N-Heterocyclic Carbenes and Cyclic (Alkyl)(amino)carbenes as Ligands for p-Block Element Compounds

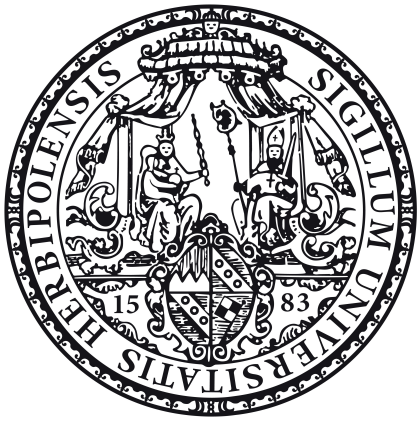

Dissertation zur Erlangung des naturwissenschaftlichen Doktorgrades

der Julius-Maximilians-Universität Würzburg

vorgelegt von

Michael Stephan Maria Philipp

aus Tegernsee

Würzburg, 2022

Eingereicht an der Fakultät für Chemie und Pharmazie der Julius-Maximilians-Universität Würzburg am:

Gutachter der schriftlichen Arbeit:

1. Gutachter: Prof. Dr. Udo Radius
2. Gutachter: Prof. Dr. Maik Finze

Prüfer des öffentlichen Promotionskolloquiums:

1. Prüfer: Prof. Dr. Udo Radius
2. Prüfer: Prof. Dr. Maik Finze
3. Prüfer: Prof. Dr. Ann-Christin Pöppler

Datum des öffentlichen Promotionskolloquiums:

14.10.2022

Doktorurkunde ausgehändigt am:

14.10.2022

Für meine Familie

Die Experimente zur vorliegenden Arbeit wurden in der Zeit von März 2018 bis März 2022 am Institut für Anorganische Chemie der Julius-Maximilians-Universität unter Anleitung von Prof. Dr. Udo Radius durchgeführt.

The publications listed below are partly reproduced in this dissertation with permission from The Royal Society of Chemistry and Copyright Wiley-VCH GmbH. The table itemizes at which position in this work, each publication has been reproduced.

Publication	Position
Michael S. M. Philipp, Rüdiger Bertermann, Udo Radius, *N-Heterocyclic Carbene and Cyclic (Alkyl)(amino)carbene Adducts of Germanium(IV) and Tin(IV) Chlorides and Organyl Chlorides*, *Eur. J. Inorg. Chem.* **2022**, e202200429, DOI: 10.1002/ejic.202200429. Licence: CC BY-NC 4.0.	Chapter II
Michael S. M. Philipp, Rüdiger Bertermann, Udo Radius, *Activation of Ge–H and Sn–H bonds with N-Heterocyclic Carbenes and a Cyclic (Alkyl)(amino)carbene*, *Chem. Eur. J* **2022**, e202202493, DOI: 10.1002/chem.202202493. Licence: CC BY-NC 4.0.	Chapter III
Michael S. M. Philipp, Rüdiger Bertermann, Udo Radius *N-Heterocyclic Carbene and Cyclic (Alkyl)(amino)carbene adducts of Plumbanes and Plumbylenes*, *Dalton Trans*. **2022**, Accepted Manuscript, DOI: 10.1039/D2DT02462D. Order License ID: 1261281-1. Permission was conveyed through Copyright Clearance Center, Inc.	Chapter IV
Michael S. M. Philipp, Mirjam J. Krahfuss, Krzysztof Radacki, Udo Radius, *N-Heterocyclic Carbene and Cyclic (Alkyl)(amino)carbene Adducts of Antimony(III)*, *Eur. J. Inorg. Chem.* **2021**, *38*, 4007-4019, DOI:10.1002/ejic.202100632. Licence: CC BY-NC 4.0.	Chapter V
Michael S. M. Philipp, Udo Radius, *A Versatile Route To Cyclic (Alkyl)(Amino)Carbene-Stabilized Stibinidenes*, *Z. anorg. allg. Chem.* **2022**, e202200085. DOI: 10.1002/zaac.202200085. Licence: CC BY-NC 4.0.	Chapter VI

Further publications:

Marcus Schulze, Michael Philipp, Waldemar Waigel, David Schmidt, Frank Würthner, *Library of Azabenz-Annulated Core-Extended Perylene Derivatives with Diverse Substitution Patterns and Tunable Electronic and Optical Properties*, *J. Org. Chem.* **2016**, *81*, 8394-8405, DOI: 10.1021/acs.joc.6b01573.

Luis Werner, Günther Horrer, Michael Philipp, Katharina Lubitz, Maximilian W. Kuntze-Fechner, Udo Radius, *A General Synthetic Route to NHC-Phosphinidenes: NHC-mediated Dehydrogenation of Primary Phosphines*, *Z. Anorg. Allg. Chem.* **2021**, *647*, 1-16, DOI: 10.1002/zaac.202000405.

Table of Contents

Chapter I

N-Heterocyclic Carbene and Cyclic (Alkyl)(amino)carbene ligated Group 14 and Group 15 Element Compounds

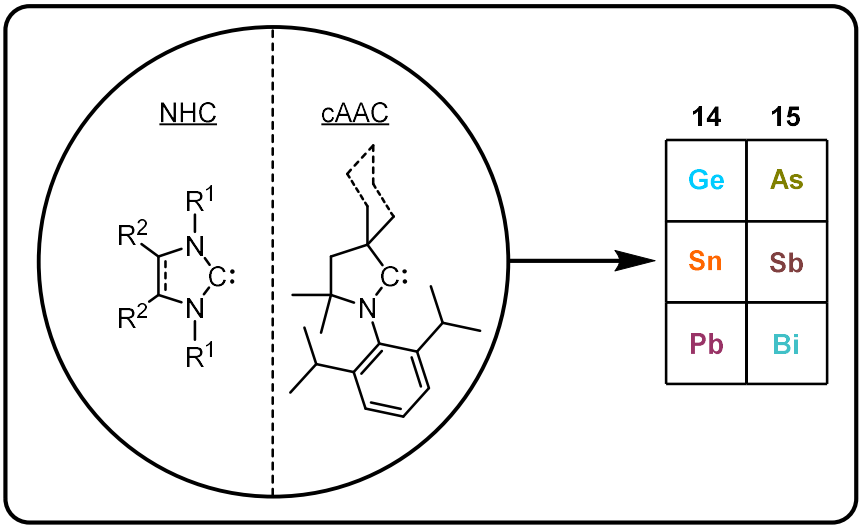

1 Introduction

1.1 N-Heterocyclic Carbenes (NHCs) and Cyclic (Alkyl)(amino)carbenes (cAACs) as ligands in main group chemistry

Since the isolation of the first free ***N*-H**eterocyclic **C**arbene (**NHC**) by Arduengo *et al.* in 1991[1] and the first **c**yclic (**A**lkyl)(**A**mino)**C**arbene (**cAAC**) by Bertrand *et al.* in 2005[2] their use as ligands in main group element chemistry is on the rise.[3][4] This is mainly due to their tunable ambiphilicity and steric properties, which can be varied significantly.[5] Both NHCs and cAACs (Figure 1.1) were reported to facilitate a plethora of low-valent compounds with interesting reactivities in particular for the elements silicon[3g-j, 4c, 6] and phosphorus[7]. In comparison, the chemistry of the heavier homologues of groups 14 and 15 is much less studied, mainly due to the weaker element-carbon bonds observed as the groups are descended.[8]

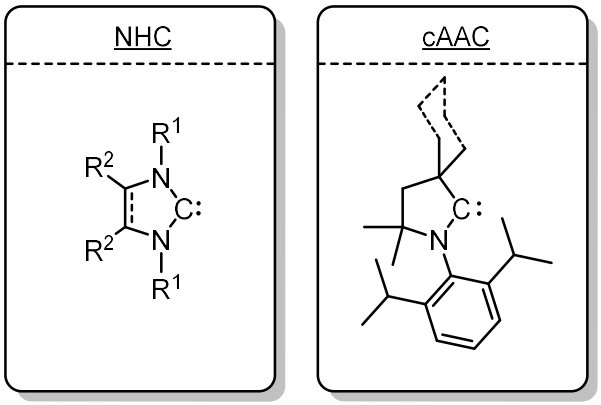

Figure 1.1 General structure of *N*-**H**eterocyclic **C**arbenes (**NHC**s) and **c**yclic (**A**lkyl)(**A**mino) **C**arbenes (**cAAC**s).

1.2 NHC- and cAAC-ligated tetrel compounds

1.2.1 NHC and cAAC adducts of silicon

As mentioned above, great progress has been made in NHC and cAAC supported silicon chemistry in des last decades.[3g-j, 4c, 6] For example, our group recently observed the thermally induced rearrangement of *i*Pr$_2$Im·SiCl$_2$Ph$_2$ to the backbone tethered salt [(^{a}*i*Pr$_2$Im)$_2$·SiPh$_2$]$^{2+}$2[Cl]$^-$ (**1.1**, Figure 1.2) ("a" denotes abnormal or backbone coordination) with loss of SiCl$_2$Ph$_2$.[9] Furthermore, the isolation of interesting carbene-stabilized subvalent silicon compounds such as the monomeric cAAC$^{Me/Cy}_2$·Si (**1.2**),[10] the dimeric (Dipp$_2$Im·Si)$_2$ (**1.3**),[11] and (cAAC$^{Me/Cy}$·Si)$_2$ (**1.4**)[12] as well as the trimeric (cAAC^{Me}·Si)$_3$ (**1.5**)[13] Si(0) adducts have been reported in recent years (Figure 1.2). A variety of Si(IV) precursors such as NHC·SiCl$_4$[3f, 11, 14] and cAAC·SiCl$_4$,[15] which can subsequently be reduced to the Si(0) compounds, were found to be essential for the formation of these products.

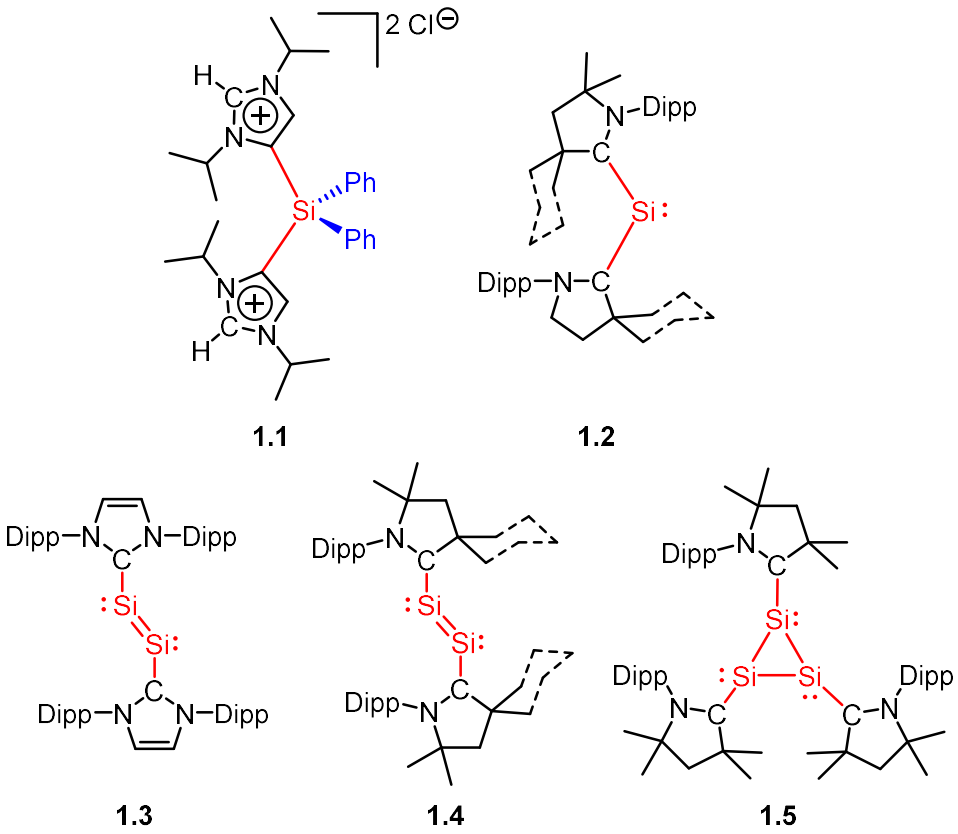

Figure 1.2 Selected NHC- and cAAC-stabilized silicon compounds.[9-13]

1.2.2 NHC- and cAAC-ligated germanium and tin chlorides

For the heavy homologues of group 14, Ge and Sn, the chemistry of low-valent NHC- and cAAC-ligated E(II) compounds (E = Ge, Sn) offers a wide range of substitution patterns as well as diverse reactivities.[3j, 6c, 16] The adducts NHC·ECl_2 and cAAC·ECl_2 (E = Ge, Sn), which can be synthesized from the corresponding free carbene and the commercially available precursors $GeCl_2$·dioxane[16b, 16c, 17] and $SnCl_2$,[14a, 16c, 17b, 18] respectively, represent the most common starting materials for this chemistry. The NHC·$ECl_{4-n}R_n$ adducts (E in the oxidation state (IV)) are also potential starting points for NHC and cAAC supported germanium and tin chemistry. These adducts are obtained by reacting of the corresponding free carbenes with the easy to handle compounds $ECl_{4-n}R_n$ (E = Ge, Sn; n = 0-4). However, only a few Ge(IV) and Sn(IV) adducts of this kind have been described in the literature so far and thus their properties, trends and reactivities remain remarkably underdeveloped.[9, 14a, 16c, 17b, 18-19]

Recently, the syntheses of a small number of such Ge(IV) compounds were reported. In 2010, Baines and co-workers synthesized the Ge(IV) chloride adduct *i*Pr_2Im·$GeCl_2$(DMB) (**1.6**, Figure 1.3) starting from $GeCl_2$(DMB) and *i*Pr_2Im. Further, thermally induced elimination of 2,3-dimethylbutadiene from **1.6** led to *i*Pr_2Im·$GeCl_2$.[19b] Subsequently, Röschenthaler *et al.* reported on the reaction of ^{s}Me_2ImF_2 with $GeCl_2$·dioxane which led to both, the chloride adduct ^{s}Me_2Im·$GeCl_4$ (**1.7**, Figure 1.3) and the fluoride adduct ^{s}Me_2Im·GeF_4 (**1.8**, Figure 1.3) in a ratio of 1:1.[19c] Based on this synthetic approach, Rivard *et al.* selectively prepared **1.7** starting from the salt [^{s}Me_2ImCl]$^+$[Cl]$^-$ and $GeCl_2$·dioxane. Furthermore, the reaction of $GeCl_4$ with the free NHCs *i*Pr_2Im^{Me} and $Dipp_2$Im, afforded the corresponding adducts *i*Pr_2Im^{Me}·$GeCl_4$ (**1.9a**, Figure 1.3)[19f] and $Dipp_2$Im·$GeCl_4$ (**1.9b**, Figure 1.3),[19d] respectively.

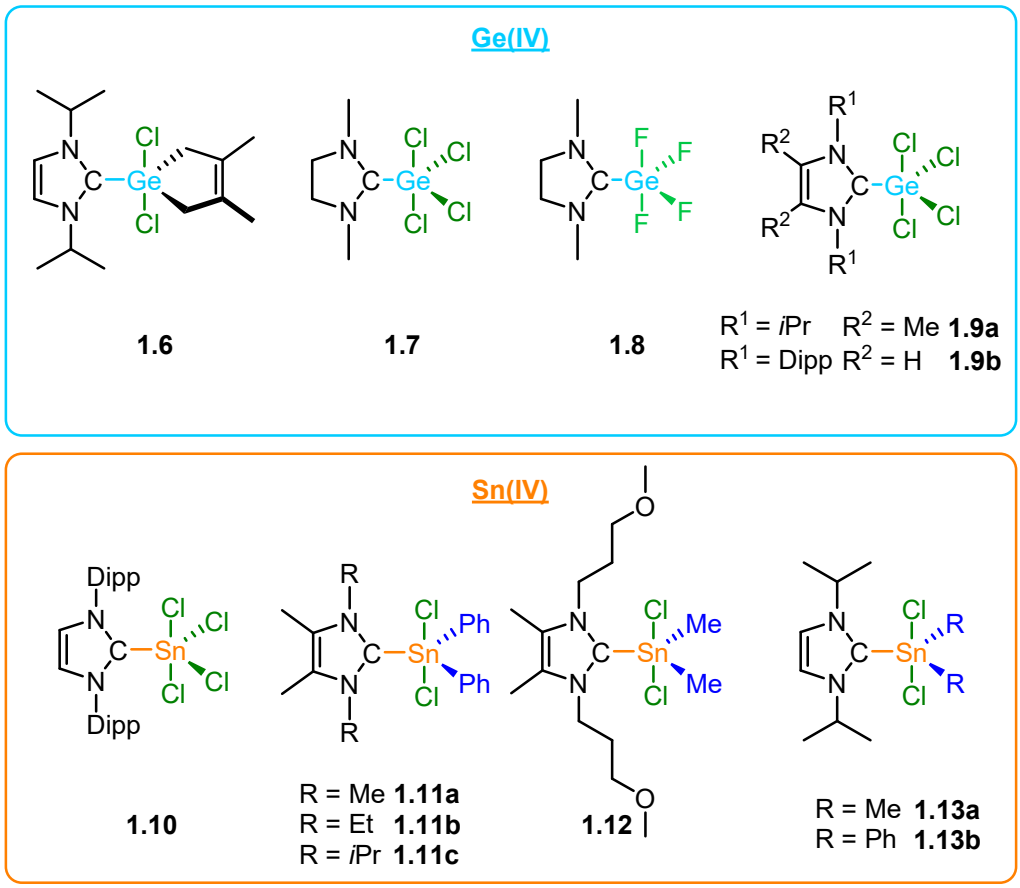

Figure 1.3 Literature known NHC Ge(IV)[19b-d, 19f] and NHC Sn(IV) halogenide adducts.[9, 14a, 19d, 19e]

Analogously to the synthesis of the Ge(IV) adducts **1.9a−b**, the reaction of $Dipp_2Im$ with $SnCl_4$ yielded the adduct $Dipp_2Im{\cdot}SnCl_4$ (**1.10**, Figure 1.3).[19d] Similar Sn(IV) adducts $R_2Im^{Me}{\cdot}SnCl_2Ph_2$ were already obtained in 1995 by Boese and co-workers by the reaction of $SnCl_2Ph_2$ with R_2Im^{Me} (R = Me (**1.11a**), Et (**1.11b**), *i*Pr (**1.11c**); Figure 1.3).[14a] Additionally, the methyl-substituted derivative $DMP_2Im^{Me}{\cdot}SnCl_2Me_2$ (**1.12** Figure 1.3) was isolated, upon combination of $SnCl_2Me_2$ and DMP_2Im^{Me}.[19a] In the course of the aforementioned studies on the rearrangement of $iPr_2Im{\cdot}SiCl_2Ph_2$ into the backbone-coordinated adduct **1.1**,[9] the corresponding NHC-coordinated tin compounds $iPr_2Im{\cdot}SnCl_2R_2$ (R = Me (**1.13a**), Ph (**1.13b**); Figure 1.3) were obtained by reacting iPr_2Im with $SnCl_2R_2$, too. However, the desired corresponding backbone coordination of the NHC could not be observed for the tin compounds.[19e] Despite their simple synthetic accessibility and promising use as starting materials, examples of such NHC- or cAAC-coordinated E(IV) (E =Ge, Sn) compounds still remain scarce in the literature.

1.2.3 Reactivity of NHCs and cAACs with germanium and tin hydride compounds

The reactivity of tetrel hydrides towards NHCs and cAACs has also been investigated in the past decades. Recently, our group reported on the reaction of the silicon hydrides SiH_3Ph, SiH_2Ph_2 and $SiHPh_3$ with different NHCs leading to an insertion of silylene moieties into the C−N bond of NHCs in a **R**ing **E**xpansion **R**eaction (RER) and subsequent formation of the diaza-silinanes **1.14a−c** (Scheme 1.1, left). In the reaction of $SiHPh_3$ in contrast to mono- and diphenylsilane, the migration of a phenyl group was observed.[20] Furthermore, Bertrand *et al.* reported on the insertion of $cAAC^{Cy}$ into one Si−H bond of various silanes. For example the equimolar reaction of $cAAC^{Cy}$ with SiH_2Ph_2 yielded the stable insertion product $cAAC^{Cy}H{-}SiHPh_2$ (**1.15**, Scheme 1.1, right).[21]

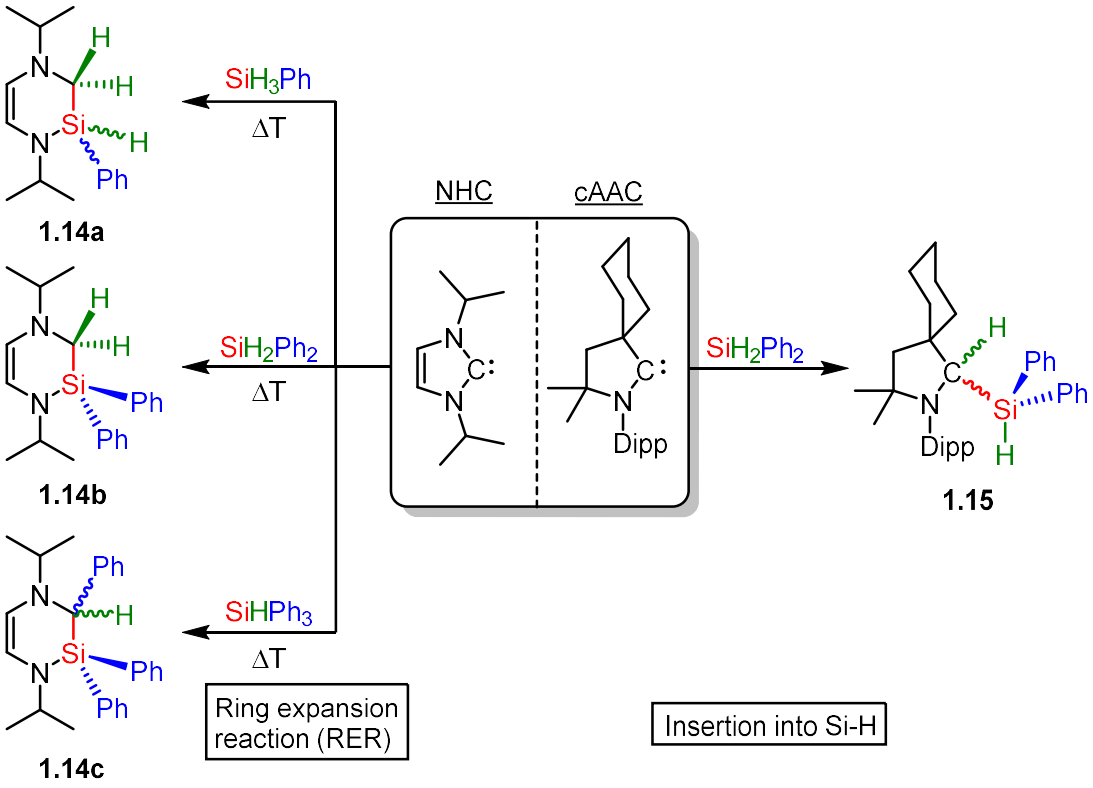

Scheme 1.1 Ring **E**xpansion **R**eaction (RER) of *i*Pr$_2$Im with SiH_3Ph, SiH_2Ph_2 and $SiHPh_3$ forming the diaza-silinanes **1.14a−c**. Insertion of $cAAC^{Cy}$ into one Si−H bond of SiH_2Ph_2 yielding $cAAC^{Cy}H{-}SiHPh_2$ (**1.15**).[20-21]

For the heavier homologue germanium, the NHC- and cAAC-containing chemistry of the hydrides is mainly based on the hydrogenation of various chloride adducts with reagents such as $LiBH_4$ to form the corresponding hydrides. The group of Rivard carried out pioneering work in a series of publications, starting with the NHC-stabilized adduct $Dipp_2Im{\cdot}GeH_2{\cdot}BH_3$ (**1.16a**, Scheme 1.2), which was synthesized from the chloride precursors $Dipp_2Im{\cdot}GeCl_2$,[17b] $Dipp_2Im{\cdot}GeCl_4$,[19d] or $Dipp_2Im{\cdot}GeCl_2GeCl_2$[22] by hydrogenation with $LiBH_4$. The compounds $Me_2Im^{Me}{\cdot}GeH_2{\cdot}BH_3$ (**1.16b**, Scheme 1.2) and $iPr_2Im^{Me}{\cdot}GeH_2{\cdot}BH_3$ (**1.16c**, Scheme 1.2) were analogously prepared by hydrogenation of $Me_2Im^{Me}{\cdot}GeCl_2$ and $iPr_2Im^{Me}{\cdot}GeCl_2$, respectively.[19f] Compound **1.16a** could further be reacted with $[W(CO)_5THF]$ *via* exchange of the *Lewis*-acid BH_3 to form $[Dipp_2Im{\cdot}GeH_2{\cdot}W(CO)_5]$ (**1.17**, Scheme 1.2).[23] This compound can also be prepared from the NHO-stabilized $[Dipp_2ImCH_2{\cdot}GeH_2{\cdot}W(CO)_5]$ by exchange of the NHO with $Dipp_2Im$ or by hydrogenation of the corresponding chloride precursor $[Dipp_2Im{\cdot}GeCl_2{\cdot}W(CO)_5]$, respectively.[24] In addition, the reaction of **1.16a** with MeOTf led to $Dipp_2Im{\cdot}GeH_2{\cdot}BH_2OTf$ (**1.18**, Scheme 1.2), which further reacts with different group 15 *Lewis*-bases (LB) to form the corresponding salts $[Dipp_2Im{\cdot}GeH_2LB]^+[OTf]^-$ (LB = PH_2tBu (**1.19a**), $PHPh_2$ (**1.19b**), PPh_3 (**1.19c**) and $AsPh_3$ (**1.19d**)).

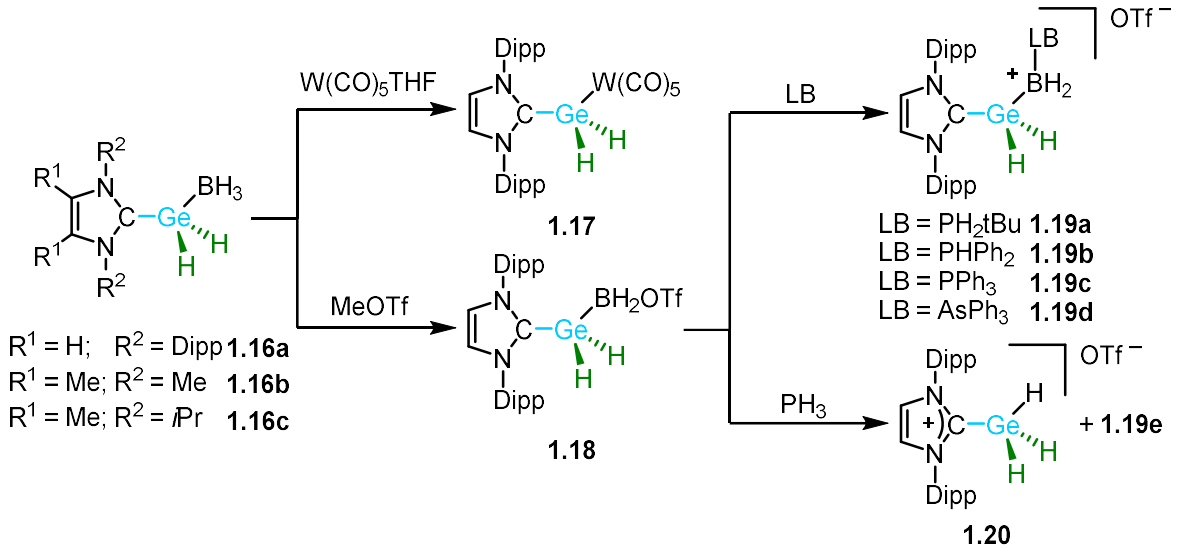

Scheme 1.2 Synthesis of NHC-stabilized germanium hydride compounds.[17b, 19d, 19f, 22-23, 25]

An exception within this series of *Lewis*-bases is PH_3, which gives compound $[Dipp_2Im{\cdot}GeH_2PH_3]^+[OTf]^-$ (**1.19e**) and the additional product $[Dipp_2Im{\cdot}GeH_3]^+[OTf]^-$ (**1.20**) (Scheme 1.2).[25] Moreover, the reaction of $Dipp_2Im{\cdot}GeCl_2$ with $[THF{\cdot}GeCl_2{\cdot}W(CO)_5]$ and $LiBH_4$ yields a mixture of the NHC-stabilized digermene $[Dipp_2Im{\cdot}GeH_2GeH_2{\cdot}W(CO)_5]$ (**1.21**), **1.16a** and **1.17**.[26]

Furthermore, the hydrogenation of $Dipp_2Im{\cdot}GeClR$ with $LiBH_4$ yielded the corresponding hydrides $Dipp_2Im{\cdot}GeHR{\cdot}BH_3$ (R = NHDipp (**1.22a**), $OSiMe_3$ (**1.22b**)). Whereas in the case of the amidohydride **1.22a** a mixture of $Dipp_2Im{\cdot}BH_3$, $Dipp_2ImH_2$ and $Dipp_2Im{\cdot}BH_2NHDipp$ was obtained. In the reaction of **1.22b** with HBPin, the formation of elemental germanium and $NHCH_2$ was observed.[27] Additionally, Tobita and co-workers reported on the insertion of a germanium atom of the cationic metallo-germylene $[Cp^*(CO)_3WGe{-}Dipp_2Im]^+[BAr^F{}_4]^-$ (**1.23**) into the respective E−H bonds of H_2, HBpin or $SiHMe_2Et$, with formation of the corresponding hydride salts $[Cp^*(CO)_3WGeHR{-}Dipp_2Im)]^+[BAr^F{}_4]^-$ (R = H (**1.24a**), Bpin (**1.24b**), $SiMe_2Et$ (**1.24c**); Scheme 1.3).[28]

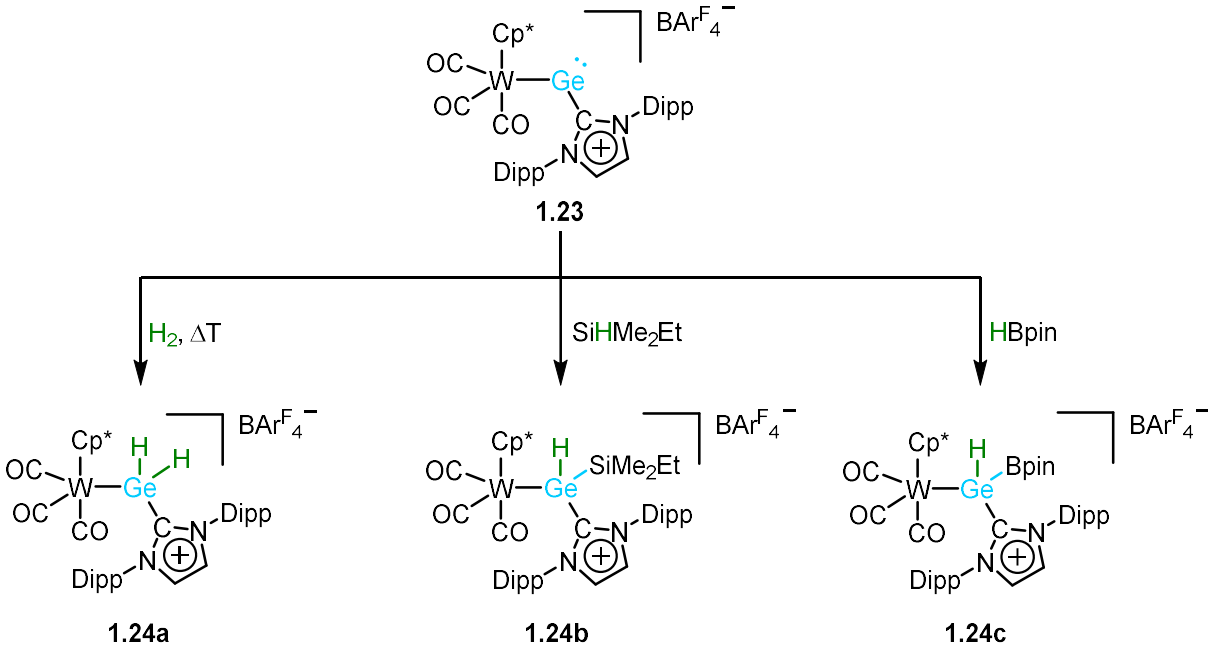

Scheme 1.3 Activation of H_2, $SiHMe_2Et$ and HBpin by $[Cp^*(CO)_3WGe{\cdot}Dipp_2Im]^+[BAr^F{}_4]^-$ (**1.23**) yielding the salts $[Cp^*(CO)_3WGeHR{\cdot}Dipp_2Im)]^+[BAr^F{}_4]^-$ (R = H (**1.24a**), Bpin (**1.24b**), $SiMe_2Et$ (**1.24c**)).[28]

The same group also described the formation of a W≡Ge triple bond by an intramolecular dehydrogenation of the NHC-stabilized germylene complex [Cp*(CO)$_2$HW−GeH(C(TMS)$_3$)·Me$_2$Im^{Me}] (**1.25**) yielding Me$_2$Im^{Me}H$_2$ and [Cp*(CO)$_2$W≡Ge(C(TMS)$_3$)] (**1.26**).[29] Driess *et al.* hydrogenated the bis(NHC)borate-stabilized zwitterionic germyliumylidene chloride Ph$_2$B(N-*t*BuIm)$_2$·GeCl with [K]$^+$[BH(*s*Bu)$_3$]$^-$ to the corresponding hydride Ph$_2$B(N-*t*BuIm)$_2$·GeH (**1.27**), which was treated with half an equivalent of [Ph$_3$C]$^+$[B(C$_6$F$_5$)$_4$]$^-$ to afford the compound [Ph$_2$B(N-*t*BuIm)$_2$·GeH·Ge·(*t*BuIm-N)$_2$BPh$_2$]$^+$[B(C$_6$F$_5$)$_4$]$^-$ (**1.28**, Scheme 1.4).[30]

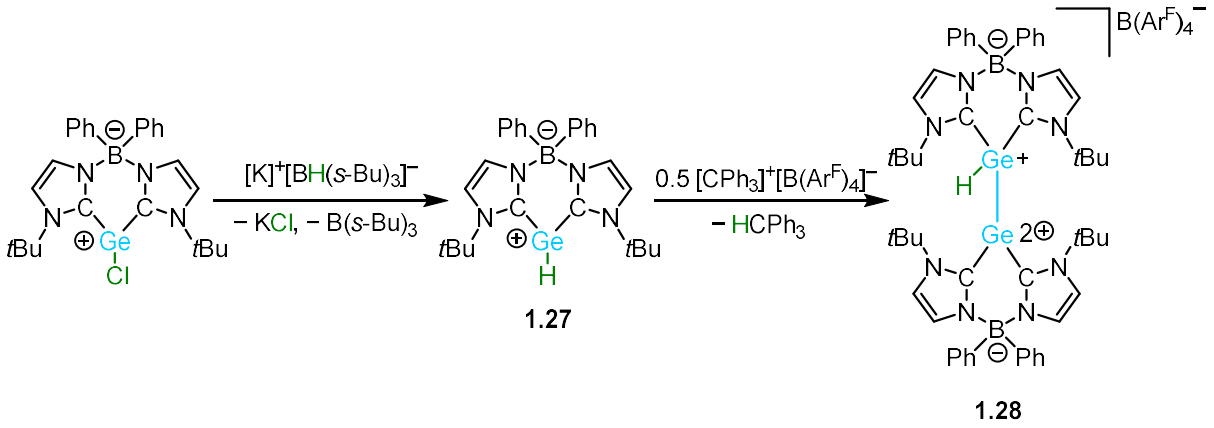

Scheme 1.4 Synthesis of Ph$_2$B(N-*t*BuIm)$_2$·GeH (**1.27**) and subsequent reaction with 0.5 eq [Ph$_3$C]$^+$[B(C$_6$F$_5$)$_4$]$^-$ to form [Ph$_2$B(N-*t*BuIm)$_2$·GeH·Ge·(*t*BuIm-N)$_2$BPh$_2$]$^+$[B(C$_6$F$_5$)$_4$]$^-$ (**1.28**).[30]

In addition, the activation of the E−H bonds of H_2, SiH_3Ph and $SiHEt_3$ by the NHC-stabilized Ge(II) cation of the salt $[(B(NDippCH)_2)(iPr_2Im^{Me})\cdot Ge\cdot THF]^+[Al(OR^F)_4]^-$ with the subsequent formation of the corresponding salts $[(B(NDippCH)_2)(iPr_2Im^{Me})\cdot GeHR]^+[Al(OR^F)_4]^-$ (R = H (**1.29a**), SiH_2Ph (**1.29b**), $SiEt_3$ (**1.29c**)) was recently observed in the group of Aldridge (Scheme 1.5). The triethylsilyl substituted product **1.29c** reacts with water to form **1.29a** and $Et_3SiOSiEt_3$.[31] Similarly, the NHC-stabilized dicationic dimer of the salt $[((iPr_2Im^{Me})\cdot GeAr^{Mes})_2]^{2+}2[Al(OR^F)_4]^-$ activates SiH_3Ph, resulting in the germanium hydride compound $[Me_2Im^{Me}\cdot GeH(SiH_2Ph)Ar^{Mes}]^+[Al(OR^F)_4]^-$ (**1.30**, Scheme 1.5).[32] Furthermore, Jones *et al.* reacted the tetrameric germanium hydride $(GeH(N(Dipp)(tBu))_4$ with Me_2Im^{Me} to yield the NHC-stabilized germylene hydride $Me_2Im^{Me}\cdot GeH(N(Dipp)(tBu))$ (**1.31**).[33]

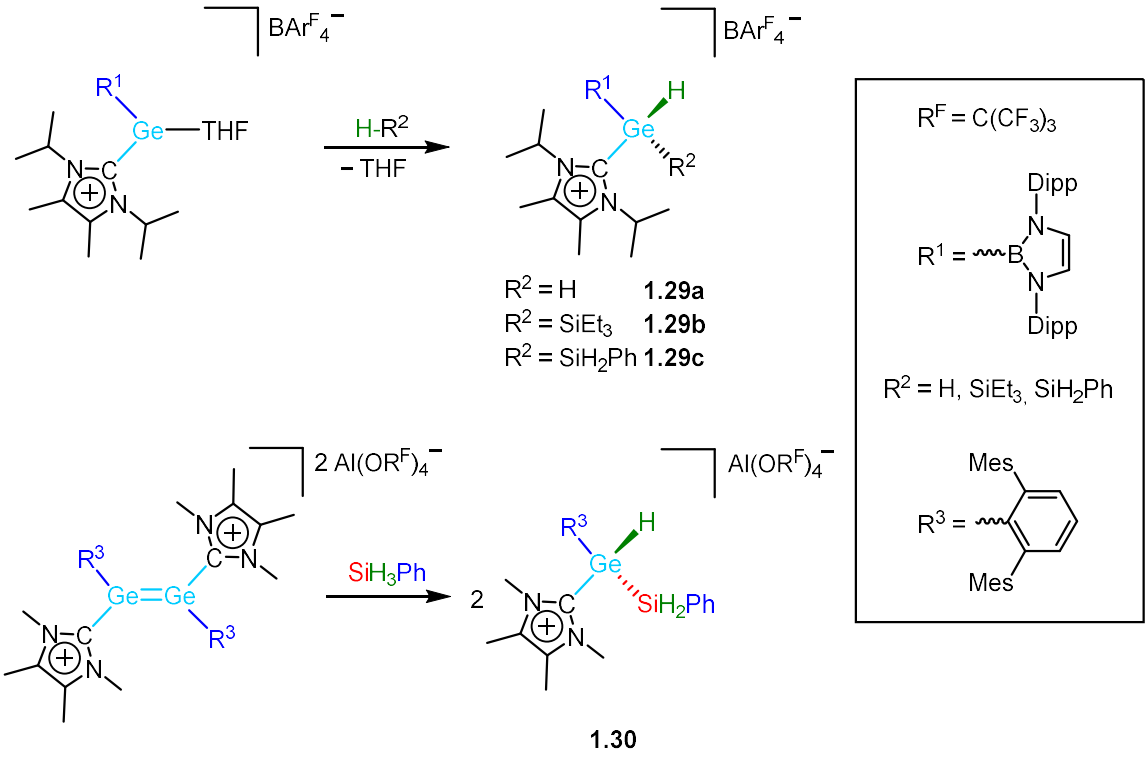

Scheme 1.5 Activation of H_2, $SiHEt_3$ SiH_3Ph by $[(B(NDippCH)_2)(iPr_2Im^{Me})\cdot Ge\cdot THF]^+[Al(OR^F)_4]^-$yielding $[(B(NDippCH)_2)(iPr_2Im^{Me})\cdot GeHR]^+[Al(OR^F)_4]^-$ (R = H (**1.29a**), SiH_2Ph (**1.29b**), $SiEt_3$ (**1.29c**)).[31] Activation of SiH_3Ph by $[((iPr_2Im^{Me})\cdot GeAr^{Mes})_2]^{2+}2[Al(OR^F)_4]^-$ yielding $[Me_2Im^{Me}\cdot GeH(SiH_2Ph)Ar^{Mes}]^+[Al(OR^F)_4]^-$ (**1.30**).[32]

Moreover, the group of Wesemann reported on the dehydrogenative synthesis of the NHC-stabilized germylenes Me_2Im^{Me}·GeHR (R = 2,6-$Trip_2C_6H_3$ (**1.32a**); R = Tbb (**1.32b**)) with concomitant formation of $NHCH_2$ starting from GeH_3R and Me_2Im^{Me}. The NHC-stabilized stannylene iPr_2Im^{Me}·SnHTbb (**1.33**, Scheme 1.6, (i)) was prepared analogously.[34]

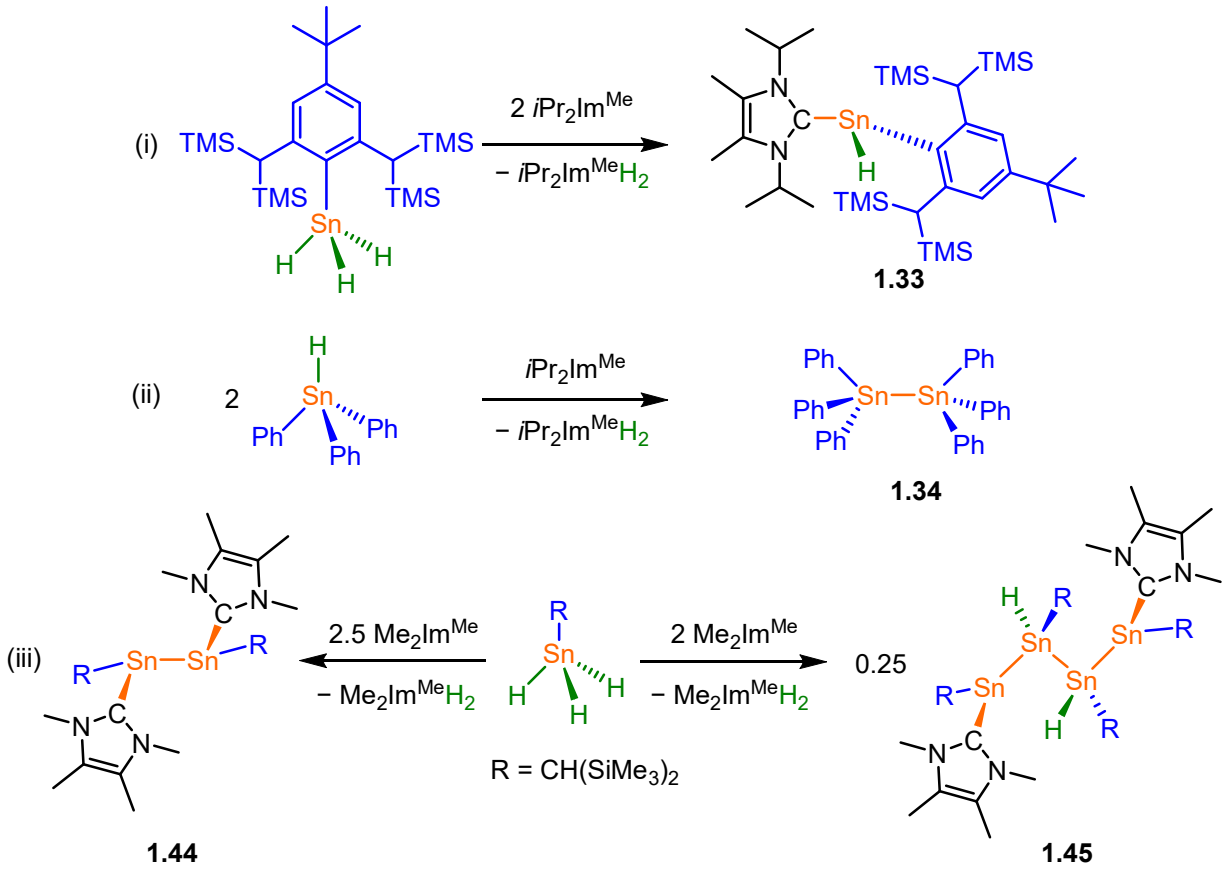

Scheme 1.6 (i) Synthesis of iPr_2Im^{Me}·SnHTbb (**1.33**) *via* dehydrogenation of SnH_3Tbb by iPr_2Im^{Me}.[34] (ii) iPr_2Im^{Me} mediated dehydrogenative coupling of $SnHPh_3$ to form Sn_2Ph_6 (**1.34**) and $iPr_2Im^{Me}H_2$.[19e] (iii) Dehydrogenative coupling of $SnH_3(CH(SiMe_3)_2)$ to form $(CH(SiMe_3)_2)_2Sn_2(Me_2Im^{Me})_2$ (**1.44**) and $(Me_2Im^{Me}$·SnR−SnHR$)_2$ (**1.45**).[35]

Our group observed a similar pathway for the reaction of the NHCs iPr_2Im and iPr_2Im^{Me} with $SnHPh_3$. The dehydrogenative coupling (DHC) of the stannane afforded the hexaaryldistannane Sn_2Ph_6 (**1.34**, Scheme 1.6, (ii)) and the aminal $NHCH_2$. The knowledge about carbene-mediated DHC of stannanes is mainly based on the work of the Wesemann group. They reported on the reaction of the diarylstannane SnH_2Ar_2 (Ar = Ph, Trip) with Et_2Im^{Me} in a ratio of 2:1 (SnH_2Trip_2:Et_2Im^{Me}) which yielded the tetraorganodistannane $Sn_2H_2Trip_4$ (**1.35**). The reaction with inverse stoichiometry of 1:2 (SnH_2Ar_2:Et_2Im^{Me}) led to the isolation of the NHC-stabilized stannylenes

Et_2Im^{Me}·$SnAr_2$ (Ar = Ph (**1.36a**), Trip (**1.36b**)).[36] Correspondingly, both the reaction of Me_2Im^{Me} with SnH_2Trip_2 and the reaction of the mono-organostannane SnH_3Ar^{Trip} with the NHCs Me_2Im^{Me} (**a**) and Et_2Im^{Me} (**b**) afforded the NHC-stabilized stannylenes Me_2Im^{Me}·$SnTrip_2$ (**1.37**)[37] and NHC·$SnHAr^{Trip}$ (**1.38a−b**)[36, 38], respectively. If SnH_3Trip and Et_2Im^{Me} were reacted in a stoichiometry of 1:1.5 (SnH_3Trip:Et_2Im^{Me}), the subvalent tin cluster Sn_6Trip_6 (**1.39**) was obtained.[36] Further, the reactions of SnH_3Ar^{Mes} with the NHCs Me_2Im^{Me} (**a**) and *i*Pr_2Im^{Me} (**b**) led to different products depending on the stoichiometry. The stannyl-stannylenes $Ar^{Mes}Sn(NHC)SnH_2Ar^{Mes}$ (**1.40a−b**) were formed by a stoichiometry of 1:1.5 (SnH_3Ar^{Mes}:NHC) while a ratio of 1:2 (SnH_3Ar^{Mes}:NHC) led to the stannylenes NHC·$SnHAr^{Mes}$ (**1.41a−b**). The obtained stannyl-stannylenes **1.40a−b** react with another equivalent $Ar^{Mes}SnH_3$ to give the corresponding distannane $Sn_2H_4ArMes_2$ (**1.42**) through formation of $NHCH_2$.[39] In addition, the neutral cluster $(SnMes)_{10}$ (**1.43**) was isolated from an Et_2Im^{Me}-mediated DHC of SnH_3Mes.[35] In contrast, the carbene-mediated DHC of the monoorganostannane SnH_3R (R = $CH(SiMe_3)_2$) yielded different products depending on the reaction conditions. Through altering stoichiometry both, the dialkyldistannyne $R_2Sn_2(Me_2Im^{Me})_2$ (R = $CH(SiMe_3)_2$) (**1.44**) and the tin chain $(Me_2Im^{Me}$·SnR−SnHR$)_2$ (**1.45**) were afforded *via* NHC-mediated DHC of $SnH_3(CH(SiMe_3)_2)$ (Scheme 1.6, (iii)).[35] The reaction of such tin hydrides with NHCs offers a variety of different products, but has so far been limited to sterically demanding substituents on tin.

1.2.4 NHC- and cAAC-ligated lead compounds

In contrast to its lighter homologues the carbene chemistry of lead is remarkably underdeveloped. The first NHC-stabilized plumbylene *i*Pr_2Im^{Me}·$PbTrip_2$ (**1.46**) was obtained from the reaction of Pb_2Trip_4, with *i*Pr_2Im^{Me} by Weidenbruch and co-workers (Scheme 1.7, (i)).[40] Wesemann's group followed with the synthesis of the first NHC-stabilized plumbylene hydride Me_2Im^{Me}·$PbAr^{Trip}H$ (**1.47**, Scheme 1.7, (ii)), which was obtained by trapping the dimeric $Pb_2H_2Ar^{Trip}_2$ intermediate from the reaction of $PbAr^{Trip}R$ (R = $CHPh(PPh_2)$) and catecholborane with free Me_2Im^{Me}.[41] In addition,

Gerhus *et al.* reacted the *N*-heterocyclic plumbylene (NHPb) $Pb(NNeop)_2^{(C6H4)}$ with $Neop_2Im^{(C6H4)}$, which led to the adduct $Neop_2Im^{(C6H4)}{\cdot}Pb(NNeop)_2^{(C6H4)}$ (**1.48**, Scheme 1.7, (iii)).[42] For the aforementioned plumbylenes, equilibria between adducts and the corresponding starting materials were observed.[40-42]

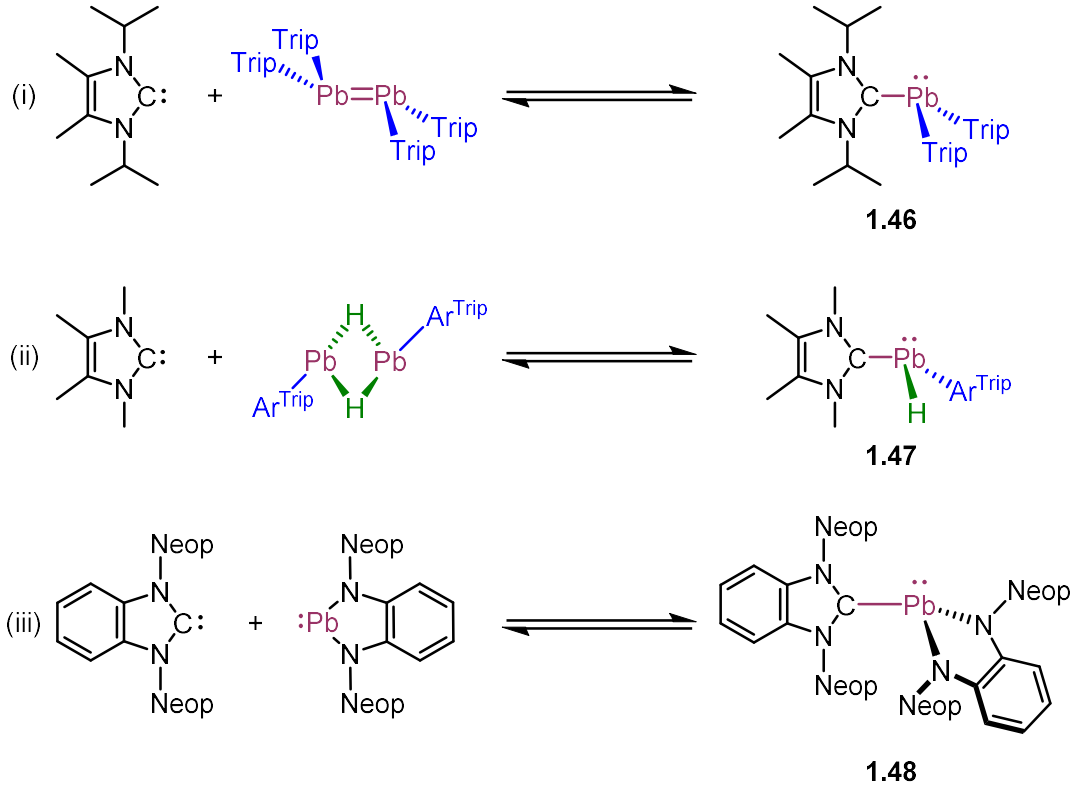

Scheme 1.7 Equilibria between the starting materials and the corresponding adducts $iPr_2Im^{Me}PbTrip_2$ (**1.46**, (i)),[40] $Me_2Im^{Me}PbHTer^{Trip}$ (**1.47**, (ii))[41] and $Neop_2Im^{(C6H4)}{\cdot}Pb(NNeop)_2^{(C6H4)}$ (**1.48**, (iii)).[42]

Similarly, further adducts of *N*-heterocyclic plumbylenes $[Fe((\eta^5\text{-}C_5H_4)NSiMe_2R)_2Pb{\cdot}Me_2Im^{Me}]$ (R = Me (**1.49a**), *t*Bu (**1.49b**)), $Me_2Im^{Me}{\cdot}Pb(N(SiMe_3)_2)_2$ and Ph-1,2-$(NSiMe_3)_2Pb{\cdot}$L (L = Me_2Im^{Me} (**1.50a**), $cAAC^{Et}$ (**1.50a**)) were synthesized by Siemling *et al.*[43] Furthermore, an NHC-linked bisphosphanyl plumbylene $[Fe((\eta^5\text{-}C_5H_4)P\textit{t}Bu)_2Pb{\cdot}Me_2Im^{Me}]$ (**1.51**) was obtained by Pietschnig and co-workers from the reaction of $[Fe((\eta^5\text{-}C_5H_4)P\textit{t}Bu)_2Pb]$ and free Me_2Im^{Me}.[44] In addition to the aforementioned sterically demanding Pb(II) compounds, an NHC adduct of $PbBr_2$ was synthesized in the same manner. The obtained adduct $Dipp_2Im{\cdot}PbBr_2$ (**1.52**) was thought to be used as starting point for a reduction to yield a Pb=Pb double bond, however this was unsuccessful.[45]

The reaction of **1.52** with $[Li]^+[NHDipp]^-$ afforded the first stable amide-substituted adduct of lead, $Dipp_2Im{\cdot}PbBrNHDipp$ (**1.53**).[19d] Another carbene adduct of $PbBr_2$ was obtained by Munz *et al.* by coordination of the pincer carbene 2,6-(^{s}DippImN)$_2$-pyridine (^{pincer}NHC). Exchange of the lead bound substituents of (^{pincer}NHC)·$PbBr_2$ (**1.54**) with TlOTf led to (^{pincer}NHC)·$PbOTf_2$ (**1.55**).[46] In addition to the NHC-coordinated plumbocenes reported by Schäfer *et al.*,[47] the backbone-coordinated ^{a}NHC salts $[K]^+[^{a}Dipp_2Im^{NHDC}{\cdot}Pb(N(TMS)_2)_2]^-$ (**1.56**) and $[M]^+[(^{a}Dipp_2Im^{NHDC})_2{\cdot}Pb(N(TMS)_2)_2]^-$ (**1.57**) (M = Li, K) obtained from the reaction of $[M]^+[NHDC]^-_n$ with $Pn(N(TMS)_2)_2$ was reported by the group of Goicoechea (Scheme 1.8).[48]

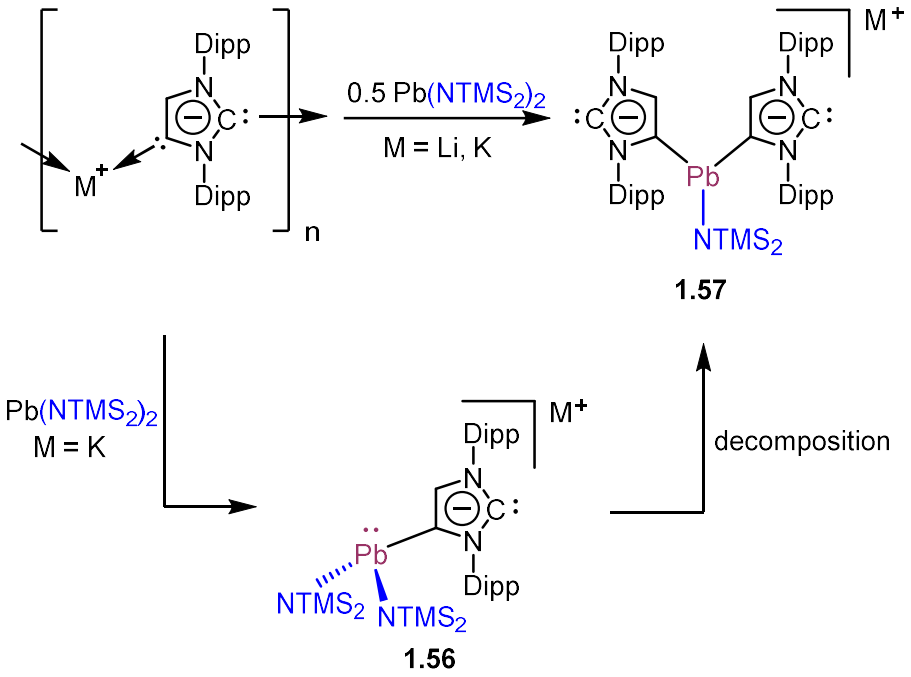

Scheme 1.8 Synthesis of the backbone-coordinated salts $[K]^+[^{a}Dipp_2Im^{NHDC}{\cdot}Pb(N(TMS)_2)_2]^-$ (**1.56**) and $[M]^+[(^{a}Dipp_2Im^{NHDC})_2{\cdot}Pb(N(TMS)_2)_2]^-$ (**1.57**) (M = Li, K).[48]

1.3 NHC- and cAAC-ligated pnictogen compounds

1.3.1 NHC and cAAC adducts of phosphorus

A plethora of NHC supported phosphorus compounds are reported in the literature.[7] These compounds feature phosphorus centers in low oxidation states and uncommon binding modes such as carbene-stabilized P_2, P_4 and P_{12} moieties,[7i, 49] as well as NHC-stabilized phosphinidenes (NHC·PR), which can be used for phosphinidene transfer reactions.[7m, 14c, 49m, 49o, 50] Such NHC-ligated phosphinidenes can be obtained from a variety of phosphinidene precursors,[50d, 51] by the cleavage of *cyclo*-phosphines $(RP)_n$ with NHCs, [7n, 49n, 50a, 50b, 52] the reduction of NHC·PCl_2R adducts, [5f, 50e, 50i] as well as the DHC of RPH_2 in the presence of the corresponding NHCs.[49f, 50f, 50g, 50k, 53] In contrast to the large amount of interesting NHC supported phosphorus compounds and their reactivities, the chemistry of the heavier homologues is significantly less developed. This is mainly due to the intrinsic decrease in stability of the corresponding adducts and the decreasing *π*-interactions with increasing atomic number, which is essential for the stability of the corresponding subvalent compounds.[8]

1.3.2 NHC and cAAC adducts of arsenic, antimony and bismuth

First representatives of arsenic NHC adducts, $Mes_2Im{\cdot}AsR$ (**1.58a**−**b**, Scheme 1.9) were synthesized by Arduengo *et al*. starting from Mes_2Im and the corresponding *cyclo*-arsanes $(AsR)_n$ (n = 6, R = Ph (**a**), n = 4, R = C_6F_5 (**b**)).[50a] Following an analogous route, $Me_2Im^{Me}{\cdot}AsTrip$ (**1.59**, Scheme 1.9) was prepared in the group of Hering-Junghans by reacting the *cyclo*-trimer $(AsTrip)_3$ with free Me_2Im^{Me}.[54]

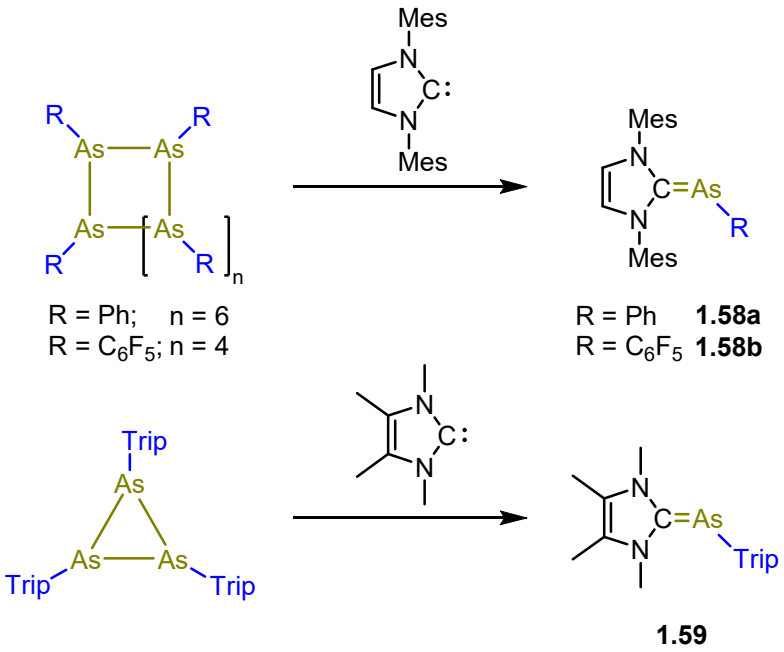

Scheme 1.9 Synthesis of $Mes_2Im{\cdot}AsR_2$ (n = 6, R = Ph (**1.58a**); n = 4, R = C_6F_5 (**1.58b**))[50a] and $Me_2Im^{Me}{\cdot}AsTrip$ (**1.59**).[54]

In a collaborative work by the groups of Tamm, Scheer, and Goicoechea, the arsinidenes $R_2Im{\cdot}AsTMS$ (R = Mes (**1.60a**), Dipp (**1.60b**)) were obtained after the reaction of $R_2Im\text{-}F_2$ with $As(TMS)_3$ with elimination of TMSF. Furthermore, both **1.60a** and **1.60b** can be reacted with methanol to give the H-arsinidenes $R_2Im{\cdot}AsH$ (**1.61a–b**) *via* desilylation. The compounds **1.61a–b**, as well as $Ar^*_2Im{\cdot}AsH$ (**1.61c**), can additionally be synthesized from the corresponding imidazolium salt $[R_2ImH]^+[Cl]^-$ and $[Na(dioxane)_{3.31}]^+[AsCO]^-$ with formation of NaCl and CO.[55] Another path to obtain low-valent pnictogen compounds is the reduction of the corresponding halide adducts.

Various pnictogen halide carbene adducts, such as $Dipp_2Im{\cdot}PnCl_3$ (Pn = As (**1.62**)[3f], Bi (**1.63**)[56]) and $Dipp_2Im{\cdot}PnBr_3$ (Pn = Sb (**1.64**), Bi (**1.65**)),[57] have been synthesized starting from $Dipp_2Im$ and the corresponding PnX_3 (Scheme 1.10). Halide compounds coordinated to cAACs such as $cAAC^{Me/Et}{\cdot}AsCl_3$ (**1.66a–b**)[58] and $cAAC^{Me/Cy}{\cdot}SbCl_3$ (**1.67a–b**)[58b, 59] were prepared analogously. In the next step, such chlorides can be reduced to subvalent pnictogen compounds. For example, the stabilized diarsene $(Dipp_2Im{\cdot}As)_2$ (**1.68**, Scheme 1.10) was obtained by Robinson and co-workers by reduction of $Dipp_2Im{\cdot}AsCl_3$ with KC_8.[3f]

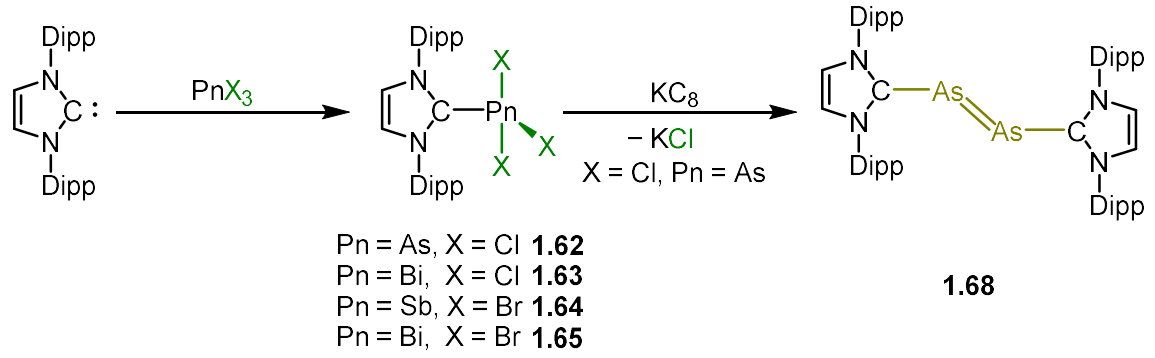

Scheme 1.10 Synthesis of $Dipp_2Im{\cdot}PnX_3$ (X = Cl, Pn = As (**1.62**),[3f] Bi (**1.63**);[56] X = Br, Pn = Sb (**1.64**), Bi (**1.65**))[57] and subsequent reduction of **1.62** to $(Dipp_2Im{\cdot}As)_2$ (**1.68**).[3f]

Similarly, starting from $(B(C_5F_5)_3)$–^{a}Dipp$_2$ImLi(toluene) and $PnCl_3$ (Pn = As, Sb), Tamm *et al.* synthesized $(B(C_5F_5)_3)$–^{a}Dipp$_2$Im·$PnCl_2$ (Pn = As (**1.69a**), Sb (**1.69b**), Bi (**1.69c**)) *via* salt metathesis and subsequently reduced these adducts with KC_8 to the NHC-stabilized dipnictenes $[(B(C_5F_5)_3)$–^{a}Dipp$_2$Im)·Pn]$_2$ (**1.70a–c**).[60] By reacting the phosphinidene Dipp$_2$Im·PTMS with **1.69a** and Mes$_2$Im·$AsCl_3$ (**1.70**), $(B(C_5F_5)_3)$–^{a}Dipp$_2$Im·AsCl–P·Dipp$_2$Im (**1.71**), and Mes$_2$Im–AsCl–P·Dipp$_2$Im (**1.72**), were obtained, which were further reduced with bis(trimethylsilyl)-1,4-dihydropyrazine to give the neutral radical $[(B(C_5F_5)_3)$–^{a}Dipp$_2$Im–AsP·Dipp$_2$Im]$^{\cdot}$ (**1.73**) and Mes$_2$Im·As–P·Dipp$_2$Im (**1.74**), respectively.[61] Bockfeldt *et al.* modified this route to obtain the analogous As–N compound. The compound Dipp$_2$Im·NTMS was directly reacted with $AsCl_3$ to give Dipp$_2$Im·N($AsCl_2$), which was subsequently treated with Mes$_2$Im to afford the salt [Mes$_2$Im·AsClN·Dipp$_2$Im]$^+$[Cl]$^-$ (**1.75**) which was finally reduced with KC_8 to yield Mes$_2$Im·AsN·Dipp$_2$Im (**1.76**).[62] Furthermore, NHC-stabilized arsenic salts could be obtained. For instance, Acarazo's group reacted Mes$_2$Im with Ph_2AsI, which led to the imidazolium arsine [Mes$_2$Im–$AsPh_2$]$^+$[I]$^-$ (**1.77**).[63] In the group of Weigand, the reaction of [NHC–TMS]$^+$[OTf]$^-$ with $PnCl_3$ led to the corresponding compounds [NHC–$PnCl_2$]$^+$[OTf]$^-$ (NHC = *i*Pr$_2$Im^{Me}; Pn = As (**1.78a**), Sb (**1.78b**); NHC = Dipp$_2$Im; Pn = As (**1.79**)). In the case of the arsenic compounds **1.78a** and **1.79**, the chlorine substituents can subsequently be exchanged with TMSCN or $TMSN_3$ with loss of TMSCl, forming [NHC–AsX_2]$^+$[OTf]$^-$ (NHC = *i*Pr$_2$Im^{Me}; X = CN^- (**1.80a**), N_3^- (**1.80b**); NHC = Dipp$_2$Im; X = CN^- (**1.81a**), N_3^- (**1.81b**)).[7h]

In contrast to NHC-stabilized arsine compounds, only a few examples for the corresponding compounds with cAACs have been described. For example, the arsine trichloride adduct **1.66b** was reduced with tetrakis(dimethylamino)ethylene (TDAE) or KC_8 to afford cAAC^{Et}·AsCl (**1.82**) which was further reacted with another equivalent of cAAC^{Et} to give the salt [cAAC$^{Et}_2$·As]$^+$[Cl]$^-$ (**1.83**, Scheme 1.11). Subsequent reduction of [cAAC$^{Et}_2$·As]$^+$[Cl]$^-$ with one equivalent of KC_8 led to the formation of the neutral bis-cAAC^{Et}-stabilized diarsene allotrope (cAAC^{Et}·As)$_2$ (**1.84**, Scheme 1.11).[58a]

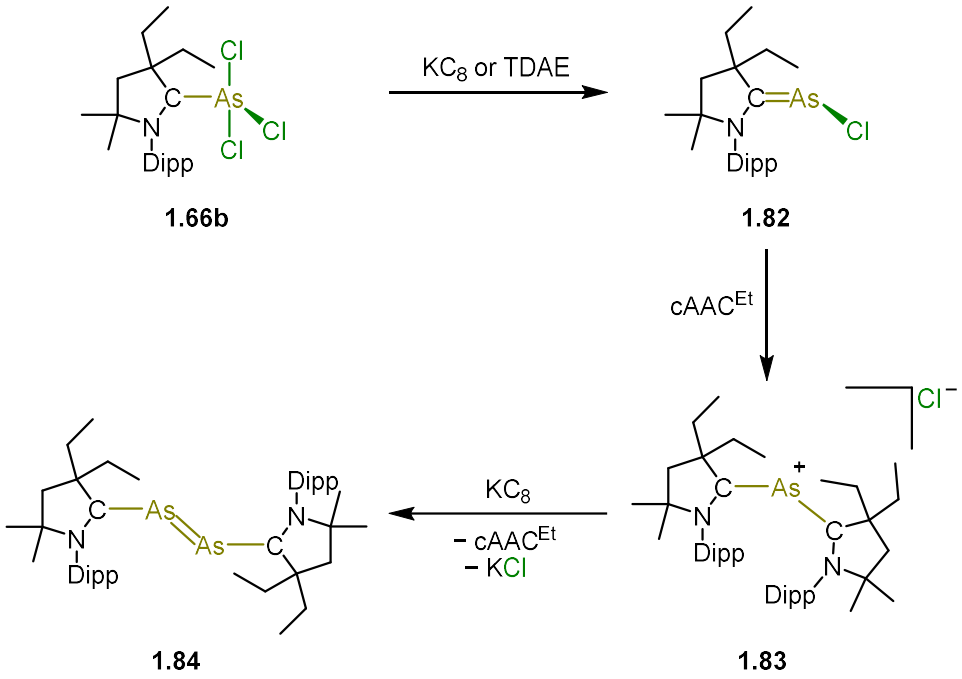

1.66b **1.82** **1.83** **1.84**

Scheme 1.11 Reduction of cAAC^{Et}·AsCl$_3$ (**1.66b**) to cAAC^{Et}·AsCl (**1.82**). Reaction of **1.82** with cAAC^{Et} to form [cAAC$^{Et}_2$·As]$^+$[Cl]$^-$ (**1.83**) and subsequent reduction to (cAAC^{Et}·As)$_2$ (**1.84**).[58a]

Moreover, the cAAC-stabilized compounds Dipp$_2$Im=CPhAs·cAAC$^{Me/Cy}$ (**1.85a–b**) were obtained by the reaction of Dipp$_2$Im=CPh(AsCl$_2$) with cAAC^{Me} (**a**) and cAAC^{Cy} (**b**) and *in situ* reduction with magnesium, respectively.[64] Recently, Schulz *et al.* reported the synthesis of the L(Cl)Ga-substituted pnictinidenes cAAC^{Me}·PnGa(Cl)L (Pn = As (**1.86a**), Sb (**1.86b**), Bi (**1.86c**); L = HC[C(Me)NDipp]$_2$) which were synthesized by different routes depending on the pnictinidene chloride used. While for arsenic the corresponding precursor cAAC^{Me}·AsCl (**1.87**) could be isolated from the reduction of **1.66a**, for Pn = Sb the reduction from **1.67b** to cAAC^{Me}·SbCl (**1.88**) had to be carried out *in situ* (Scheme 1.12). The resulting pnictinidenes **1.87** and **1.88** were further treated with LGa to give cAAC^{Me}·PnGa(Cl)L (E = As (**1.89a**), Sb (**1.89b**), Scheme 1.12). For bismuth, the reaction conditions had to be adjusted and cAAC^{Me}·BiGa(Cl)L (**1.89c**) was obtained starting from cAAC^{Me}·BiCl$_3$ (**1.90**) and two equivalents of LGa. One equivalent of LGa was used as reducing agent giving LGaCl$_2$ (Scheme 1.12).[58b]

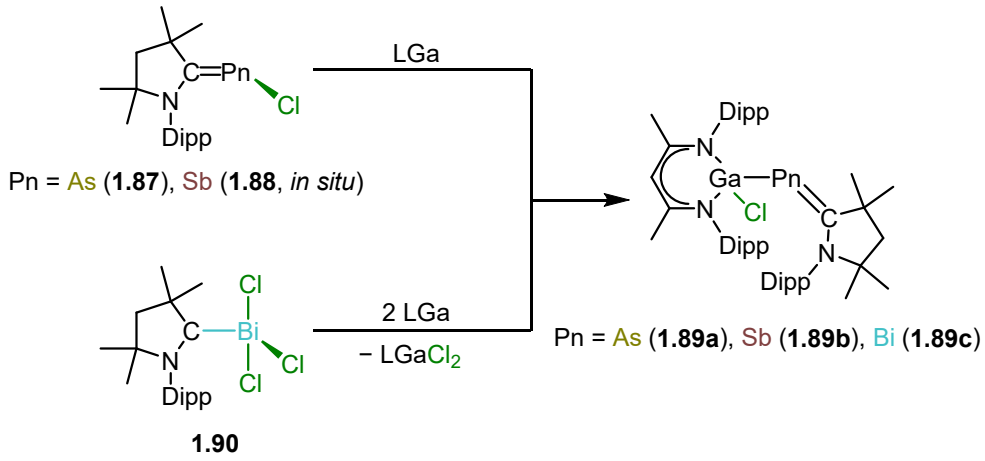

Scheme 1.12 Reaction of cAAC^{Me}·AsCl (**1.87**), the *in situ* formed cAAC^{Me}·SbCl (**1.88**) and cAAC^{Me}·BiCl$_3$ (**1.90**) with LGa to afford cAAC^{Me}·PnGa(Cl)L (E = As (**1.89a**), Sb (**1.89b**), Bi (**1.89c**)).[58b]

Subsequently, Schulz *et al.* succeeded in preparing the corresponding radical cations [cAAC^{Me}·PnGa(Cl)L]$^{\bullet+}$ (**1.90a–c**) with a [B(C$_6$F$_5$)$_4$]$^-$ counteranion in good yields by reacting **1.89a–c** with [FeCp$_2$]$^+$[B(C$_6$F$_5$)$_4$]$^-$.[65] As observed for the lighter homologue arsenic, NHC or cAAC adducts of the corresponding antimony and bismuth halides serve as ideal starting points for follow-up chemistry. Beside the abovementioned adducts **1.63–1.65** and **1.67a–b**, the fluoride substituted derivative Dipp$_2$Im·SbF$_3$ (**1.91**)[66] and even a six-membered NHC-stabilized adduct 6-Dipp$_2$Im·SbCl$_3$ (6-Dipp$_2$Im = 1,3-bis(2,6-di-*iso*-propylphenyl)-4,5,6-hexahydropyrimidin-2-yliden)[67] were reported. For the compounds **1.91** and **1.64–1.65**, thermally induced isomerization was observed, affording [(^{a}Dipp$_2$Im)(Dipp$_2$Im)SbF$_2$]$^+$[SbF$_4$]$^-$ (**1.92**) and ^{a}Dipp$_2$Im·EBr$_3$ (E = Sb (**1.93a**), Bi (**1.93b**)), respectively.[57, 66] In addition, with AlBr$_3$ and [Na]$^+$[B(3,5-(CF$_3$)$_2$C$_6$H$_3$)$_4$]$^-$ ([Na]$^+$[BAr^F$_4$]$^-$) as halide acceptors, halide abstraction from **1.64–1.65** and **1.93a–b** was observed, yielding the salts [Dipp$_2$Im·PnBr$_2$]$^+$[AlBr$_4$]$^-$ (**1.94a–b**) and [^{a}Dipp$_2$Im·PnBr$_2$]$^+$[BAr^F$_4$]$^-$ (**1.95a–b**), respectively.[57] Benjamin and co-workers extended the number of compounds with [NHC–SbX$_2$]$^+$ moieties by the isolation of the η^3-Cp* coordinated salt [Mes$_2$Im·SbCp*F]$^+$[B(C$_6$F$_5$)$_4$]$^-$ (**1.96**).[68] Antimony(III) halides also represent interesting entry points into the chemistry of subvalent antimony compounds, as was demonstrated by the synthesis of the Sb(II) radical (cAAC^{Cy})·SbCl$_2^{\bullet}$ (**1.97**) which was obtained by the reduction of **1.67b** with one equivalent of KC$_8$. In contrast, reduction with two equivalents of KC$_8$ led to the formation of the cAAC-stabilized stibinidene (cAAC^{Cy})·SbCl (**1.98**), and reduction

with three equivalents of KC_8 yielded the stibaalkene dimer $(cAAC^{Cy}{\cdot}Sb)_2$ (**1.99**).[59] The first aryl-substituted carbene-stabilized stibinidene $(DAC^{Mes})\cdot SbPh$ (**1.100**) was prepared by the reduction of $DAC^{Mes}\cdot SbCl_2Ph$ (**1.101**) with magnesium.[69] Moreover, it was previously reported that the reduction of PnX_3 (Pn = Sb, Bi; X = F, Cl) with KC_8 in the presence of $cAAC^{Me}$ and LiOTf (LiOTf = $LiCF_3SO_3$) in a molar ratio of 1:2:2:2 gave $[(cAAC^{Me})_2Pn]^+[OTf]^-$ (Pn = Sb (**1.102a**), Bi (**1.102b**)) with a cAAC-stabilized Pn(I) cation.[70]

Furthermore, the group of Gilliard reported pioneering work in the field of NHC and cAAC mediated bismuth compounds by reacting the carbenes L (L = $cAAC^{Et}$ (**a**), $cAAC^{Cy}$ (**b**),[71] iPr_2Im^{Me} (**c**)[72]) with $BiCl_2Ph$, which led to the adducts $L\cdot BiCl_2Ph$ (**1.103a–c**, Scheme 1.13). Upon reaction of $BiCl_2Ph$ with the unsaturated $Dipp_2Im$, the adduct $Dipp_2Im\cdot BiCl_2Ph$ (**1.103d**, Scheme 1.13) can also be isolated, but isomerizes within two weeks in solution at –37 °C to yield the abnormally coordinated compound $^aDipp_2Im\cdot BiCl_2Ph$ (**1.104**).[71]

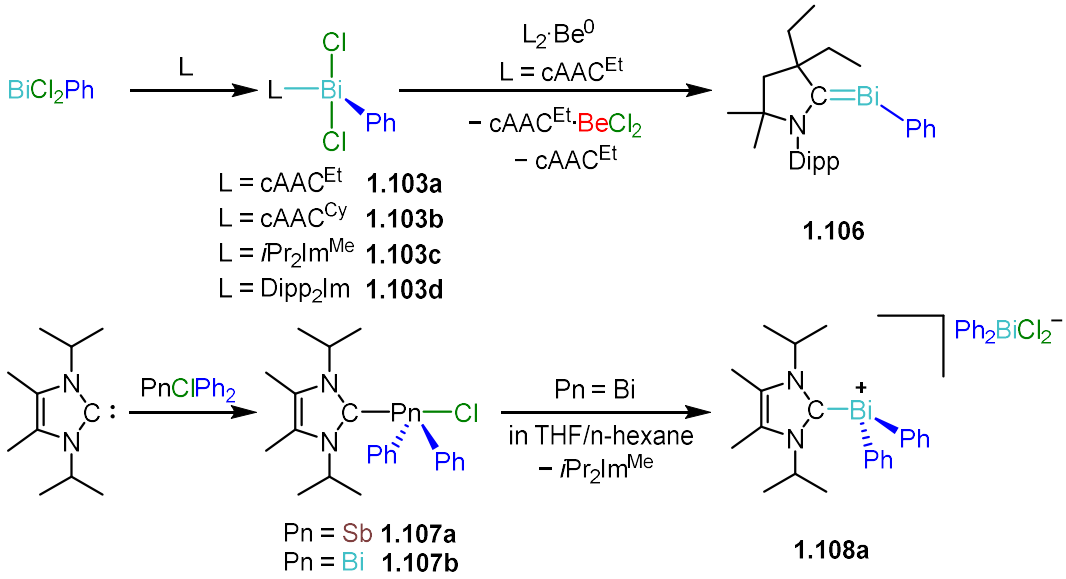

Scheme 1.13 Synthesis of $L\cdot BiCl_2Ph$ (L = $cAAC^{Et}$ (**1.103a**), $cAAC^{Cy}$ (**1.103b**),[71] iPr_2Im^{Me} (**1.103c**)[72], $Dipp_2Im$ (**1.103d**))[71] and reaction of **1.103a** with $cAAC^{Et}{}_2{\cdot}Be$ to form $cAAC^{Et}{\cdot}BiPh$ (**1.106**).[73] Synthesis of $iPr_2Im^{Me}{\cdot}SbClPh_2$ (**1.107a**) and $iPr_2Im^{Me}{\cdot}BiClPh_2$ (**1.107b**)[74] and decomposition of **1.107b** forming $[iPr_2Im^{Me}{\cdot}BiPh_2]^+[Ph_2BiCl_2]^-$ (**1.108a**).[72]

In contrast, for the reaction with ^{s}Dipp$_2$Im, the additional coordination of one THF molecule was observed, yielding ^{s}Dipp$_2$Im·BiCl$_2$Ph·THF (**1.105**).[71] Furthermore, the aforementioned cAAC adducts **1.103a−b** were considered as starting points for the synthesis of the corresponding bismuthinidenes. Since this approach was unsuccessfull, Gillard *et al.* reacted **1.103a** with the beryllium(0) reagent cAAC$^{Et}_2$Be, affording cAAC^{Et}·BeCl$_2$ and free cAAC^{Et} as well as the desired bismuthinidene cAAC^{Et}·BiPh (**1.106**, Scheme 1.13) in low yield. Quantum chemical calculations revealed partial π-bonding and a free electron pair with p-character at Bi, for the HOMO, respectively.[73] Moreover, the reaction of free *i*Pr$_2$Im^{Me} and PnClPh$_2$ led to the corresponding adducts *i*Pr$_2$Im^{Me}·PnClPh$_2$ (Pn = Sb (**1.107a**), Bi (**1.107b**); Scheme 1.13) in solution, which revealed chloride bridged dimeric structures in the solid-state.[74] The same was observed for the analogous mono phenyl substituted compound **1.103c**. Moreover, a THF solution of compound **1.107b** shows chloride abstraction and concomitant formation of free *i*Pr$_2$Im^{Me} to afford the salt [*i*Pr$_2$Im^{Me}·BiPh$_2$]$^+$[Ph$_2$BiCl$_2$]$^-$ (**1.108a**, Scheme 1.13). The reaction of sterically more demanding carbenes L with Ph$_2$BiCl led to the related compounds [L·BiPh$_2$]$^+$[Ph$_2$BiCl$_2$]$^-$ (L = ^{s}Dipp$_2$Im (**1.108b**), cAAC^{Et} (**1.108c**)), respectively.[72]

In this work, investigations about the reactivity of NHCs and cAACs towards various germanium, tin, lead as well as antimony halides are presented. In addition, the reduction of corresponding adducts to subvalent NHC- and cAAC-stabilized germylenes (L·GeR$_2$), stannylenes (L·SnR$_2$), plumbylenes (L·PbR$_2$) and stibinidenes (L·SbR) is reported in the Chapters II and IV−VI. Furthermore, studies about the reactivity of germanium and tin hydride compounds towards various NHCs and cAAC^{Me} are presented in Chapter III.

1.4 References

[1] A. J. Arduengo, R. L. Harlow, M. Kline, *J. Am. Chem. Soc.* **1991**, *113*, 361-363.

[2] V. Lavallo, Y. Canac, C. Prasang, B. Donnadieu, G. Bertrand, *Angew. Chem. Int. Ed.* **2005**, *44*, 5705-5709; *Angew. Chem.* **2005**, *117*, 5851-5855.

[3] a) W. A. Herrmann, C. Köcher, *Angew. Chem. Int. Ed.* **1997**, *36*, 2162-2187; *Angew. Chem.* **1997**, *109*, 2256-2282; b) P. P. Power, *Chem. Rev.* **1999**, *99*, 3463-3504; c) D. Bourissou, O. Guerret, F. P. Gabbai, G. Bertrand, *Chem. Rev.* **2000**, *100*, 39-92; d) F. E. Hahn, M. C. Jahnke, *Angew. Chem. Int. Ed.* **2008**, *47*, 3122-3172; *Angew. Chem.* **2008**, *120*, 3166-3216; e) T. Dröge, F. Glorius, *Angew. Chem. Int. Ed.* **2010**, *49*, 6940-6952; *Angew. Chem.* **2010**, *122*, 7094-7107; f) Y. Wang, G. H. Robinson, *Inorg. Chem.* **2011**, *50*, 12326-12337; g) M. N. Hopkinson, C. Richter, M. Schedler, F. Glorius, *Nat. Chem.* **2014**, *510*, 485-496; h) Y. Wang, G. H. Robinson, *Inorg. Chem.* **2014**, *53*, 11815-11832; i) S. Würtemberger-Pietsch, U. Radius, T. B. Marder, *Dalton Trans.* **2016**, *45*, 5880-5895; j) V. Nesterov, D. Reiter, P. Bag, P. Frisch, R. Holzner, A. Porzelt, S. Inoue, *Chem. Rev.* **2018**, *118*, 9678-9842; k) A. Doddi, M. Peters, M. Tamm, *Chem. Rev.* **2019**, *119*, 6994-7112.

[4] a) M. Melaimi, M. Soleilhavoup, G. Bertrand, *Angew. Chem. Int. Ed.* **2010**, *49*, 8810-8849; *Angew. Chem.* **2010**, *122*, 8992-9032; b) M. Soleilhavoup, G. Bertrand, *Acc. Chem. Res.* **2015**, *48*, 256-266; c) M. Melaimi, R. Jazzar, M. Soleilhavoup, G. Bertrand, *Angew. Chem. Int. Ed.* **2017**, *56*, 10046-10068; *Angew. Chem.* **2017**, *129*, 10180-10203; d) U. S. Paul, U. Radius, *Chem. Eur. J.* **2017**, *23*, 3993-4009; e) U. S. D. Paul, M. J. Krahfuß, U. Radius, *Chemie unserer Zeit* **2019**, *53*, 212-223.

[5] a) R. Dorta, E. D. Stevens, N. M. Scott, C. Costabile, L. Cavallo, C. D. Hoff, S. P. Nolan, *J. Am. Chem. Soc.* **2005**, *127*, 2485-2495; b) S. Diez-Gonzalez, S. P. Nolan, *Coord. Chem. Rev.* **2007**, *251*, 874-883; c) A. Poater, B. Cosenza, A. Correa, S. Giudice, F. Ragone, V. Scarano, L. Cavallo, *Eur. J. Inorg. Chem.* **2009**, 1759-1766; d) H. Clavier, S. P. Nolan, *Chem. Commun.* **2010**, *46*, 841-861; e) C. Lujan, S. P. Nolan, *J. Organomet. Chem.* **2011**, *696*, 3935-3938; f) O. Back, M. Henry-Ellinger, C. D. Martin, D. Martin, G. Bertrand, *Angew.*

Chem. Int. Ed. **2013**, *52*, 2939-2943; *Angew. Chem.* **2013**, *125*, 3011-3015; g) A. Liske, K. Verlinden, H. Buhl, K. Schaper, C. Ganter, *Organometallics* **2013**, *32*, 5269-5272; h) D. J. Nelson, S. P. Nolan, *Chem. Soc. Rev.* **2013**, *42*, 6723-6753; i) K. Verlinden, H. Buhl, W. Frank, C. Ganter, *Eur. J. Inorg. Chem.* **2015**, 2416-2425; j) S. V. C. Vummaleti, D. J. Nelson, A. Poater, A. Gomez-Suarez, D. B. Cordes, A. M. Z. Slawin, S. P. Nolan, L. Cavallo, *Chem. Sci.* **2015**, *6*, 1895-1904; k) K. C. Mondal, S. Roy, B. Maity, D. Koley, H. W. Roesky, *Inorg. Chem.* **2016**, *55*, 163-169; l) U. S. D. Paul, U. Radius, *Eur. J. Inorg. Chem.* **2017**, 3362-3375; m) H. V. Huynh, *Chem. Rev.* **2018**, *118*, 9457-9492; n) D. Munz, *Organometallics* **2018**, *37*, 275-289.

[6] a) C. J. Carmalt, A. H. Cowley, in *Adv. Inorg. Chem.* **2000**, *50*, 1-32; b) N. Kuhn, A. Al-Sheikh, *Coord. Chem. Rev.* **2005**, *249*, 829-857; c) G. Prabusankar, A. Sathyanarayana, P. Suresh, C. N. Babu, K. Srinivas, B. P. R. Metla, *Coord. Chem. Rev.* **2014**, *269*, 96-133; d) K. C. Mondal, S. Roy, H. W. Roesky, *Chem. Soc. Rev.* **2016**, *45*, 1080-1111.

[7] a) J. I. Bates, P. Kennepohl, D. P. Gates, *Angew. Chem. Int. Ed.* **2009**, *48*, 9844-9847; *Angew. Chem.* **2009**, *121*, 10028-10031; b) J. J. Weigand, K. O. Feldmann, F. D. Henne, *J. Am. Chem. Soc.* **2010**, *132*, 16321-16323; c) D. Mendoza-Espinosa, B. Donnadieu, G. Bertrand, *Chem. Asian J.* **2011**, *6*, 1099-1103; d) J. I. Bates, D. P. Gates, *Organometallics* **2012**, *31*, 4529-4536; e) F. D. Henne, E.-M. Schnöckelborg, K.-O. Feldmann, J. Grunenberg, R. Wolf, J. J. Weigand, *Organometallics* **2013**, *32*, 6674-6680; f) K. Schwedtmann, M. H. Holthausen, K. O. Feldmann, J. J. Weigand, *Angew. Chem. Int. Ed.* **2013**, *52*, 14204-14208; *Angew. Chem.* **2013**, *125*, 14454-14458; g) A. Doddi, D. Bockfeld, A. Nasr, T. Bannenberg, P. G. Jones, M. Tamm, *Chem. Eur. J.* **2015**, *21*, 16178-16189; h) F. D. Henne, A. T. Dickschat, F. Hennersdorf, K. O. Feldmann, J. J. Weigand, *Inorg. Chem.* **2015**, *54*, 6849-6861; i) A. Beil, R. J. Gilliard, Jr., H. Grützmacher, *Dalton Trans.* **2016**, *45*, 2044-2052; j) F. D. Henne, F. A. Watt, K. Schwedtmann, F. Hennersdorf, M. Kokoschka, J. J. Weigand, *Chem. Commun.* **2016**, *52*, 2023-2026; k) P. K. Majhi, K. C. Chow, T. H. Hsieh, E. G. Bowes, G. Schnakenburg, P. Kennepohl, R. Streubel, D. P. Gates, *Chem. Commun.* **2016**, *52*, 998-1001; l) K. Schwedtmann, R. Schoemaker, F. Hennersdorf, A. Bauza, A. Frontera, R.

Weiss, J. J. Weigand, *Dalton Trans.* **2016**, *45*, 11384-11396; m) L. Dostal, *Coord. Chem. Rev.* **2017**, *353*, 142-158; n) T. Krachko, M. Bispinghoff, A. M. Tondreau, D. Stein, M. Baker, A. W. Ehlers, J. C. Slootweg, H. Grützmacher, *Angew. Chem. Int. Ed.* **2017**, *56*, 7948-7951; *Angew. Chem.* **2017**, *129*, 8056-8059.

[8] C. Elschenbroich, *Organometallchemie*, Vol. 6 (C. Elschenbroich, F Hensel, H. Hopf), Vieweg+Teubner Verlag, Wiesbaden, Germany **2008**.

[9] H. Schneider, D. Schmidt, U. Radius, *Chem. Eur. J.* **2015**, *21*, 2793-2797.

[10] a) K. C. Mondal, H. W. Roesky, M. C. Schwarzer, G. Frenking, B. Niepötter, H. Wolf, R. Herbst-Irmer, D. Stalke, *Angew. Chem. Int. Ed.* **2013**, *52*, 2963-2967; *Angew. Chem.* **2013**, *125*, 3036-3040; b) K. C. Mondal, P. P. Samuel, M. Tretiakov, A. P. Singh, H. W. Roesky, A. C. Stückl, B. Niepötter, E. Carl, H. Wolf, R. Herbst-Irmer, D. Stalke, *Inorg. Chem.* **2013**, *52*, 4736-4743.

[11] Y. Wang, Y. Xie, P. Wei, R. B. King, H. F. Schaefer III, R. P. v. Schleyer, G. H. Robinson, *Science* **2008**, *321*, 1069-1071.

[12] a) K. C. Mondal, P. P. Samuel, H. W. Roesky, R. R. Aysin, L. A. Leites, S. Neudeck, J. Lübben, B. Dittrich, N. Holzmann, M. Hermann, G. Frenking, *J. Am. Chem. Soc.* **2014**, *136*, 8919-8922; b) K. C. Mondal, S. Roy, B. Dittrich, B. Maity, S. Dutta, D. Koley, S. K. Vasa, R. Linser, S. Dechert, H. W. Roesky, *Chem. Sci.* **2015**, *6*, 5230-5234.

[13] K. C. Mondal, S. Roy, B. Dittrich, D. M. Andrada, G. Frenking, H. W. Roesky, *Angew. Chem. Int. Ed.* **2016**, *55*, 3158-3161; *Angew. Chem.* **2016**, *128*, 3210.

[14] a) N. Kuhn, T. Kratz, D. Bläser, R. Boese, *Chem. Ber.* **1995**, *128*, 245-250; b) R. S. Ghadwal, H. W. Roesky, S. Merkel, J. Henn, D. Stalke, *Angew. Chem. Int. Ed.* **2009**, *48*, 5683-5686; *Angew. Chem.* **2009**, *121*, 5793-5796; c) T. Böttcher, B. S. Bassil, L. Zhechkov, T. Heine, G.-V. Röschenthaler, *Chem. Sci.* **2013**, *4*, 77-83; d) T. Böttcher, S. Steinhauer, B. Neumann, H. G. Stammler, G. V. Röschenthaler, B. Hoge, *Chem. Commun.* **2014**, *50*, 6204-6206; e) F. Uhlemann, R. Köppe, A. Schnepf, *Z. Anorg. Allg. Chem.* **2014**, *640*, 1658-1664; f) F. Uhlemann, A. Schnepf, *Chem. Eur. J.* **2016**, *22*, 10748-10753.

[15] K. C. Mondal, H. W. Roesky, A. C. Stückl, F. Ehret, W. Kaim, B. Dittrich, B. Maity, D. Koley, *Angew. Chem. Int. Ed.* **2013**, *52*, 11804-11807; *Angew. Chem.* **2013**, *125*, 12020-12023.

[16] a) P. A. Rupar, M. C. Jennings, K. M. Baines, *Organometallics* **2008**, *27*, 5043-5051; b) A. J. Ruddy, P. A. Rupar, K. J. Bladek, C. J. Allan, J. C. Avery, K. M. Baines, *Organometallics* **2010**, *29*, 1362-1367; c) N. Katir, D. Matioszek, S. Ladeira, J. Escudie, A. Castel, *Angew. Chem. Int. Ed.* **2011**, *50*, 5352-5355; *Angew. Chem.* **2011**, *123*, 5464-5467.

[17] a) P. A. Rupar, V. N. Staroverov, P. J. Ragogna, K. M. Baines, *J. Am. Chem. Soc.* **2007**, *129*, 15138-15139; b) K. C. Thimer, S. M. Al-Rafia, M. J. Ferguson, R. McDonald, E. Rivard, *Chem. Commun.* **2009**, 7119-7121; c) A. C. Filippou, O. Chernov, B. Blom, K. W. Stumpf, G. Schnakenburg, *Chem. Eur. J.* **2010**, *16*, 2866-2872; d) Y. Li, K. C. Mondal, H. W. Roesky, H. Zhu, P. Stollberg, R. Herbst-Irmer, D. Stalke, D. M. Andrada, *J. Am. Chem. Soc.* **2013**, *135*, 12422-12428; e) B. Lyhs, D. Bläser, C. Wölper, S. Schulz, R. Haack, G. Jansen, *Inorg. Chem.* **2013**, *52*, 7236-7241.

[18] a) B. Bantu, G. M. Pawar, U. Decker, K. Wurst, A. M. Schmidt, M. R. Buchmeiser, *Chem. Eur. J.* **2009**, *15*, 3103-3109; b) A. P. Singh, P. P. Samuel, K. C. Mondal, H. W. Roesky, N. S. Sidhu, B. Dittrich, *Organometallics* **2013**, *32*, 354-357.

[19] a) N. Kuhn, C. Maichle-Mößmer, E. Niquet, I. Walker, *Z.Naturforsch. B* **2002**, *57*, 47-52; b) P. A. Rupar, V. N. Staroverov, K. M. Baines, *Organometallics* **2010**, *29*, 4871-4881; c) T. Böttcher, B. S. Bassil, G. V. Röschenthaler, *Inorg. Chem.* **2012**, *51*, 763-765; d) I. S. M. Al-Rafia, P. A. Lummis, A. K. Swarnakar, K. C. Deutsch, M. J. Ferguson, R. McDonald, E. Rivard, *Aust. J. Chem.* **2013**, *66*, 1235-1245; e) H. Schneider, M. J. Krahfuß, U. Radius, *Z. Anorg. Allg. Chem.* **2016**, *642*, 1282-1286; f) J. Sinclair, G. Dai, R. McDonald, M. J. Ferguson, A. Brown, E. Rivard, *Inorg. Chem.* **2020**, *59*, 10996-11008.

[20] D. Schmidt, J. H. J. Berthel, S. Pietsch, U. Radius, *Angew. Chem.* **2012**, *124*, 9011-9015.

[21] G. D. Frey, J. D. Masuda, B. Donnadieu, G. Bertrand, *Angew. Chem. Int. Ed.* **2010**, *49*, 9444-9447; *Angew. Chem.* **2010**,*122*, 9634-9637.

[22] S. M. Al-Rafia, M. R. Momeni, R. McDonald, M. J. Ferguson, A. Brown, E. Rivard, *Angew. Chem. Int. Ed.* **2013**, *52*, 6390-6395; *Angew. Chem.* **2013**, *125*, 6518-6523.

[23] S. M. Al-Rafia, A. C. Malcolm, S. K. Liew, M. J. Ferguson, E. Rivard, *J. Am. Chem. Soc.* **2011**, *133*, 777-779.

[24] S. M. Al-Rafia, A. C. Malcolm, S. K. Liew, M. J. Ferguson, R. McDonald, E. Rivard, *Chem. Commun.* **2011**, *47*, 6987-6989.

[25] M. Ackermann, M. Seidl, F. Wen, M. J. Ferguson, A. Y. Timoshkin, E. Rivard, M. Scheer, *Chem. Eur. J.* **2021**, e202103780.

[26] S. M. I. Al-Rafia, M. R. Momeni, M. J. Ferguson, R. McDonald, A. Brown, E. Rivard, *Organometallics* **2013**, *32*, 6658-6665.

[27] M. M. D. Roy, S. Fujimori, M. J. Ferguson, R. McDonald, N. Tokitoh, E. Rivard, *Chem. Eur. J.* **2018**, *24*, 14392-14399.

[28] K. Inomata, T. Watanabe, Y. Miyazaki, H. Tobita, *J. Am. Chem. Soc.* **2015**, *137*, 11935-11937.

[29] T. Fukuda, H. Hashimoto, H. Tobita, *J. Organomet. Chem.* **2017**, *848*, 89-94.

[30] Y. Xiong, T. Szilvasi, S. Yao, G. Tan, M. Driess, *J. Am. Chem. Soc.* **2014**, *136*, 11300-11303.

[31] R. J. Mangan, A. Rit, C. P. Sindlinger, R. Tirfoin, J. Campos, J. Hicks, K. E. Christensen, H. Niu, S. Aldridge, *Chem. Eur. J.* **2020**, *26*, 306-315.

[32] R. J. Mangan, A. R. Davies, J. Hicks, C. P. Sindlinger, A. L. Thompson, S. Aldridge, *Polyhedron* **2021**, *196*, 115006.

[33] J. A. Kelly, M. Juckel, T. J. Hadlington, I. Fernandez, G. Frenking, C. Jones, *Chem. Eur. J.* **2019**, *25*, 2773-2785.

[34] M. Auer, F. Diab, K. Eichele, H. Schubert, L. Wesemann, *Dalton Trans.* **2022**, *51*, 5950-5961.

[35] J. J. Maudrich, C. P. Sindlinger, F. S. Aicher, K. Eichele, H. Schubert, L. Wesemann, *Chem. Eur. J.* **2017**, *23*, 2192-2200.

[36] C. P. Sindlinger, L. Wesemann, *Chem. Sci.* **2014**, *5*, 2739-2746.

[37] C. P. Sindlinger, S. Weiss, H. Schubert, L. Wesemann, *Angew. Chem. Int. Ed.* **2015**, *54*, 4087-4091; *Angew. Chem.* **2015**, *127*, 4160-4164.

[38] C. P. Sindlinger, L. Wesemann, *Chem. Commun.* **2015**, *51*, 11421-11424.

[39] C. P. Sindlinger, W. Grahneis, F. S. Aicher, L. Wesemann, *Chem. Eur. J.* **2016**, *22*, 7554-7566.

[40] F. Stabenow, W. Saak, M. Weidenbruch, *Chem. Commun.* **1999**, 1131-1132.

[41] J. Schneider, C. P. Sindlinger, K. Eichele, H. Schubert, L. Wesemann, *J. Am. Chem. Soc.* **2017**, *139*, 6542-6545.

[42] B. Gehrhus, P. B. Hitchcock, M. F. Lappert, *J. Chem. Soc., Dalton Trans.* **2000**, 3094-3099.

[43] a) R. Guthardt, J. Oetzel, J. I. Schweizer, C. Bruhn, R. Langer, M. Maurer, J. Vicha, P. Shestakova, M. C. Holthausen, U. Siemeling, *Angew. Chem. Int. Ed.* **2019**, *58*, 1387-1391; *Angew. Chem.* **2019**, *131*, 1401-1405; b) R. Guthardt, C. Bruhn, U. Siemeling, *Polyhedron* **2021**, *194*, 114959.

[44] D. Kargin, Z. Kelemen, K. Krekic, L. Nyulaszi, R. Pietschnig, *Chem. Eur. J.* **2018**, *24*, 16774-16778.

[45] C. Jones, A. Sidiropoulos, N. Holzmann, G. Frenking, A. Stasch, *Chem. Commun.* **2012**, *48*, 9855-9857.

[46] J. Messelberger, P. Pinter, F. W. Heinemann, D. Munz, *Mendeleev Commun.* **2021**, *31*, 471-474.

[47] a) L. Wirtz, M. Jourdain, V. Huch, M. Zimmer, A. Schafer, *ACS Omega* **2019**, *4*, 18355-18360; b) L. Wirtz, W. Haider, V. Huch, M. Zimmer, A. Schafer, *Chem. Eur. J.* **2020**, *26*, 6176-6184.

[48] J. B. Waters, L. S. Tucker, J. M. Goicoechea, *Organometallics* **2018**, *37*, 655-664.

[49] a) J. D. Masuda, W. W. Schoeller, B. Donnadieu, G. Bertrand, *Angew. Chem. Int. Ed*. **2007**, *46*, 7052-7055; *Angew. Chem.* **2007**, *119*, 7182-7185; b) J. D. Masuda, W. W. Schoeller, B. Donnadieu, G. Bertrand, *J. Am. Chem. Soc.* **2007**, *129*, 14180-14181; c) Y. Wang, Y. Xie, P. Wei, R. B. King, H. F. Schaefer III, P. v. R. Schleyer, G. H. Robinson, *J. Am. Chem. Soc.* **2008**, *130*, 14970-14971; d) O. Back, G. Kuchenbeiser, B. Donnadieu, G. Bertrand, *Angew. Chem. Int. Ed.* **2009**, *48*, 5530-5533; *Angew. Chem.* **2009**, *121*, 5638-5641; e) O. Back, B. Donnadieu, P. Parameswaran, G. Frenking, G. Bertrand, *Nat. Chem.* **2010**, *2*, 369-373; f) Y. Wang, Y. Xie, M. Y. Abraham, R. J. Gilliard, P. Wei, H. F. Schaefer III, P. v. R. Schleyer, G. H. Robinson, *Organometallics* **2010**, *29*, 4778-4780; g) C. L. Dorsey, B. M. Squires, T. W. Hudnall, *Angew. Chem. Int. Ed.* **2013**, *52*, 4462-4465; *Angew. Chem.* **2013**, *125*, 4558-4561; h) M. H. Holthausen, S. K. Surmiak, P. Jerabek, G. Frenking, J. J. Weigand, *Angew. Chem. Int. Ed.* **2013**, *52*, 11078-11082; *Angew. Chem.* **2013**, 125,

11284-11288; i) C. D. Martin, C. M. Weinstein, C. E. Moore, A. L. Rheingold, G. Bertrand, *Chem. Commun.* **2013**, *49*, 4486-4488; j) M. H. Holthausen, J. J. Weigand, *Chem. Soc. Rev.* **2014**, *43*, 6639-6657; k) J. B. Waters, T. A. Everitt, W. K. Myers, J. M. Goicoechea, *Chem. Sci.* **2016**, *7*, 6981-6987; l) J. E. Borger, A. W. Ehlers, J. C. Slootweg, K. Lammertsma, *Chem. Eur. J.* **2017**, *23*, 11738-11746; m) A. Doddi, D. Bockfeld, M. K. Zaretzke, C. Kleeberg, T. Bannenberg, M. Tamm, *Dalton Trans.* **2017**, *46*, 15859-15864; n) N. Hayakawa, K. Sadamori, S. Tsujimoto, M. Hatanaka, T. Wakabayashi, T. Matsuo, *Angew. Chem. Int. Ed.* **2017**, *56*, 5765-5769; *Angew. Chem.* **2017**, 129, 5859-5863; o) K. Schwedtmann, G. Zanoni, J. J. Weigand, *Chem. Asian J.* **2018**, *13*, 1388-1405.

[50] a) A. J. Arduengo III, J. C. Calabrese, A. H. Cowley, H. V. Dias, J. R. Goerlich, W. J. Marshall, B. Riegel, *Inorg. Chem.* **1997**, *36*, 2151-2158; b) I. I. I. A. J. Arduengo, H. V. R. Dias, J. C. Calabrese, *Chem. Lett.* **1997**, *26*, 143-144; c) B. D. Ellis, C. A. Dyker, A. Decken, C. L. Macdonald, *Chem. Commun.* **2005**, 1965-1967; d) A. Doddi, D. Bockfeld, T. Bannenberg, P. G. Jones, M. Tamm, *Angew. Chem. Int. Ed.* **2014**, *53*, 13568-13572; *Angew. Chem.* **2014**, *126*, 13786-13790; e) R. R. Rodrigues, C. L. Dorsey, C. A. Arceneaux, T. W. Hudnall, *Chem. Commun.* **2014**, *50*, 162-164; f) M. Bispinghoff, H. Grützmacher, *Chimia (Aarau)* **2016**, *70*, 279-283; g) M. Bispinghoff, A. M. Tondreau, H. Grützmacher, C. A. Faradji, P. G. Pringle, *Dalton Trans.* **2016**, *45*, 5999-6003; h) D. Bockfeld, A. Doddi, P. G. Jones, M. Tamm, *Eur. J. Inorg. Chem.* **2016**, 3704-3712; i) S. Roy, K. C. Mondal, S. Kundu, B. Li, C. J. Schurmann, S. Dutta, D. Koley, R. Herbst-Irmer, D. Stalke, H. W. Roesky, *Chem. Eur. J.* **2017**, *23*, 12153-12157; j) T. Krachko, J. C. Slootweg, *Eur. J. Inorg. Chem.* **2018**, 2734-2754; k) L. Werner, G. Horrer, M. Philipp, K. Lubitz, M. W. Kuntze-Fechner, U. Radius, *Z. Anorg. Allg. Chem.* **2021**, *647*, 881-895.

[51] a) F. E. Hahn, D. Le Van, M. C. Moyes, T. v. Fehren, R. Fröhlich, E. U. Würthwein, *Angew. Chem. Int. Ed.* **2001**, *40*, 3144-3148; *Angew. Chem.* **2001**, *113*, 3241-3244; b) D. Heift, Z. Benko, H. Grützmacher, *Dalton Trans.* **2014**, *43*, 5920-5928; c) M. Cicac-Hudi, J. Bender, S. H. Schlindwein, M. Bispinghoff, M. Nieger, H. Grützmacher, D. Gudat, *Eur. J. Inorg. Chem.* **2016**, 649-658; d)

Z. Li, X. Chen, Y. Li, C. Y. Su, H. Grützmacher, *Chem. Commun.* **2016**, *52*, 11343-11346.

[52] A. K. Adhikari, T. Grell, P. Lönnecke, E. Hey-Hawkins, *Eur. J. Inorg. Chem.* **2015**, 620-622.

[53] H. Schneider, D. Schmidt, U. Radius, *Chem. Commun.* **2015**, *51*, 10138-10141.

[54] A. Schumann, J. Bresien, M. Fischer, C. Hering-Junghans, *Chem. Commun.* **2021**, *57*, 1014-1017.

[55] A. Doddi, M. Weinhart, A. Hinz, D. Bockfeld, J. M. Goicoechea, M. Scheer, M. Tamm, *Chem. Commun.* **2017**, *53*, 6069-6072.

[56] A. Aprile, R. Corbo, K. Vin Tan, D. J. Wilson, J. L. Dutton, *Dalton Trans.* **2014**, *43*, 764-768.

[57] J. B. Waters, Q. Chen, T. A. Everitt, J. M. Goicoechea, *Dalton Trans.* **2017**, *46*, 12053-12066.

[58] a) K. M. Melancon, M. B. Gildner, T. W. Hudnall, *Chem. Eur. J.* **2018**, *24*, 9264-9268; b) J. Krüger, C. Wölper, G. Haberhauer, S. Schulz, *Inorg. Chem.* **2022**, *61*, 597-604.

[59] R. Kretschmer, D. A. Ruiz, C. E. Moore, A. L. Rheingold, G. Bertrand, *Angew. Chem. Int. Ed.* **2014**, *53*, 8176-8179; *Angew. Chem.* **2014**, *126*, 8315-8318.

[60] L. P. Ho, A. Nasr, P. G. Jones, A. Altun, F. Neese, G. Bistoni, M. Tamm, *Chem. Eur. J.* **2018**, *24*, 18922-18932.

[61] a) A. Doddi, D. Bockfeld, M. K. Zaretzke, T. Bannenberg, M. Tamm, *Chem. Eur. J.* **2019**, *25*, 13119-13123; b) L. P. Ho, M. K. Zaretzke, T. Bannenberg, M. Tamm, *Chem. Commun.* **2019**, *55*, 10709-10712.

[62] D. Bockfeld, M. Tamm, *Z. Anorg. Allg. Chem.* **2020**, *646*, 866-872.

[63] J. W. Dube, Y. Zheng, W. Thiel, M. Alcarazo, *J. Am. Chem. Soc.* **2016**, *138*, 6869-6877.

[64] M. K. Sharma, S. Blomeyer, B. Neumann, H. G. Stammler, A. Hinz, M. van Gastel, R. S. Ghadwal, *Chem. Commun.* **2020**, *56*, 3575-3578.

[65] J. Krüger, J. Haak, C. Wölper, G. E. Cutsail III, G. Haberhauer, S. Schulz, *Inorg. Chem.* **2022**, *61*, 5878-5884.

[66] B. Alič, A. Štefančič, G. Tavčar, *Dalton Trans.* **2017**, *46*, 3338-3346.

[67] A. Sidiropoulos, B. Osborne, A. N. Simonov, D. Dange, A. M. Bond, A. Stasch, C. Jones, *Dalton Trans.* **2014**, *43*, 14858-14864.

[68] O. Coughlin, T. Krämer, S. L. Benjamin, *Dalton Trans.* **2020**, *49*, 1726-1730.

[69] C. L. Dorsey, R. M. Mushinski, T. W. Hudnall, *Chem. Eur. J.* **2014**, *20*, 8914-8917.

[70] M. M. Siddiqui, S. K. Sarkar, M. Nazish, M. Morganti, C. Kohler, J. Cai, L. Zhao, R. Herbst-Irmer, D. Stalke, G. Frenking, H. W. Roesky, *J. Am. Chem. Soc.* **2021**, *143*, 1301-1306.

[71] G. Wang, L. A. Freeman, D. A. Dickie, R. Mokrai, Z. Benko, R. J. Gilliard, Jr., *Inorg. Chem.* **2018**, *57*, 11687-11695.

[72] J. E. Walley, L. S. Warring, G. Wang, D. A. Dickie, S. Pan, G. Frenking, R. J. Gilliard, Jr., *Angew. Chem. Int. Ed.* **2021**, *60*, 6682-6690; *Angew. Chem.* **2021**, *133*, 6756-6764.

[73] G. Wang, L. A. Freeman, D. A. Dickie, R. Mokrai, Z. Benko, R. J. Gilliard, Jr., *Chem. Eur. J.* **2019**, *25*, 4335-4339.

[74] J. E. Walley, L. S. Warring, E. Kertesz, G. Wang, D. A. Dickie, Z. Benko, R. J. Gilliard, Jr., *Inorg. Chem.* **2021**, *60*, 4733-4743.

Chapter II

N-Heterocyclic Carbene and Cyclic (Alkyl)(amino)carbene Adducts of Germanium(IV) and Tin(IV) Chlorides and Organyl Chlorides

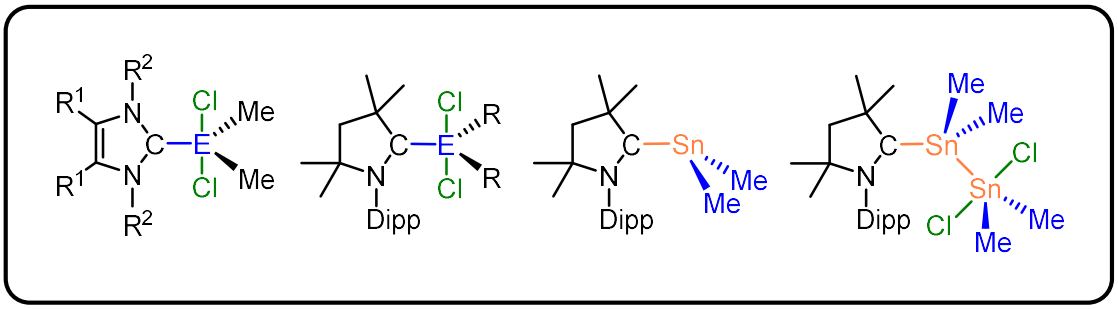

2 *N*-Heterocyclic Carbene and Cyclic (Alkyl)(amino)carbene Adducts of Germanium(IV) and Tin(IV) Chlorides and Organyl Chlorides

2.2 Introduction

N-heterocyclic carbenes (NHCs)[1] and cyclic (alkyl)(amino)carbenes (cAACs)[1j, 2] have a major impact in main group chemistry and their use allowed to realize molecular scaffolds and reaction pathways which would not be feasible without the support of this type of ligand. Their use as such ligands is mainly due to their tunable ambiphilicity and steric properties.[2b, 3] In the recent years, we investigated the synthesis and the reactivity of different silicon[4] and tin compounds.[5] For group 14, especially NHC silicon chemistry is well developed[1g-j, 2c, 6] and a wide range of Si(IV) precursors such as NHC·$SiCl_x$[7] and cAAC·$SiCl_x$[8] are already known. For the higher homologues Ge and Sn, common precursors are subvalent adducts L·ECl_2 (L = NHC, cAAC; E = Ge, Sn) which can be prepared from the corresponding carbenes and commercially available $GeCl_2$·dioxane[9] and $SnCl_2$,[7a, 9b, 9e, 10] respectively. The reaction of different carbenes with $ECl_{4-n}R_n$ (E = Ge, Sn; n = 0-4) to yield the corresponding adducts NHC·$ECl_{4-n}R_n$ was also used as a starting point into germanium[11] and tin chemistry.[7a, 12]

It has been demonstrated on several occasions that these compounds are potential starting materials for carbene-stabilized subvalent tetrel compounds. For example, Baines *et al.* reported the Ge(IV) chloride adduct *i*Pr_2Im·$GeCl_2$(DMB) (DMB = 2,3-dimethylbut-2-enyl) (Scheme 2.1, **2.A**), which was synthesized starting from $GeCl_2$(DMB) and *i*Pr_2Im (1,3-di-*iso*-propyl-4,5-dimethyl-imidazolin-2-ylidene), and subsequently converted into the Ge(II)-adduct *i*Pr_2Im·$GeCl_2$ (Scheme 2.1, **2.B**).[11a] Another interesting example was reported by Röschenthaler *et al.* who reacted $^{S}Me_2ImF_2$ (2,2-difluoro-1,3-dimethylimidazolidine; "S" denotes saturated backbone) with $GeCl_2$·dioxane, yielding both, $^{S}Me_2Im$·$GeCl_4$ (Me_2Im = 1,3,4,5-tetramethyl-imidazolin-2-ylidene; Scheme 2.1, **2.C**) and $^{S}Me_2Im$·GeF_4 (Scheme 2.1, **2.D**).[11b] Based on this research, Rivard *et al.* reacted the NHC salt [$^{S}Me_2ImCl$][Cl] with $GeCl_2$·dioxane, which led selectively to $^{S}Me_2Im$·$GeCl_4$ (Scheme 2.1, **2.C'**). In addition, the adducts *i*Pr_2Im^{Me}·$GeCl_4$[11d] (Scheme 2.1, **2.E**) and $Dipp_2$Im·$GeCl_4$[11c] (Scheme 2.1, **2.F**) were reported, which were synthesized starting from $GeCl_4$ and the NHCs *i*Pr_2Im^{Me}

and Dipp$_2$Im (1,3-bis-(2,6-di-*iso*-propylphenyl)-imidazolin-2-ylidene) respectively. Reduction with LiBH$_4$ afforded the borane-stabilized adducts *i*Pr$_2$Im^{Me}·GeH$_2$·BH$_3$[11d] (Scheme 2.1, **2.G**) and Dipp$_2$Im·GeH$_2$·BH$_3$[11c] (Scheme 2.1, **2.H**). Similarly, the reaction of Dipp$_2$Im with SnCl$_4$ afforded the corresponding Sn(IV) compound Dipp$_2$Im·SnCl$_4$ (Figure 2.1, **2.I**).[11c]

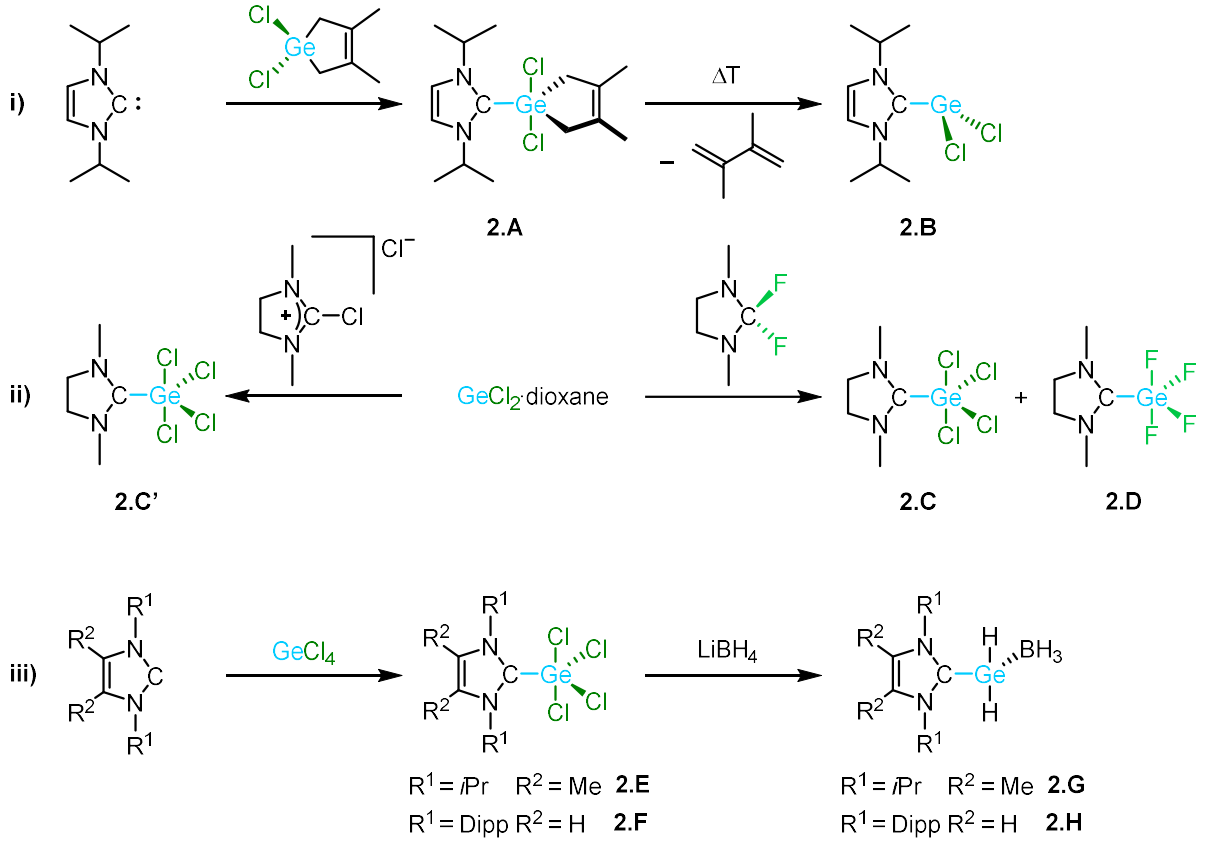

Scheme 2.1: (i) Synthesis of *i*Pr$_2$Im·GeCl$_2$(DMB) (**2.A**) and *i*Pr$_2$Im·GeCl$_2$ (**2.B**); (ii) Synthesis of ^{S}Me$_2$Im·GeCl$_4$ (**2.C** and **2.C'**) and ^{S}Me$_2$Im·GeF$_4$ (**2.D**); (iii) Synthesis of *i*Pr$_2$Im·GeCl$_4$ (**2.E**) and Dipp$_2$Im·GeCl$_4$ (**2.F**) and subsequent reaction with LiBH$_4$ to yield *i*Pr$_2$Im·GeH$_2$·BH$_3$ (**2.G**) and Dipp$_2$Im·GeH$_2$·BH$_3$ (**2.H**).

Similarly, Sn(IV) adducts were already reported previously by Boese *et al.* in 1995, who reacted R_2Im^{Me} (R = Me, Et, *i*Pr) with $SnCl_2Ph_2$ to isolate the corresponding compounds $R_2Im^{Me}{\cdot}SnCl_2Ph_2$ (Figure 2.1, **2.J**).[7a] In addition, an adduct of $SnCl_2Me_2$ was realized by coordination of the NHC DMP_2Im^{Me} (DMP = 2,3-dihydro-1,3-di-3'-methoxypropyl) to give the adduct $DMP_2Im^{Me}{\cdot}SnCl_2Me_2$ (Figure 2.1, **2.K**).[12] In the course of our work on the reactivity of NHCs with $SiCl_2Ph_2$ to yield $iPr_2Im{\cdot}SiCl_2Ph_2$ and the rearrangement of this adduct into a backbone coordinated ("abnormal" coordination) adduct $[(^aiPr_2ImH)_2SiPh_2]^{2+}2[Cl]^-$ ("a" denotes "abnormal" coordination mode of the NHC)[4c] we synthesized the NHC adducts $iPr_2Im{\cdot}SnCl_2R_2$ (R = Me, Ph; Figure 2.1, **2.L**) starting from iPr_2Im and $SnCl_2R_2$. However, the corresponding rearrangement was not observed, most probably due to the larger *Lewis*-acidity of the tin compounds.[5] As the number of such NHC (or cAAC) adducts of E(IV) halides or organohalides are rather limited, and to explore the possibility whether adducts $NHC{\cdot}EX_2R_2$ (E = Ge, Sn) are prone to rearrangement into the abnormally coordinated isomers and thus pave the way to germanium and tin tethered bis(carbene) ligands,[4c] we further explored this type of adducts and report our results here.

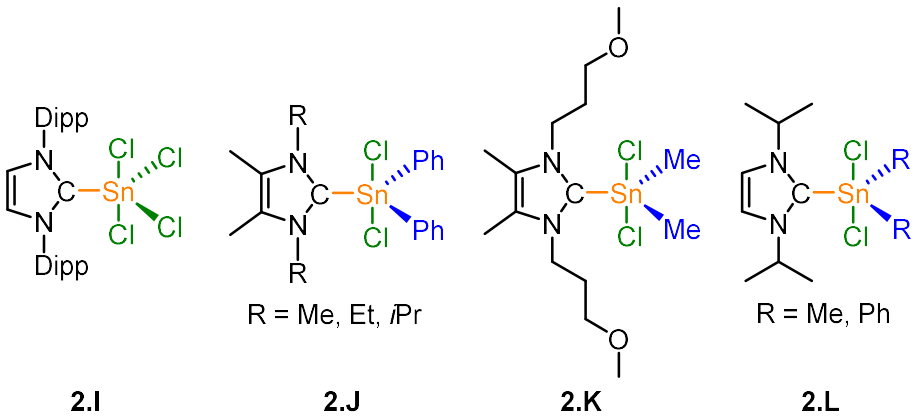

Figure 2.1: Selected NHC-Sn(IV) adducts.

2.2 Results and Discussion

We started our investigations with the reaction of *Lewis*-acidic Ge(IV) and Sn(IV) halides with different NHCs. The reaction of ECl_2Me_2 (E = Ge, Sn), with the NHCs Me_2Im^{Me} (**a**), iPr_2Im^{Me} (**b**) and $Dipp_2Im$ (**c**) in *n*-hexane at room temperature led to the corresponding adducts $NHC{\cdot}ECl_2Me_2$ (**2.1a-2.2c**) as colorless solids in fair to high yields (60 – 95 %; Scheme 2.2). Similarly, the reaction of $GeCl_4$ with Me_2Im^{Me} in *n*-hexane at room temperature afforded $Me_2Im^{Me}{\cdot}GeCl_4$ (**2.3**) as a colorless solid in 80 % yield (Scheme 2.2). In contrast, the formation of the tin adduct $Me_2Im^{Me}{\cdot}SnCl_4$ was not observed due to decomposition of the carbene to unknown salts with $[Me_2Im^{Me}\text{-}H]^+$ cations. However, the reaction of iPr_2Im^{Me} with $SnCl_4$ in THF led to formation of $iPr_2Im^{Me}{\cdot}SnCl_4{\cdot}THF$ (**2.4**) as a colorless solid in 85 % yield (Scheme 2.2).

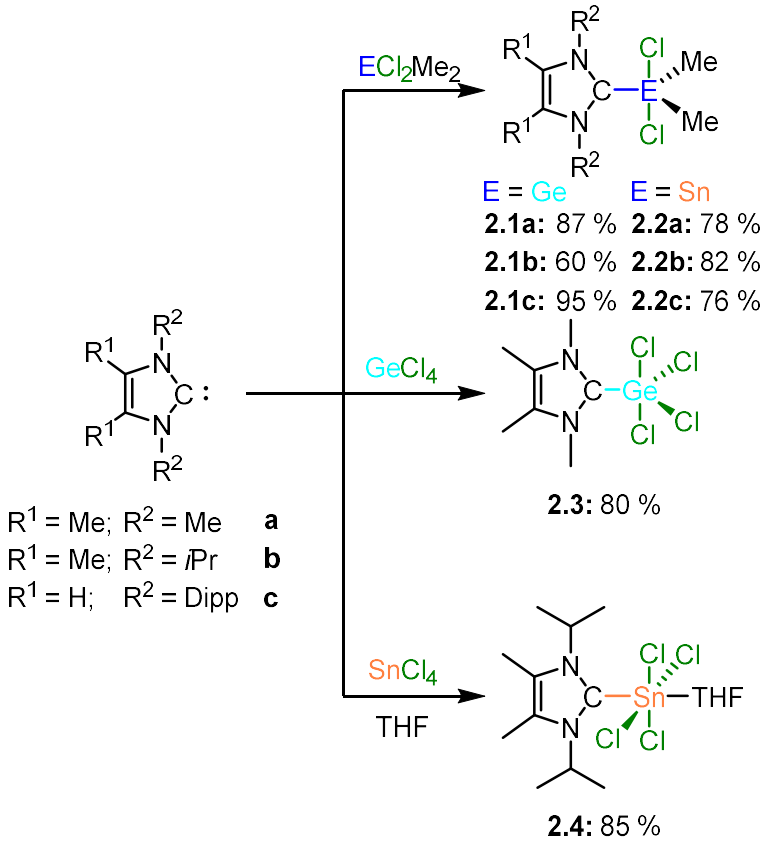

Scheme 2.2: Synthesis of the NHC-stabilized adducts of $GeCl_2Me_2$ (**1a-c**), $SnCl_2Me_2$ (**2a-c**), $GeCl_4$ (**3**) and $SnCl_4$ (**4**).

Adduct formation of these compounds is evident from ^{1}H, $^{13}C\{^{1}H\}$ and $^{119}Sn\{^{1}H\}$ NMR spectroscopy (Table 2.1) as well as elemental analysis. In the $^{13}C\{^{1}H\}$ NMR spectra, the N*C*N carbene carbon resonances of the adducts **2.1a**-**2.2c** (155.8 ppm to 165.9 ppm), are ca. 50 ppm upfield-shifted compared to the corresponding uncoordinated carbene (Table 2.1) due to coordination of the *Lewis*-acid. The Sn(IV) adducts **2.2a**-**c** revealed characteristic resonances in the ^{119}Sn NMR spectra in a range from −227.8 ppm to −217.6 ppm, similar to the ^{119}Sn NMR shift for *i*Pr$_2$Im·SnCl$_2$Me$_2$ (δ_{119Sn} = −227.0 ppm) reported previously.[5] The N*C*N resonance of **2.3** at 153.6 ppm in the $^{13}C\{^{1}H\}$ NMR spectrum is almost identical to that of literature known *i*Pr$_2$Im·GeCl$_4$[11d] (155.7 ppm). The additional THF coordination in the six-coordinate tin adduct *i*Pr$_2$Im^{Me}·SnCl$_4$·THF (**2.4**) led to a low-field shift in the $^{13}C\{^{1}H\}$ NMR spectrum of the N*C*N resonance to 160.1 ppm and to a upfield-shift of the corresponding $^{119}Sn\{^{1}H\}$ resonance to −446.5 ppm (cf. 146.7 ppm and −422.6 ppm for Dipp$_2$Im·SnCl$_4$).[11c]

Table 2.1: Selected $^{13}C\{^{1}H\}$ and $^{119}Sn\{^{1}H\}$ NMR chemical shifts (ppm) of the compounds NHC·ECl$_2$Me$_2$ (**2.1a**-**2.2c**), Me$_2$Im^{Me}·GeCl$_4$ (**2.3**), *i*Pr$_2$Im^{Me}·SnCl$_4$·THF (**2.4**) and related compounds (*), recorded in C_6D_6, unless otherwise noted.

		Me$_2$Im^{Me}	*i*Pr$_2$Im^{Me}	Dipp$_2$Im
2.1a-c	$\delta^{13}C$	155.8	157.5	160.5
2.2a-c	$\delta^{13}C$ $\delta^{119}Sn$	160.0 −222.5	162.6 −227.8	165.9 −217.6
2.3	$\delta^{13}C$	153.6	155.7*[11d]	156.5*a[11c]
2.4	$\delta^{13}C$ $\delta^{119}Sn$	/ /	160.1 −446.5 (THF adduct)	146.7*[11c] −422.6*[11c]
free NHC	$\delta^{13}C$	212.4	207.6	220.1

a) recorded in CD_2Cl_2.

Crystals suitable for X-ray diffraction were obtained for the compounds **2.1a-c** (benzene, 6 °C), **2.2b**, **2.2c** (benzene, rt) (Figure 2.2), **2.3** (toluene, rt) and **2.4** (THF layered with *n*-hexane, –30 °C) (Figure 2.3). The adducts crystallize in the monoclinic space groups $P2_1/c$ (**2.1c**) and $P2_1/n$ (**2.2b** and **2.2c**), in the triclinic space group $P\bar{1}$ (**2.4**) as well as in the orthorhombic space groups *Pbca* (**2.1a**), $Pca2_1$ (**2.1b**) and $P2_12_12_1$ (**2.3**), respectively, with one molecule in the asymmetric unit. Selected bonding parameters are summarized in Table 2.2. All adducts, except for **2.4**, adopt a trigonal bipyramidal arrangement of the ligands at the Ge or Sn atom with two chloride substituents in axial positions and the remaining substituents at equatorial sites. The C1–E distances of **2.1a-c** and **2.2b-c** (Table 2.2) are within 3σ in the range of the corresponding distances in other NHC-coordinated Ge(IV) (C1–Ge: 1.987(2) Å – 1.9921(14) Å)[11a-c] and Sn(IV) (C1–Sn: 2.1773(19) Å – 2.203(3) Å) compounds reported previously.[5, 11c, 12] The axial chlorides are slightly tilted towards the carbene with Cl1–E–Cl2 angles ranging from 172.39(2)° to 179.445(17)° and C1–Cl distances in the range from 2.9679(30) Å (**2.3**) to 3.1704(16) Å (**2.1c**) for the germanium compounds and 3.1251(50) Å (**2.12**) to 3.5048(29) Å (**2.7**) for the tin compounds. Non-bonding inter-ligand interactions between the carbene carbon p_π-orbitals and the lone pairs of the chloride ligands Cl1 and Cl2 might be the reason for this distortion. Such non-bonding interactions might additionally stabilize the compounds, as has been noticed for NHC complexes of early transition metals in their high to highest oxidation states before. [13]

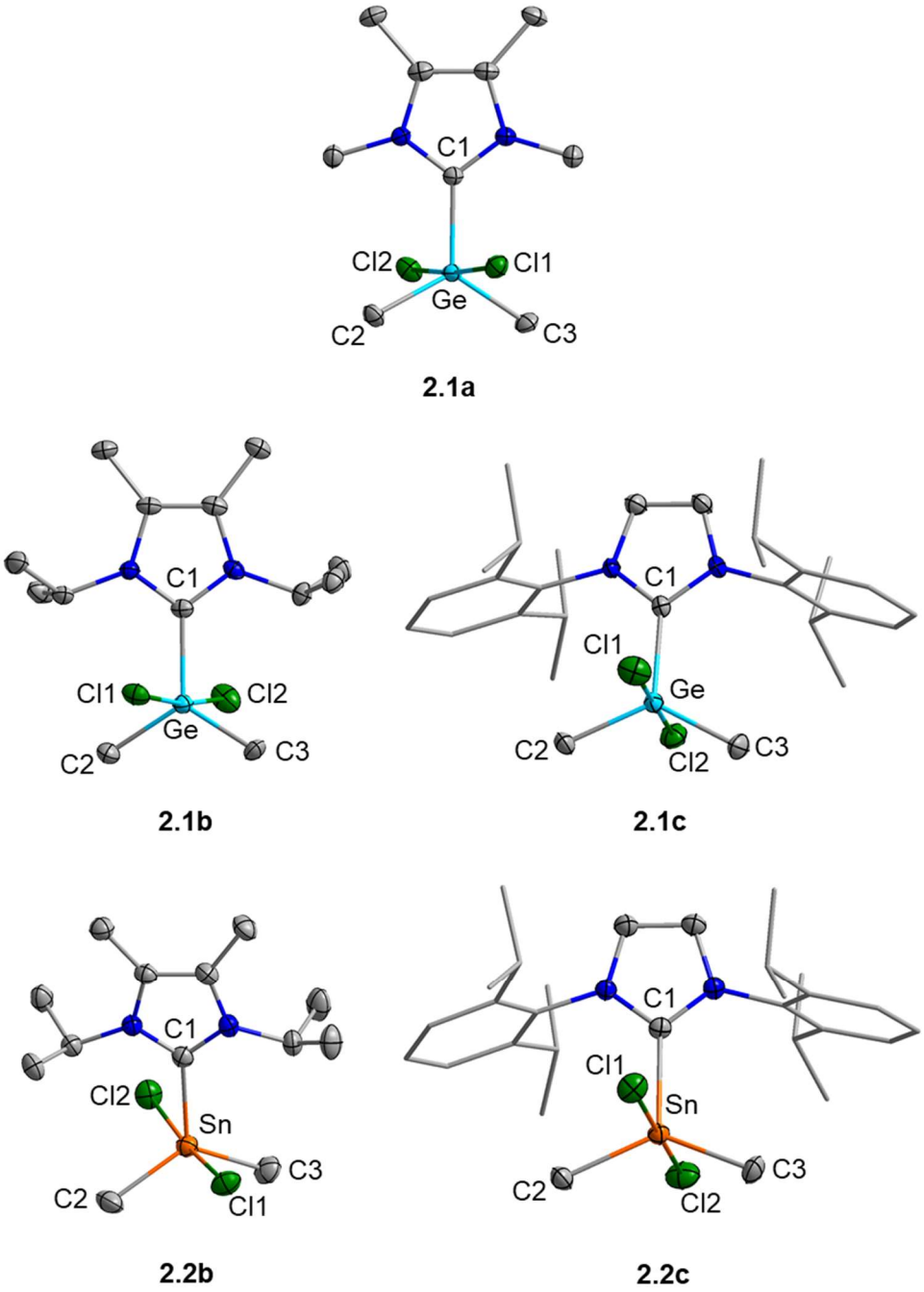

Figure 2.2: Molecular structures of $Me_2Im^{Me}{\cdot}GeCl_2Me_2$ (**2.1a**), $iPr_2Im^{Me}{\cdot}GeCl_2Me_2$ (**2.1b**), $Dipp_2Im{\cdot}GeCl_2Me_2$ (**2.1c**), $iPr_2Im^{Me}{\cdot}SnCl_2Me_2$ (**2.2b**) and $Dipp_2Im{\cdot}SnCl_2Me_2$ (**2.2c**), in the solid-state. Hydrogen atoms are omitted for clarity. Atomic displacement ellipsoids are set at the 50 % probability level and Dipp groups are shown as wire-and-stick models. Selected bond lengths [Å] and angles [°] (Table 2.2): **2.1a**: Ge–C1, 1.9803(18); Ge–Cl1, 2.4513(5); Ge–Cl2, 2.4910(5); Ge–C2, 1.9395(17); Ge–C3, 1.9305(18); Cl1–Ge–Cl2, 175.292(17); C2–Ge–C3, 121.29(8); **2.1b**: Ge–C1, 1.984(3); Ge–Cl1, 2.5348(9); Ge–Cl2, 2.3634(9); Ge–C2, 1.950(4); Ge–C3, 1.933(3); Cl1–Ge–Cl2, 172.58(4); C2–Ge–C3, 118.41(16); **2.1c**: Ge–C1, 1.9987(15); Ge–Cl1, 2.3603(4); Ge–Cl2, 2.5199(4); Ge–C2, 1.9355(16); Ge–C3, 1.9386(17); Cl1–Ge–Cl2, 179.445(17); C2–Ge–C3, 128.20(7); **2.2b**: Sn–C1, 2.189(3); Sn–Cl1, 2.5540(7); Sn–Cl2, 2.5638(7); Sn–C2, 2.122(3); Sn–C3, 2.121(3); Cl1–Sn–Cl2, 172.39(2); C2–Sn–C3, 125.83(13); **2.2c**: Sn–C1, 2.202(2); Sn–Cl1, 2.5692(6); Sn–Cl2, 2.5107(6); Sn–C2, 2.115(2); Sn–C3, 2.122(2); Cl1–Sn–Cl2, 178.11(2); C2–Sn–C3, 132.16(10).

The structure of compound **2.4** reveals an octahedral coordination sphere at the central tin atom with the NHC as well as one THF ligand coordinated *trans* to each other and the chloride substituents occupying the remaining coordination sites. From the angles Cl1–Sn–Cl2 (170.23(4)°) and Cl3–Sn–Cl4 (165.73(3)°) it can be concluded that the chloride substituents are slightly bent towards the THF ligand.

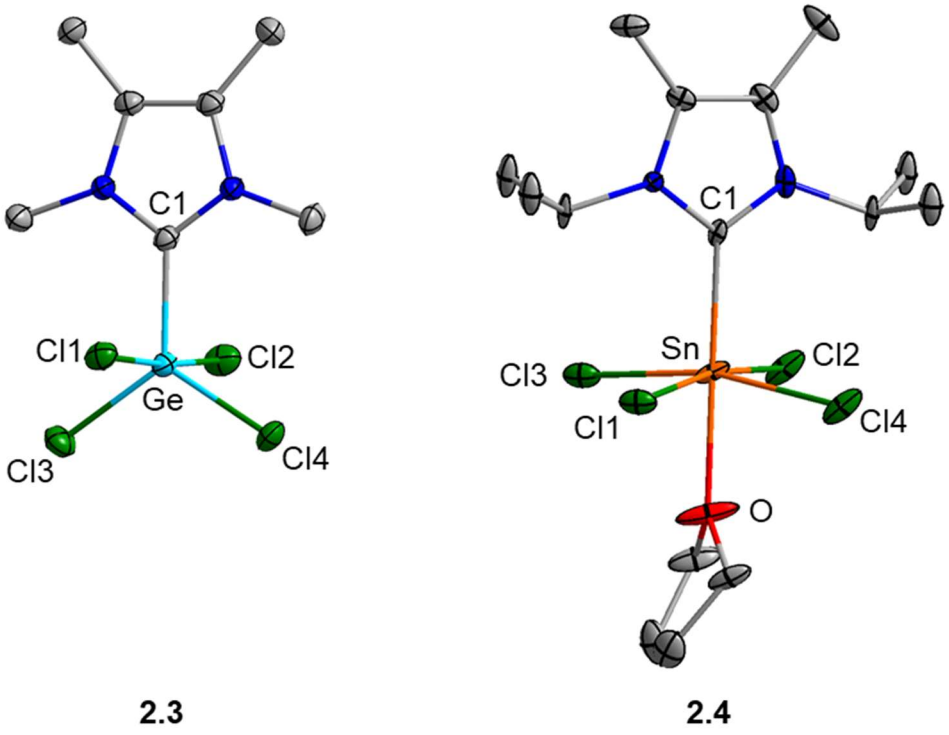

2.3 **2.4**

Figure 2.3: Molecular structures of $Me_2Im^{Me}\cdot GeCl_4$ (**2.3**), and $iPr_2Im^{Me}\cdot SnCl_2Me_2\cdot THF$ (**2.4**), in the solid-state. Hydrogen atoms and solvent molecules (**2.4**: THF) are omitted for clarity. Atomic displacement ellipsoids are set at 50 % probability. Selected bond lengths [Å] and angles [°] (Table 2.2): **2.3**: Ge–C1, 1.976(3); Ge–Cl1, 2.2960(7); Ge–Cl2, 2.3117(8); Ge–Cl3, 2.1604(8); Ge–Cl4, 2.1565(7); Cl1–Ge–Cl2, 174.53(3); Cl3–Ge–Cl4, 114.74(3); **2.4**: Sn–C1, 2.231(4); Sn–Cl1, 2.4131(11); Sn–Cl2, 2.4205(11); Sn–Cl3, 2.4029(12); Sn–Cl4, 2.4166(12); Sn–O, 2.257(4); Cl1–Sn–Cl2, 170.23(4); Cl3–Sn–Cl4, 165.73(4).

Recently, our group has demonstrated that *i*Pr$_2$Im·SiCl$_2$Ph$_2$ rearranges to the backbone-coordinated and silicon-bridged compound [(^{a}*i*Pr$_2$Im)$_2$·SiPh$_2$]$^{2+}$2[Cl]$^-$ upon heating.[4c] However, so far we did not observe similar reactivity for the related tin compounds reported herein.[5] Furthermore, we did not observe the controlled formation of Ge(II) or Sn(II) compounds NHC·ECl$_2$ after heating benzene solutions of NHC·ECl$_2$Me$_2$ to reflux for several days. However, the Ge(IV) adduct **2.1c** isomerized after heating in benzene to give a colorless precipitate of the salt [^{a}Dipp$_2$Im·GeClMe$_2$]$^+$[Cl]$^-$ (**2.5**), which was isolated in 71 % yield (Scheme 2.3).

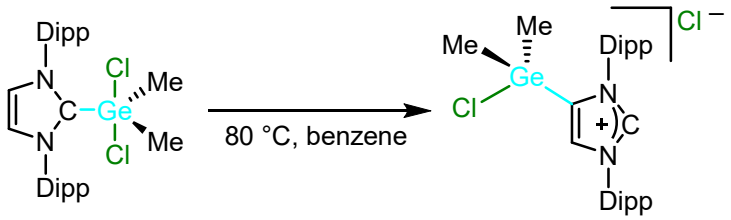

1c **5**

Scheme 2.3: Thermal induced isomerization of Dipp$_2$Im·GeCl$_2$Me$_2$ (**2.1c**) into the abnormal coordinated salt [^{a}Dipp$_2$Im·GeClMe$_2$]$^+$[Cl]$^-$ (**2.5**).

It has been demonstrated previously that abnormal coordination is often thermodynamically favored.[1,2] The abnormal coordination of **2.5** is evident from ^{1}H and ^{13}C{^{1}H} NMR spectroscopy. The signal sets of the Dipp groups are doubled in the ^{1}H and ^{13}C{^{1}H} NMR spectra due to the asymmetry of **2.5**. Two characteristic resonances in the ^{1}H NMR spectrum are indicative for a change in the coordination mode, namely one singlet with an intensity of one for the remaining backbone proton at 7.68 ppm and a second singlet for the new imidazolium proton were observed at 12.2 ppm. The N*C*N resonance in the ^{13}C{^{1}H} NMR is shifted from 160.5 ppm (**2.1c**) to 146.0 ppm (**2.5**).

Table 2.2: Selected bond lengths [Å] and angles [°] of the NHC adducts **2.1a-c**, **2.2b**, **2.2c**, **2.3** and **2.4**.

trigonal bipyramidal	**E–C1**	**E–Cl1**	**E–Cl2**	**E–C2**	**E–C3**	**Cl1–E–Cl2**	**C2–E–C3**
(2.1a) Me_2Im^{Me}·$GeCl_2Me_2$	1.9803(18)	2.4513(5)	2.4910(5)	1.9395(17)	1.9305(18)	175.292(17)	121.29(8)
(2.1b) *i*Pr_2Im^{Me}·$GeCl_2Me_2$	1.984(3)	2.5348(9)	2.3634(9)	1.950(4)	1.933(3)	172.58(4)	118.41(16)
(2.1c) $Dipp_2Im^{Me}$·$GeCl_2Me_2$	1.9987(15)	2.3603(4)	2.5199(4)	1.9355(16)	1.9386(17)	179.445(17)	128.20(7)
(2.2b) *i*Pr_2Im^{Me}·$SnCl_2Me_2$	2.189(3)	2.5540(7)	2.5638(7)	2.122(3)	2.121(3)	172.39(2)	125.83(13)
(2.2c) $Dipp_2Im$·$SnCl_2Me_2$	2.202(2)	2.5692(6)	2.5107(6)	2.115(2)	2.122(2)	178.11(2)	132.16(10)
trigonal bipyramidal	**E–C1**	**E–Cl1**	**E–Cl2**	**E–Cl3**	**E–Cl4**	**Cl1–E–Cl2**	**Cl3–E–Cl4**
(2.3) Me_2Im^{Me}·$GeCl_4$	1.976(3)	2.2960(7)	2.3117(8)	2.1604(8)	2.1565(7)	174.53(3)	114.74(3)
octahedral	**E–C1**	**E–Cl1**	**E–Cl2**	**E–Cl3**	**E–Cl4**	**Cl1–E–Cl2**	**Cl3–E–Cl4**
(2.4) *i*Pr_2Im^{Me}·$SnCl_4$·THF	2.231(4)	2.4131(11)	2.4205(11)	2.4029(12)	2.4166(12)	170.23(4)	165.73(4)

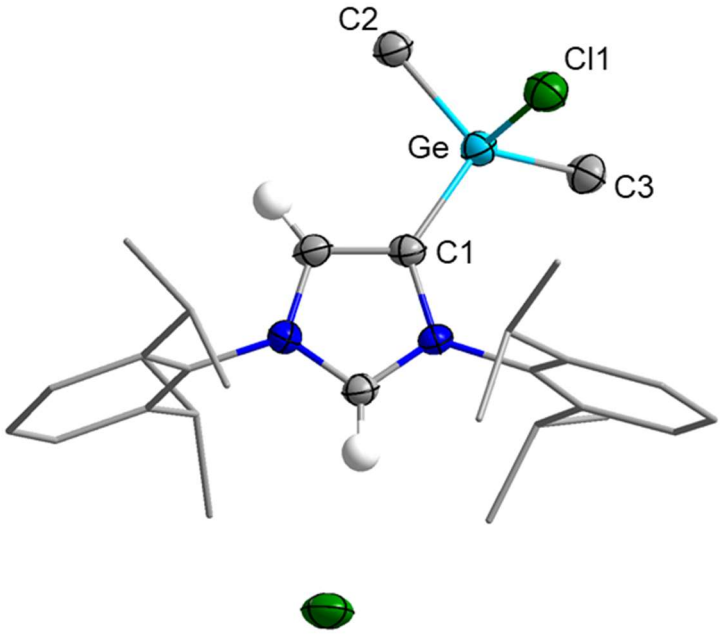

2.5

Figure 2.4: The molecular structure of [^{a}Dipp$_2$Im·GeClMe$_2$]$^+$[Cl]$^-$ (**2.5**) in the solid-state. Hydrogen atoms (except the imidazolium protons) and solvent molecules (benzene) are omitted for clarity. Only one of two independent molecules of the asymmetric unit is shown. Atomic displacement ellipsoids are set at 50 % probability and Dipp groups are shown as wire-and-stick-model. Selected bond lengths [Å] and angles [°]: **2.5**: Ge–C1, 1.944(2); Ge–Cl1, 2.2325(8); Ge–C2, 1.938(3); Ge–C3, 1.922(3); C1–Ge–Cl1, 99.99(8); C1–Ge–C2, 108.48(11); C1–Ge–C3, 120.20(11); Cl1–Ge–C2, 101.67(8); Cl1–Ge–C3, 101.43(9); C2–Ge–C3, 120.48(12)

Crystals of **2.5** suitable for X-ray diffraction were obtained by cooling an at reflux saturated benzene solution of the compound to room temperature (Figure 2.4). Compound **2.5** crystallizes in the triclinic space group $P\bar{1}$ with two molecules in the asymmetric unit. The structure reveals a tetrahedral coordination sphere at germanium, which deviates from the five-coordinated nature of the other adducts reported here, most probably due to steric repulsion of the methyl groups and the Dipp substituents of the backbone-bonded NHC.

Thus, salt formation is preferred and one of the chloride substituents is expelled from the coordination sphere of germanium. It is also interesting to note that the methyl groups at germanium keep intact in the presence of the acidic imidazole hydrogen atoms. The Ge–C1 distance of the covalent Ge–C single bond of **2.5** (1.944(2) Å) is smaller compared to the Ge–C distance observed for the NHC adduct **2.1c** (C1–Ge: 1.9987(15) Å), which is most probably due to the better donation properties of ^{a}NHC

compared to the NHC ligand and the lower coordination number of **2.5** compared to that of **2.1c**. Compound **2.5** represents a rare example of an NHC backbone-coordinated to germanium. For the formation of **2.5** we assume a mechanism similar to that reported previously by Goicoechea *et al.* for the formation of $^{a}Dipp_2Im{\cdot}EBr_3$ from $Dipp_2Im{\cdot}EBr_3$ (E = Sb, Bi).[14] This isomerization likely proceeds *via* cleavage of the Ge–C bond generating free $Dipp_2Im$ in solution, which allows deprotonation of another coordinated $Dipp_2Im$ ligand and isomerization.

In contrast to the NHC adducts of Ge(IV) and Sn(IV), adducts with cAACs are unknown so far. For this reason we also investigated the behavior of various Ge(IV) and Sn(IV) compounds towards $cAAC^{Me}$ (1-(2,6-di-*iso*-propylphenyl)-3,3,5,5-tetramethyl-pyrrolidin-2-ylidene) (Scheme 2.4). Like the syntheses of **2.1a**-**2.2c**, the reactions of $cAAC^{Me}$ with $GeCl_2Me_2$, $SnCl_2Me_2$ and $GeCl_2Ph_2$, respectively, afforded the corresponding $cAAC^{Me}$ adducts $cAAC^{Me}{\cdot}GeCl_2Me_2$ (**2.6**), $cAAC^{Me}{\cdot}SnCl_2Me_2$ (**2.7**) and $cAAC^{Me}{\cdot}GeCl_2Ph_2$ (**2.8**) as benzene-soluble, colorless solids in good to very good yields (68 % – 88 %, Scheme 2.4). The reaction of $cAAC^{Me}$ with $GeClMe_3$ and $GeCl_4$, respectively, afforded colorless precipitates which are poorly soluble in non-polar solvents. Isolation of these precipitates led to the characterization of the salts $[cAAC^{Me}GeMe_3]^+[Cl]^-$ (**2.9**) and $[cAAC^{Me}Cl]^+[GeCl_3]^-$ (**2.10**) as dichloromethane-soluble, colorless solids in 60 % (**2.9**) and 87 % (**2.10**) yield, respectively. Note that salt formation depends on the halide content of the germane, as the reaction of $cAAC^{Me}$ with $GeClMe_3$ led to chloride elimination to yield the chloride salt $[cAAC^{Me}GeMe_3]^+[Cl]^-$ (**2.9**) ($[cAAC^{Me}GeMe_3]^+$ cation) whereas the reaction of $cAAC^{Me}$ with $GeCl_4$ afforded with chlorine transfer to the cAAC of $[cAAC^{Me}Cl]\ ]^+[GeCl_3]^-$ ($[GeCl_3]^-$ anion; see below).

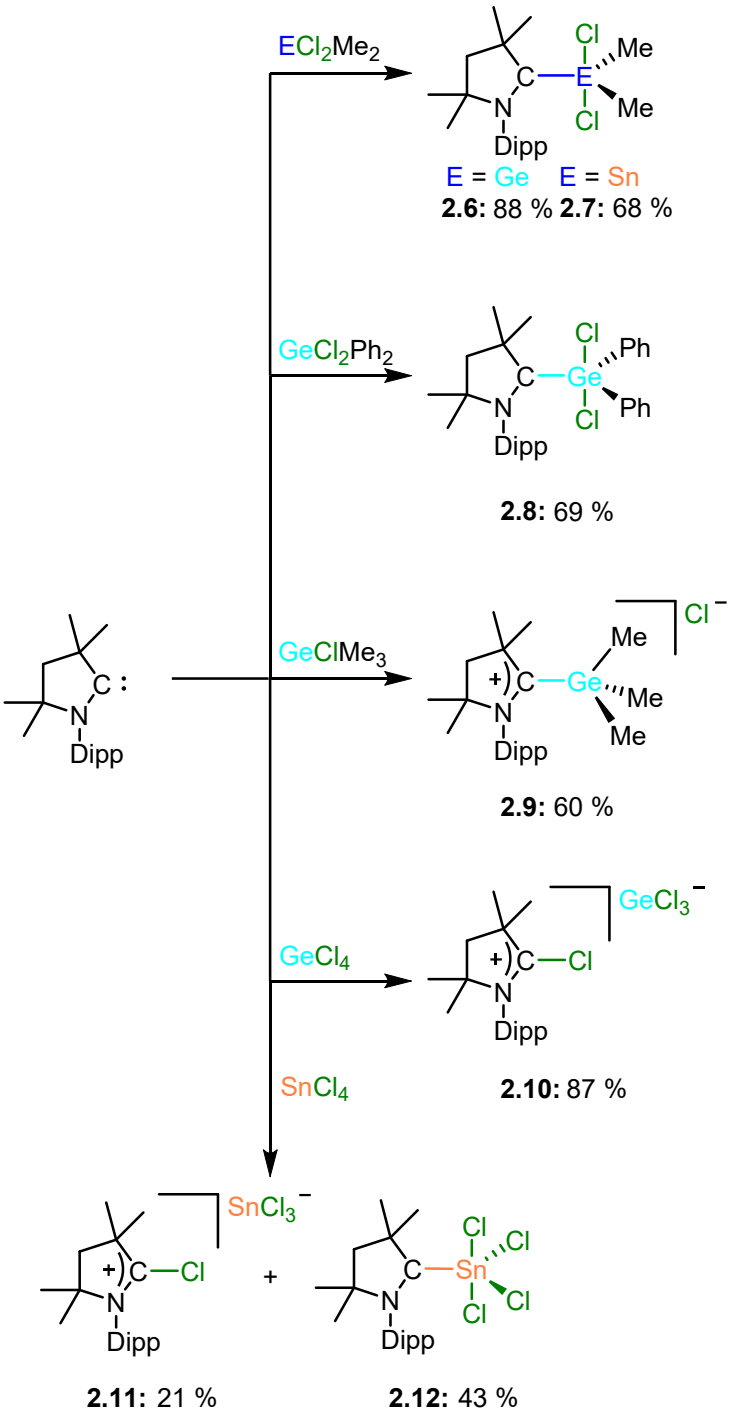

Scheme 2.4: Synthesis of the cAAC^{Me}-stabilized adducts cAAC^{Me}·$GeCl_2Me_2$ (**2.6**), cAAC^{Me}·$SnCl_2Me_2$ (**2.7**), cAAC^{Me}·$GeCl_2Ph_2$ (**2.8**), and the salts $[cAAC^{Me}GeMe_3]^+[Cl]^-$ (**2.9**), $[cAAC^{Me}Cl]^+[GeCl_3]^-$ (**2.10**) and $[cAAC^{Me}Cl]^+[SnCl_3]^-$ (**2.11**) and cAAC^{Me}·$SnCl_4$ (**2.12**).

Evidence for the formation of the compounds **2.6**-**2.10** was obtained by NMR and IR spectroscopy as well as elemental analysis. Due to the strong broadening of the resonances of the methyl groups in C_6D_6 at room temperature, the NMR spectra of the compounds **2.6** and **2.7** were recorded in toluene-d_8 at −40 °C. In the ^{1}H NMR spectra, the characteristic resonances of the backbone CH_2 unit (**2.6**: 1.28 ppm; **2.7**: 1.21 ppm) and the methine protons (**2.6**: 3.23 ppm; **2.7**: 3.06 ppm) of the Dipp groups are shifted towards higher field compared to free cAAC^{Me} (CH_2: 1.52 ppm; *i*Pr-C*H*: 3.10 ppm; in toluene-d_8).

The carbene carbon N*C*E (E = Ge, Sn) resonances in the ^{13}C{^{1}H} NMR spectra are significantly upfield-shifted to 214.1 ppm (**2.6**) and 226.3 ppm (**2.7**) compared to uncoordinated cAAC^{Me} (313.9 ppm; in toluene-d_8). In the ^{119}Sn{^{1}H} NMR spectrum of compound **2.7** a signal was detected at −214.1 ppm. Similar coordination shifts were observed for the adduct **2.8** (see 7.5 Synthetic Procedures for Chapter II). The spectroscopy of the compounds **2.9** and **2.10** differ significantly from that of **2.6**-**2.8**. In the ^{1}H NMR spectrum of **2.9**, a broad resonance at 0.35 ppm with a relative intensity of **2.9** was observed for the germanium-bound methyl groups.

In the ^{13}C{^{1}H} NMR spectrum, the N*C*Ge resonance was detected at 222.9 ppm, which is slightly up field shifted compared to other germanium-coordinated cAAC^{Me} carbene carbon atoms (N*C*Ge: 226.3 – 249.8 ppm).[9d, 15] Formation of the cation [cAAC^{Me}Cl]$^+$ in [cAAC^{Me}Cl]$^+$[GeCl$_3$]$^-$ (**2.10**) is evident from the ^{13}C{^{1}H} NMR spectrum of **2.10**, in which the N*C*Cl resonance was detected at 190.6 ppm which is in range of N*C*Cl signals of literature known [cAAC–Cl]$^+$ cations (188.5 – 190.6 ppm).[16]

Additional evidence for the formation of the compounds **2.6**-**2.9** was obtained from X-ray crystallography, and the solid-state structures of these compounds are depicted in Figure 2.5. Crystals suitable for X-ray diffraction were obtained by storing a saturated solution in benzene at 6 °C (**2.6**, **2.8**), by slow evaporation of a benzene solution at room temperature (**2.7**) and storing a saturated solution in THF at room temperature (**2.9**), respectively. The adducts crystallize in the triclinic space group $P\bar{1}$ (**2.7**), in the monoclinic space group *P*2$_1$/*n* (**2.8**), in the orthorhombic space group *Pbca* (**2.6**), and the tetragonal space group *I*4$_1$*cd* (**2.9**), respectively, in each case with one molecule in the asymmetric unit. Selected bonding parameters are summarized in Table 2.3.

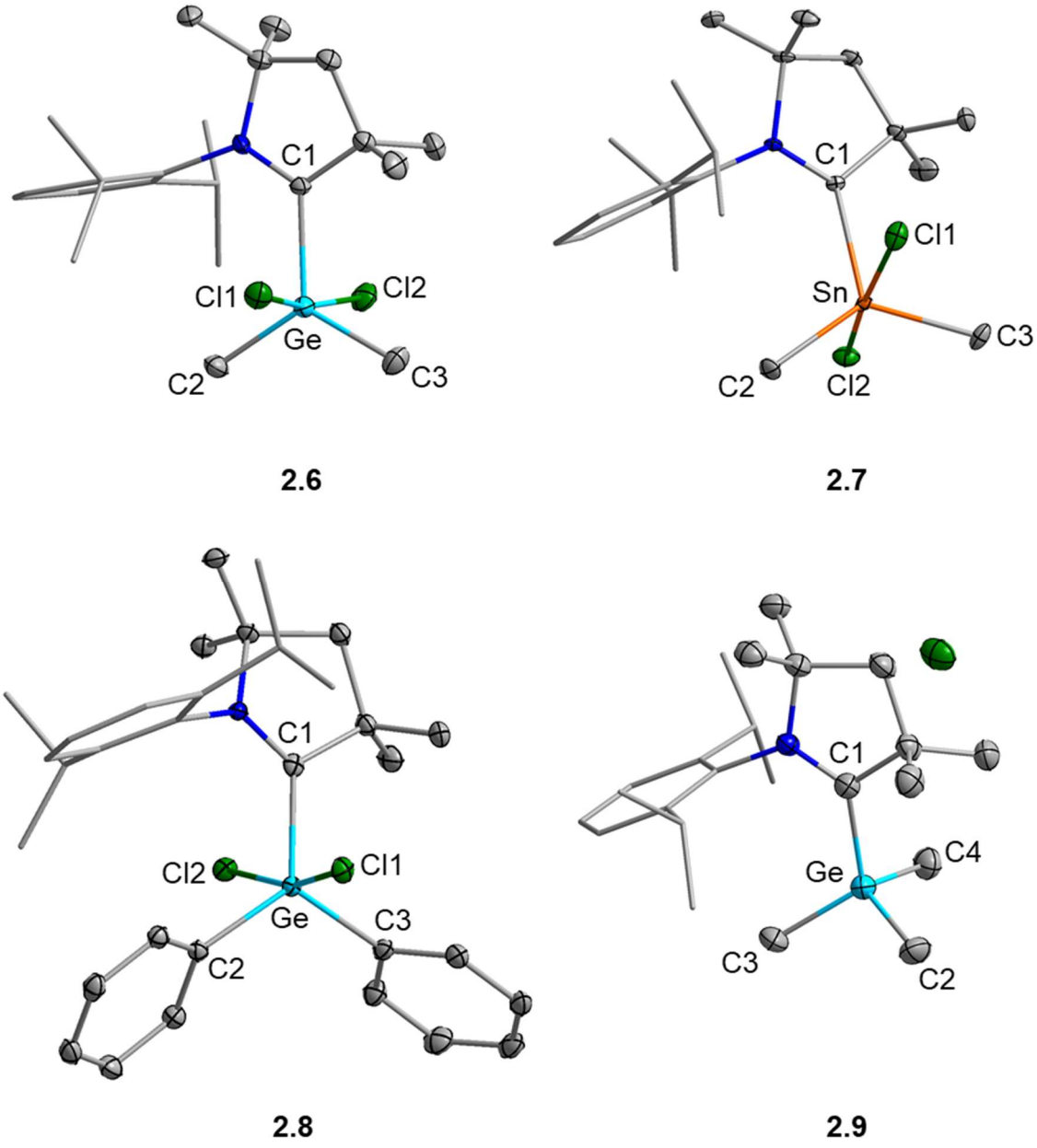

Figure 2.5: Molecular structures of cAAC^{Me}·$GeCl_2Me_2$ (**2.6**), cAAC^{Me}·$SnCl_2Me_2$ (**2.7**), cAAC^{Me}·$GeCl_2Ph_2$ (**2.8**) and [cAAC^{Me}$GeMe_3$]$^+$[Cl]$^-$ (**2.9**), in the solid-state. Hydrogen atoms and solvent molecules (**2.6** and **2.8**: benzene) are omitted for clarity. Atomic displacement ellipsoids are set at 50 % probability and Dipp groups are shown as wire-and-stick model. Selected bond lengths [Å] and angles [°] (Table 2.3): **2.6**: Ge–C1 (part 1), 1.964(12); Ge–C1 (part 2), 2.078(18); Ge–Cl1, 2.4303(4); Ge–Cl2, 2.4325(4); Ge–C2, 1.9379(15); Ge–C3, 1.9426(16); Cl1–Ge–Cl2, 169.355(14); C2–Ge–C3, 119.72(7); **2.7**: Sn–C1, 2.231(2); Sn–Cl1, 2.5502(7); Sn–Cl2, 2.5726(7); Sn–C2, 2.122(3); Sn–C3, 2.124(3); Cl1–Sn–Cl2, 170.59(2); C2–Sn–C3, 127.95(11); **2.8**: Ge–C1, 2.0177(19); Ge–Cl1, 2.2965(5); Ge–Cl2, 2.5488(5); Ge–C2, 1.9485(18); Ge–C3, 1.9762(19); Cl1–Ge–Cl2, 166.582(18); C2–Ge–C3, 115.03(8); **2.9**: Ge–C1, 2.030(4); Ge–C2, 1.947(4); Ge–C3, 1.943(4); Ge–C4, 1.954(4); C2–Ge–C3, 107.86(18); C3–Ge–C4, 110.41(19); C2–Ge–C4, 111.17(19).

The compounds **2.6**-**2.8** adopt – similar to the NHC adducts **2.1a**-**2.3** – trigonal bipyramidal structures. The axial chloride substituents are slightly more tilted towards the cAAC than in the NHC adducts **2.1a**-**2.3** (Cl1–E–Cl2: 172.39(2)° – 179.445(17)°) with Cl1–E–Cl2 angles from 166.582(18)° to 170.59(2)°, owing to the better donor properties of the cAAC.[1i, 2c, 3l] Interestingly, the C1–E bond lengths of **2.6**-**2.8** (**2.6**: 2.078(18) Å; **2.7**: 2.231(2) Å; **2.8**: 2.0177(19) Å; Table 2.3) are slightly longer as observed in the structures of the NHC supported compounds **2.1a-c** (1.9803(18) – 1.9987(15) Å; Table 2.2) and **2.2b-c** (2.189(3) – 2.202(2) Å; Table 2.2), respectively. The crystal structure of **2.9** reveals the formation of a ionic structure featuring a chloride anion and the $[cAAC^{Me}GeMe_3]^+$ cation, which adopts a tetrahedral coordination at germanium with three methyl groups and one $cAAC^{Me}$ ligand occupying the coordination sites. Similarly, the crystal structure of **2.10** (Figure 2.6) does not confirm the formation of an adduct $cAAC^{Me}{\cdot}GeCl_4$, but the formation of the salt $[cAAC^{Me}Cl]^+[GeCl_3]^-$ instead, featuring the discrete cation $[cAAC^{Me}Cl]^+$ and the $[GeCl_3]^-$ counterion.

In contrast to the synthesis of **2.10**, the reaction of $SnCl_4$ with $cAAC^{Me}$ does not lead to clean formation of the salt $[cAAC^{Me}Cl]^+[SnCl_3]^-$ (**2.11**). In fact, a mixture of **2.11** and the adduct $cAAC^{Me}{\cdot}SnCl_4$ (**2.12**) (Scheme 2.4) was obtained. Compound **2.12** is partially soluble in benzene and can be extracted and isolated in a yield of 43 % from the crude product. Subsequent recrystallization of the remaining solid afforded **2.11** in 21 % yield. The formation of the $[cAAC^{Me}Cl]^+$ cation can be concluded from a resonance at 190.7 ppm of the former carbene carbon atom in the $^{13}C\{^1H\}$ NMR spectrum of **2.11**, which was already observed for compound **2.10**. For compound **2.12** a characteristic N*C*Sn signal was detected at 218.9 ppm, in a similar region as observed for compound **2.7** (NCSn, 225.3 ppm; in toluene-d_8). In the $^{119}Sn\{^1H\}$ NMR spectra, resonances were detected at −34.8 ppm for **2.11** and at −406.3 ppm for **2.12**, the latter close to that observed for $Dipp_2Im{\cdot}SnCl_4$ (−422.6 ppm, in toluene-d_8).[11c]

Crystals suitable for X-ray diffraction were obtained for **2.10** by slow evaporation of a dichloromethane solution at room temperature, for **2.11** by slow diffusion of *n*-hexane into a saturated dichloromethane solution and for **2.12** by slow evaporation of a saturated benzene solution at room temperature, respectively (Figure 2.6). The compounds **2.10**, **2.11** and **2.12** crystallize in the orthorhombic space group $P2_12_12_1$

with one molecule in the asymmetric unit. Selected bonding parameters of **2.10**, **2.11** and **2.12** are summarized in Table 2.3. The germanium and tin salts **2.10** (Figure 2.6) and **2.11** (Figure 2.6) are isostructural with an $[ECl_3]^-$ (E = Ge, **2.10**; Sn, **2.11**) anion and the $[cAAC^{Me}Cl]^+$ cation, whereas compound **2.12** (Figure 2.6) shows a slightly distorted trigonal bipyramidal coordinated tin atom as found for the related dichlorodimethyl compound **2.7** (Figure 2.5).

Table 2.3: Selected bond lengths [Å] and angles [°] of the compounds **2.6**-**2.12**.

trigonal bipyramidal	E–C1	E–Cl1	E–Cl2	E–C2/Cl3	E–C3/Cl4	Cl1–E–Cl2	Cl2–E–Cl3
(2.6) **cAAC^{Me}·GeCl$_2$Me$_2$**	2.078(18)	2.4303(4)	2.4325(4)	1.9379(15)	1.9426(16)	169.355(14)	119.72(7)
(2.7) **cAAC^{Me}·SnCl$_2$Me$_2$**	2.231(2)	2.5502(7)	2.5726(7)	2.122(3)	2.124(3)	170.59(2)	127.95(11)
(2.8) **cAAC^{Me}·GeCl$_2$Ph$_2$**	2.0177(19)	2.2965(5)	2.5488(5)	1.9485(18)	1.9762(19)	166.582(18)	115.03(8)
(2.12) **cAAC^{Me}·SnCl$_4$**	2.214(5)	2.3878(5)	2.4385(13)	2.3181(12)	2.3356(15)	165.83(5)	110.31(5)
tetrahedral	**E–C1**	**E–C2**	**E–C3**	**E–C4**	**C2–E–C3**	**C3–E–C4**	**C2–E–C4**
(2.9) **[cAAC^{Me}GeMe$_3$]$^+$[Cl]$^-$**	2.030(4)	1.947(4)	1.943(4)	1.954(4)	107.86(18)	110.41(19)	111.17(19)
trigonal pyramidal	**C1–Cl1**	**E–Cl2**	**E–Cl3**	**E–Cl4**	**Cl2–E–Cl3**	**Cl3–E–Cl4**	**Cl2–E–Cl4**
(2.10) **[cAAC^{Me}Cl]$^+$[GeCl$_3$]$^-$**	1.691(3)	2.3085(9)	2.2975(9)	2.2914(8)	94.63(3)	97.30(3)	97.79(3)
(2.11) **[cAAC^{Me}Cl]$^+$[SnCl$_3$]$^-$**	1.683(7)	2.477(3)	2.462(4)	2.458(3)	92.53(14)	95.97(12)	96.53(12)

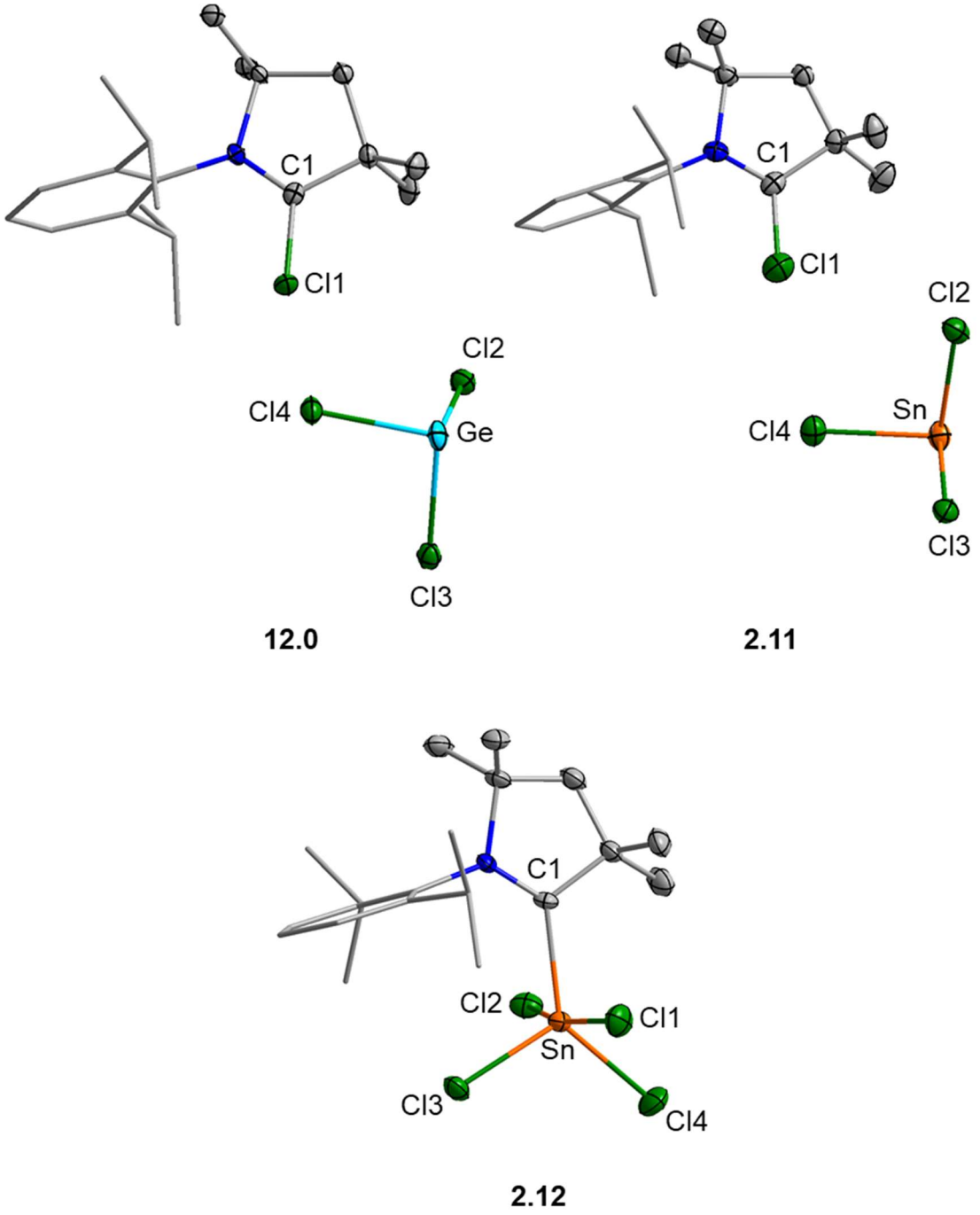

Figure 2.6: Molecular structures of $[cAAC^{Me}Cl]^+[GeCl_3]^-$ (**2.10**), $[cAAC^{Me}Cl]^+[SnCl_3]^-$ (**2.11**) and $cAAC^{Me}{\cdot}SnCl_4$ (**2.12**), in the solid-state. Hydrogen atoms are omitted for clarity. The $[SnCl_3]^-$ anion in compound **2.11** is disordered and the data corresponds to the part with 86 % occupancy. Atomic displacement ellipsoids are set at 50 % probability and Dipp groups are shown as wire-and-stick model. Selected bond lengths [Å] and angles [°] (Table 2.3): **2.10**: Ge–Cl1, 1.691(3); Ge–Cl2, 2.3085(9); Ge–Cl3, 2.2975(9); Ge–Cl4, 2.2914(8); Cl2–Ge–Cl3, 94.63(3); Cl3–Ge–Cl4, 97.30(3); Cl2–Ge–Cl4, 97.79(3); **2.11**: Sn–Cl1, 1.683(7); Sn–Cl2, 2.477(3); Sn–Cl3, 2.462(4); Sn–Cl4, 2.458(3); Cl2–Sn–Cl3, 92.53(14); Cl3–Sn–Cl4, 95.97(12); Cl2–Sn–Cl4, 96.53(12); **2.12**: Sn–C1, 2.214(5); Sn–Cl1, 2.3878(15); Sn–Cl2, 2.4385(13); Sn–Cl3, 2.3181(12); Sn–Cl4, 2.3556(15); Cl1–Sn–Cl2, 165.83(5); Cl3–Sn–Cl4, 110.31(5).

Furthermore, the Sn–C1 distances of **2.12** (Sn–C1: 2.214(5) Å) and **2.7** (Sn–C1: 2.231(2) Å) are identical within 3σ. However, the angles in the coordination sphere of the tin atom are noticeably reduced in **2.12** (Cl1–Sn–Cl2: 165.83(5)°, Cl3–Sn–Cl4: 110.31(5)°) compared to the dimethyl analogue **2.7** (Cl1–Sn–Cl2: 170.59(2)°, C2–Sn–C3: 127.95(11)°), which reflects the lower steric demand of the chlorine atoms in comparison to the methyl groups.

We also performed preliminary experiments concerning the reduction chemistry of the NHC adducts. Reduction of **2.2a** with KC_8 led to the NHC-stabilized stannylene $Me_2Im^{Me}{\cdot}SnMe_2$ (**2.13**) as a yellow solid in 67 % yield (Scheme 2.5). However, analogous experiments with the NHCs $i Pr_2Im^{Me}$ and $Dipp_2Im$ or reduction of the adducts **2.2b** and **2.2c**, respectively, were unsuccessful. The ^1H NMR spectrum of **2.13** reveals strongly shifted methyl group resonances (SnC*H*$_3$, 0.73 ppm; NCC*H*$_3$, 1.31 ppm; NC*H*$_3$, 3.19 ppm) compared to the adduct **2.2a** (SnC*H*$_3$, 0.05 ppm; NCC*H*$_3$, 1.59 ppm; NC*H*$_3$, 3.66 ppm), and the $^{13}C\{^1H\}$ NMR carbene carbon resonance was shifted from 160.0 ppm (**2.2a**) to 183.4 ppm (**2.13**).

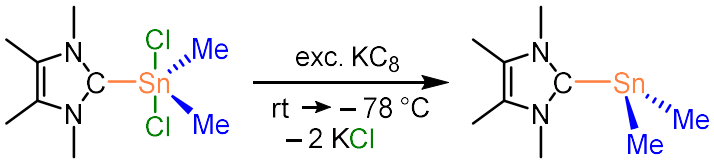

2.2a **2.13**

Scheme 2.5: Synthesis of $Me_2Im^{Me}{\cdot}SnMe_2$ (**2.13**).

Most significant, a resonance at −83.3 ppm was recorded for **2.13** in the $^{119}Sn\{^1H\}$ NMR spectrum, clearly downfield-shifted compared to the signal observed for $Me_2Im^{Me}{\cdot}SnCl_2Me_2$ (δ_{119Sn} = −222.5 ppm), but also downfield-shifted compared to closely related NHC adducts of diarylsubstituted stannylenes $Et_2Im^{Me}SnAr_2$ (Ar = Ph, δ_{119Sn} = −121.0 ppm; Ar = Trip, δ_{119Sn} = −150.7 ppm) reported previously.[17]

The molecular structure of **2.13** (Figure 2.7) confirms stannylene formation. Crystals of **2.13** suitable for X-ray diffraction were obtained by slow evaporation of a concentrated solution in toluene at room temperature. Stannylene **2.13** crystallizes in the orthorhombic space group *Pnma* with one molecule in the asymmetric unit, and a crystallographically imposed mirror plane runs through the tin atom and NHC plane. The molecular structure clearly reveals a trigonal pyramidal coordination at tin with almost ideal perpendicular angles (C1−Sn−C2: 93.33(11)° and C2−Sn−C2': 95.66(18)°) and is thus isostructural to the literature known stannylenes.[17,18] The NHC σ-orbital (occupied sp²-hybrid orbital) is donating into the vacant stannylene p-orbital and thus stabilizes the stannylene. The Sn−C1 distance 2.316(4) Å lies in the upper range of other NHC-stabilized organo-substituted stannylenes (Sn–C1: 2.230(2) – 2.295(2) Å).[17,18]

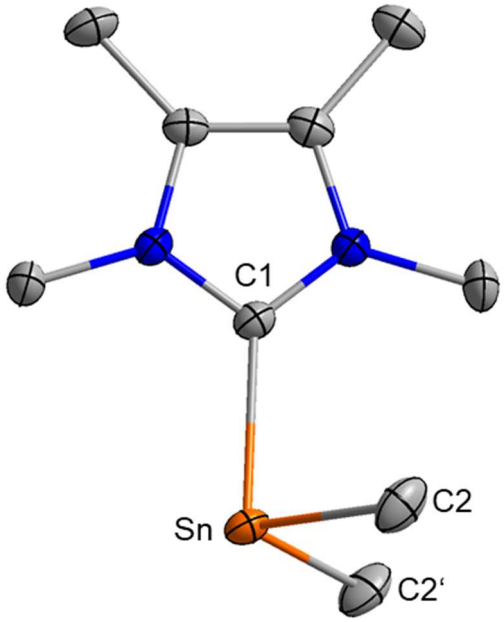

2.13

Figure 2.7: Molecular structure of $Me_2Im^{Me}{\cdot}SnMe_2$ (**2.13**) in the solid-state. Hydrogen atoms are omitted for clarity. Atomic displacement ellipsoids are set at 50 % probability and Dipp groups are shown as wire-and-stick model. Symmetry generated atoms and their associated values are indicated with ^{Sym}. Selected bond lengths [Å] and angles [°]: **2.13**: Sn–C1, 2.316(4); Sn–C2 = Sn–C2', 2.212(3); C1–Sn–C2 = C1–Sn–C2', 93.33(11); C2–Sn–C2', 95.66(18).

Furthermore, we also attempted to synthesize the stannylene $cAAC^{Me}{\cdot}SnMe_2$ *via* metallic reduction in analogy to **2.13**. The reduction of **2.7** with KC_8 (Scheme 2.6) quickly led to a red colored reaction mixture, which completely decolorized after a short

time and turned pale brown at room temperature. We failed so far to isolate the unstable red intermediate, but obtained a colorless crystal suitable for X-ray diffraction (Figure 2.8) after cooling a reaction mixture in toluene shortly after the onset of the red coloration to −78 °C, filtration at this temperature and storage of the resulting solution at −30 °C.

The molecular structure revealed the formation of a stannylene-stannane adduct cAAC^{Me}·SnMe$_2$·SnMe$_2$Cl$_2$ (**2.14**), which can also be regarded as a push-pull-stabilized stannylene, i.e., the stannylene SnMe$_2$ is stabilized by the donor cAAC^{Me} and the acceptor SnMe$_2$Cl$_2$.

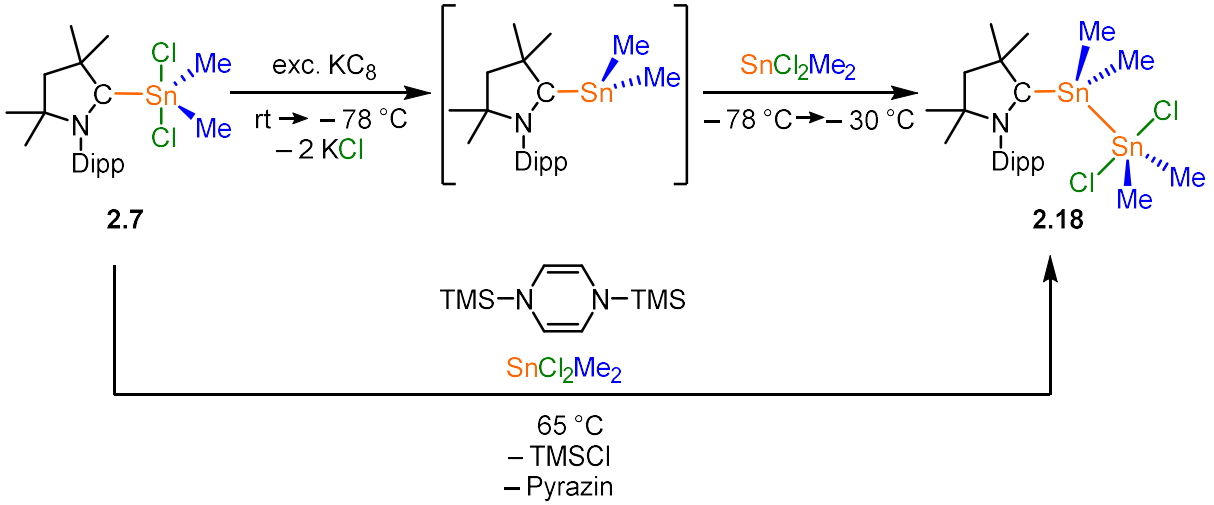

Scheme 2.6: *In situ* formation of cAAC^{Me}·SnMe$_2$ by reduction of cAAC^{Me}·SnMe$_2$Cl$_2$ (**2.7**) with excess KC$_8$ and subsequent stabilization of the intermediate cAAC^{Me}·SnMe$_2$ with SnMe$_2$Cl$_2$ to form cAAC^{Me}·SnMe$_2$·SnMe$_2$Cl$_2$ (**2.14**) (top). Reduction of cAAC^{Me}·SnMe$_2$Cl$_2$ (**2.7**) with 1,4-bis(trimethylsilyl)-1,4-dihydropyrazin in the presence of SnMe$_2$Cl$_2$ to form cAAC^{Me}·SnMe$_2$·SnMe$_2$Cl$_2$ (**2.14**) (bottom).

Compound **2.14** crystallizes in the triclinic space group $P\bar{1}$, with one molecule in the asymmetric unit. The stannylene center Sn1 is tetrahedral coordinated by two methyl groups, the cAAC^{Me} ligand and one molecule SnMe$_2$Cl$_2$. The Sn1–C1 bond length (2.243(3) Å) is longer than the two single bonds between tin and the methyl substituents (Sn1–C2: 2.148(3) Å, Sn1–C3: 2.147(3) Å). The tin(IV) atom Sn2 is trigonal bipyramidal coordinated, with Sn1 and the methyl substituents in equatorial positions. The Sn1–Sn2 bond length is 2.7667(3) Å, which is similar to Sn–Sn distances observed for other distannanes, for example Sn$_2$H$_4$Trip$_2$ (Sn1–Sn2: 2.7449(2) Å; Figure 2.1, **2.C**; R^1 = H).[17b]

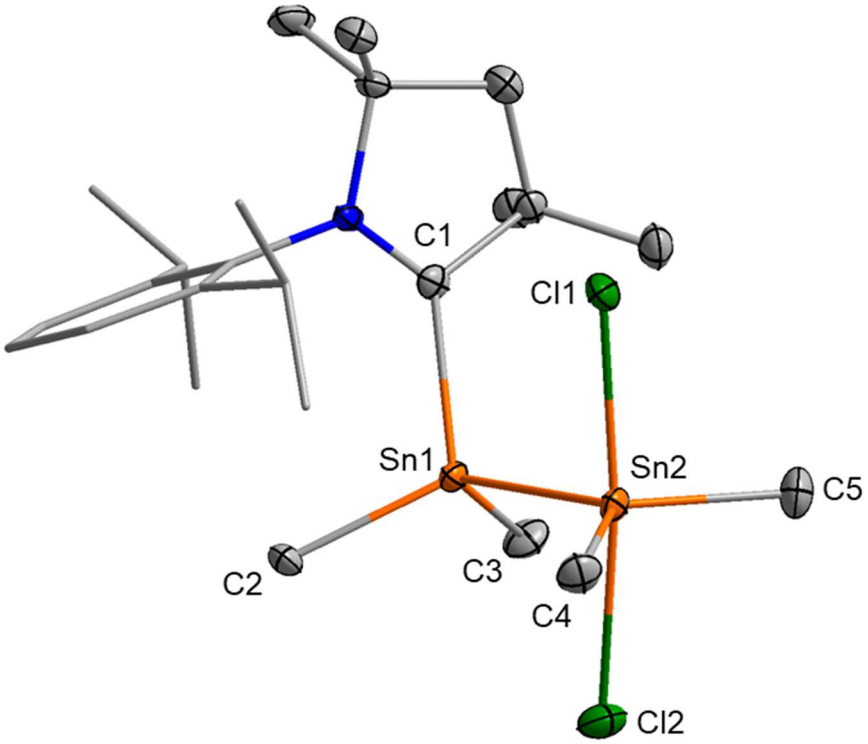

2.14

Figure 2.8: Molecular structure of cAAC^{Me}·SnMe$_2$·SnCl$_2$Me$_2$ (**2.14**), in the solid-state. Hydrogen atoms and solvent molecules (benzene) are omitted for clarity. Atomic displacement ellipsoids are set at 50 % probability and Dipp groups are shown as wire-and-stick model. Selected bond lengths [Å] and angles [°]: **2.14**: Sn1–C1, 2.243(3); Sn1–C2, 2.148(3); Sn1–C3, 2.147(3); Sn1–Sn2, 2.7667(3); Sn2–Cl1, 2.5714(7); Sn1–Cl2, 2.6684(8); Sn1–C4, 2.133(3); Sn1–C5, 2.136(3); C1–Sn1–C2, 111.01(12); C2–Sn1–C3, 107.30(13); C1–Sn1–C3, 106.02(7); Cl1–Sn2–Cl2, 173.08(3); C4–Sn2–C5, 114.99(14).

As metallic reduction failed for the isolation of cAAC^{Me}·SnMe$_2$ (which most likely causes the red color) compound cAAC^{Me}·SnMe$_2$·SnMe$_2$Cl$_2$ (**2.14**) was prepared by reacting the red solution with another equivalent SnCl$_2$Me$_2$ (see 7.5 Synthetic Prodcedures for Chapter II). Furthermore, we discovered that 1,4-bis(trimethylsilyl)-1,4-dihydropyrazin is a suitable reductant for cAAC^{Me}·SnMe$_2$Cl$_2$ (**2.7**), which led to isolation of **2.14** in good yield (Scheme 2.6) and to characterization of the compound by using NMR and IR spectroscopy, as well as elemental analysis. In the ^{1}H NMR spectrum of **2.14**, two broad resonances were observed for the stannylene methyl substituents at 0.24 ppm and a sharp singlet at 0.96 ppm for the chlorostannane methyl protons. Two sets of tin satellites were detected for the latter, with ^2J-coupling of the methyl protons with ^{119}Sn ($^2J_{H\text{-}119Sn}$ = 67.8 Hz) and ^{117}Sn ($^2J_{H\text{-}117Sn}$ = 64.9 Hz) to the stannane tin atom and ^3J-coupling to the stannylene tin atom with coupling

constants of 11.3 Hz ($^3J_{H\text{-}117Sn}$ = $^3J_{H\text{-}119Sn}$ = 11.3 Hz). The ^{119}Sn{^{1}H} NMR spectrum of **2.14** (Figures 2.S45 and 2.S46) shows two signals for the two tin atoms, the resonance of the stannylene tin atom was observed at −120.6 ppm and is therefore only slightly downfield shifted compared to the signal of the stannane tin atom at −127.1 ppm.

Both signals show satellite sets with a $^1J_{119Sn\text{-}117Sn}$-coupling constant of 9492 Hz. Furthermore, an AB system was observed for the ^{119}Sn satellites, from which a $^1J_{119Sn\text{-}119Sn}$ coupling constant of 9910 Hz emerged. To precisely determine the $^1J_{119Sn\text{-}119Sn}$ coupling constant, the corresponding ^{119}Sn{^{1}H} NMR spectrum was simulated based on the experimentally determined coupling constants (Figure 2.S46), which also allowed the identification of the position of the signals of the AB system with very low intensity.

2.3 Conclusion

We present here a study on the synthesis, spectroscopic properties and molecular structures of various NHC-stabilized Ge(IV) and Sn(IV) adducts. The synthesis of NHC·ECl_2Me_2 (**2.1a**-**2c**) was performed by the reaction of ECl_2Me_2 (E = Ge, Sn), with the NHCs Me_2Im^{Me} (**a**), *i*Pr_2Im^{Me} (**b**) and $Dipp_2Im$ (**c**), respectively. The reaction of Me_2Im^{Me} with $GeCl_4$ and *i*Pr_2Im^{Me} with $SnCl_4$ in THF led to different coordinated adducts (trigonal bipyramidal: Me_2Im^{Me}·$GeCl_4$ (**2.3**); octahedral: *i*Pr_2Im^{Me}·$SnCl_4$·THF (**2.4**)). Thermal treatment of the NHC adduct **2.1c** led to formation of an isomer salt with abnormally coordinated NHC $[^aDipp_2Im{\cdot}GeClMe_2]^+[Cl]^-$ (**2.5**). The reaction of $cAAC^{Me}$ with ECl_2Me_2 (E = Ge, Sn) and $GeCl_2Ph_2$, respectively, afforded the adducts $cAAC^{Me}$·$GeCl_2Me_2$ (**2.6**), $cAAC^{Me}$·$SnCl_2Me_2$ (**2.7**) and $cAAC^{Me}$·$GeCl_2Ph_2$ (**2.8**). In contrast to similar reactions with NHCs, the reaction of $cAAC^{Me}$ with $GeClMe_3$ and $GeCl_4$ led to formation of the salts $[cAAC^{Me}GeMe_3]^+[Cl]^-$ (**2.9**) and $[cAAC^{Me}Cl]^+[GeCl_3]^-$ (**2.10**), respectively. Unlike the synthesis of **2.10**, both the isostructural salt $[cAAC^{Me}Cl]^+[SnCl_3]^-$ (**2.11**) and the adduct $cAAC^{Me}$·$SnCl_4$ (**2.12**) were isolated from the reaction of $cAAC^{Me}$ with $SnCl_4$. Starting from Me_2Im^{Me}·$SnCl_2Me_2$ (**2.2a**), the stannylene Me_2Im^{Me}·$SnMe_2$ (**2.13**) was obtained by reduction with KC_8. Analogous reduction of $SnCl_2Me_2$ in the presence of *i*Pr_2Im^{Me} or $Dipp_2Im$ as well as reduction of the adducts **2.2b** and **2.2c**, respectively, was unsuccessful. In contrast, the reduction of **2.7** resulted in an unstable stannylene, which was stabilized by an additional equivalent of $SnCl_2Me_2$ to afford $cAAC^{Me}$·$SnMe_2$·$SnMe_2Cl_2$ (**2.14**).

2.4 References

[1] a) W. A. Herrmann, C. Köcher, *Angew. Chem. Int. Ed.* **1997**, *36*, 2162-2187; *Angew. Chem.* **1997**, *109*, 2256-2282; b) P. P. Power, *Chem. Rev.* **1999**, *99*, 3463-3504; c) D. Bourissou, O. Guerret, F. P. Gabbai, G. Bertrand, *Chem. Rev.* **2000**, *100*, 39-92; d) F. E. Hahn, M. C. Jahnke, *Angew. Chem. Int. Ed.* **2008**, *47*, 3122-3172; *Angew. Chem.* **2008**, *120*, 3166-3216; e) T. Dröge, F. Glorius, *Angew. Chem. Int. Ed.* **2010**, *49*, 6940-6952; *Angew. Chem.* **2010**, *122*, 7094-7107; f) Y. Wang, G. H. Robinson, *Inorg. Chem.* **2011**, *53*, 12326-12337; g) M. N. Hopkinson, C. Richter, M. Schedler, F. Glorius, *Nat. Chem.* **2014**, *510*, 485-496; h) Y. Wang, G. H. Robinson, *Inorg. Chem.* **2014**, *53*, 11815-11832; i) S. Würtemberger-Pietsch, U. Radius, T. B. Marder, *Dalton Trans.* **2016**, *45*, 5880-5895; j) V. Nesterov, D. Reiter, P. Bag, P. Frisch, R. Holzner, A. Porzelt, S. Inoue, *Chem. Rev.* **2018**, *118*, 9678-9842; k) A. Doddi, M. Peters, M. Tamm, *Chem. Rev.* **2019**, *119*, 6994-7112.

[2] a) M. Melaimi, M. Soleilhavoup, G. Bertrand, *Angew. Chem. Int. Ed.* **2010**, *49*, 8810-8849; *Angew. Chem.* **2010**, *122*, 8992-9032; b) M. Soleilhavoup, G. Bertrand, *Acc. Chem. Res.* **2015**, *48*, 256-266; c) M. Melaimi, R. Jazzar, M. Soleilhavoup, G. Bertrand, *Angew. Chem. Int. Ed.* **2017**, *56*, 10046-10068; *Angew. Chem.* **2017**, *129*, 10180-10203; d) U. S. Paul, U. Radius, *Chem. Eur. J.* **2017**, *23*, 3993-4009; e) U. S. D. Paul, M. J. Krahfuß, U. Radius, *Chem. unserer Zeit* **2019**, *53*, 212-223.

[3] a) R. Dorta, E. D. Stevens, N. M. Scott, C. Costabile, L. Cavallo, C. D. Hoff, S. P. Nolan, *J. Am. Chem. Soc.* **2005**, *127*, 2485-2495; b) S. Diez-Gonzalez, S. P. Nolan, *Coord. Chem. Rev.* **2007**, *251*, 874-883; c) A. Poater, B. Cosenza, A. Correa, S. Giudice, F. Ragone, V. Scarano, L. Cavallo, *Eur. J. Inorg. Chem.* **2009**, 1759-1766; d) H. Clavier, S. P. Nolan, *Chem. Commun.* **2010**, *46*, 841-861; e) C. Lujan, S. P. Nolan, *J. Organomet. Chem.* **2011**, *696*, 3935-3938; f) O. Back, M. Henry-Ellinger, C. D. Martin, D. Martin, G. Bertrand, *Angew. Chem. Int. Ed.* **2013**, *52*, 2939-2943; *Angew. Chem.* **2013**, *125*, 3011-3015; g) A. Liske, K. Verlinden, H. Buhl, K. Schaper, C. Ganter, *Organometallics* **2013**, *32*, 5269-5272; h) D. J. Nelson, S. P. Nolan, *Chem. Soc. Rev.* **2013**, *42*, 6723-6753; i) K. Verlinden, H. Buhl, W. Frank, C. Ganter, *Eur. J. Inorg. Chem.* **2015**, 2416-2425;

j) S. V. C. Vummaleti, D. J. Nelson, A. Poater, A. Gomez-Suarez, D. B. Cordes, A. M. Z. Slawin, S. P. Nolan, L. Cavallo, *Chem. Sci.* **2015**, *6*, 1895-1904; k) K. C. Mondal, S. Roy, B. Maity, D. Koley, H. W. Roesky, *Inorg. Chem.* **2016**, *55*, 163-169; l) U. S. D. Paul, U. Radius, *Eur. J. Inorg. Chem.* **2017**, 3362-3375; m) H. V. Huynh, *Chem. Rev.* **2018**, *118*, 9457-9492; n) D. Munz, *Organometallics* **2018**, *37*, 275-289.

[4] a) D. Schmidt, J. H. J. Berthel, S. Pietsch, U. Radius, *Angew. Chem. Int. Ed.* **2012**, *51*, 8881-8885; *Angew. Chem.* **2012**, *124*, 9011-9015; b) P. Hemberger, A. Bodi, J. H. Berthel, U. Radius, *Chem. Eur. J.* **2015**, *21*, 1434-1438; c) H. Schneider, D. Schmidt, U. Radius, *Chem. Eur. J.* **2015**, *21*, 2793-2797.

[5] H. Schneider, M. J. Krahfuß, U. Radius, *Z. Anorg. Allg. Chem.* **2016**, *642*, 1282-1286.

[6] a) C. J. Carmalt, A. H. Cowley, *Adv. Inorg. Chem.* **2000**, 50, 1-32; b) N. Kuhn, A. Al-Sheikh, *Coord. Chem. Rev.* **2005**, *249*, 829-857; c) C. E. Willans, in *Organomet. Chem.* **2010**, *36*, 1-28; d) G. Prabusankar, A. Sathyanarayana, P. Suresh, C. N. Babu, K. Srinivas, B. P. R. Metla, *Coord. Chem. Rev.* **2014**, *269*, 96-133; e) K. C. Mondal, S. Roy, H. W. Roesky, *Chem. Soc. Rev.* **2016**, *45*, 1080-1111.

[7] a) N. Kuhn, T. Kratz, D. Bläser, R. Boese, *Chem. Ber.* **1995**, *128*, 245-250; b) Y. Wang, Y. Xie, P. Wei, R. B. King, H. F. Schaefer III, R. P. v. Schleyer, G. H. Robinson, *Science* **2008**, *321*, 1069-1071; c) R. S. Ghadwal, H. W. Roesky, S. Merkel, J. Henn, D. Stalke, *Angew. Chem. Int. Ed.* **2009**, *48*, 5683-5686; *Angew. Chem.* **2009**, *121*, 5793-5796; d) Y. Wang, G. H. Robinson, *Inorg. Chem.* **2011**, *50*, 12326-12337; e) T. Böttcher, B. S. Bassil, L. Zhechkov, T. Heine, G.-V. Röschenthaler, *Chem. Sci.* **2013**, *4*, 77-83; f) T. Böttcher, S. Steinhauer, B. Neumann, H. G. Stammler, G. V. Röschenthaler, B. Hoge, *Chem. Commun.* **2014**, *50*, 6204-6206; g) F. Uhlemann, R. Köppe, A. Schnepf, *Z. Anorg. Allg. Chem.* **2014**, *640*, 1658-1664; h) F. Uhlemann, A. Schnepf, *Chem. Eur. J.* **2016**, *22*, 10748-10753.

[8] K. C. Mondal, H. W. Roesky, A. C. Stückl, F. Ehret, W. Kaim, B. Dittrich, B. Maity, D. Koley, *Angew. Chem. Int. Ed.* **2013**, *52*, 11804-11807; *Angew. Chem.* **2013**, *125*, 12020-12023.

[9] a) P. A. Rupar, V. N. Staroverov, P. J. Ragogna, K. M. Baines, *J. Am. Chem. Soc.* **2007**, *129*, 15138-15139; b) K. C. Thimer, S. M. Al-Rafia, M. J. Ferguson, R. McDonald, E. Rivard, *Chem. Commun.* **2009**, 7119-7121; c) A. C. Filippou, O. Chernov, B. Blom, K. W. Stumpf, G. Schnakenburg, *Chem. Eur. J.* **2010**, *16*, 2866-2872; d) A. J. Ruddy, P. A. Rupar, K. J. Bladek, C. J. Allan, J. C. Avery, K. M. Baines, *Organometallics* **2010**, *29*, 1362-1367; e) N. Katir, D. Matioszek, S. Ladeira, J. Escudie, A. Castel, *Angew. Chem. Int. Ed.* **2011**, *50*, 5352-5355; *Angew. Chem.* **2011**, *123*, 5464-5467; f) Y. Li, K. C. Mondal, H. W. Roesky, H. Zhu, P. Stollberg, R. Herbst-Irmer, D. Stalke, D. M. Andrada, *J. Am. Chem. Soc.* **2013**, *135*, 12422-12428; g) B. Lyhs, D. Bläser, C. Wölper, S. Schulz, R. Haack, G. Jansen, *Inorg. Chem.* **2013**, *52*, 7236-7241.

[10] a) B. Bantu, G. M. Pawar, U. Decker, K. Wurst, A. M. Schmidt, M. R. Buchmeiser, *Chem. Eur. J.* **2009**, *15*, 3103-3109; b) A. P. Singh, P. P. Samuel, K. C. Mondal, H. W. Roesky, N. S. Sidhu, B. Dittrich, *Organometallics* **2013**, *32*, 354-357.

[11] a) P. A. Rupar, V. N. Staroverov, K. M. Baines, *Organometallics* **2010**, *29*, 4871-4881; b) T. Böttcher, B. S. Bassil, G. V. Röschenthaler, *Inorg. Chem.* **2012**, *51*, 763-765; c) I. S. M. Al-Rafia, P. A. Lummis, A. K. Swarnakar, K. C. Deutsch, M. J. Ferguson, R. McDonald, E. Rivard, *Aust. J. Chem.* **2013**, *66*, 1235-1245; d) J. Sinclair, G. Dai, R. McDonald, M. J. Ferguson, A. Brown, E. Rivard, *Inorg. Chem.* **2020**, *59*, 10996-11008.

[12] N. Kuhn, C. Maichle-Mößmer, E. Niquet, I. Walker, *Z. Naturforsch. B* **2002**, *57*, 47-52.

[13] a) G. Horrer, M. J. Krahfuss, K. Lubitz, I. Krummenacher, H. Braunschweig, U. Radius, *Eur. J. Inorg. Chem.* **2020**, 281-291; b) G. Horrer, I. Krummenacher, S. Mann, H. Braunschweig, U. Radius, *Dalton Trans.* **2022**, *51*, 11054-11071.

[14] J. B. Waters, Q. Chen, T. A. Everitt, J. M. Goicoechea, *Dalton Trans.* **2017**, *46*, 12053-12066.

[15] C. Gendy, J. M. Rautiainen, A. Mailman, H. M. Tuononen, *Chem. Eur. J.* **2021**, *27*, 14405-14409.

[16] a) A. S. Romanov, M. Bochmann, *Organometallics* **2015**, *34*, 2439-2454; b) M. S. M. Philipp, U. Radius, *Z. Anorg. Allg. Chem.* **2022**, e202200085.

[17] a) A. Schäfer, M. Weidenbruch, W. Saak, S. Pohl, *J. Chem. Soc., Chem. Commun.* **1995**, 1157-1158; b) C. P. Sindlinger, L. Wesemann, *Chem. Sci.* **2014**, *5*, 2739-2746.

[18] a) T. G. Kocsor, D. Matioszek, G. Nemes, A. Castel, J. Escudie, P. M. Petrar, N. Saffon, I. Haiduc, *Inorg. Chem.* **2012**, *51*, 7782-7787; b) C. P. Sindlinger, W. Grahneis, F. S. Aicher, L. Wesemann, *Chem. Eur. J.* **2016**, *22*, 7554-7566.

Chapter III

Activation of Ge–H and Sn–H bonds with *N*-Heterocyclic Carbenes and a Cyclic (Alkyl)(amino)carbene

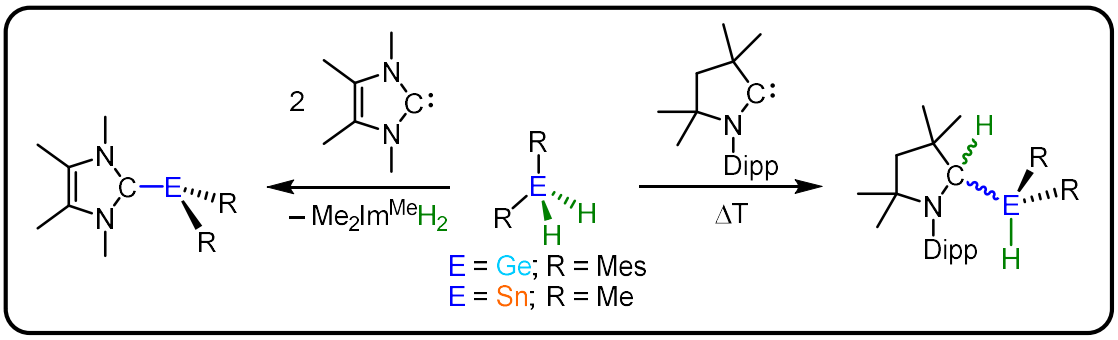

3 Activation of Ge–H and Sn–H bonds with *N*-Heterocyclic Carbenes and a Cyclic (Alkyl)(amino)carbene

3.1 Introduction

N-heterocyclic carbenes (NHCs)[1] and the related cyclic (Alkyl)(amino)carbenes (cAACs)[1j, 2] are first class ligands for a large variety of molecules and render reactivities in main group element chemistry which would not be feasible without this particular ligand support. Their electronic and steric properties can be precisely adjusted depending on the substitution pattern of the carbene.[3] Our group has been working on the synthesis and the reactivity of various carbene-stabilized main group element compounds in the recent years[4] including the reactivity of NHCs towards several group 14 compounds.[5]

This work originates from our previous studies on the reactivity of group 14 element hydrides with different NHCs.[5a, 5b, 5d] We demonstrated earlier that NHCs react with the silicon hydrides SiH_3Ph, SiH_2Ph_2 and $SiHPh_3$ with insertion of silylene moieties into the C–N bond of the NHCs, which leads to ring expansion (RER = ring expansion reaction) of the NHC and formation of diaza-silinanes **3.A**-**3.C** (Scheme 3.1).[5a] RERs were feasible using primary, secondary and tertiary silanes $Ph_{4-n}SiH_n$ and a variety of NHCs, i.e. saturated and unsaturated NHCs with *N*-alkyl and *N*-aryl substituents. In the meantime, we[4a, 4b, 4d-f, 5a, 6] and others (for the elements Be[7], B[8], Al[8g, 9] and Si[10]) demonstrated that RERs are rather general processes in NHC main group chemistry. The products isolated are typically six-membered heterocycles which were formed *via* C–N bond cleavage within the NHC, migration of two hydrogen atoms to the (former) NHC-carbene-carbon atom and formal insertion of a subvalent (e.g. a silylene) moiety into the C–N bond. For the reaction of Ph_3SiH even migration of a phenyl group was observed.[5a]

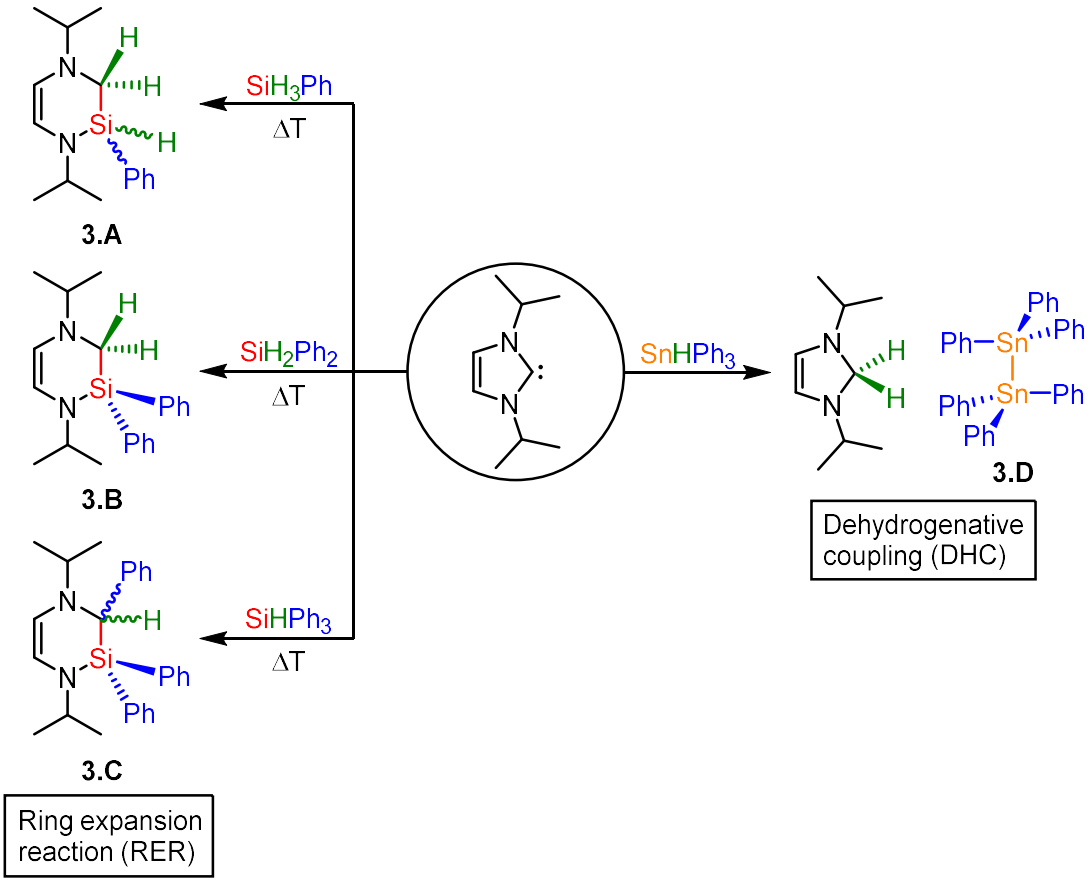

Scheme 3.1: Previous work from our group on the reactivity of group 14 element hydrides with *i*Pr$_2$Im.

Bertrand *et al.* reported prior to our work the insertion of cAAC^{Cy} (cAAC^{Cy} = 2-azaspiro[4.5]dec-2-(2,6-di-*iso*-propylphenyl)-3,3-dimethyl-1-ylidene) into the Si−H bond of different silanes leading to stable cAAC insertion products, for example cAAC^{Cy}H−SiHPh$_2$ from the equimolar reaction of cAAC^{Cy} with SiH$_2$Ph$_2$.[11]

For the reaction of the NHCs *i*Pr$_2$Im and *i*Pr$_2$Im^{Me} with the higher homologue SnHPh$_3$ a completely different reaction pathway was observed, which led not to SnAr$_2$ insertion but to NHC-mediated dehydrogenative coupling (DHC) of the stannane with formation of the hexaaryl distannane Ph$_6$Sn$_2$ **3.D** and the aminal NHCH$_2$ (Scheme 3.1).[5d] We[5d, 12] and others[13] demonstrated that NHCs are very good hydrogen acceptors and that NHC-mediated DHC may be used on a preparative scale for element element bond formation, as for example for the synthesis of NHC-phosphinidene adducts, for diphosphines and cyclic oligophosphines.[12]

Wesemann and co-workers exploited NHC-mediated DHC in tin chemistry rather systematically and demonstrated in their beautiful work that the reaction of the

diarylstannanes SnH_2Ar_2 (Ar = Ph, Trip; Trip = 2,4,6-tri-*iso*-propylphenyl) with Et_2Im^{Me} (Et_2Im^{Me} = 1,3-diethyl-4,5-dimethyl-imidazolin-2-ylidene) or Me_2Im^{Me} as the hydrogen acceptor lead to the formation of different reaction products, depending on the tin hydride and the stoichiometry used (Figure 3.1).

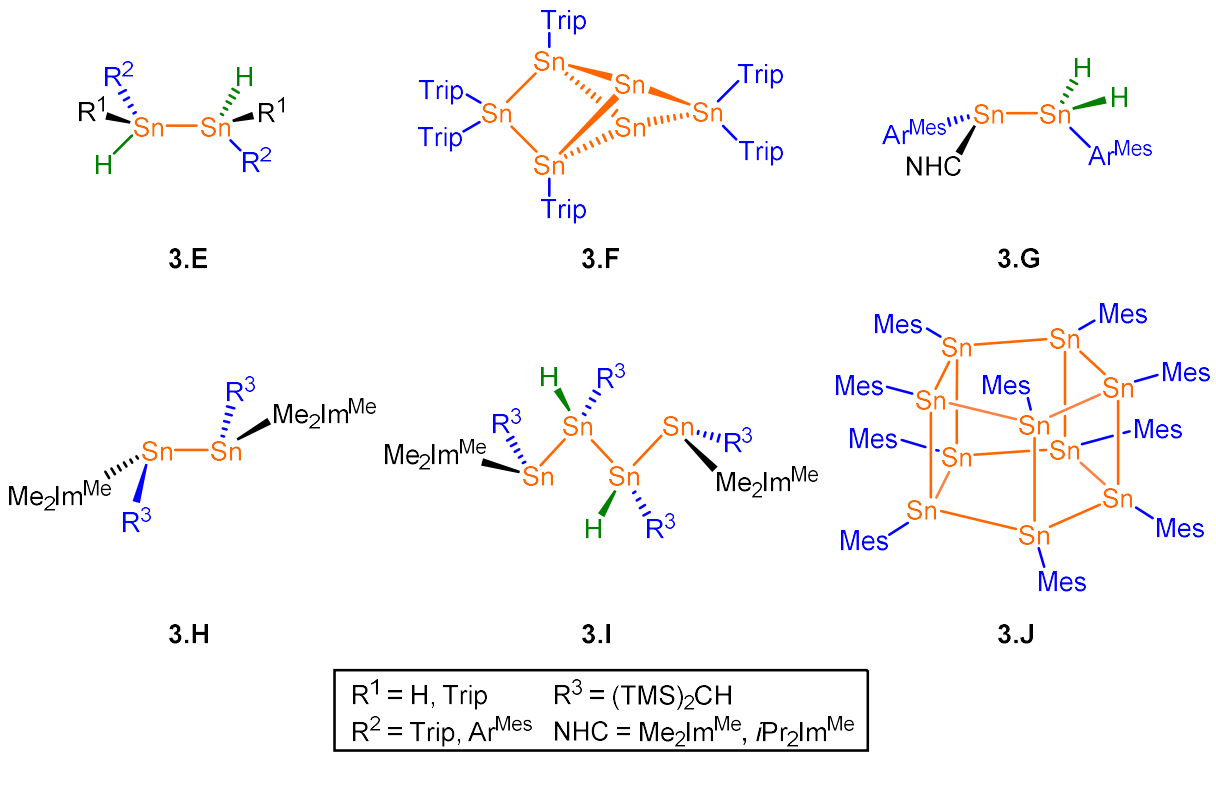

Figure 3.1: NHC-mediated dehydrogenative Sn−Sn coupling.

Using a 2:1 ratio of SnH_2Trip_2:Et_2Im^{Me}, the tetraorganyl distannane $Sn_2H_2Trip_4$ (Figure 3.1, **3.E**; R^1 = Trip,) was obtained from NHC-mediated DHC, whereas from a 1:2 ratio SnH_2Ar_2:Et_2Im^{Me} the NHC-stabilized stannylenes Et_2Im^{Me}·$SnAr_2$ (Ar = Ph, Trip) were formed.[14] Similarly, the reaction of Me_2Im^{Me} with SnH_2Trip_2 afforded the NHC-stabilized stannylene Me_2Im^{Me}·$SnTrip_2$.[15] Analogous reactions of the mono-organyl stannane SnH_3Trip with different NHCs (NHC = Et_2Im^{Me}, Me_2Im^{Me}) led to the corresponding NHC-stabilized stannylenes NHC·SnHTrip.[14,16] At a ratio of 1:1.5 (SnH_3Trip:Et_2Im^{Me}) the reaction yielded the interesting tin cluster Sn_6Trip_6 (Figure 3.1, **3.F**).[14] Reacting the backbone methylated NHCs Me_2Im^{Me} and iPr_2Im^{Me} (1,3-di-*iso*-propyl-4,5-dimethyl-imidazolin-2-ylidene) with SnH_3Ar^{Mes} (Ar^{Mes} = 2,6-dimesitylphenyl, mesityl = 2,4,6-trimethylphenyl) in a ratio of 1:2 (SnH_3Ar^{Mes}:NHC) afforded the stannylene NHC·$SnHAr^{Mes}$, whereas the stannyl-stannylenes

$Ar^{Mes}Sn(NHC)SnH_2Ar^{Mes}$ (Figure 3.1, **3.G**) were formed by using a ratio of 1:1.5 (SnH_3Ar^{Mes}:NHC). The latter was exploited for the reaction with another equivalent of $Ar^{Mes}SnH_3$, which gave the distannane $Sn_2H_4Ar^{Mes}_2$ (Figure 3.1, **3.E**; R^1 = H, R^2 = Ar^{Mes}) with loss of $NHCH_2$.[17] Furthermore, the Me_2Im^{Me} induced DHC of the mono-organyl stannane SnH_3R (R = $CH(SiMe_3)_2$) offered a wide range of interesting compounds, such as the dialkyl distannyne $R^3_2Sn_2(Me_2Im^{Me})_2$ (Figure 3.1, **3.H**; R^3 = $CH(SiMe_3)_2$) and the tin chain $(Me_2Im^{Me}{\cdot}SnR^3{-}SnHR^3)_2$ (Figure 3.1, **3.I**), depending on the reaction conditions. A very interesting neutral Sn_{10} cluster, $(SnMes)_{10}$ (Figure 3.1, **3.J**), was obtained from the Et_2Im^{Me}-mediated DHC of SnH_3Mes.[18] In addition, the NHC-stabilized stannylene *i*$Pr_2Im^{Me}{\cdot}SnHTbb$ as well as the germylenes $Me_2Im^{Me}{\cdot}GeHR$ (R = 2,6-$Trip_2C_6H_3$, Tbb; Tbb = 2,6-$(CH(SiMe_3)_2)_2$-4-(*t*Bu)C_6H_2) were isolated starting from the corresponding stannane or germane EH_3R and a NHC.[19] However, with the latter exception the reactivity of NHCs with respect to germanium hydrides is rather unexplored and mainly restricted on the formation of NHC germanium hydride adducts from the corresponding NHC germanium chloride adducts.[8a,20,21] With respect of our investigations on the RER of silicon hydrides we were interested in the reactivity of NHCs with similar germanium and tin hydrides and report here first results on the reactivity of various carbenes towards hydride compounds of the heavier tetreles.

3.2 Results and Discussion

Briefly after our report on RER several groups reported theoretical investigations on the reaction mechanism of the ring expansion, based on our original proposal.[5b, 8g, 10b, 22] This mechanism can be in principle divided into four steps, which involve the adduct formation between the *Lewis*-basic NHC and the *Lewis*-acidic hydride, the hydride migration from the main group element hydride to the carbene carbon atom, C−N bond cleavage and ring expansion of the NHC with insertion of the main group element unit into the NHC ring, and a potential stabilization of the ring-expanded NHC by migration of substituents or by additional coordination of a *Lewis*-base, like an NHC. Wilson and Dutton *et al.* presented a theoretical study on the detailed reaction pathway and indicated that formation of C–H bonds is the crucial factor in the over-all transformation, resulting in an exothermic process.[22a] For SiH_2Ph_2 and Me_2Im, the insertion of the NHC into the Si-H bond was calculated to be the rate determining step, associated with a barrier of 113.4 kJ/mol at the M06-2x/6-31G(d) (optimized geometries)//MP2/TZVP (single-point energy) level of theory. Furthermore, these authors stated that the trends observed in the reaction energetics were largely independent of the method (SCS-MP2, PBE1PBE, M06-2x) and basis set used (6-31G(d), TZVP), with deviations from the MP2/TZVP reaction energetics of less than 5 kJ/mol. Similarly, calculations with solvent effects (toluene) had only minimal influence on the geometries and energies obtained (±5 kJ/mol). After that, this group presented variations of these calculations for beryllium and boron hydrides and for the carbene employed.[22b,c,e,g-i] This mechanism was also confirmed by work of other groups, although on different occasions the C−N bond cleavage and ring expansion of NHC was calculated to be the rate-determining step.[22d] Of interest for this work were calculations presented by Su, who evaluated the potential-energy surfaces for the ring-expansion reactions of $i Pr_2Im$ with EH_2Ph_2 (E = C, Si, Ge, Sn, Pb) at the M06-2x/def2-TZVP level of theory.[22f

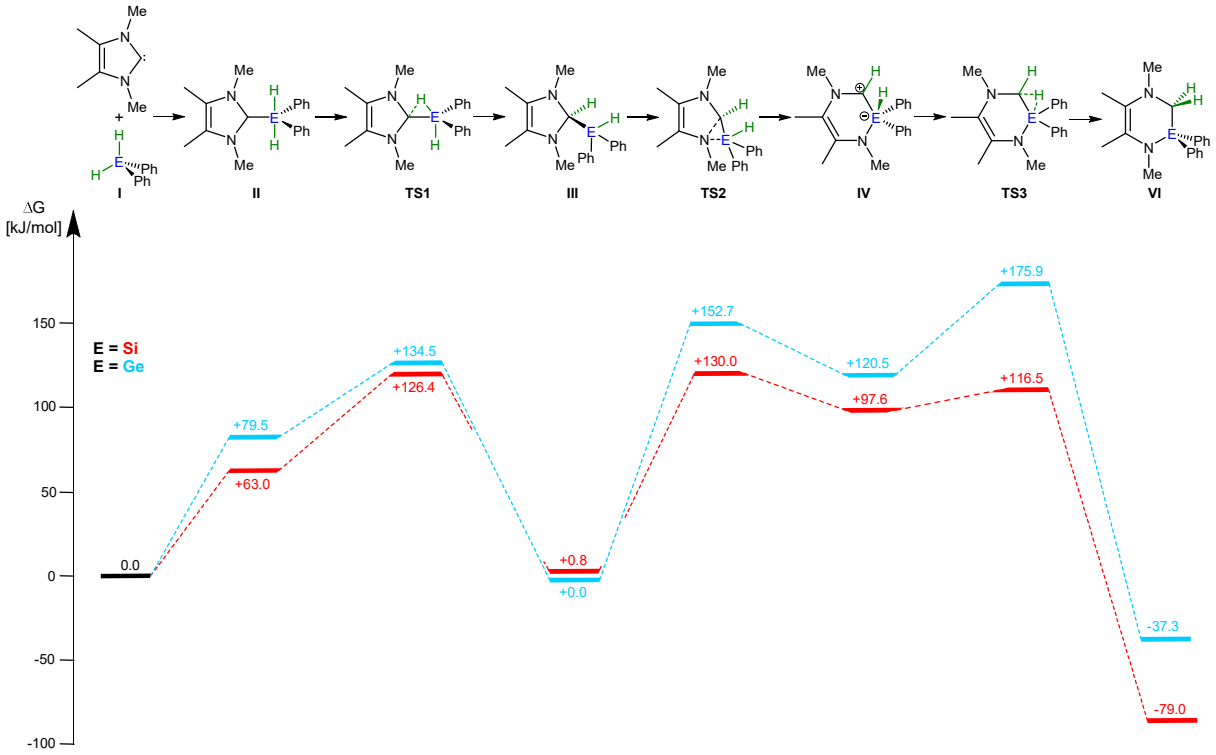

Figure 3.2: Molecular structures free energy profile (kJ/mol) for the RER of Me_2Im^{Me} and EH_2Ph_2 (E = Si, Ge; TURBOMOLE, M06-2x//def2-TZVPP).

These investigations suggested that the reactivity of the EH_2Ph_2 molecule that undergoes the ring-expansion reaction decreases in the order $SiH_2Ph_2 \approx GeH_2Ph_2 \approx SnH_2Ph_2 > PbH_2Ph_2 \gg CH_2Ph_2$. They also indicated that both the electronic structure and steric effects play a crucial role for the reactivity. As steric effects certainly influence the reactivity within these systems, we set out to compare the RER of the methyl-substituted NHC Me_2Im^{Me} with EH_2Ph_2 (E = Si, Ge) in some detail, and the results of the calculations performed on these systems at the M06-2x//def2-TZVPP level of theory are provided in Figure 3.2.

The calculations revealed for the reaction of the NHC Me_2Im^{Me} with SiH_2Ph_2 that an initial, endothermic adduct $Me_2Im^{Me}{\cdot}SiH_2Ph_2$ **II**, five-coordinated at silicon and repulsive on the energy hyper surface by 63.0 kJ/mol, is formed. The corresponding adduct $Me_2Im^{Me}{\cdot}GeH_2Ph_2$ lies +79.5 kJ/mol above the starting materials. The crucial transition state **TS1** for the hydrogen atom transfer can be described as an NHC-H-$EHPh_2$ σ-complex, which lies 126.4 kJ/mol (Si) and 134.5 kJ/mol (Ge) higher in energy compared to the starting material. This barrier agrees with the experimentally observed

high temperature conditions for the RER using the silane. The insertion product **III** lies for both, SiH_2Ph_2 and GeH_2Ph_2, within the error of the calculations at the same energy level as the starting materials. The reaction profiles for SiH_2Ph_2 and GeH_2Ph_2 then differ significantly as the pathway after the formation of adduct **III** shows considerable higher barriers for the reaction of GeH_2Ph_2. The transition state **TS2** for amide transfer is calculated to be +22.7 kJ/mol higher in energy (130.0 kJ/mol, Si, vs. 152.7 kJ/mol, Ge), and the energetically very high transition state **TS3** for the hydride shift from Ge to the former NHC carbene carbon atom of 175.9 kJ/mol (instead of 116.5 kJ/mol calculated for the reaction of SiH_2Ph_2) should prevent RER for the Ge system at ambient temperatures. Therefore, another reaction pathway can be predicted, which must be evaluated experimentally.

Reaction of different carbenes with GeH_2Mes_2

We started our experimental investigations with the reaction of GeH_2Mes_2[23] and $cAAC^{Me}$ (Scheme 3.2). Since no reaction was observed at room temperature, the reaction mixture was heated to 85 °C overnight. Monitoring of the reaction by ^1H NMR spectroscopy revealed full conversion into a new compound, the cAAC insertion product into the Ge–H bond $cAAC^{Me}H–GeHMes_2$ (**3.1**, Scheme 3.2). A similar insertion of $cAAC^{Cy}$ into the Si−H bond of different silanes was reported previously by Bertrand *et al.*, leading to stable $cAAC^{Cy}$ insertion products such as $cAAC^{Cy}H−SiHPh_2$.[11] Compound **3.1** was isolated in 77 % yield by recrystallization from a saturated solution of **3.1** in *n*-hexane. This molecule is stable at room temperature for several weeks in solution and in the solid-state.

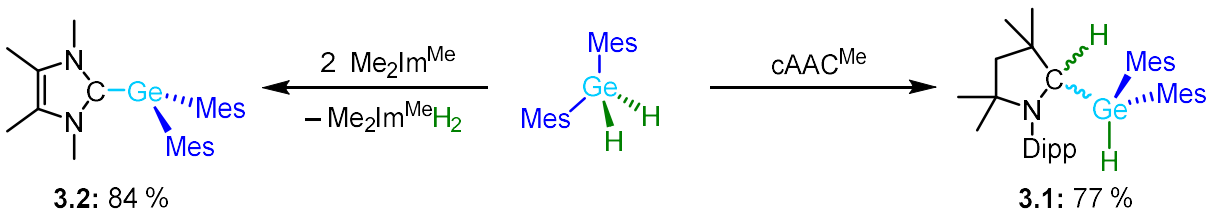

Scheme 3.2: Reaction of $cAAC^{Me}$ and Me_2Im^{Me} with GeH_2Mes_2.

In the ^{1}H NMR spectrum of **3.1** a splitting of the signal sets of the cAAC ligand was observed, which is characteristic for an asymmetric substitution at the cAAC carbene carbon atom. For instance, two doublets were detected for the C*H*$_2$ group of the cAAC^{Me} at 1.72 ppm and 2.23 ppm with a coupling constant of 12.4 Hz. Additional evidence for the insertion of the carbon atom into the Ge−H bond arises from the occurrence of two doublets at 4.66 ppm and 5.95 ppm (NC*H*N and Ge*H*) with a mutual coupling constant of 6.6 Hz. In the ^{1}H,^{13}C{^{1}H} HSQC-NMR spectrum of **3.1** the signal at 5.95 ppm does not show cross coupling, which indicates bonding of one proton to the germanium atom. The signal at 4.66 ppm exhibits a strong coupling to the NCC(*C*H$_3$)$_2$ carbon atoms and a weak coupling to the *C*H$_2$ carbon atom, which proofs binding of the proton to the former carbene carbon atom. In addition, a band was detected at 2056 cm^{-1} in the IR spectrum of **3.1**, which is characteristic for a Ge−H stretching vibration and shifted hypsochromic compared to the precursor GeH$_2$Mes$_2$ ($\nu_{Ge\text{-}H}$ = 2040 cm^{-1}).[24]

Crystals of **3.1** suitable for X-ray diffraction were obtained from cooling an at room temperature saturated solution in *n*-hexane to −30 °C. Compound **3.1** crystallizes as a racemic mixture in the monoclinic space group *P*2$_1$/*c* with one molecule in the asymmetric unit (Figure 3.3). The solid-state structure confirms the insertion of the cAAC into the Ge−H bond. The Ge−C1 of 2.051(2) Å is unexceptional. The two hydrogen atoms at Ge and C1 are aligned *anti* to each other in the solid-state. This *anti* alignment might be forced due to the steric repulsion of the mesityl groups and the substituents of cAAC^{Me}.

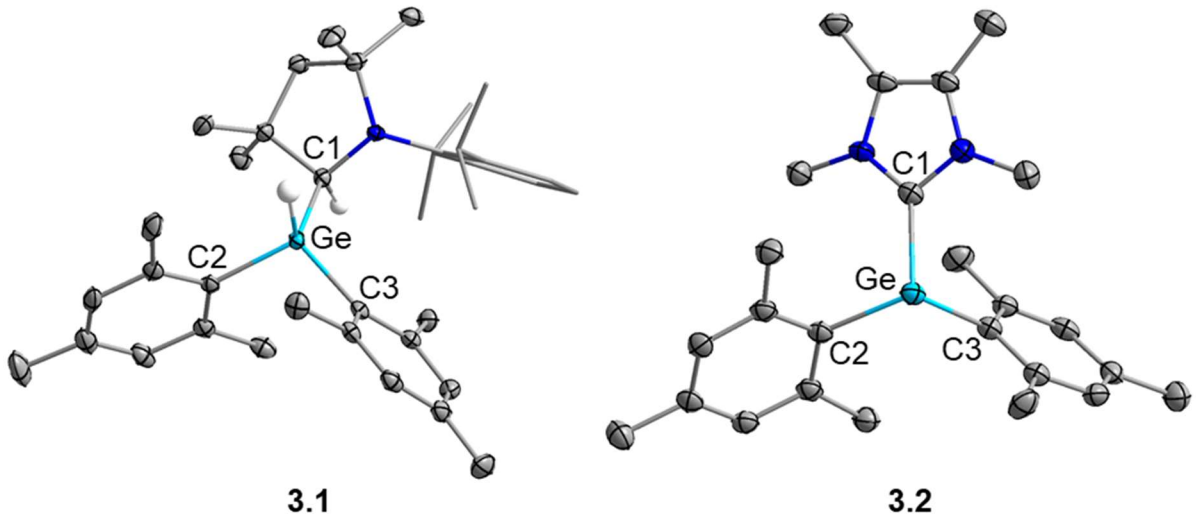

Figure 3.3: Molecular structures of cAAC^{Me}H–GeHMes$_2$ (**3.1**, left) and Me$_2$Im^{Me}·GeMes$_2$ (**3.2**, right), in the solid-state. Hydrogen atoms and one enantiomer of the racemic mixture of **3.1** are omitted for clarity. Atomic displacement ellipsoids are set at 50 % probability, the Dipp substituent of **3.1** is shown as wire-and-stick model. Selected bond lengths [Å] and angles [°]: **3.1**: Ge–C1, 2.026(2); Ge–C2, 1.989(2); Ge–C3, 1.997(2); C1–Ge–C2, 112.78(8); C2–Ge–C3, 107.06(8); C1–Ge–C3, 120.49(8); **3.2**: Ge–C1, 2.051(2); Ge–C2, 2.029(2); Ge–C3, 2.036(2); C1–Ge–C2, 103.96(9); C2–Ge–C3, 110.82(10); C1–Ge–C3, 97.63(9); N–C1–Ge-C3: 124.201(236)°.

GeH$_2$Mes$_2$ was also reacted with the NHCs Me$_2$Im^{Me}, *i*Pr$_2$Im^{Me} and Dipp$_2$Im. No reaction occurred with the bulkier *i*Pr$_2$Im^{Me} and Dipp$_2$Im, whereas heating of GeH$_2$Mes$_2$ with two equivalents Me$_2$Im^{Me} to 65 °C in benzene led to full conversion into Me$_2$Im^{Me}·GeMes$_2$ (**3.2**) after 10 days (Scheme 3.2). After removal of all volatile material including the side product Me$_2$Im^{Me}H$_2$, the NHC stabilized germylene was isolated in 84 % yield. Me$_2$Im^{Me}·GeMes$_2$ (**3.2**) was synthesized before, and the NMR and IR spectroscopic data are in accordance with those reported in the literature.[25] In addition, we obtained single crystals of **3.2** suitable for X-ray diffraction by slow evaporation of a concentrated toluene solution of **3.2** at room temperature. In contrast to the orthorhombic structure reported by Baines and co-workers,[25] **3.2** crystallizes in our case in the monoclinic space group *P*2$_1$/*c* (Figure 3.3).

However, there are no significant differences in the bond lengths with the reported structure, the major difference lies in the torsion angle N–C1–Ge–C3, which was reported to be 87.845(307)°)[25] and is significantly larger in our case (N–C1–Ge–C3: 124.201(236)°). Consequently the C2–Ge–C3 angle of 110.82(10)° is slightly larger compared to that reported in the literature (106.60(12)°)[25] due to lower steric repulsion of the mesityl groups with the NHC.

Reaction of carbenes with SnH_2Me_2

As the mesityl groups of GeH_2Mes_2 prevented reactions with the NHCs *i*Pr_2Im^{Me} and $Dipp_2Im$ and the Wesemann group already reported a comprehensive study on the reactivity of NHCs with aryl stannanes (see Introduction), we set out to investigate the reactivity of $cAAC^{Me}$ and the NHCs Me_2Im^{Me}, *i*Pr_2Im^{Me}, and $Dipp_2Im$ towards the steric less protected methyl-substituted stannane SnH_2Me_2. Whereas SiH_2Ph_2 and GeH_2Mes_2 react with cAACs at higher temperatures, the corresponding reaction of $cAAC^{Me}$ with SnH_2Me_2 must be performed at low temperatures to avoid side reactions (see below). The insertion product $cAAC^{Me}H–SnHMe_2$ (**3.3**) was obtained in 77 % yield after workup (Scheme 3.3).

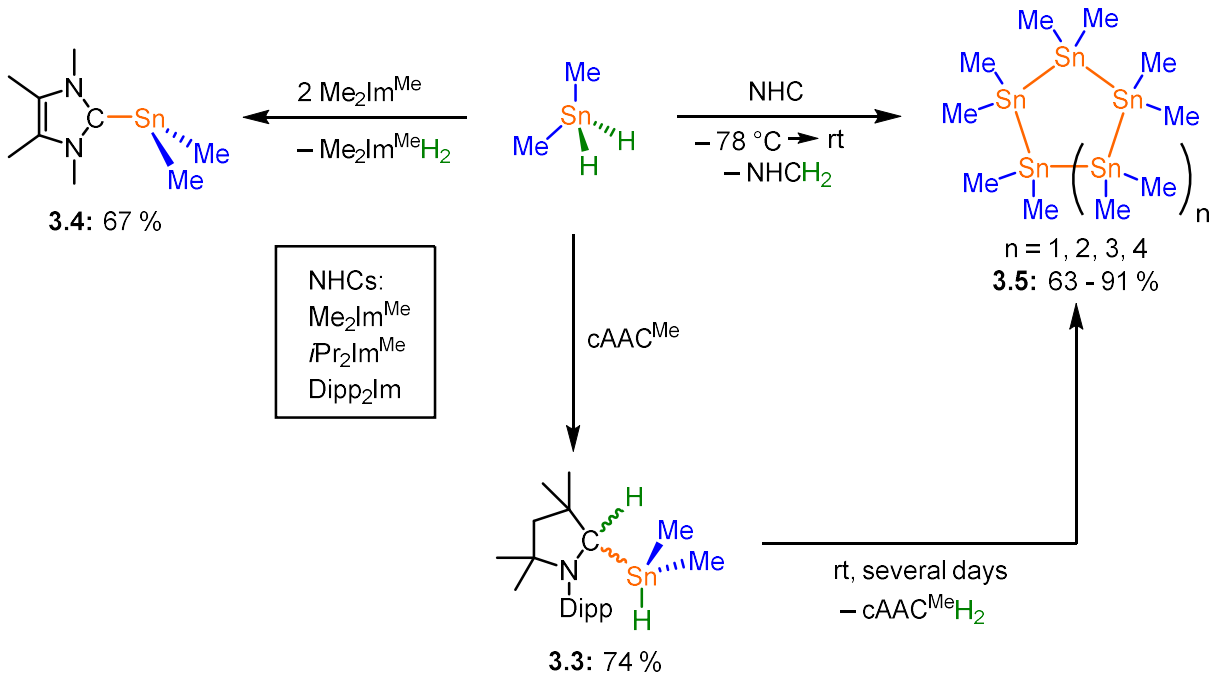

Scheme 3.3: Reaction of the NHCs Me_2Im^{Me}, *i*Pr_2Im^{Me}, $Dipp_2Im$ and $cAAC^{Me}$ with SnH_2Me_2.

Compound **3.3** can be stored at −30 °C for several weeks but readily decomposes in a controlled manner in solution at room temperature to yield {$SnMe_2$} oligomeric rings **3.5** (see Scheme 3.3 and discussion below). This reaction starts immediately after the isolated product is dissolved in solvents such as benzene, toluene or THF. The reaction typically reaches completeness at room temperature after a few days. Formation of **3.3** from $cAAC^{Me}$ and SnH_2Me_2 was evidenced from NMR spectroscopy. For example, the

methyl groups located at tin became inequivalent in the ^{1}H NMR spectrum of **3.3** leading to two separate doublets, each of them equipped with ^{117}Sn and ^{119}Sn satellites, and a $^{4}J_{H\text{-}H}$ coupling constant of 2.5 Hz. The Sn*H* resonance was detected as a doublet of septets at 5.02 ppm due to coupling to the methyl protons ($^{3}J_{H\text{-}H}$ = 2.5 Hz) and coupling to a single adjacent proton bound to the former carbene carbon atom ($^{3}J_{H\text{-}H}$ = 3.9 Hz). In addition, satellites with a $^{1}J_{H\text{-}117Sn}$ coupling constant of 1588 Hz and a $^{1}J_{H\text{-}119Sn}$ coupling constant of 1661 Hz were observed, which indicated direct bonding of the hydrogen atom to tin. For the proton bound to the carbenic carbon atom, a doublet with a $^{3}J_{H\text{-}H}$ coupling constant of 3.9 Hz was observed at 4.02 ppm with coupling constants to ^{117}Sn and ^{119}Sn of ca. 30.5 Hz each. The cAAC^{Me} moiety gives rise to two sets of resonances due to the asymmetry of the molecule, as observed previously. In the ^{13}C{^{1}H} NMR spectrum a resonance at 72.0 ppm was detected for the former carbene carbon atom, which shows cross-coupling in the ^{1}H,^{13}C{^{1}H} HSQC-NMR spectrum with the proton resonance at 4.02 ppm. The ^{119}Sn NMR spectrum of **3.3** reveals a doublet of multiplets at 139.6 ppm with a coupling constant of 1661 Hz, which collapses upon proton decoupling to a singlet. Furthermore, an IR band at 1805 cm^{-1} was assigned to the Sn−H stretching mode.[17] The solid-state structure of **3.3** (Figure 3.4) also confirms the formation of the insertion product.

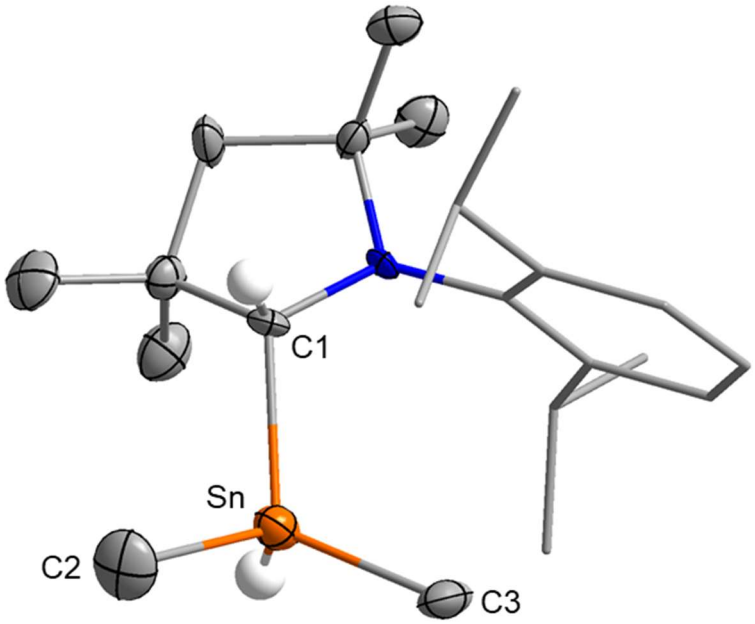

3.3

Figure 3.4: Molecular structure of cAAC^{Me}H-SnHMe$_2$ (**3.3**) in the solid-state. Hydrogen atoms are omitted for clarity. Atomic displacement ellipsoids are set at 50 % probability and the Dipp substituent is shown as wire-and-stick model. Selected bond lengths [Å] and angles [°]: Sn–C1, 2.206(10); Sn–C2, 2.163(13); Sn–C3, 2.147(12); C1–Sn–C2, 104.9(5); C2–Sn–C3, 105.4(5); C1–Sn–C3, 116.9(4).

Compound **3.3** crystallizes in the monoclinic space group *P*2$_1$/*c* with one molecule in the asymmetric unit. The molecular structure reveals tetrahedral coordination of both the C1 carbon atom and the tin atom. The Sn–C bond lengths to the sp^3 carbon atoms are identical within 3σ (Sn–C1: 2.206(10) Å; Sn–C2: 2.163(13) Å and Sn–C3: 2.147(12) Å) and are in accordance with C–Sn single bonds. The hydrogen atoms at Sn and C1 are arranged *anti* to each other in the solid-state, presumably due to steric effects, as already observed for the related germanium compound **3.1**.

The reaction of SnH$_2$Me$_2$ with two equivalents of Me$_2$Im^{Me} at room temperature led to the formation of the aminal Me$_2$Im^{Me}H$_2$ and the NHC-stabilized stannylene Me$_2$Im^{Me}·SnMe$_2$ (**3.4**) (Scheme 3.3). As the aminal Me$_2$Im^{Me}H$_2$ is volatile the separation is easy, and the reaction yielded **3.4** as a yellow solid in 67 % isolated yield. Me$_2$Im^{Me}·SnMe$_2$ (**3.4**) can also be synthesized *via* the metallic reduction of Me$_2$Im^{Me}·SnMe$_2$Cl$_2$, which was reported – including the molecular structure of the compound (Figure 2.7) – just recently by us.[5e]

The reaction of SnH_2Me_2 with one of the larger NHCs *i*Pr_2Im^{Me} and $Dipp_2Im$ at low temperature did not lead to formation of NHC-stabilized stannylenes analogous to **3.4**. Instead, the formation of an in toluene sparingly soluble yellow solid and the corresponding aminal $NHCH_2$ was observed (Scheme 3.3). Similarly, if only one equivalent of Me_2Im^{Me} is used instead of the two equivalents used for the synthesis of **3.4**, the same yellow solid was formed, which was isolated by simple filtration in yields of 63 – 91%, depending on the NHC used. The ^{1}H NMR spectrum of this product showed only one multiplet at 0.53 ppm for equivalent methyl groups and no resonance for the NHCs used for synthesis.

The ^{119}Sn{^{1}H} NMR spectrum of C_6D_6 solutions of the soluble products of this reaction revealed three resonances at −246.4 ppm, −244.6 ppm, and −242.7 ppm (major component). A similar mixture was reported by Neumann et al.[26] previously, obtained from the equimolar condensation of SnH_2Me_2 and $SnMe_2(NEt_2)_2$. These resonances there were assigned at that time to the *cyclo*-pentamer (δ_{119Sn} = −241.4 ppm) and the cyclo-heptamer or *cyclo*-octamer (δ_{119Sn} = −243.4 ppm, −244.9 ppm). In addition, Neumann et al. observed an additional product leading to a broad and significantly more intense resonance at −231 ppm, which was assigned to the *cyclo*-hexamer. Later on, Wrackmeyer *et al.* pointed out that the intensity pattern of the ^{117}Sn satellites (2:2:1) of the signal at −241.4 ppm would correspond to the *cyclo*-hexamer.[27] Consistently, this would mean that the resonance at −231 ppm should be associated with the *cyclo*-pentamer or another oligomeric or polymeric compound.

Therefore, we assign our resonances to the *cyclo*-heptamer, the *cyclo*-octamer (−246.4 ppm, −244.6 ppm), and the *cyclo*-hexamer (−242.7 ppm) as the main products of the solution. Even with high resolution ^{119}Sn{^{1}H} NMR experiments we were not able to resolve different resonances or use coupling constants to clarify the assignment of the *cyclo*-heptamer and the *cyclo*-octamer to the corresponding signals.

As the tin *cyclo*-oligomers were reported to be well soluble substances in various hydrocarbons,[26] we further investigated the poorly soluble yellow solid by using solid-state NMR spectroscopy. In both the ^{1}H DP/MAS and ^{13}C{^{1}H} CP/MAS solid-state NMR spectra a singlet was detected at 0.92 and −10.4 ppm, respectively, for the methyl groups. In contrast to the ^{119}Sn{^{1}H} NMR investigations in solution, only one signal was detected at −226.0 ppm in the ^{119}Sn{^{1}H} CP/MAS solid-state NMR

spectrum. As the NMR shifts obtained from solution NMR and solid-state NMR are often difficult to compare, the only conclusion that can be made is that the yellow solid contains only one product of (nearly) equivalent tin atoms. Interestingly, the yellow solid dissolves completely after heating in benzene to 80 °C for a few seconds. In addition to the resonances obtained for the solution of the product, as discussed above, new broad resonances were detected in the ^{1}H and ^{119}Sn{^{1}H} NMR spectra of the resulting solution at 0.64 ppm (^{1}H NMR) and −232.4 ppm (^{119}Sn{^{1}H} NMR), respectively. We attribute the latter to the *cyclo*-pentamer and assume that the ^{119}Sn solid-state NMR resonance at −226.0 ppm is the signal of the *cyclo*-pentamer. Note that the resonances typically observed for chain oligomers or polymers, i. e. alkyl-substituted polystannanes, are typically observed in the range between −172.2 ppm to −194.8 ppm in their solution ^{119}Sn NMR spectra.[28] Thus, the *cyclo*-pentamer *cyclo*-$(SnMe_2)_5$ seems to be the favored product of the DHC of SnH_2Me_2 with the NHCs Me_2Im^{Me}, iPr_2Im^{Me}, and $Dipp_2Im$ (isolation in 63 – 91% yield). Unfortunately, we could not obtain crystals of this product suitable for X-ray diffraction or meaningful high-res mass-spec data of this product.

Interestingly, a mixture of *cyclo*-stannanes can also be obtained from the decomposition of $cAAC^{Me}H–SnHMe_2$ (**3.3**). We noted before that **3.3** easily decomposes in a controlled manner, and the reaction products of this decomposition are *cyclo*-stannanes and $cAAC^{Me}H_2$, which can be easily detected in the ^{1}H NMR spectrum. However, for the DHC using $cAAC^{Me}H–SnHMe_2$ (**3.3**) only the *cyclo*-heptamer, the *cyclo*-octamer (−246.4 ppm, −244.6 ppm), and the *cyclo*-hexamer (−242.7 ppm) were formed.

As oligomer mixtures were obtained from the DHC of SnH_2Me_2 using one equivalent of the NHC Me_2Im^{Me}, iPr_2Im^{Me} and $Dipp_2Im$ at room temperature or by heating a benzene solution of compound **3.3** to 80 °C overnight, we assume that insertion products of the carbene into the Sn–H bond and reductive elimination of $NHCH_2$ and/or $cAACH_2$ play a major role in the formation of these tin *cyclo*-oligomers of different sizes.

3.3 Conclusion

This work is based on our previous studies on the reactivity of silicon element hydrides SiH_3Ph, SiH_2Ph_2 and $SiHPh_3$ with different NHCs, which led to the formation of diaza-silinanes with insertion of silylene moieties into the C–N bond of the NHCs and RER of the NHC, and on DFT calculations on the RER of Me_2Im^{Me} with EH_2Ph_2 (E = Si, Ge), which predicted a different reaction path for the germane. Therefore, we investigated the reactivity of several different NHCs and the cyclic (alkyl)(amino)carbene $cAAC^{Me}$ the tetrel hydrides GeH_2Mes_2 and SnH_2Me_2 of the higher congeners of silicon.

The reaction of GeH_2Mes_2 with $cAAC^{Me}$ led to insertion of the cAAC carbene carbon atom into one of the Ge–H bond and formation of $cAAC^{Me}H–GeHMes_2$ (**3.1**). Similar insertion products of $cAAC^{Cy}$ into the Si−H bond of silanes was reported previously by Bertrand and co-workers. The reaction of GeH_2Mes_2 with two equivalents of Me_2Im^{Me} at elevated temperatures led to complete dehydrogenation of GeH_2Mes_2. One equivalent of the NHC acts as excellent hydrogen acceptor and yielded $NHCH_2$, the other equivalent NHC stabilizes the resulting germylene $GeMes_2$ to yield $Me_2Im^{Me}{\cdot}GeMes_2$ (**3.2**). The reaction of SnH_2Me_2 with $cAAC^{Me}$ afforded in analogy to selected silicon and germanium hydrides the insertion product $cAAC^{Me}H–SnHMe_2$ (**3.3**). Dehydrogenation of SnH_2Me_2 by using Me_2Im^{Me} also led to the formation of a NHC-stabilized stannylene, i.e. $Me_2Im^{Me}{\cdot}SnMe_2$ (**3.4**). Using just one equivalent or the sterically more demanding NHCs iPr_2Im^{Me} and $Dipp_2Im$ afforded dehydrogenative coupling of the *in situ* formed {$SnMe_2$} moieties to tin *cyclo*-oligomers $(SnMe_2)_n$ (**3.5**) (n = 6, 7, 8). The formation of the *cyclo*-pentamer *cyclo*-$(SnMe_2)_5$ seems to be the dominant product of this reaction and the compound was isolated in 63 to 91% yield. A mixture of cyclostannanes was also obtained from the decomposition of $cAAC^{Me}H–SnHMe_2$ (**3.3**) with formation of $cAAC^{Me}H_2$. We were not successful to obtain oligomer mixtures starting from the isolated NHC-stabilized stannylene $Me_2Im^{Me}{\cdot}SnMe_2$ (**3.4**), which contrasts the situation observed for phosphines.[12] The dehydrogenative coupling of primary and secondary phosphines with NHCs afforded diphosphines $R_2P–PR_2$ for secondary phosphines and mixtures of NHC phosphinidene adducts NHC=PAr and cyclic oligophosphines P_4Ar_4, P_5Ar_5 and P_6Ar_6, depending on the stoichiometry used. The NHC phosphinidene adducts can act as synthons for the phosphinidene moieties {PAr}, which oligomerize in an equilibrium

to give the *cyclo*-oligophosphines. As this reactivity was not observed for the NHC stannylene **3.4**, we currently assume that insertion products of the carbene into the Sn–H bond and reductive elimination of $NHCH_2$ and/or $cAACH_2$ with liberation of $SnMe_2$ and subsequent oligomerization or more complex reaction mechanisms play a major role in the formation of the tin *cyclo*-oligomers of different sizes.

3.4 References

[1] a) W. A. Herrmann, C. Köcher, *Angew. Chem. Int. Ed.* **1997**, *36*, 2162-2187; *Angew. Chem.* **1997**, *109*, 2256-2282; b) P. P. Power, *Chem. Rev.* **1999**, *99*, 3463-3504; c) D. Bourissou, O. Guerret, F. P. Gabbai, G. Bertrand, *Chem. Rev.* **2000**, *100*, 39-92; d) F. E. Hahn, M. C. Jahnke, *Angew. Chem. Int. Ed.* **2008**, *47*, 3122-3172; *Angew. Chem.* **2008**, *120*, 3166-3216; e) T. Dröge, F. Glorius, *Angew. Chem. Int. Ed.* **2010**, *49*, 6940-6952; *Angew. Chem.* **2010**, *122*, 7094-7107; f) Y. Wang, G. H. Robinson, *Inorg. Chem.* **2011**, *50*, 12326-12337; g) M. N. Hopkinson, C. Richter, M. Schedler, F. Glorius, *Nat. Chem.* **2014**, *510*, 485-496; h) Y. Wang, G. H. Robinson, *Inorg. Chem.* **2014**, *53*, 11815-11832; i) S. Würtemberger-Pietsch, U. Radius, T. B. Marder, *Dalton Trans.* **2016**, *45*, 5880-5895; j) V. Nesterov, D. Reiter, P. Bag, P. Frisch, R. Holzner, A. Porzelt, S. Inoue, *Chem. Rev.* **2018**, *118*, 9678-9842; k) A. Doddi, M. Peters, M. Tamm, *Chem. Rev.* **2019**, *119*, 6994-7112.

[2] a) M. Melaimi, M. Soleilhavoup, G. Bertrand, *Angew. Chem. Int. Ed.* **2010**, *49*, 8810-8849; *Angew. Chem.* **2010**, *122*, 8992-9032; b) M. Soleilhavoup, G. Bertrand, *Acc. Chem. Res.* **2015**, *48*, 256-266; c) M. Melaimi, R. Jazzar, M. Soleilhavoup, G. Bertrand, *Angew. Chem. Int. Ed.* **2017**, *56*, 10046-10068; *Angew. Chem.* **2017**, *129*, 10180-10203; d) U. S. Paul, U. Radius, *Chem. Eur. J.* **2017**, *23*, 3993-4009; e) U. S. D. Paul, M. J. Krahfuß, U. Radius, *Chemie unserer Zeit* **2019**, *53*, 212-223.

[3] a) R. Dorta, E. D. Stevens, N. M. Scott, C. Costabile, L. Cavallo, C. D. Hoff, S. P. Nolan, *J. Am. Chem. Soc.* **2005**, *127*, 2485-2495; b) S. Diez-Gonzalez, S. P. Nolan, *Coord. Chem. Rev.* **2007**, *251*, 874-883; c) A. Poater, B. Cosenza, A. Correa, S. Giudice, F. Ragone, V. Scarano, L. Cavallo, *Eur. J. Inorg. Chem.* **2009**, 1759-1766; d) H. Clavier, S. P. Nolan, *Chem. Commun.* **2010**, *46*, 841-861; e) C. Lujan, S. P. Nolan, *J. Organomet. Chem.* **2011**, *696*, 3935-3938; f) O. Back, M. Henry-Ellinger, C. D. Martin, D. Martin, G. Bertrand, *Angew. Chem. Int. Ed.* **2013**, *52*, 2939-2943; *Angew. Chem.* **2013**, *125*, 3011-3015; g) A. Liske, K. Verlinden, H. Buhl, K. Schaper, C. Ganter, *Organometallics* **2013**, *32*, 5269-5272; h) D. J. Nelson, S. P. Nolan, *Chem. Soc. Rev.* **2013**, *42*, 6723-6753; i) K. Verlinden, H. Buhl, W. Frank, C. Ganter, *Eur. J. Inorg. Chem.* **2015**,

2416-2425; j) S. V. C. Vummaleti, D. J. Nelson, A. Poater, A. Gomez-Suarez, D. B. Cordes, A. M. Z. Slawin, S. P. Nolan, L. Cavallo, *Chem. Sci.* **2015**, *6*, 1895-1904; k) K. C. Mondal, S. Roy, B. Maity, D. Koley, H. W. Roesky, *Inorg. Chem.* **2016**, *55*, 163-169; l) U. S. D. Paul, U. Radius, *Eur. J. Inorg. Chem.* **2017**, 3362-3375; m) H. V. Huynh, *Chem. Rev.* **2018**, *118*, 9457-9492; n) D. Munz, *Organometallics* **2018**, *37*, 275-289.

[4] a) S. Pietsch, U. Paul, I. A. Cade, M. J. Ingleson, U. Radius, T. B. Marder, *Chem. Eur. J.* **2015**, *21*, 9018-9021; b) S. Würtemberger-Pietsch, H. Schneider, T. B. Marder, U. Radius, *Chem. Eur. J.* **2016**, *22*, 13032-13036; c) M. Eck, S. Würtemberger-Pietsch, A. Eichhorn, J. H. Berthel, R. Bertermann, U. S. Paul, H. Schneider, A. Friedrich, C. Kleeberg, U. Radius, T. B. Marder, *Dalton Trans.* **2017**, *46*, 3661-3680; d) A. F. Eichhorn, S. Fuchs, M. Flock, T. B. Marder, U. Radius, *Angew. Chem. Int. Ed.* **2017**, *56*, 10209-10213; *Angew. Chem.* **2017**, *129*, 10343-10347; e) A. F. Eichhorn, L. Kuehn, T. B. Marder, U. Radius, *Chem. Commun.* **2017**, *53*, 11694-11696; f) H. Schneider, A. Hock, R. Bertermann, U. Radius, *Chem. Eur. J.* **2017**, *23*, 12387-12398; g) A. Hock, H. Schneider, M. J. Krahfuss, U. Radius, *Z. Anorg. Allg. Chem.* **2018**, *644*, 1243-1251; h) H. Schneider, A. Hock, A. D. Jaeger, D. Lentz, U. Radius, *Eur. J. Inorg. Chem.* **2018**, 4031-4043; i) L. Kuehn, M. Stang, S. Würtemberger-Pietsch, A. Friedrich, H. Schneider, U. Radius, T. B. Marder, *Faraday Discuss.* **2019**, *220*, 350-363; j) A. Hock, L. Werner, C. Luz, U. Radius, *Dalton Trans.* **2020**, *49*, 11108-11119; k) A. Hock, L. Werner, M. Riethmann, U. Radius, *Eur. J. Inorg. Chem.* **2020**, 4015-4023; l) S. A. Föhrenbacher, V. Zeh, M. Krahfuss, N. V. Ignat'ev, M. Finze, U. Radius, *Eur. J. Inorg. Chem.* **2021**, 1941-1960; m) M. S. M. Philipp, M. J. Krahfuss, K. Radacki, U. Radius, *Eur. J. Inorg. Chem.* **2021**, 4007-4019; n) M. S. M. Philipp, U. Radius, *Z. Anorg. Allg. Chem.* **2022**, e202200085.

[5] a) D. Schmidt, J. H. J. Berthel, S. Pietsch, U. Radius, *Angew. Chem. Int. Ed.* **2012**, *51*, 8881-8885; *Angew. Chem.* **2012**, *124*, 9011-9015; b) P. Hemberger, A. Bodi, J. H. Berthel, U. Radius, *Chem. Eur. J.* **2015**, *21*, 1434-1438; c) H. Schneider, D. Schmidt, U. Radius, *Chem. Eur. J.* **2015**, *21*, 2793-2797; d) H. Schneider, M. J. Krahfuß, U. Radius, *Z. Anorg. Allg. Chem.* **2016**, *642*, 1282-

1286; e) M. S. M. Philipp, R. Bertermann, U. Radius, *Eur. J. Inorg. Chem.* **2022**, e202200429.

[6] a) M. Eck, S. Würtemberger-Pietsch, A. Eichhorn, J. H. Berthel, R. Bertermann, U. S. Paul, H. Schneider, A. Friedrich, C. Kleeberg, U. Radius, T. B. Marder, *Dalton Trans.* **2017**, *46*, 3661-3680; b) J. Lorkowski, M. Krahfuss, M. Kubicki, U. Radius, C. Pietraszuk, *Chem. Eur. J.* **2019**, *25*, 11365-11374.

[7] a) M. Arrowsmith, M. S. Hill, G. Kociok-Köhn, D. J. MacDougall, M. F. Mahon, *Angew. Chem. Int. Ed.* **2012**, *51*, 2098-2100; *Angew. Chem.* **2012**, *124*, 2140-2142; b) M. Arrowsmith, M. S. Hill, G. Kociok-Köhn, *Organometallics* **2015**, *34*, 653-662.

[8] a) S. M. Al-Rafia, R. McDonald, M. J. Ferguson, E. Rivard, *Chem. Eur. J.* **2012**, *18*, 13810-13820; b) S. K. Bose, K. Fucke, L. Liu, P. G. Steel, T. B. Marder, *Angew. Chem. Int. Ed.* **2014**, *53*, 1799-1803; *Angew. Chem.* **2014**, *126*, 1829-1834; c) T. Wang, D. W. Stephan, *Chem. Eur. J.* **2014**, *20*, 3036-3039; d) J. Lam, B. A. Günther, J. M. Farrell, P. Eisenberger, B. P. Bestvater, P. D. Newman, R. L. Melen, C. M. Crudden, D. W. Stephan, *Dalton Trans.* **2016**, *45*, 15303-15316; e) D. N. Lastovickova, C. W. Bielawski, *Organometallics* **2016**, *35*, 706-712; f) D. N. Lastovickova, C. W. Bielawski, *Catalysts* **2016**, *6*, 141; g) M. D. Anker, A. L. Colebatch, K. J. Iversen, D. J. D. Wilson, J. L. Dutton, L. García, M. S. Hill, D. J. Liptrot, M. F. Mahon, *Organometallics* **2017**, *36*, 1173-1178; h) M. Arrowsmith, J. Böhnke, H. Braunschweig, M. A. Celik, *Angew. Chem. Int. Ed.* **2017**, *56*, 14287-14292; *Angew. Chem.* **2017**, *129*, 14475-14480; i) B. Su, Y. Li, R. Ganguly, R. Kinjo, *Angew. Chem. Int. Ed.* **2017**, *56*, 14572-14576; *Angew. Chem.* **2017**, *129*, 14764-14768; j) J. J. Clarke, P. Eisenberger, S. S. Piotrkowski, C. M. Crudden, *Dalton Trans.* **2018**, *47*, 1791-1795; k) T. Brückner, M. Arrowsmith, M. Hess, K. Hammond, M. Müller, H. Braunschweig, *Chem. Commun.* **2019**, *55*, 6700-6703; l) D. Prieschl, M. Dietz, J. H. Muessig, K. Wagner, I. Krummenacher, H. Braunschweig, *Chem. Commun.* **2019**, *55*, 9781-9784; m) T. Thiess, S. K. Mellerup, H. Braunschweig, *Chem. Eur. J.* **2019**, *25*, 13572-13578; n) D. Prieschl, M. Arrowsmith, M. Dietz, A. Rempel, M. Müller, H. Braunschweig, *Chem. Commun.* **2020**, *56*, 5681-5684; o) L. Englert, U. Schmidt, M. Dömling, M. Passargus, T. E. Stennett, A. Hermann, M. Arrowsmith, M. Härterich, J.

Müssig, A. Phillipps, D. Prieschl, A. Rempel, F. Röhm, K. Radacki, F. Schorr, T. Thiess, J. O. C. Jimenez-Halla, H. Braunschweig, *Chem. Sci.* **2021**, *12*, 9506-9515; p) Z. Guven, L. Denker, H. Dolati, D. Wullschlager, B. Trzaskowski, R. Frank, *Chem. Eur. J.* **2022**, *28*, e202200673; q) W. Lu, A. Jayaraman, F. Fantuzzi, R. D. Dewhurst, M. Härterich, M. Dietz, S. Hagspiel, I. Krummenacher, K. Hammond, J. Cui, H. Braunschweig, *Angew. Chem. Int. Ed.* **2022**, *61*, e202113947; *Angew. Chem.* **2022,** *134*, e202113947.

[9] K. J. Blakeney, P. D. Martin, C. H. Winter, *Organometallics* **2020**, *39*, 1006-1013.

[10] a) W. C. Chen, W. C. Shih, T. Jurca, L. Zhao, D. M. Andrada, C. J. Peng, C. C. Chang, S. K. Liu, Y. P. Wang, Y. S. Wen, G. P. A. Yap, C. P. Hsu, G. Frenking, T. G. Ong, *J. Am. Chem. Soc.* **2017**, *139*, 12830-12836; b) L. Garcia, K. H. M. Al Furaiji, D. J. D. Wilson, J. L. Dutton, M. S. Hill, M. F. Mahon, *Dalton Trans.* **2017**, *46*, 12015-12018.

[11] G. D. Frey, J. D. Masuda, B. Donnadieu, G. Bertrand, *Angew. Chem. Int. Ed.* **2010**, *49*, 9444-9447; *Angew. Chem.* **2010**, *122*, 9634-9637.

[12] a) H. Schneider, D. Schmidt, U. Radius, *Chem. Commun.* **2015**, *51*, 10138-10141; b) L. Werner, G. Horrer, M. Philipp, K. Lubitz, M. W. Kuntze-Fechner, U. Radius, *Z. Anorg. Allg. Chem.* **2021**, *647*, 881-895.

[13] a) G. D. Frey, V. Lavallo, B. Donnadieu, W. W. Schoeller, G. Bertrand, *Science* **2007**, *316*, 439-441; b) D. Martin, M. Soleilhavoup, G. Bertrand, *Chem. Sci.* **2011**, *2*, 389-399; c) M. M. D. Roy, A. A. Omana, A. S. S. Wilson, M. S. Hill, S. Aldridge, E. Rivard, *Chem. Rev.* **2021**, *121*, 12787-12965.

[14] C. P. Sindlinger, L. Wesemann, *Chem. Sci.* **2014**, *5*, 2739-2746.

[15] C. P. Sindlinger, S. Weiss, H. Schubert, L. Wesemann, *Angew. Chem. Int. Ed.* **2015**, *54*, 4087-4091; *Angew. Chem.* **2015**, *127*, 4160-4164.

[16] C. P. Sindlinger, L. Wesemann, *Chem. Commun.* **2015**, *51*, 11421-11424.

[17] C. P. Sindlinger, W. Grahneis, F. S. Aicher, L. Wesemann, *Chem. Eur. J.* **2016**, *22*, 7554-7566.

[18] J. J. Maudrich, C. P. Sindlinger, F. S. Aicher, K. Eichele, H. Schubert, L. Wesemann, *Chem. Eur. J.* **2017**, *23*, 2192-2200.

[19] M. Auer, F. Diab, K. Eichele, H. Schubert, L. Wesemann, *Dalton Trans.* **2022**, *51*, 5950-5961.

[20] a) Y. Xiong, T. Szilvasi, S. Yao, G. Tan, M. Driess, *J. Am. Chem. Soc.* **2014**, *136*, 11300-11303; b) K. Inomata, T. Watanabe, Y. Miyazaki, H. Tobita, *J. Am. Chem. Soc.* **2015**, *137*, 11935-11937; c) T. Fukuda, H. Hashimoto, H. Tobita, *J. Organomet. Chem.* **2017**, *848*, 89-94; d) J. A. Kelly, M. Juckel, T. J. Hadlington, I. Fernandez, G. Frenking, C. Jones, *Chem. Eur. J.* **2019**, *25*, 2773-2785; e) R. J. Mangan, A. Rit, C. P. Sindlinger, R. Tirfoin, J. Campos, J. Hicks, K. E. Christensen, H. Niu, S. Aldridge, *Chem. Eur. J.* **2020**, *26*, 306-315; f) R. J. Mangan, A. R. Davies, J. Hicks, C. P. Sindlinger, A. L. Thompson, S. Aldridge, *Polyhedron* **2021**, *196*, 115006.

[21] a) K. C. Thimer, S. M. Al-Rafia, M. J. Ferguson, R. McDonald, E. Rivard, *Chem. Commun.* **2009**, 7119-7121; b) S. M. Al-Rafia, A. C. Malcolm, S. K. Liew, M. J. Ferguson, R. McDonald, E. Rivard, *Chem. Commun.* **2011**, *47*, 6987-6989; c) S. M. Al-Rafia, A. C. Malcolm, S. K. Liew, M. J. Ferguson, E. Rivard, *J. Am. Chem. Soc.* **2011**, *133*, 777-779; d) I. S. M. Al-Rafia, P. A. Lummis, A. K. Swarnakar, K. C. Deutsch, M. J. Ferguson, R. McDonald, E. Rivard, *Aust. J. Chem.* **2013**, *66*, 1235-1245; e) S. M. Al-Rafia, M. R. Momeni, R. McDonald, M. J. Ferguson, A. Brown, E. Rivard, *Angew. Chem. Int. Ed.* **2013**, *52*, 6390-6395; *Angew. Chem.* **2013**, *125*, 6518-6523; f) S. M. I. Al-Rafia, M. R. Momeni, M. J. Ferguson, R. McDonald, A. Brown, E. Rivard, *Organometallics* **2013**, *32*, 6658-6665; g) M. M. D. Roy, S. Fujimori, M. J. Ferguson, R. McDonald, N. Tokitoh, E. Rivard, *Chem. Eur. J.* **2018**, *24*, 14392-14399; h) J. Sinclair, G. Dai, R. McDonald, M. J. Ferguson, A. Brown, E. Rivard, *Inorg. Chem.* **2020**, *59*, 10996-11008; i) M. Ackermann, M. Seidl, F. Wen, M. J. Ferguson, A. Y. Timoshkin, E. Rivard, M. Scheer, *Chem. Eur. J.* **2021**, 28, e202103780.

[22] a) K. J. Iversen, D. J. Wilson, J. L. Dutton, *Dalton Trans.* **2013**, *42*, 11035-11038; b) K. J. Iversen, D. J. D. Wilson, J. L. Dutton, *Organometallics* **2013**, *32*, 6209-6217; c) M. R. Momeni, E. Rivard, A. Brown, *Organometallics* **2013**, *32*, 6201-6208; d) R. Fang, L. Z. Yang, Q. Wang, *Organometallics* **2014**, *33*, 53-60; e) K. J. Iversen, D. J. Wilson, J. L. Dutton, *Dalton Trans.* **2014**, *43*, 12820-12823; f) M. D. Su, *Inorg. Chem.* **2014**, *53*, 5080-5087; g) K. J. Iversen, D. J. Wilson, J. L. Dutton, *Dalton Trans.* **2015**, *44*, 3318-3325; h) K. J. Iversen, J. L. Dutton, D. J. D. Wilson, *Chem. Asian J.* **2017**, *12*, 1499-1508; i) K. H. M.

Al Furaiji, K. J. Iversen, J. L. Dutton, D. J. D. Wilson, *Chem. Asian J.* **2018**, *13*, 3745-3752.

[23] J. A. Cooke, C. E. Dixon, M. R. Netherton, G. M. Kollegger, R. M. Baines, *Synth. React. Inorg. Met.-Org. Chem.* **1996**, *26*, 1205-1217.

[24] A. Castel, P. Riviere, J. Satge, H. Y. Ko, *Organometallics* **1990**, *9*, 205-210.

[25] A. J. Ruddy, P. A. Rupar, K. J. Bladek, C. J. Allan, J. C. Avery, K. M. Baines, *Organometallics* **2010**, *29*, 1362-1367.

[26] B. Watta, W. P. Neumann, J. Sauer, *Organometallics* **1985**, *4*, 1954-1957.

[27] a) B. Wrackmeyer, in *Tin Chemistry: Fundamentals, Frontiers, and Apllications*, (M. Gielen, A. G. Davies, K. Pannell, E. Tiekink), Wiley-VCH, Weinheim, Germany **1996**, Ch. 2; b) B. Wrackmeyer, U. Klaus, *J. Organomet. Chem.* **1996**, *520*, 211-226.

[28] a) T. Imori, V. Lu, H. Cai, T. D. Tilley, *J. Am. Chem. Soc.* **1995**, *117*, 9931-9940; b) V. Y. Lu, T. D. Tilley, *Macromolecules* **2000**, *33*, 2403-2412; c) F. Choffat, S. Käser, P. Wolfer, D. Schmid, R. Mezzenga, P. Smith, W. Caseri, *Macromolecules* **2007**, *40*, 7878-7889; d) D. Foucher, in *Main Group Strategies towards Functional Hybrid Materials*, (Eds: H. Baumgartner, F. Jäkle), Wiley-VCH, Weinheim, Germany **2018**, ch. 9.

Chapter IV

N-Heterocyclic Carbene and Cyclic (Alkyl)(amino) carbene Adducts of Plumbanes and Plumbylenes

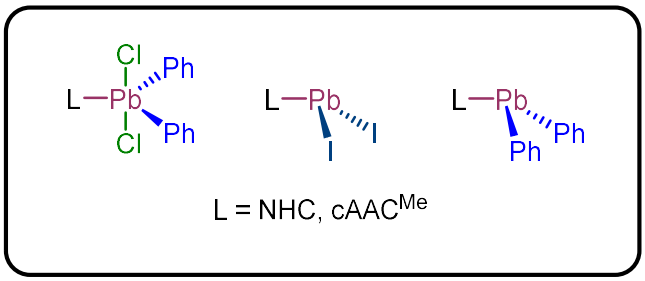

4 *N*-Heterocyclic Carbene and Cyclic (Alkyl)(amino)carbene Adducts of Plumbanes and Plumbylenes

4.1 Introduction

The use of *N*-heterocyclic carbenes (NHCs)[1] and related cyclic (alkyl)(amino)carbenes (cAACs) has led to important developments in main group element chemistry.[1i, 2] Our group has been interested in NHC coordination chemistry and reactivity of the p-block elements over years,[3] lately especially in the chemistry of the heavier p-block elements such as gallium,[4] tin[5] and antimony[6]. Investigations on NHC-supported group 14 elements in general led to a plethora of new compounds and reactivities in recent years,[1g-i, 2c, 7] for example various group 14 element motifs in the oxidation state 0, such as monomeric $(cAAC^{R})_2E$ (R = Me, Cy; E = Si,[8] Ge[9]), the dimeric $(Dipp_2Im)_2E_2$ (E = Si,[10] Ge,[11] Sn[12]) (1,3-bis-(2,6-di-*iso*-propylphenyl)-imidazolin-2-ylidene), $(cAAC^{R})_2Si_2$[13] (R = Me, Cy) and the trimeric $(cAAC^{Me})_3Si_3$.[14] In contrast, the chemistry of carbene-ligated lead compounds is remarkably underdeveloped.

In 1997 Schumann and Tamm *et al.* reported the synthesis of the first carbene-ligated lead compound. The reaction of $[(i\text{PrN})_2C_3Cl]^+[OTf]^-$ with *n*-BuLi led *in situ* to the formation of the bis(dialkylamino)cyclopropenylidene $(i\text{PrN})_2C_3$, which was reacted with $Pb(N(SiMe_3)_2)_2$ to yield the first carbene ligated lead(II) adduct $(i\text{PrN})_2C_3{\cdot}Pb(N(SiMe_3)_2)_2$.[15] In 1999 the group of Weidenbruch reported on the first NHC lead adduct, $i\text{Pr}_2\text{Im}^{Me}{\cdot}\text{PbTrip}_2$ ($i\text{Pr}_2\text{Im}^{Me}$ = 1,3-di-*iso*-propyl-4,5-dimethyl-imidazolin-2-ylidene, Trip = 2,4,6-tri-*iso*-propylphenyl; Figure 4.1, **4.A**) synthesized from the dimeric plumbylene Pb_2Trip_4, which is in equilibrium with its monomer $PbTrip_2$, with $i\text{Pr}_2\text{Im}^{Me}$.[16] However, this compound, isolated in 43 % yield, could only be characterized by X-ray diffraction. It was reported that this adduct is sensitive to light and air, and that it decomposes already as a solid at room temperature. In solution, it was found only stable if an excess of the plumylene was present, and all attempts to record NMR spectra of pure $i\text{Pr}_2\text{Im}^{Me}{\cdot}\text{PbTrip}_2$ have failed because decomposition with formation of 1,3,5-tri-*iso*-propylbenzene occurs even at -70 °C.[16] The Wesemann group later on reported the first lead hydride $Me_2Im^{Me}{\cdot}PbTer^{Trip}H$ (Me_2Im^{Me} = 1,3,4,5-

tetramethyl-imidazolin-2-ylidene; Figure 4.1, **4.B**), using the very bulky Ter^{Trip} substituent (Ter = C_6H_3-2,6-$Trip_2$),[17] The NHC Me_2Im^{Me} was used to trap a hydride-bridged dimer $Pb_2H_2Ter^{Trip}_2$, an intermediate of the reaction of $PbTer^{Trip}R$ (R = $CHPh(PPh_2)$) with catecholborane. Reaction with an excess of the NHC afforded the NHC adduct Me_2Im^{Me}·$PbTer^{Trip}H$, whereas the use of one equivalent NHC led to formation of an equilibrium mixture containing Me_2Im^{Me}·$PbTer^{Trip}H$ and the dimer $Pb_2H_2Ter^{Trip}_2$.[17] The stability of NHC adducts of Pb(II) increases if more electronegative substituents were used at Pb(II). Gerhus *et al.* reported the existence of an equilibrium between the precursors and the corresponding adduct $Neop_2Im^{(C6H4)}$·$Pb(NNeop)_2(C_6H_4)$ ($Neop_2Im^{(C6H4)}$ = 1,3,-di-neopentylbenzimidazolin-2-ylidene; Figure 4.1, **4.C**) upon treatment of the *N*-heterocyclic plumbylene (NHPb) with $Neop_2Im^{(C6H4)}$.[18]

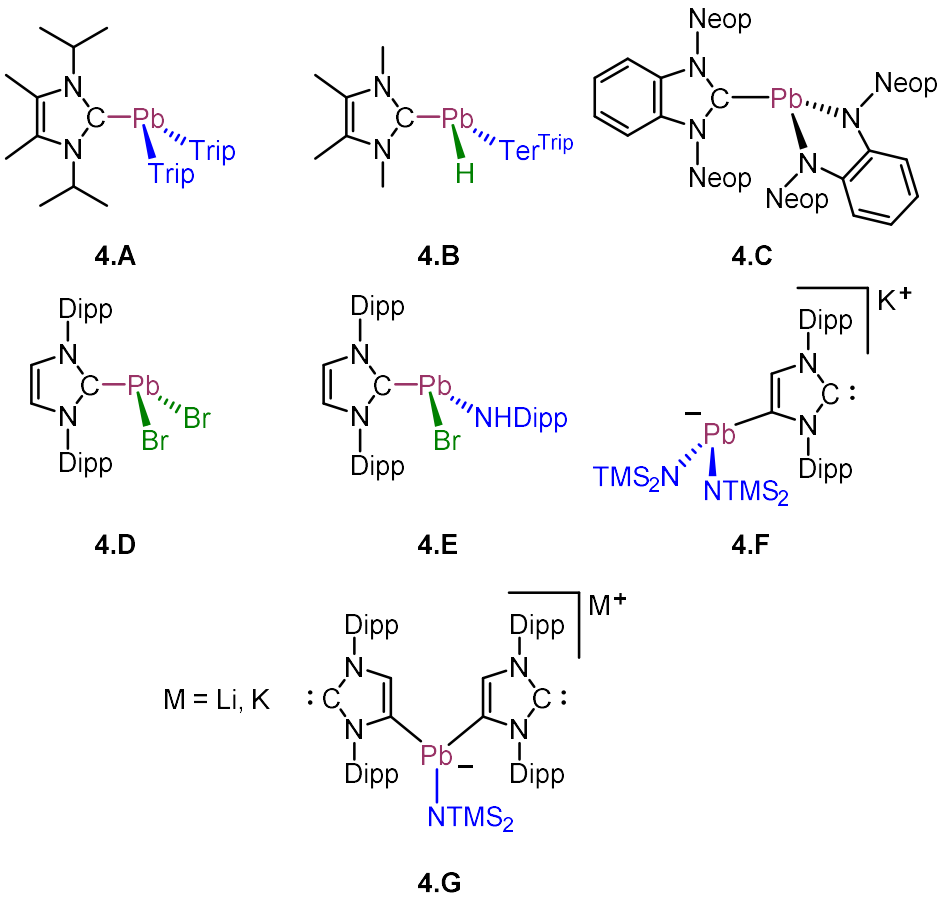

4.A **4.B** **4.C**

4.D **4.E** **4.F**

4.G

Figure 4.1: Carbene-ligated lead compounds *via* reaction of NHCs with the lead(II) precursors.

Siemeling *et al.* reported the Me_2Im^{Me} adduct of the *N*-heterocyclic plumbylenes [$Fe((\eta^5$-$C_5H_4)NSiMe_2R)_2Pb$·Me_2Im^{Me}] (R = Me, *t*Bu) with a ferrocenylene

backbone.[19] In course of this work the NHC-ligated plumbylene $Me_2Im^{Me}{\cdot}Pb(N(SiMe_3)_2)_2$ was also synthesized, starting from the precursors Me_2Im^{Me} and $Pb(N(SiMe_3)_2)_2$.[19] Similarly, adducts of the *N*-heterocyclic plumbylene (*o*-C_6H_4)-1,2-$(NSiMe_3)_2Pb$ with Me_2Im^{Me} and $cAAC^{Et}$ (1-(2,6-di-*iso*-propylphenyl)-3,3-diethyl-5,5-dimethyl-pyrrolidin-2-ylidene) were prepared by the same group.[19, 20] A NHC bound Bisphosphanyl-plumbylene $[Fe((\eta^5\text{-}C_5H_4)P\textit{t}Bu)_2Pb{\cdot}Me_2Im^{Me}]$ was prepared from $[Fe((\eta^5\text{-}C_5H_4)P\textit{t}Bu)_2Pb]$ and Me_2Im^{Me} by Pietschnig *et al*.[21] Jones, Frenking and Stasch reported the NHC-plumbylene adduct $Dipp_2Im{\cdot}PbBr_2$ (Figure 4.1, **4.D**), which was synthesized starting from $Dipp_2Im$ and $PbBr_2$. All attempts to reduce compound **4.D** in analogy to similar tin compounds to yield molecules featuring a Pb=Pb double bond were unsuccessful.[12] However, Rivard and co-workers reported the reaction of $Dipp_2Im{\cdot}PbBr_2$ (Figure 4.1, **4.D**) with $[Li]^+[NHDipp]^-$ to afford the stable amide-substituted NHC-plumbylene adduct $Dipp_2Im{\cdot}PbBrNHDipp$ (Figure 4.1, **4.E**).[22] Munz *et al.* reacted the pyridine based CNC-pincer-type ligand 2,6-$(^S DippImN)_2$-C_5H_3N (^{pincer}NHC; "S" denotes saturated backbone) with $PbBr_2$ to obtain the corresponding plumbylene (^{pincer}NHC)·$PbBr_2$ which was then converted to (^{pincer}NHC)·$PbOTf_2$ upon treatment with TlOTf.[23] Moreover, a number of NHC-coordinated plumbocenes were reported recently by Schäfer *et al.*,[24] and the backbone-coordinated ^{a}NHC salts ("a" denotes abnormal coordination) $[K]^+[^aDipp_2Im^{NHDC}{\cdot}Pb(N(TMS)_2)_2]^-$ (TMS = $SiMe_3$; NHDC = :C[N(2,6-*i*$Pr_2C_6H_3$)]$_2$(CH)C:)) (Figure 4.1, **4.F**) and $[M]^+[(^aDipp_2Im^{NHDC})_2{\cdot}Pb(N(TMS)_2)_2]^-$ (M = Li, K) (Figure 4.1, **4.G**) were also accessible.[25] Compared to the lighter homologues, the chemistry of carbene bound lead compounds is thus still in its infancy and only a few substitution patterns at lead are realized so far, which are based almost exclusively on sterically demanding substituents such as Ter^{Trip}, Trip, NHDipp and $NTMS_2$ or tethered plumbylene substituents. Moreover, to the best of our knowledge, carbene-supported Pb(IV) compounds have not been investigated at all. Therefore, we report herein *Lewis*-acid/base adducts of different NHCs and $cAAC^{Me}$ with PbI_2 and $PbCl_2Ph_2$, as well as first attempts to reduce NHC adducts of $PbCl_2Ph_2$.

4.2 Results and Discussion

We started our investigations with the reaction of PbI_2 with the NHCs Me_2Im^{Me}, iPr_2Im^{Me}, $Dipp_2Im$ and with $cAAC^{Me}$, respectively. The reactions in THF at room temperature led to the corresponding adducts NHC·PbI_2 (NHC = Me_2Im^{Me} (**4.1**), iPr_2Im^{Me} (**4.2**), $Dipp_2Im$ (**4.3**)) and $cAAC^{Me}$·PbI_2 (**4.4**) as colorless to pale yellow solids in 32 – 87 % yield (Scheme 4.1).

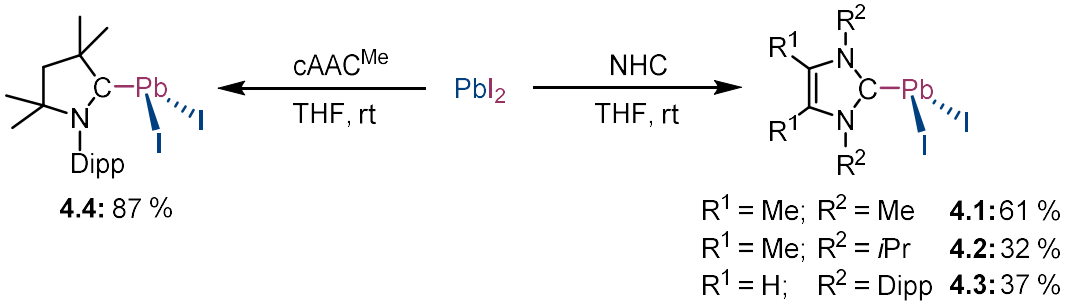

Scheme 4.1: Synthesis of the NHC-ligated plumbylenes Me_2Im^{Me}·PbI_2 (**4.1**), iPr_2Im^{Me}·PbI_2 (**4.2**) and $Dipp_2Im$·PbI_2 (**4.3**) as well as the $cAAC^{Me}$ plumbylene adduct $cAAC^{Me}$·PbI_2 (**4.4**).

Adduct formation of these compounds is evident from NMR data (Table 4.1) and elemental analysis. However, for **4.3** and **4.4** no resonances for the carbene carbon atom were detected in the $^{13}C\{^1H\}$ NMR spectra of these compounds, and we also failed to detect resonances in the $^{207}Pb\{^1H\}$ NMR spectra of all adducts **4.1**-**4.4**, which might be due to the high quadrupole moment of the iodine atoms attached to lead in those cases. Moreover, the NMR resonances of the adducts **4.1** and **4.2** are clearly shifted compared to the values obtained for the NHC in C_6D_6 or related solvents, but these compounds had to be measured in $CDCl_3$ for solubility reasons. This solvent reacts with free carbenes, which thus prevents a direct comparison. Furthermore, even if crystalline material of **4.1** and **4.2** was used for NMR spectroscopic measurements in $CDCl_3$, partial decomposition (about 10 % in 10 h) occurred.

Table 4.1: Selected $^{13}C\{^1H\}$ and ^{207}Pb NMR chemical shifts (ppm) of the compounds NHC·PbI_2 (**4.1**-**4.4**) NHC·$PbCl_2Ph_2$ (**4.5**-**4.8**), recorded in C_6D_6, unless otherwise noted.

	NMR	Me_2Im^{Me}	iPr_2Im^{Me}	$Dipp_2Im$	$cAAC^{Me}$
NHC	$\delta^{13}C_{carbene}$	212.4	207.6	220.1	313.8[b]
NHC·PbI_2 (**4.1**-**4.4**)	$\delta^{13}C_{carbene}$	137.5[a]	133.6[a]	/	/
NHC·$PbCl_2Ph_2$ (**4.5**-**4.8**)	$\delta^{13}C_{carbene}$ $\delta^{207}Pb$	175.9 –394.0	179.1 –397.3	180.2 –397.2	241.2[b] –401.7[b]

a) recorded in $CDCl_3$. b) recorded in toluene-d_8.

In the $^{13}C\{^1H\}$ NMR spectra of **4.1** and **4.2** the N*C*N carbon resonances were observed at 137.5 (**4.1**) and 133.6 ppm (**4.2**), respectively. The ^1H and $^{13}C\{^1H\}$ NMR spectra of the adducts **4.3** and **4.4** of the sterically more demanding ligands $Dipp_2Im$ and $cAAC^{Me}$ (measured in C_6D_6) revealed the expected number of resonances, which are typically shifted upon coordination.

Single crystals of compound **4.2** ($^1{}_\infty[iPr_2Im^{Me}\cdot PbI_2]$) and **4.4** ($cAAC^{Me}\cdot PbI_2$) were obtained by slow evaporation of a saturated THF (**4.2**) or dichloromethane (**4.4**) solution at room temperature. The crystal structure of **4.2** is presented in Figure 4.2, the molecular structure of **4.4** is shown in Figure 4.3 and important bonding parameters are summarized in Table 4.2.

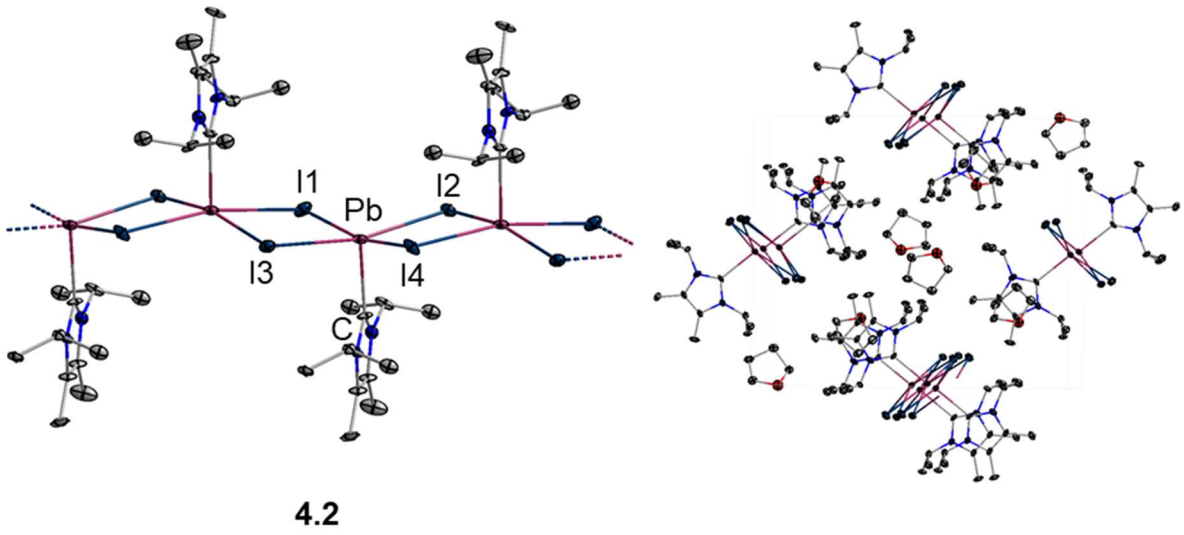

4.2

Figure 4.2: The crystal structure of $^{1}_{\infty}$[*i*Pr$_2$Im^{Me}·PbI$_2$] (**4.2**) in the solid-state: strand of the coordination polymer (left side) and projection of the coordination polymer along the *c*-axis (right side). Hydrogen atoms and solvent molecules (THF) are omitted for clarity. Atomic displacement ellipsoids are set at 50 % probability. Selected bond lengths [Å] and angles [°] (Table 4.2): **4.2**: Pb–C, 2.464(8); Pb–I1, 3.0893(12); Pb–I2, 3.0868(11); Pb–I3, 3.4134(11); Pb–I4, 3.4187(11); I1–Pb–I2, 94.985(17); I3–Pb–I4, 82.692(15); I1–Pb–I3, 89.42(4); I2–Pb–I4, 89.36(4); I1–Pb–I4, 164.44(2); I2–Pb–I3, 164.432(16).

Compound **4.2** crystallizes in the orthorhombic *space group Pna*2$_1$ and forms a one-dimensional coordination polymer of *i*Pr$_2$Im^{Me}·PbI$_2$ *via* iodide bridges in the solid-state, i.e. $^{1}_{\infty}$[*i*Pr$_2$Im^{Me}·PbI$_2$] (Figure 4.2, left side). The strands of the coordination polymer are aligned in direction of the crystallographic *c*-axis (Figure 4.2, right side). For packing reasons, the adjacent strands are twisted by 90° with respect to each other. The Pb–I bond lengths differ remarkably and reflect that *i*Pr$_2$Im^{Me}·PbI$_2$ is bound in the solid-state *via* weaker Pb-I interactions to the next plumbylene moiety. While two iodine atoms of *i*Pr$_2$Im^{Me}·PbI$_2$, I1 and I2 (Figure 4.2, left side), are relatively strongly bound to the lead atom with bond lengths of 3.0893(12) Å and 3.0868(11) Å, respectively, the distances Pb–I3 (3.4134(11) Å) and Pb–I4 (3.4187(11) Å) are significantly longer. The coordination sphere around the central Pb atom is thus a slightly distorted (I1–Pb–I4, 164.44(2)°; I2–Pb–I3, 164.432(16)°) tetragonal pyramid. The Pb–C distance of 2.464(8) Å is within 3σ identical to those observed for the trigonal pyramidal coordinated monomeric Dipp$_2$Im·PbBr$_2$ (Pb–C1, 2.443(11) Å)[12] and cAAC^{Me}·PbI$_2$ (Figure 4.3, Pb–C1, 2.449(2) Å), which adopt a molecular structure featuring one isolated L·PbX$_2$ unit in the solid-state. Compound **4.4**

crystallizes in the monoclinic space group $P2_1/c$ with one molecule in the asymmetric unit. X-ray analysis clearly reveals a molecular structure with pyramidal coordination at lead. The substituents are almost ideally perpendicularly arranged with angles ranging from 92.96(5)° to 96.253(5)° (Table 4.2) and a Pb–C1 bond length of 2.449(2) Å. The Pb–I1 (2.9272(2) Å) and Pb–I2 (2.9209(2) Å) distances are slightly shorter compared to those of compound **4.2** (Pb–I1, 3.0893(12) Å; Pb–I2, 3.0868(11) Å), since these are not additionally coordinated to neighboring substituents as observed for the coordination polymer of compound **4.2**. The bonding parameter obtained for **4.4** are in good agreement with those observed previously for the compound $Dipp_2Im{\cdot}PbBr_2$ ((Pb–C1, 2.443(11) Å; C–Pb–Br1, 93.3(3)°; Br1–Pb–Br2, 93.79(5)°).[12]

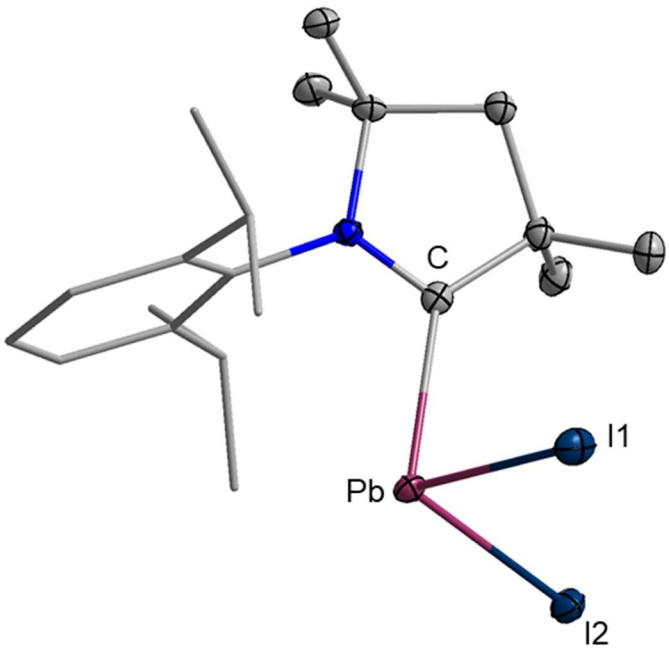

4.4

Figure 4.3: The molecular structure of $cAAC^{Me}{\cdot}PbI_2$ (**4.4**) in the solid-state. Hydrogen atoms are omitted for clarity. Atomic displacement ellipsoids are set at 50 % probability. Selected bond lengths [Å] and angles [°] (Table 4.2): **4.4**: Pb–C, 2.449(2); Pb–I1, 2.9272(2); Pb–I2, 2.9209(2); I1–Pb–I2, 96.253(5); C–Pb–I1, 92.96(5); C–Pb–I2, 95.71(5).

Arylation experiments on **4.1**-**4.4** using RLi or RMgBr (R = Ph, Mes) led to decomposition of the Pb(II) compounds. Therefore, we were interested to synthesize carbene adducts of lead(IV) aryl chlorides and to investigate

reduction chemistry. The reaction of $PbCl_2Ph_2$ with the carbenes Me_2Im^{Me}, iPr_2Im^{Me}, $Dipp_2Im$ and $cAAC^{Me}$ in THF or benzene at room temperature yielded the corresponding adducts NHC·$PbCl_2Ph_2$ (Me_2Im^{Me} (**4.5**), iPr_2Im^{Me} (**4.6**), $Dipp_2Im$ (**4.7**)) and $cAAC^{Me}$·$PbCl_2Ph_2$ (**4.8**), respectively, as colorless to off-white solids in fair to high yields (76 – 92 %; Scheme 4.2). For the reaction of $cAAC^{Me}$ with $PbCl_2Ph_2$ longer reaction times than three hours led to decomposition of the product.

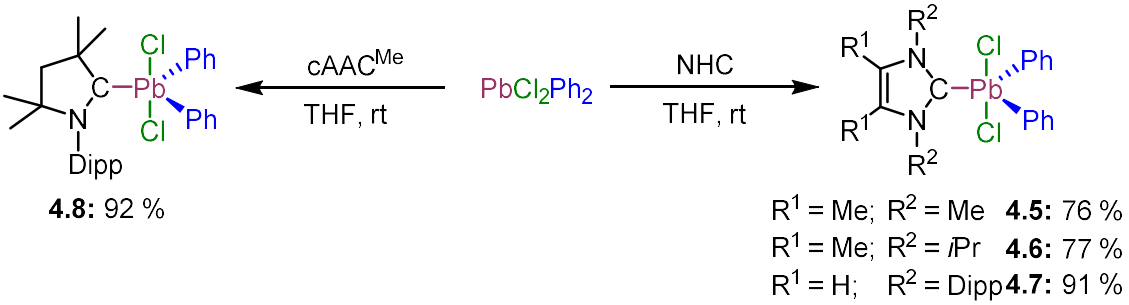

Scheme 4.2: Synthesis of the NHC-containing Pb(IV) adducts Me_2Im^{Me}·$PbCl_2Ph_2$ (**4.5**), iPr_2Im^{Me}·$PbCl_2Ph_2$ (**4.6**) and $Dipp_2Im$·$PbCl_2Ph_2$ (**4.7**) (left) as well as the $cAAC^{Me}$-ligated $cAAC^{Me}$·$PbCl_2Ph_2$ (**4.8**) (right).

Adduct formation of **4.5-4.8** is evident from the ^{1}H, $^{13}C\{^{1}H\}$ and $^{207}Pb\{^{1}H\}$ NMR spectroscopic data (Table 4.1) as well as elemental analyses. Most important, the carbene carbon resonances of the adducts **4.5-4.7** (175.9 to 180.2 ppm) and **4.8** (241.2 ppm) were recorded in the $^{13}C\{^{1}H\}$ NMR spectra and are shifted approximately 40 ppm (**4.5-4.7**) and 73 ppm (**4.8**) towards higher field compared to the uncoordinated carbenes (Table 4.1). The adducts **4.5-4.8** also show characteristic resonances in the ^{207}Pb NMR spectra, ranging from −394.0 to −401.7 ppm, which is similar to the shifts observed for phosphine(oxide) based *Lewis*-base adducts *e.g.* L·$PbCl_2Ph_2$ (L = P*n*Bu_3, −251 ppm; L = O=P*n*Bu_3, −524 ppm).[26] Low temperature NMR measurements on solutions of compound **4.8** had to be performed due to broadening of the signal sets at room temperature (Figure 4.S1). At −40 °C, the NMR spectra of compound **4.8** showed a splitting of the signal sets of the lead bound phenyl groups, which might be caused by hindered rotation of the phenyl rings (and the cAAC) due to steric repulsion between the phenyl groups and the Dipp group of $cAAC^{Me}$.

Table 4.2. Selected bond lengths [Å] and angles [°] of the compounds **4.2**, **4.4-4.10**.

Tetragonal pyramidal	**Pb–C**	**Pb–I1**	**Pb–I2**	**Pb–I3**	**Pb–I4**	**I1–Pb–I2**	**I1–Pb–I3**
(4.2) ***i*Pr$_2$Im^{Me}·PbI$_2$** (coordination polymer)	2.464(8)	3.0893(12)	3.0868(11)	3.4134(11)	3.4187(11)	94.985(17)	89.42(4)
Trigonal pyramidal	**Pb–C**	**Pb–I1**	**Pb–I2**	**I1–Pb–I2**	**C–Pb–I1**	**C–Pb–I2**	
(4.4) cAAC^{Me}·PbI$_2$	2.241	2.9272(2)	2.9209(2)	96.253(5)	92.96(5)	95.71(5)	
Trigonal bipyramidal	**Pb–C1**	**Pb–Cl1**	**Pb–Cl2**	**Pb–C2**	**Pb–C3**	**Cl1–Pb–Cl2**	**C2–Pb–C3**
(4.5) Me$_2$Im^{Me}·PbCl$_2$Ph$_2$	2.241(2)	2.6549(6)	2.6881(5)	2.203(2)	2.1911(19)	168.89(2)	127.84(7)
(4.6) ***i*Pr$_2$Im^{Me}·PbCl$_2$Ph$_2$**	2.263(3) 2.243(5)	2.6618(8) 2.6802(8)	2.6604(7) 2.6802(8)^{sym}	2.211(3) 2.191(3)	2.205(3) 2.191(3)^{Sym}	170.26(2) 167.04(4)	128.95(12) 127.62(17)
(4.7) Dipp$_2$Im·PbCl$_2$Ph$_2$	2.320(3)	2.6324(9)	2.6987(8)	2.204(3)	2.212(3)	171.63(3)	135.12(13)
(4.8) cAAC^{Me}·PbCl$_2$Ph$_2$	2.35(3) 2.28(2)	2.582(17) 2.752(17)	2.740(17) 2.587(17)	2.19(2) 2.23(2)	2.24(2) 2.22(2)	175.9(8) 124.8(10)	128.3(10) 177.6(8)
Trigonal pyramidal	**Pb–C1**	**Pb–C2**	**Pb–C3**	**C2–Pb–C3**	**C1–Pb–C2**	**C1–Pb–C3**	
(4.9) Me$_2$Im^{Me}·PbPh$_2$	2.443(5)	2.311(5)	2.305(4)	90.93(16)	92.47(17)	93.96(17)	
(4.10) ***i*Pr$_2$Im^{Me}·PbPh$_2$**	2.457(3)	2.302(3)	2.320(3)	94.62(12)	95.15(12)	93.68(11)	

^{Sym} denotes symmetry generated.

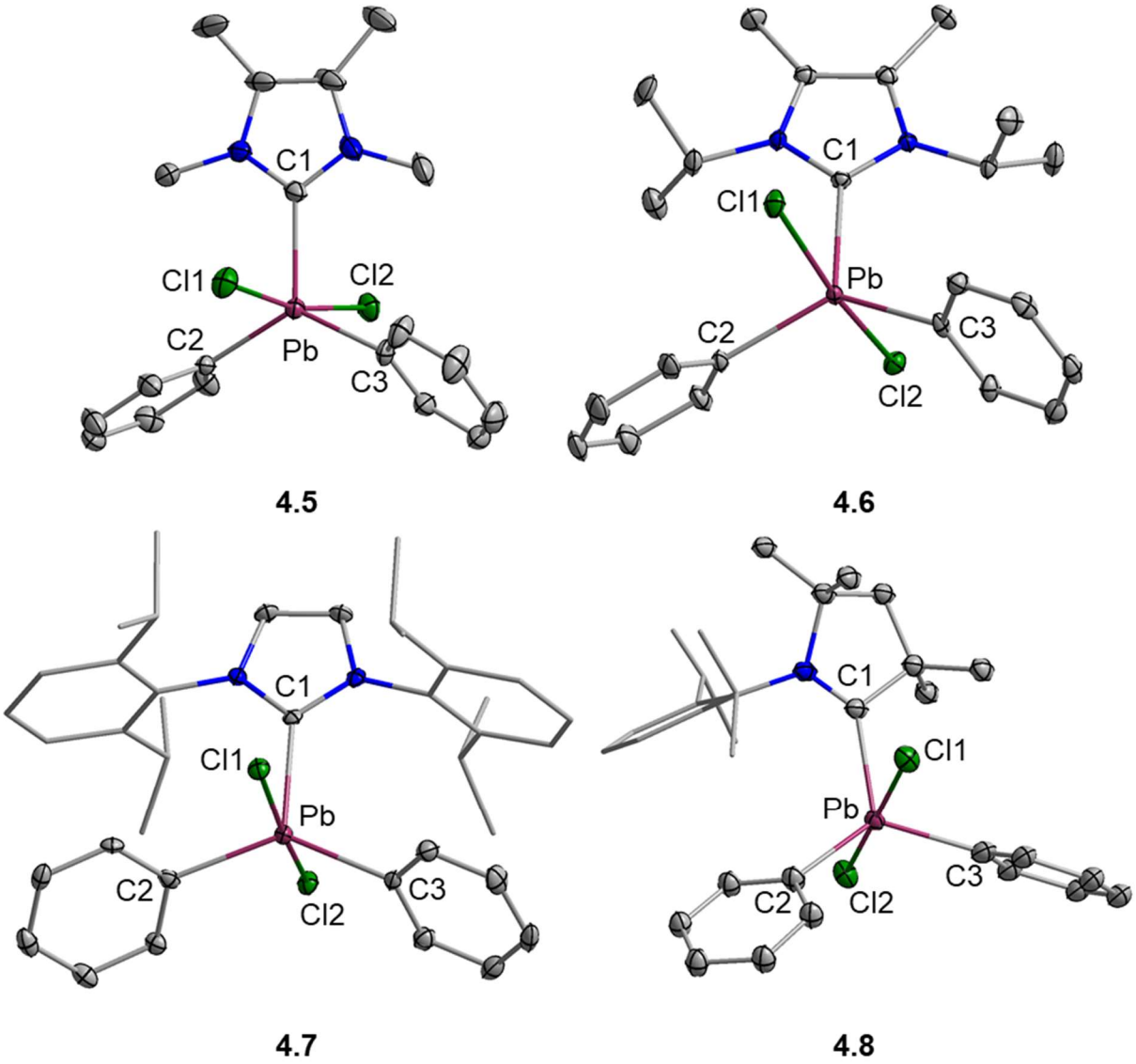

Figure 4.4: Molecular structures of $Me_2Im^{Me}{\cdot}PbCl_2Ph_2$ (**4.5**), $iPr_2Im^{Me}{\cdot}PbCl_2Ph_2$ (**4.6**), $Dipp_2Im{\cdot}PbCl_2Ph_2$ (**4.7**) and $cAAC^{Me}{\cdot}PbCl_2Ph_2$ (**4.8**) in the solid-state. Hydrogen atoms and solvent molecules (**4.5**: toluene; **4.6**-**4.7**: benzene) are omitted for clarity. Only one part of the disordered molecule **4.8** is shown. Atomic displacement ellipsoids are set at 50 % probability. Selected bond lengths [Å] and angles [°] (Table 4.2): **4.5**: Pb–C1, 2.241(2); Pb–C2, 2.203(2); Pb–C3, 2.1911(19); Pb–Cl1, 2.6549(6); Pb–Cl2, 2.6881(5); C2–Pb–C3, 127.84(7); Cl1–Pb–Cl2, 168.89(2); **4.6**: Pb–C1, 2.263(3); Pb–C2, 2.211(3); Pb–C3, 2.205(3); Pb–Cl1, 2.6618(8); Pb–Cl2, 2.6604(7); C2–Pb–C3, 128.95(12); Cl1–Pb–Cl2, 170.26(2); **4.7**: Pb–C1, 2.320(3); Pb–C2, 2.204(3); Pb–C3, 2.212(3); Pb–Cl1, 2.6324(9); Pb–Cl2, 2.6987(8); C2–Pb–C3, 135.12(13); Cl1–Pb–Cl2, 171.63(3); **4.8** (part 1): Pb–C1, 2.35(3); Pb–C2, 2.19(2); Pb–C3, 2.24(2); Pb–Cl1, 2.582(17); Pb–Cl2, 2.740(17); C2–Pb–C3, 128.3(10); Cl1–Pb–Cl2, 175.9(8); **4.8** (part 2): Pb–C1, 2.28(2); Pb–C2, 2.23(2); Pb–C3, 2.22(2); Pb–Cl1, 2.752(17); Pb–Cl2, 2.587(17); C2–Pb–C3, 124.8(10); Cl1–Pb–Cl2, 177.6(8).

Crystals suitable for X-ray diffraction were obtained for the compounds **4.5**-**4.8** (Figure 4.4, Table 4.2). These adducts crystallize in the monoclinic *space group*s *C*2/*c* (**4.5**, **4.6**) and *P*2$_1$/m (**4.7**) and in the triclinic space group $P\bar{1}$ (**4.8**),

respectively, with one (**4.5**, **4.7**, **4.8**) or one and a half (**4.6**) molecules in the asymmetric unit. A crystallographically imposed C_2 rotation axis is running through Pb and C1 of the second molecule in the asymmetric unit of compound **4.6**, generating the second part of the molecule. The complete molecule of **4.8** is disordered (ratio of the two parts: 49:51 %) leading to low precision of the bonding parameters. All lead(IV) adducts adopt a trigonal bipyramidal geometry with two chloride substituents in axial positions and the remaining substituents at equatorial sites. The axial chlorides are slightly tilted towards the carbene with Cl1–E–Cl2 angles ranging from 167.04(4) to 171.63(3)°. The C1–Pb distances of **4.5-4.7** (Table 4.2) range from 2.243(5) to 2.320(3) Å which is smaller than those observed for the plumbylenes **4.A**, **4.C**, **4.D** and **4.E** ((Pb–C1: 2.332(2) – 2.540(5) Å) previously.[12, 16-17, 22]

The Pb(IV) adducts **4.5-4.8** were reacted with an excess of KC_8 in the hope to synthesize the corresponding Pb(II) adducts NHC·$PbPh_2$. However, for adducts of the sterical demanding carbenes **4.7** and **4.8** only decomposition to unknown insoluble solids was observed, whereas the reduction of **4.5** and **4.6** afforded pale yellow solutions (Scheme 4.3). Filtration of the reaction mixture and subsequent removal of all volatile material *in vacuo* gave the plumbylene adducts Me_2Im^{Me}·$PbPh_2$ (**4.9**) and iPr_2Im^{Me}·$PbPh_2$ (**4.10**) in low yield. However, reacting a mixture of $PbCl_2Ph_2$, NHC and the reducing agent KC_8 afforded these compounds in 63 % and 12 % yield, respectively. The yields obtained for these products already reflect the significantly higher stability of plumbylene **4.9** compared to **4.10**.

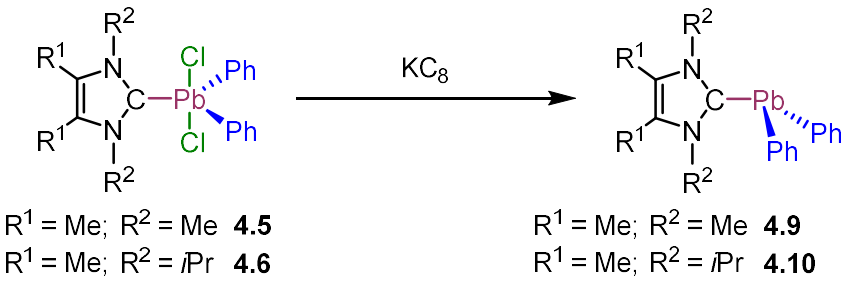

Scheme 4.3: Synthesis of the NHC plumbylene adducts Me_2Im^{Me}·$PbPh_2$ (**4.9**) and iPr_2Im^{Me}·$PbPh_2$ (**4.10**).

The corresponding resonances of the protons in *meta*-positions were observed as triplets of multiplets at 7.50 (**4.9**) and 7.52 ppm (**4.10**) with $^{3}J_{H\text{-}H}$ coupling constants of 7.7 and 7.4 Hz (**4.9**, **4.10**). In the $^{13}C\{^{1}H\}$ NMR spectra, the resonances of the phenyl carbon atoms in *ortho*-position were detected at 139.9 and 139.7 ppm with lead satellites revealing a $^{2}J_{13C\text{-}207Pb}$ coupling of 57.8 (**4.9**) and 56.5 Hz (**4.10**), respectively. The corresponding signals of the *meta*-positions were observed at 129.7 (**4.9**) and 129.8 ppm (**4.10**) with lead satellites disclosing a $^{3}J_{13C\text{-}207Pb}$ of 29.6 (**4.9**) and 30.6 Hz (**4.10**), respectively.

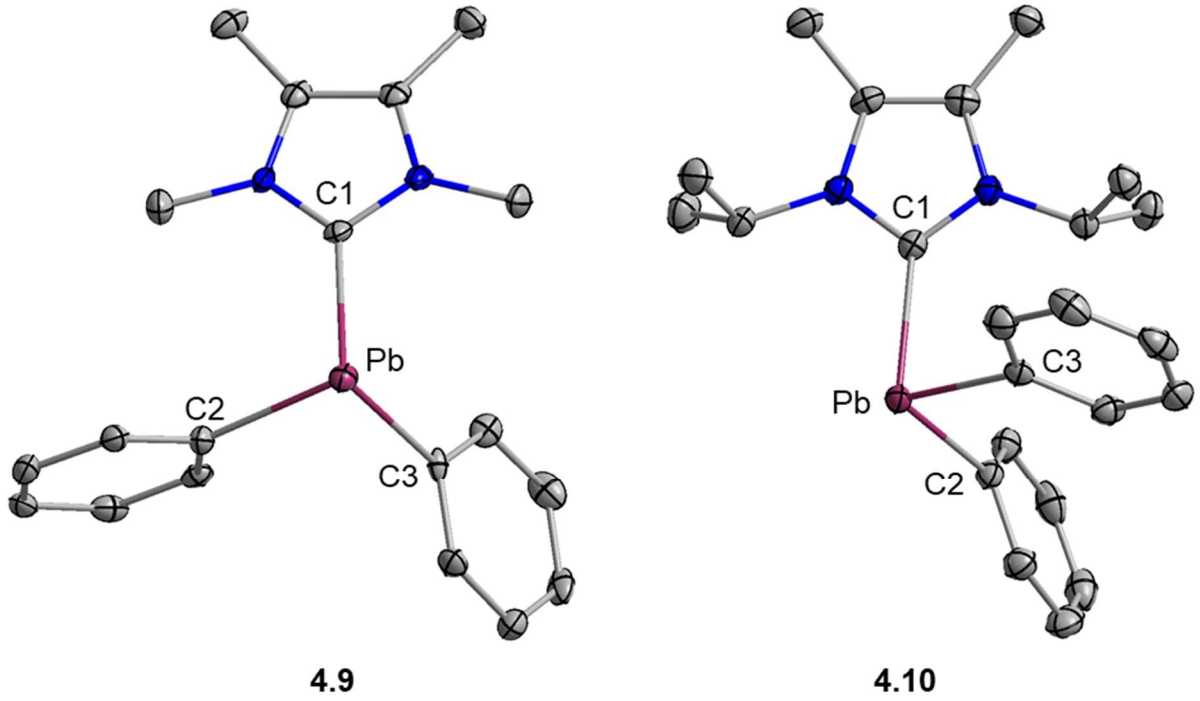

4.9 **4.10**

Figure 4.5: Molecular structures of $Me_2Im^{Me}{\cdot}PbPh_2$ (**4.9**) and $i Pr_2Im^{Me}{\cdot}PbPh_2$ (**4.10**) in the solid-state. Hydrogen atoms are omitted for clarity. Atomic displacement ellipsoids are set at 50 % probability. Selected bond lengths [Å] and angles [°] (Table 4.2): **4.9**: Pb–C1, 2.443(5); Pb–C2, 2.311(5); Pb–C3, 2.305(4); C1–Pb–C2, 92.47(17); C1–Pb–C3, 93.96(17); C2–Pb–C3, 90.93(16); **4.10**: Pb–C1, 2.457(3); Pb–C2, 2.302(3); Pb–C3, 2.320(3); C1–Pb–C2, 95.15(12); C1–Pb–C3, 93.68(11); C2–Pb–C3, 94.62(12).

For both compounds, the *ipso*-carbon signals of the phenyl groups were found at 195.9 (**4.9**) and 198.3 ppm (**4.10**), but a $^{1}J_{13C\text{-}207Pb}$ coupling of 1059.2 Hz could only be determined for **4.9**. In addition, both, NCN resonance and the corresponding lead signal in the ^{207}Pb NMR at 1403 ppm could only be detected for compound **4.9**. However, upon standing of the sample for a short time it was

noticeable that the resonances of the NHC ligands shifted with respect to those of the $PbPh_2$ moieties. The results are in accordance with, but do not prove, an equilibrium exists between the adduct NHC·$PbPh_2$ and its components NHC and $PbPh_2$ in solution, similar to those reported earlier by Weidenbruch *et al.* [16] for *i*Pr_2Im^{Me}·$PbTrip_2$ **4.A** and Wesemann *et al.* for Me_2Im^{Me}·$PbTer^{Trip}H$ **4.B**.[17] This was corroborated by the step-wise addition of NHC to the solutions, which led to a step-wise convergence of the NHC resonances to the resonances of the corresponding free carbene. A second set of signals was not observed for the NHC. VT-NMR (VT = variable temperature) experiments gave no further insight into the nature of the compounds in solution. DOSY NMR measurements then confirmed dissociation of the compounds **4.9** (Figure 4.6) and **4.10** (Figure 4.7) in solution. However, elemental analyses of the isolated solids as well as X-ray diffraction on crystals of the compounds **4.9** and **4.10** (Figure 5, Table 4.2) provide evidence for the formation of these adducts. The substance amounts of the products **4.9** and **4.10** were not sufficient to carry out corresponding solid-state NMR measurements.

The NHC-containing plumbylenes crystallize in the triclinic *space group* $P\overline{1}$ (**4.10**) and the orthorhombic space group *Pbca* (**4.9**), respectively, with one molecule in the asymmetric unit. The molecular structures of both compounds **4.9** and **4.10** confirm the proposed connectivity of these molecules in the solid-state. The molecular structures clearly reveal pyramidal coordination at lead and an almost ideal perpendicular arrangement of the substituents with angles between 90.93(16) and 95.15(12)° and C1–Pb bond lengths of 2.443(5) (**4.9**) and 2.457(3) Å (**4.10**) (see Table 4.2). The structures are isostructural to and the C1–Pb bond lengths in the same range as for the plumbylenes **4.A**, **4.C**, **4.D** and **4.E** ((Pb–C1: 2.332(2) – 2.540(5) Å).[12, 16-17, 22]

.

4.3 Conclusion

The reaction of PbI_2 with different carbenes led to the NHC-ligated plumbylenes $Me_2Im^{Me}{\cdot}PbI_2$ (**4.1**), $iPr_2Im^{Me}{\cdot}PbI_2$ (**4.2**), $Dipp_2Im{\cdot}PbI_2$ (**4.3**) and $cAAC^{Me}{\cdot}PbI_2$ (**4.4**), and the reaction with $PbCl_2Ph_2$ to the Pb(IV) NHC-adducts $NHC{\cdot}PbCl_2Ph_2$ (**4.5**-**4.7**) and $cAAC^{Me}{\cdot}PbCl_2Ph_2$ (**4.8**), respectively. In contrast to the sterically more demanding Pb(IV) adducts **4.7** and **4.8**, the reduction of **4.5** and **4.6** yielded the diphenylplumbylene NHC adducts $Me_2Im^{Me}{\cdot}PbPh_2$ (**4.9**) and $iPr_2Im^{Me}{\cdot}PbPh_2$ (**4.10**). NMR spectroscopic studies suggest an equilibrium of these adducts with NHC and $PbPh_2$ in solution. However, these adducts are stable in the solid-state, which is in accordance with the elemental analyses and X-ray single crystal structures of **4.9** and **4.10**.

4.4 References

[1] a) W. A. Herrmann, C. Köcher, *Angew. Chem. Int. Ed.* **1997**, *36*, 2162-2187; *Angew. Chem.* **1997**, *109*, 2256-2282; b) P. P. Power, *Chem. Rev.* **1999**, *99*, 3463-3504; c) D. Bourissou, O. Guerret, F. P. Gabbai, G. Bertrand, *Chem. Rev.* **2000**, *100*, 39-92; d) F. E. Hahn, M. C. Jahnke, *Angew. Chem. Int. Ed.* **2008**, *47*, 3122-3172; *Angew. Chem.* **2008**, *120*, 3166-3216; e) T. Dröge, F. Glorius, *Angew. Chem. Int. Ed.* **2010**, *49*, 6940-6952; *Angew. Chem.* **2010**, *122*, 7094-7107; f) M. N. Hopkinson, C. Richter, M. Schedler, F. Glorius, *Nat. Chem.* **2014**, *510*, 485-496; g) Y. Wang, G. H. Robinson, *Inorg. Chem.* **2014**, *53*, 11815-11832; h) S. Würtemberger-Pietsch, U. Radius, T. B. Marder, *Dalton Trans.* **2016**, *45*, 5880-5895; i) V. Nesterov, D. Reiter, P. Bag, P. Frisch, R. Holzner, A. Porzelt, S. Inoue, *Chem. Rev.* **2018**, *118*, 9678-9842; j) A. Doddi, M. Peters, M. Tamm, *Chem. Rev.* **2019**, *119*, 6994-7112.

[2] a) M. Melaimi, M. Soleilhavoup, G. Bertrand, *Angew. Chem. Int. Ed.* **2010**, *49*, 8810-8849; *Angew. Chem.* **2010**, *122*, 8992-9032; b) M. Soleilhavoup, G. Bertrand, *Acc. Chem. Res.* **2015**, *48*, 256-266; c) M. Melaimi, R. Jazzar, M. Soleilhavoup, G. Bertrand, *Angew. Chem. Int. Ed.* **2017**, *56*, 10046-10068; *Angew. Chem.* **2017**, *129*, 10180-10203; d) U. S. Paul, U. Radius, *Chem. Eur. J.* **2017**, *23*, 3993-4009; e) U. S. D. Paul, M. J. Krahfuß, U. Radius, *Chemie unserer Zeit* **2019**, *53*, 212-223.

[3] a) D. Schmidt, J. H. Berthel, S. Pietsch, U. Radius, *Angew. Chem. Int. Ed.* **2012**, *51*, 8881-8885; *Angew. Chem.* **2012**, *124*, 9011-9015; b) P. Hemberger, A. Bodi, J. H. Berthel, U. Radius, *Chem. Eur. J.* **2015**, *21*, 1434-1438; c) S. Pietsch, U. Paul, I. A. Cade, M. J. Ingleson, U. Radius, T. B. Marder, *Chem. Eur. J.* **2015**, *21*, 9018-9021; d) H. Schneider, D. Schmidt, U. Radius, *Chem. Eur. J.* **2015**, *21*, 2793-2797; e) M. Eck, S. Würtemberger-Pietsch, A. Eichhorn, J. H. Berthel, R. Bertermann, U. S. Paul, H. Schneider, A. Friedrich, C. Kleeberg, U. Radius, T. B. Marder, *Dalton Trans.* **2017**, *46*, 3661-3680; f) A. F. Eichhorn, S. Fuchs, M. Flock, T. B. Marder, U. Radius, *Angew. Chem. Int. Ed.* **2017**, *56*, 10209-10213; *Angew. Chem.* **2017**, *129*, 10343-10347; g) A. F. Eichhorn, L. Kuehn, T. B. Marder, U. Radius, *Chem. Commun.* **2017**, *53*, 11694-11696; h) A. Hock, H. Schneider, M. J. Krahfuss, U. Radius, *Z. Anorg.*

Allg. Chem. **2018**, *644*, 1243-1251; i) H. Schneider, A. Hock, A. D. Jaeger, D. Lentz, U. Radius, *Eur. J. Inorg. Chem.* **2018**, 4031-4043; j) L. Kuehn, M. Stang, S. Würtemberger-Pietsch, A. Friedrich, H. Schneider, U. Radius, T. B. Marder, *Faraday Discuss.* **2019**, *220*, 350-363; k) S. A. Föhrenbacher, V. Zeh, M. Krahfuss, N. V. Ignat'ev, M. Finze, U. Radius, *Eur. J. Inorg. Chem.* **2021**, 1941-1960.

[4] a) A. Hock, L. Werner, C. Luz, U. Radius, *Dalton Trans.* **2020**, *49*, 11108-11119; b) A. Hock, L. Werner, M. Riethmann, U. Radius, *Eur. J. Inorg. Chem.* **2020**, 4015-4023.

[5] H. Schneider, M. J. Krahfuß, U. Radius, *Z. Anorg. Allg. Chem.* **2016**, *642*, 1282-1286.

[6] a) M. S. M. Philipp, M. J. Krahfuss, K. Radacki, U. Radius, *Eur. J. Inorg. Chem.* **2021**, 4007-4019; b) M. S. M. Philipp, U. Radius, *Z. Anorg. Allg. Chem.* **2022**, e202200085; c) M. S. M. Philipp, R. Bertermann, U. Radius, *Eur. J. Inorg. Chem.* **2022**, e202200429.

[7] a) C. J. Carmalt, A. H. Cowley, *Adv. Inorg. Chem.* **2000**, *50*, 1-32; b) N. Kuhn, A. Al-Sheikh, *Coord. Chem. Rev.* **2005**, *249*, 829-857; c) C. E. Willans, *Organomet. Chem.* **2010**, *36*, 1-28; d) G. Prabusankar, A. Sathyanarayana, P. Suresh, C. N. Babu, K. Srinivas, B. P. R. Metla, *Coord. Chem. Rev.* **2014**, *269*, 96-133; e) K. C. Mondal, S. Roy, H. W. Roesky, *Chem. Soc. Rev.* **2016**, *45*, 1080-1111.

[8] a) K. C. Mondal, P. P. Samuel, M. Tretiakov, A. P. Singh, H. W. Roesky, A. C. Stückl, B. Niepötter, E. Carl, H. Wolf, R. Herbst-Irmer, D. Stalke, *Inorg. Chem.* **2013**, *52*, 4736-4743; b) K. C. Mondal, H. W. Roesky, M. C. Schwarzer, G. Frenking, B. Niepötter, H. Wolf, R. Herbst-Irmer, D. Stalke, *Angew. Chem. Int. Ed.* **2013**, *52*, 2963-2967; *Angew. Chem.* **2013**, *125*, 3036-3040.

[9] Y. Li, K. C. Mondal, H. W. Roesky, H. Zhu, P. Stollberg, R. Herbst-Irmer, D. Stalke, D. M. Andrada, *J. Am. Chem. Soc.* **2013**, *135*, 12422-12428.

[10] Y. Wang, Y. Xie, P. Wei, R. B. King, H. F. Schaefer III, R. P. v. Schleyer, G. H. Robinson, *Science* **2008**, *321*, 1069-1071.

[11] A. Sidiropoulos, C. Jones, A. Stasch, S. Klein, G. Frenking, *Angew. Chem. Int. Ed.* **2009**, *48*, 9701-9704; *Angew. Chem.* **2009**, *121*, 9881-9884.

[12] C. Jones, A. Sidiropoulos, N. Holzmann, G. Frenking, A. Stasch, *Chem. Commun.* **2012**, *48*, 9855-9857.

[13] a) K. C. Mondal, P. P. Samuel, H. W. Roesky, R. R. Aysin, L. A. Leites, S. Neudeck, J. Lübben, B. Dittrich, N. Holzmann, M. Hermann, G. Frenking, *J. Am. Chem. Soc.* **2014**, *136*, 8919-8922; b) K. C. Mondal, S. Roy, B. Dittrich, B. Maity, S. Dutta, D. Koley, S. K. Vasa, R. Linser, S. Dechert, H. W. Roesky, *Chem. Sci.* **2015**, *6*, 5230-5234.

[14] K. C. Mondal, S. Roy, B. Dittrich, D. M. Andrada, G. Frenking, H. W. Roesky, *Angew. Chem. Int. Ed.* **2016**, *55*, 3158-3161; *Angew. Chem.* **2016**, *128*, 3210.

[15] H. Schumann, M. Glanz, F. Girgsdies, E. Hahn, M. Tamm, A. Grzegorzewski, *Angew. Chem. Int. Ed.* **1997**, *36*, 2232-2234.

[16] F. Stabenow, W. Saak, M. Weidenbruch, *Chem. Commun.* **1999**, 1131-1132.

[17] J. Schneider, C. P. Sindlinger, K. Eichele, H. Schubert, L. Wesemann, *J. Am. Chem. Soc.* **2017**, *139*, 6542-6545.

[18] B. Gehrhus, P. B. Hitchcock, M. F. Lappert, *J. Chem. Soc., Dalton Trans.* **2000**, 3094-3099.

[19] R. Guthardt, J. Oetzel, J. I. Schweizer, C. Bruhn, R. Langer, M. Maurer, J. Vicha, P. Shestakova, M. C. Holthausen, U. Siemeling, *Angew. Chem. Int. Ed.* **2019**, *58*, 1387-1391; *Angew. Chem.* **2019**, *131*, 1401-1405.

[20] R. Guthardt, C. Bruhn, U. Siemeling, *Polyhedron* **2021**, *194*, 114959.

[21] D. Kargin, Z. Kelemen, K. Krekic, L. Nyulászi, R. Pietschnig *Chem. Eur. J.* **2018**, *24*, 16774-16778.

[22] I. S. M. Al-Rafia, P. A. Lummis, A. K. Swarnakar, K. C. Deutsch, M. J. Ferguson, R. McDonald, E. Rivard, *Aust. J. Chem.* **2013**, *66*, 1235-1245.

[23] J. Messelberger, P. Pinter, F. W. Heinemann, D. Munz, *Mendeleev Commun.* **2021**, *31*, 471-474.

[24] a) L. Wirtz, M. Jourdain, V. Huch, M. Zimmer, A. Schäfer, *ACS Omega* **2019**, *4*, 18355-18360; b) S. Danés, C. Müller, L. Wirtz, V. Huch, T. Block, R. Pöttgen, A. Schäfer, D. M. Andrada, *Organometallics* **2020**, *39*, 516-527.

[25] J. B. Waters, L. S. Tucker, J. M. Goicoechea, *Organometallics* 2018, **37**, 655-664.

[26] L. A. Margolis, C. D. Schaeffer Jr, C. H. Yoder, Appl. Organomet. Chem. **2003**, *17*, 236-238.

Chapter V

N-Heterocyclic Carbene and Cyclic (Alkyl)(amino)carbene Adducts of Antimony(III)

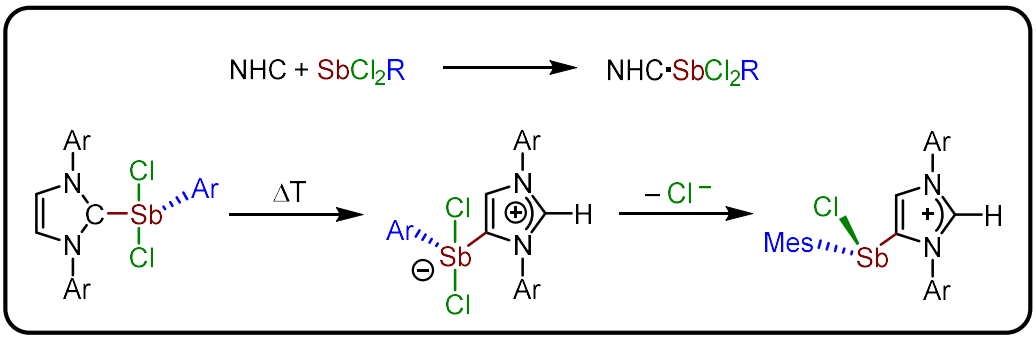

5 *N*-Heterocyclic Carbene and Cyclic (Alkyl)(amino)carbene Adducts of Antimony(III)

5.1 Introduction

N-Heterocyclic carbenes (NHCs) and related molecules play currently an important role in main-group chemistry,[1] mainly due to their tuneable ambiphilicity and steric properties.[1e, 2] Over the last few years we and others reported on the reactivity of NHCs and related molecules towards compounds of group 13,[1d,j,m, 3] 14[1d,j,m, 4] and 15[1m,j, 5] elements. A plethora of NHC-ligated phosphorus compounds is known,[6] including phosphorus in low oxidation states as in phosphinidenes (NHC·PR)[5b, 7] and molecules with uncommon binding modes such as carbene-stabilized P_2, P_4 and P_{12}.[6l, 8] In contrast, reports on carbene-stabilized compounds of the heavier homologues arsenic[6h, 9] and bismuth[9b, 10] are rather scarce, whereas some antimony compounds are known. Most of them are based on antimony(III) halides ($L{\cdot}SbX_3$) (Figure 5.1).

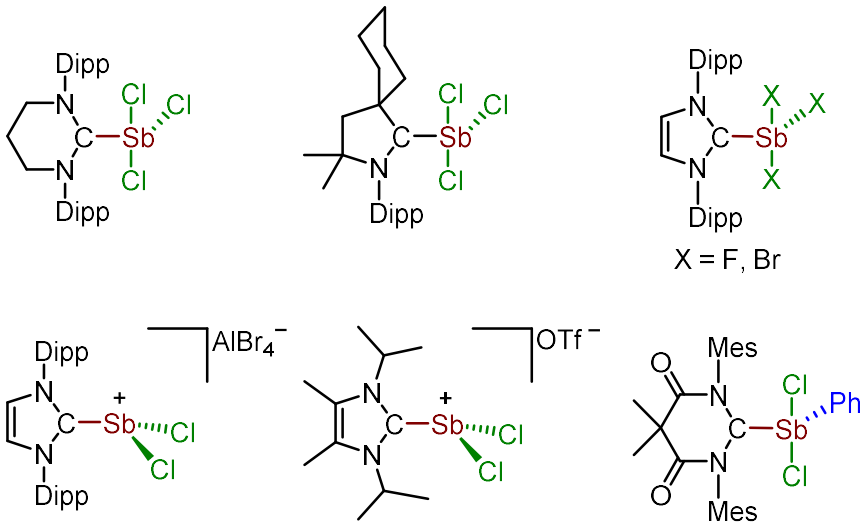

Figure 5.1: NHC-stabilized Sb(III) compounds.

To date, only a number of *Lewis*-acid/base adducts of the type $L{\cdot}SbX_3$ of NHCs and related molecules were isolated (Figure 5.1, top), i.e. 6-Dipp·$SbCl_3$[11] (6-Dipp = 1,3-bis(2,6-di-*iso*-propylphenyl)-4,5,6-hexahydropyrimidine-2-ylidene) $cAAC^{Cy}{\cdot}SbCl_3$[12] ($cAAC^{Cy}$ = 2-Azaspiro[4.5]dec-2-(2,6-di-*iso*-propylphenyl)-3,3-dimethyl-1-ylidene)

and $Dipp_2Im{\cdot}SbX_3$ (X = F, Br)[10b-c] ($Dipp_2Im$ = 1,3-bis(2,6-di-*iso*-propylphenyl)-imidazolin-2-ylidene). For the latter thermal induced isomerization processes from carbene carbon ligated $Dipp_2Im{\cdot}SbX_3$ to the backbone position ligated compounds $[(^aDipp_2Im)(Dipp_2Im)SbF_2]^+[SbF_4]^-$ and $^aDipp_2Im{\cdot}SbBr_3$ (^{a} denotes "abnormal coordination"), respectively, were observed.[10b-c] Halide abstraction of $Dipp_2Im{\cdot}SbBr_3$ and $^aDipp_2Im{\cdot}SbBr_3$ by using $AlBr_3$ and $[Na]^+[B(3,5\text{-}\{CF_3\}_2C_6H_3)_4]^-$ ($[Na]^+[BAr^F{}_4]^-$) as halide acceptor afforded $[Dipp_2Im{\cdot}SbBr_2]^+[AlBr_4]^-$ (Figure 5.1, bottom left) and $[^aDipp_2Im{\cdot}SbBr_2]^+[BAr^F{}_4]^-$, respectively.[10c] Recently the number of substances with $[NHC{\cdot}SbX_2]^+$ moieties was extended as the reaction of $SbCl_3$ with $[i Pr_2Im^{Me}{\cdot}SiMe_3]^+[OTf]^-$ led to the isolation of $[i Pr_2Im^{Me}{\cdot}SbCl_2]^+[OTf]^-$ (Figure 5.1, bottom middle; $i Pr_2Im^{Me}$ = 1,3-di-*iso*-propyl-4,5-dimethylimidazolin-2-ylidene; OTf = trifluoromethane-sulfonate).[6h] More unconvenient ionic compounds were synthesized by the group of Tamm who reported recently the zwitterionic adduct $((B(C_6F_5)_3)\text{-}Dipp_2Im){\cdot}SbCl_2$ and by Benjamin and co-workers who isolated the η^3-Cp* coordinated compound $[Mes_2Im{\cdot}SbCp^*F]^+[B(C_6F_5)_4]^-$.[13]

It has been demonstrated over the last few years for selected examples, that *Lewis*-acid/base adducts of antimony(III) halides are interesting entry-points into the chemistry of subvalent antimony compounds, including antimony radicals, stibinidenes and multiply bonded antimony dimers.[10g, 12-14] However, the examples for the stabilization of these species are scarce in the literature and the carbenes involved in the stabilization process of each different compound seems to be rather specific. So far, different cAACs, DACs (DAC = 4-6-diketo-1,3-diorganyl-5,5-dimethyl-pyrimidine-2-ylidenes) and NHCs have been involved in this type of chemistry. A systematic study is currently missing, even on synthesis and characterization of *Lewis*-acid/base adducts of antimony halides with NHCs. We thus provide herein a detailed report on *Lewis*-acid/base adducts of NHCs and the cyclic (alkyl)(amino)carbene $cAAC^{Me}$ (1-(2,6-di-*iso*-propylphenyl)-3,3,5,5-tetramethyl-pyrrolidin-2-yli-dene) with antimony(III) chlorides of the general formula $SbCl_2R$ (R = Cl, Ph, Mes).

5.2 Results and Discussion

Synthesis of NHC·$SbCl_3$ and NHC·$SbCl_2Ar$ (Ar = Ph, Mes)

We started our investigations with the reaction of *Lewis*-acidic antimony compounds and selected NHCs. Reaction of $SbCl_3$ (in Et_2O), $SbCl_2Ph$[15] (in toluene) and $SbCl_2Mes$[15-16] (in Et_2O) with the corresponding NHC (Me_2Im^{Me} (**a**), iPr_2Im^{Me} (**b**), $Dipp_2Im$ (**c**), Mes_2Im (**d**) and $cAAC^{Me}$ (**e**)) led to formation of NHC·$SbCl_3$ (**5.4a**-**e**), NHC·$SbCl_2Ph$ (**5.5a**-**e**) and NHC·$SbCl_2Mes$ (**5.6a**-**d**) in high yields (64–93 %; Scheme 5.1). A solution of $SbCl_2R$ was added at –78 °C to a solution or suspension (depending on the carbene) of the corresponding carbene and the reaction mixture was allowed to warm to room temperature overnight. In all cases the reaction led to a colorless precipitate, which was isolated by filtration. As for the Me_2Im^{Me} antimony compounds an unknown impurity was formed in course of the reaction, these adducts, **5.4a**, **5.5a** and **5.6a**, had to be recrystallized by slow diffusion of *n*-hexane into a dichloromethane solution of the crude product. Furthermore, adduct **5.6d** is very unstable in solution and decomposes within several minutes.

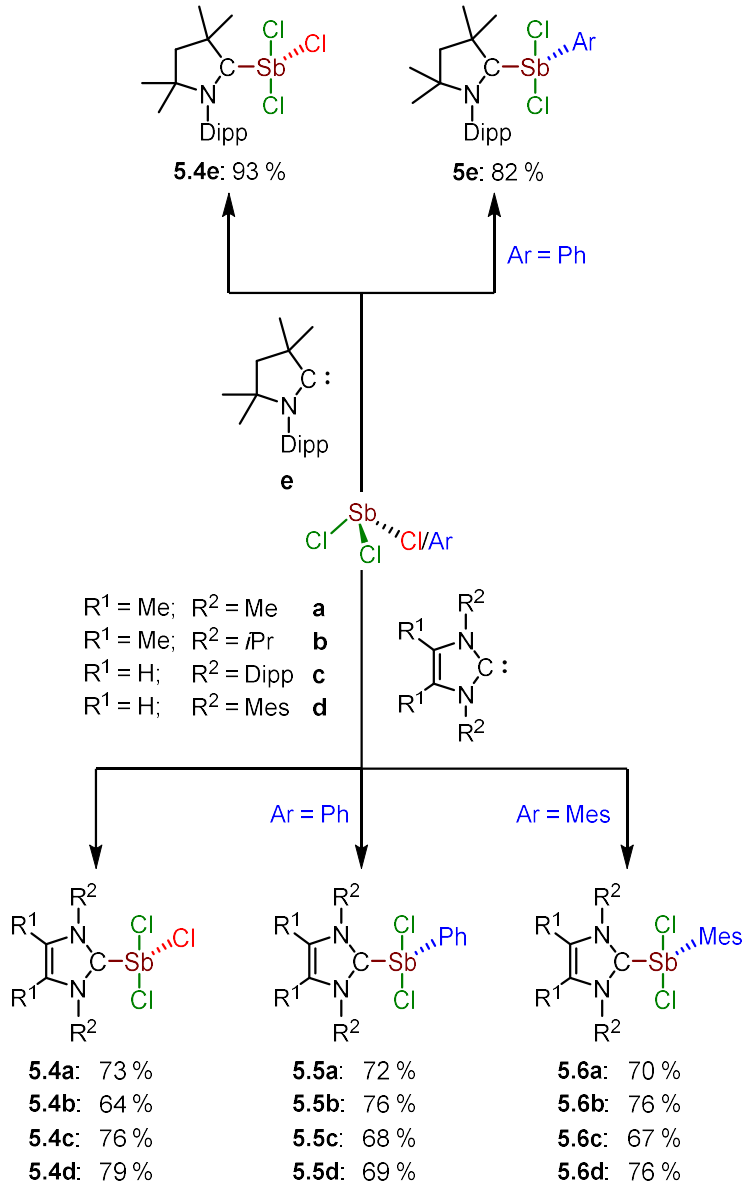

Scheme 5.1: Synthesis of cAAC^{Me}- (top) and NHC- (bottom) stabilized $SbCl_3$ (**5.4a-e**), $SbCl_2Ph$ (**5.5a-e**) and $SbCl_2Mes$ (**5.6a-d**) adducts

Adduct formation is evident from ^{1}H and $^{13}C\{^{1}H\}$ NMR spectroscopy as well as elemental analysis. The resonances of the carbene carbon atoms (C2) in the $^{13}C\{^{1}H\}$ NMR spectra of **5.4a-6d** show a strong upfield shift compared to the corresponding free carbene (Table 5.1). Additionally, the ^{1}H NMR methine proton resonances of the *iso*-propyl substituents of **5.4b**, **5.5b**, **5.6b** and **5.4c**, **5.5c**, **5.6c** are considerably shifted compared to the signals of the free carbenes (**5.4b**, 5.45 ppm, **5.5b**, 5.08 ppm and 5.57 ppm, **5.6b**, 5.55 ppm; free *i*Pr$_2$Im^{Me} 3.95 ppm; **5.4c**, 3.25 ppm, **5.5c**, 3.30 ppm and **5.6c**, 2.92 ppm; free Dipp$_2$Im 2.96 ppm; Table 5.1). The $^{13}C\{^{1}H\}$ NMR resonance of the

carbenic carbon atom is shifted to lower frequencies depending on the substitution pattern at antimony starting from the adducts of $SbCl_3$, *via* $SbCl_2Ph$ to $SbCl_2Mes$ (Table 5.1). The adducts **5.6c** and **5.6d** are quite unstable and show decomposition in solution already at ambient conditions.

Table 5.1: Selected ^1H NMR and $^{13}C\{^1H\}$ NMR chemical shifts (ppm) of the NHC-adducts **5.4**-**5.6** recorded in C_6D_6, unless otherwise noted.

	NHC·$SbCl_3$ **5.4a-e**		NHC·$SbCl_2Ph$ **5.5a-e**		NHC·$SbCl_2Mes$ **5.6a-e**		Free NHC	
	$\delta^{13}C$ ($C_{Carbene}$)	δ^1H (*i*Pr-C*H*)	$\delta^{13}C$ (NCN)	δ^1H (*i*Pr-C*H*)	$\delta^{13}C$ (NCN)	δ^1H (*i*Pr-C*H*)	$\delta^{13}C$ ($C_{Carbene}$)	δ^1H (*i*Pr-C*H*)
Me_2Im^{Me}	162.5[a]	/	157.7[a]	/	155.7[b]	/	212.4	/
iPr_2Im^{Me}	164.3	5.45	161.3	5.08, 5.57	158.4	5.55	207.6	3.95
$Dipp_2Im$	165.7	3.25	162.1	3.30	/	2.92	220.1	2.96
Mes_2Im	164.1	/	161.0	/	174.0[c]	/	215.8[a]	/
$cAAC^{Me}$	231.0	3.11	225.8	3.25	/	/	313.6	3.13

[a] recorded in THF-d_8. [b] recorded in $CDCl_3$. [c] recorded in CD_2Cl_2.

Crystals suitable for X-ray diffraction were obtained for the compounds **5.4a**-**5.4e**, **5.5a**, **5.5b**, **5.5d**, **5.5e**, **5.6a**, **5.6b** and **5.6d** (Figure 5.2). The adducts crystallize in the monoclinic space groups *C*2/*c* (**5.4a** and **5.4b**), $P2_1/n$ (**5.4c, 5.4d, 5.5d, 5.5e** and **5.6d**), $P2_1/c$ (**5.4e**) and *Cc* (**5.6a**) and in the triclinic space group $P\bar{1}$ (**5.5a**, **5.5b** and **5.6b**), respectively, with one molecule in the asymmetric unit. The most important bonding parameters of the adducts **5.4a**-**5.5b**, **5.5d**-**5.6b** and **5.6d** are summarized in Table 5.2. The solid-state structures, with the exception of **5.6d**, were found to be essentially isostructural and adopt a disphenoidal geometry about the antimony center with the angles C1–Sb–C2/Cl3 and Cl1–Sb–Cl2 varying from 96.70(5) to 104.5(2)° and 164.772(19) to 173.064(15)°, respectively. The axial positions are occupied by the two chlorine atoms Cl1 and Cl2 while C1 and Cl3/C2 are bound in equatorial positions.

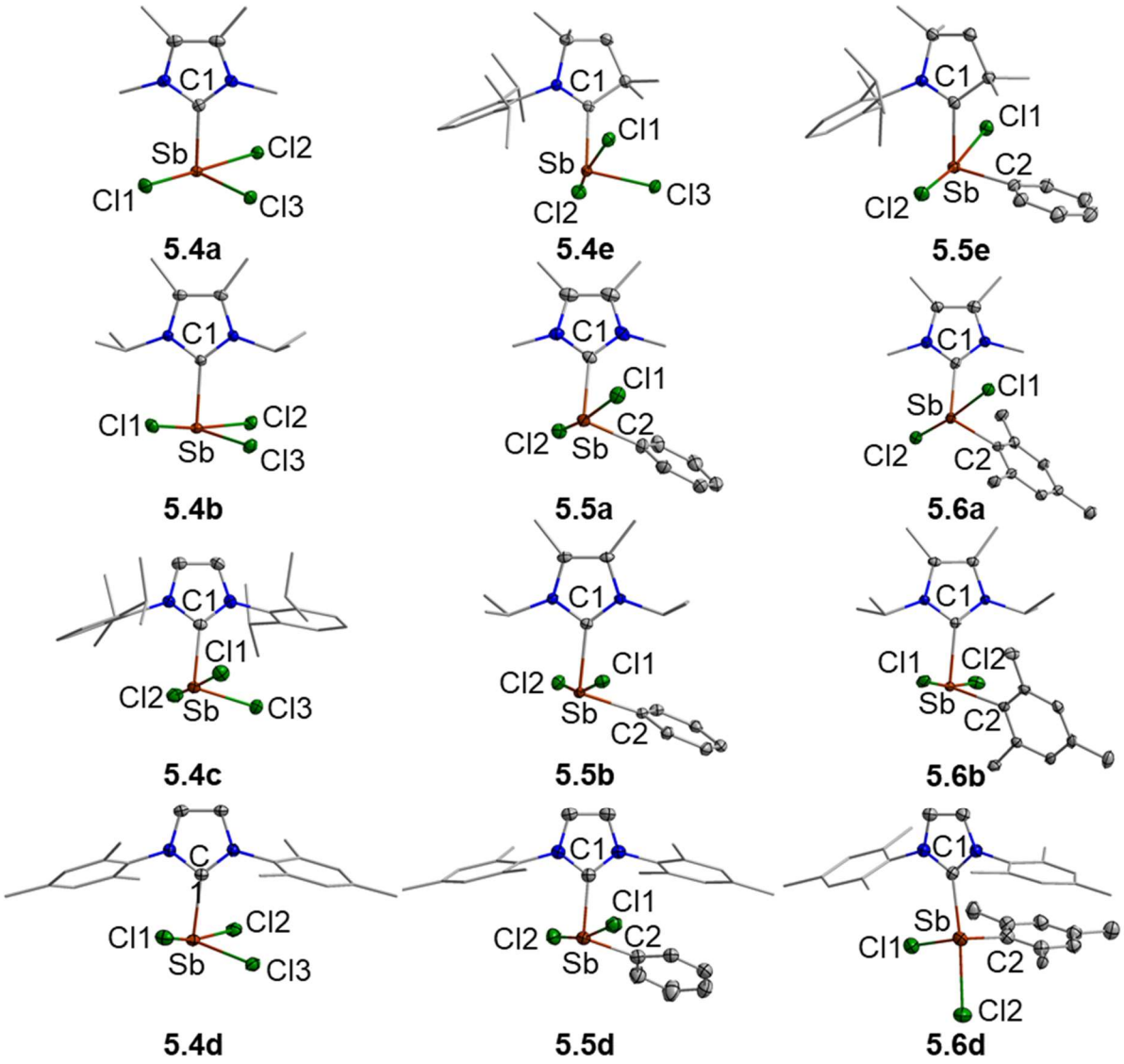

Figure 5.2: Molecular structures of $Me_2Im^{Me}{\cdot}SbCl_3$ (**5.4a**), $iPr_2Im^{Me}{\cdot}SbCl_3$ (**5.4b**), $Dipp_2Im{\cdot}SbCl_3$ (**5.4c**), $Mes_2Im{\cdot}SbCl_3$ (**5.4d**), $cAAC^{Me}{\cdot}SbCl_3$ (**5.4e**), $Me_2Im^{Me}{\cdot}SbCl_2Ph$ (**5.5a**), $iPr_2Im^{Me}{\cdot}SbCl_2Ph$ (**5.5b**), $Mes_2Im{\cdot}SbCl_2Ph$ (**5.5d**), $cAAC^{Me}{\cdot}SbCl_2Ph$ (**5.5e**), $Me_2Im^{Me}{\cdot}SbCl_2Mes$ (**5.6a**), $iPr_2Im^{Me}{\cdot}SbCl_2Mes$ (**5.6b**) and $Mes_2Im{\cdot}SbCl_2Mes$ (**5.6d**) in the solid-state. Hydrogen atoms and solvent molecules (**5.4a**, **5.4d**, **5.5a** and **5.6b**: benzene; **5.4b**: THF) are omitted for clarity. Atomic displacement ellipsoids are set at 50 % probability. Selected bond lengths [Å] and angles[°]: **5.4a**: Sb–C1, 2.2031(18); Sb–Cl1, 2.6351(5); Sb–Cl2, 2.5598(5); Sb–Cl3, 2.3858(5); C1–Sb–Cl3, 96.70(5); Cl1–Sb–Cl2, 171.202(17); **5.4b**: Sb–C1, 2.229(2); Sb–Cl1, 2.5682(5); Sb–Cl2, 2.5795(5); Sb–Cl3, 2.4012(5); C1–Sb–Cl3, 98.46(5); Cl1–Sb–Cl2, 169.362(18); **5.4c**: Sb–C1, 2.2192(2); Sb–Cl1, 2.5734(8); Sb–Cl2, 2.5084(7); Sb–Cl3, 2.3506(6); C1–Sb–Cl3, 97.99(6); Cl1–Sb–Cl2, 171.26(2). **5.4d**: Sb–C1, 2.220(2); Sb–Cl1, 2.5107(6); Sb–Cl2, 2.5915(6); Sb–Cl3, 2.3692(6); C1–Sb–Cl3, 100.72(6); Cl1–Sb–Cl2, 166.38(2); **5.4e**: Sb–C1, 2.239(2); Sb–Cl1, 2.4990(6); Sb–Cl2, 2.5968(5); Sb–Cl3, 2.3616(6); C1–Sb–Cl3, 99.28(6); Cl1–Sb–Cl2, 166.68(2); **5.5a**: Sb–C1, 2.1942(2); Sb–C2, 2.159(3); Sb–Cl1, 2.6251(6); Sb–Cl2, 2.5777(6); C1–Sb–C2, 101.85(9); Cl1–Sb–Cl2, 165.87(2); **5.5b**: Sb–C1, 2.210(2); Sb–C2, 2.170(2); Sb–Cl1, 2.6184(5); Sb–Cl2, 2.5785(5); C1–Sb–C2, 101.55(8); Cl1–Sb–Cl2, 164.772(19); **5.5d**: Sb–C1, 2.220(3); Sb–C2, 2.173(3); Sb–Cl1, 2.6183(8); Sb–Cl2, 2.5747(8); C1–Sb–C2, 100.75(11); Cl1–Sb–Cl2, 168.41(3); **5.5e**: Sb–C1, 2.243(3); Sb–C2, 2.184(3); Sb–Cl1,

2.6229(8); Sb–Cl2, 2.5425(8); C1–Sb–C2, 99.03(12); Cl1–Sb–Cl2, 170.73(3). **5.6a**: Sb–C1, 2.193(6); Sb–C2, 2.170(6); Sb–Cl1, 2.5912(19); Sb–Cl2, 2.6136(16); C1–Sb–C2, 104.5(2); Cl1–Sb–Cl2, 171.42(6); **5.6b**: Sb–C1, 2.2255(17); Sb–C2, 2.1748(18); Sb–Cl1, 2.6017(5); Sb–Cl2, 2.6097(5); C1–Sb–C2, 104.65(7); Cl1–Sb–Cl2, 173.064(15); **5.6d**: Sb–C1, 2.367(6); Sb–C2, 2.142(9); Sb–Cl1, 2.353(2); Sb–Cl2, 2.737(2); C1–Sb–C2, 92.73(3); Cl1–Sb–Cl2, 83.77(8).

This geometry was also found in carbene-stabilized Sb(III) compounds reported previously.[10b-c, 11-12] The bond lengths from antimony to the substituents are by and large unaffected by the substitution pattern of the carbene. The distances Sb–C1 in the $SbCl_3$ adducts **5.4a**-**5.e** range from 2.2031(18) to 2.239(2) Å, which is consistent with those observed in $cAAC^{Cy}{\cdot}SbCl_3$ (Sb–C1: 2.223(3) Å)[12] and 6-$Dipp_2Im{\cdot}SbCl_3$ (Sb–C1: 2.288(2) Å)[11]. The bond lengths Sb–Cl1 and Sb–Cl2 for the chlorine atoms in axial positions (2.4990(6) to 2.6351(5) Å) are notably longer than the Sb–Cl distances of the chlorines in equatorial position (Sb–Cl3: 2.3506(6) to 2.3858(5) Å) in the compounds **5.4a**-**5.e**. This is in line with the understanding of a three-center, four electron bond of the axial moiety X–Sb–X (X = Cl, Br), as reported previously for $Dipp_2Im{\cdot}SbBr_3$. Furthermore, some electron donation of the NHC into an anti-bonding σ^*-orbital of Sb–X_{axial} may weaken and thus elongates these bonds further. [10c, 17] For the $SbCl_2Ar$ (Ar = Ph, Mes) adducts **5.5a**, **5.5b** and **5.5d**-**5.6b** the Sb–C1 distances are in the same range as determined for **5.4a**-**e** and are slightly longer than those observed for the bond to the aryl substituent (Sb–C2: 2.159(3) to 2.184(3) Å). Compared to $DAC^{Mes}{\cdot}SbCl_2Ph$ (Sb–C1: 2.330(4) Å, Sb–C2: 2.364(4) Å; average of two independent molecules in the asymmetric unit) the difference between Sb–C1 and Sb–C2 is slightly smaller. In contrast to $DAC{\cdot}SbCl_2Ph$ (Sb–Cl1: 2.6550(12) Å Sb–Cl2: 2.5157(13) Å; average)[14a] *d*(Sb–Cl1) and *d*(Sb–Cl2) of **5.5a**, **5.5b**, **5.5d**, **5.6a** and **5.6b** are in the small range from 2.5777(6) Å to 2.6251(6) Å. However, the corresponding distances of **5.5e** (Sb–Cl1: 2.6229(8) Å, Sb–Cl2: 2.5425(8) Å) differ remarkably. In contrast to the aforementioned adducts, compound **5.6d** shows an anomaly in its molecular structure. The chlorine atom Cl1 is in *cis*-position to Cl2 which is caused by the approaching and repulsive *ortho*-methyl groups of the mesityl substituent. To get some deeper insight into the bonding situation, quantum-mechanical DFT calculations on the B3LYP/def2-SV(P) level of theory were performed.[18,19] According to these calculations this geometry is energetically favored by 15.8 kJ/mol compared to the disphenoidal geometry found for the other adducts.

Table 5.2: Selected bond lengths [Å] and angles [°] of the NHC-adducts **5.4a**-**5.4e**, **5.5a**, **5.5b**, **5.5d**, **5.5e**, **5.6a** and **5.6b** as well as the [a]NHC adducts **5.7** and **5.8**.

	Sb–C1	Sb–C2/Cl3	Sb–Cl1	Sb–Cl2	C1–Sb–Cl3/C2	Cl1–Sb–Cl2
(5.4a) Me_2Im^{Me}·$SbCl_3$	2.2031(18)	2.3858(5)	2.6351(5)	2.5598(5)	96.70(5)	171.202(17)
(5.4b) *i*Pr_2Im^{Me}·$SbCl_3$	2.229(2)	2.4012(5	2.5682(5)	2.5795(5)	98.46(5)	169.362(18)
(5.4c) $Dipp_2Im$·$SbCl_3$	2.2192(2)	2.3506(6)	2.5734(8)	2.5084(7)	97.99(6)	171.26(2)
(5.4d) Mes_2Im·$SbCl_3$	2.220(2)	2.3692(6)	2.5107(6)	2.5915(6)	100.72(6)	166.38(2)
(5.4e) $cAAC^{Me}$·$SbCl_3$	2.239(2)	2.3616(6)	2.4990(6)	2.5968(5)	99.28(6)	166.68(2)
(5.5a) Me_2Im^{Me}·$SbCl_2Ph$	2.1942(2)	2.159(3)	2.6251(6)	2.5777(6)	101.85(9)	165.87(2)
(5.5b) *i*Pr_2Im^{Me}·$SbCl_2Ph$	2.210(2)	2.170(2)	2.6184(5)	2.5785(5)	101.55(8)	164.772(19)
(5.5d) Mes_2Im·$SbCl_2Ph$	2.220(3)	2.173(3)	2.6183(8)	2.5747(8)	100.75(11)	168.41(3)
(5.5e) $cAAC^{Me}$·$SbCl_2Ph$	2.243(3)	2.184(3)	2.6229(8)	2.5425(8)	99.03(12)	170.73(3)
(5.6a) Me_2Im^{Me}·$SbCl_2Mes$	2.193(6)	2.170(6)	2.5912(19)	2.6136(16)	104.5(2)	171.42(6)
(5.6b) *i*Pr_2Im^{Me}·$SbCl_2Mes$	2.2255(17)	2.1748(18)	2.6017(5)	2.6097(5)	104.65(7)	173.064(15)
(5.6d) Mes_2Im·$SbCl_2Mes$[a]	2.367(6)	2.142(9)	2.353(2)	2.737(2)	92.73(3)	83.77(8)

	Sb–C3	Sb–C2	Sb–Cl1	Sb–Cl2	C2–Sb–C3	Cl1–Sb–Cl2
(5.7) [a]$Dipp_2Im$·$SbCl_2Mes$	2.1639(18)	2.1716(19)	2.6578(5)	2.5752(5)	100.80(7)	169.969(15)
(5.8) [a]$Dipp_2Im$·$SbCl_2Ph$[b]	2.1582(18) 2.1545(18)	2.163(2) 2.1656(19)	2.6093(5) 2.6627(5)	2.5641(5) 2.5388(5)	93.16(7) 95.39(7)	170.303(17) 180.233(17)

[a] The molecule is disordered and the data reported corresponds to the part with 84 % occupancy. [b] Two independent molecules were found in the unit cell.

Thermal induced isomerization of 5c and 6c

It has been reported previously that sterically demanding NHCs may switch coordination mode from „normal" (coordination *via* the C2 carbon atom) to "abnormal" (coordination *via* the backbone C4 carbon atom). Two examples were presented earlier for antimony chemistry with thermally induced isomerization of $Dipp_2Im{\cdot}SbX_3$ to $[(^aDipp_2Im)(Dipp_2Im)SbF_2]^+[SbF_4]^-$ and $^aDipp_2Im{\cdot}SbBr_3$, respectively.[10b-c] Similarly, heating solutions of **5.5c** and **5.6c** in benzene to 80 °C overnight and removal of all volatiles *in vacuo* afforded the zwitterionic ^{a}NHC adducts $^aDipp_2Im{\cdot}SbCl_2Mes$ (**5.7**) and $^aDipp_2Im{\cdot}SbCl_2Ph$ (**5.8**) in nearly quantitative yields (route A: **5.7**, 98 %; **5.8**, 95 %; Scheme 5.2, top). Another synthetic approach towards the ^{a}NHC adducts **5.7** and **5.8** was the reaction of $SbCl_2Mes$ and $SbCl_2Ph$, respectively, with $Dipp_2Im$ in benzene at elevated temperatures. Heating these reaction mixtures to 80 °C overnight led in both cases to a colorless precipitate, which was collected by filtration and afforded **5.7** and **5.8** in very good yields (route B: **5.7,** 89 %; **5.8**, 86 %). For other adducts, similar rearrangements were detected in traces or minor amounts after prolonged heating.

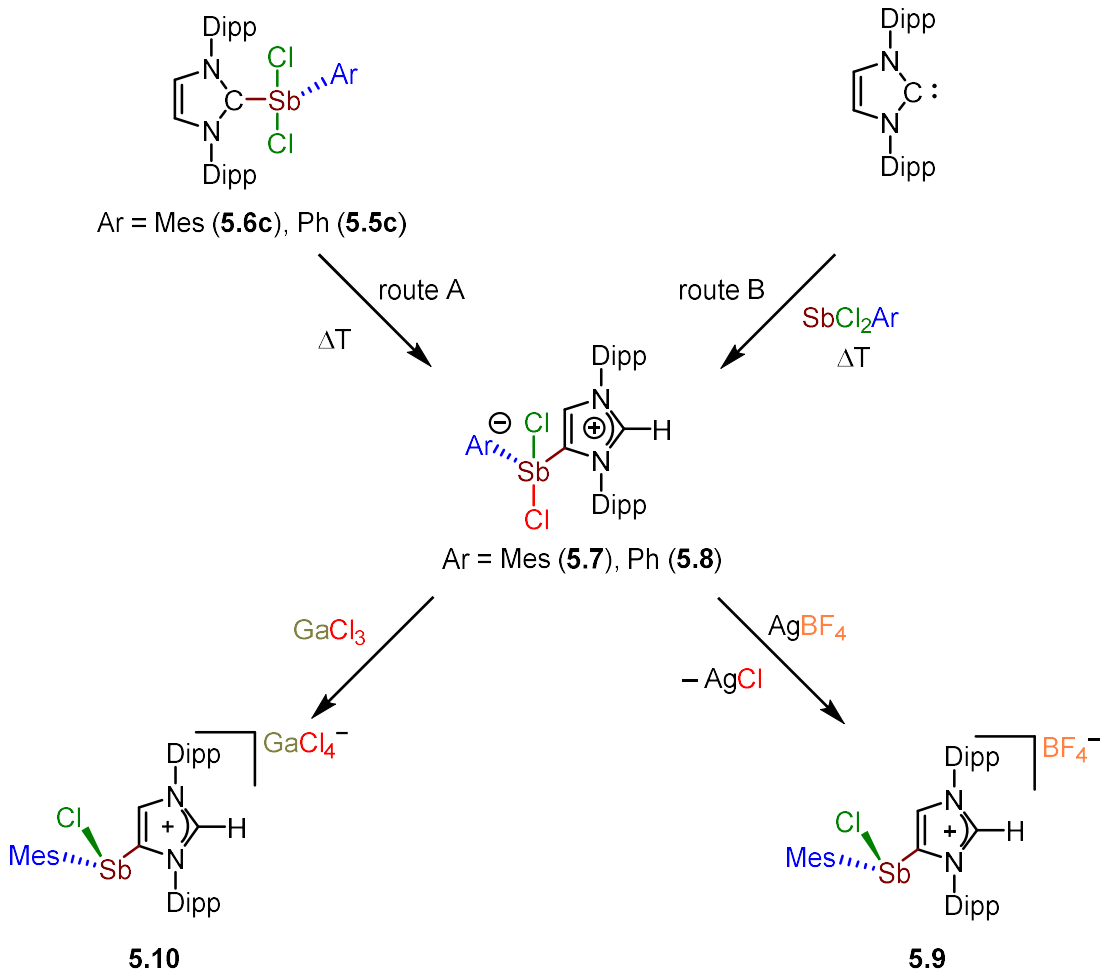

Scheme 5.2: Synthesis of ^{a}Dipp$_2$Im·SbCl$_2$Mes (**5.7**) and ^{a}Dipp$_2$Im·SbCl$_2$Ph (**5.8**) (top) and chloride abstraction from **5.7** by $GaCl_3$ and $AgBF_4$ to form the salts [^{a}Dipp$_2$Im·SbCl$_2$Mes]$^+$[BF_4]$^-$ (**5.9**) and [^{a}Dipp$_2$Im·SbCl$_2$Mes]$^+$[$GaCl_4$]$^-$ (**5.10**) (bottom).

Both compounds show two characteristic resonances in their ^{1}H NMR spectra (Table 5.3), i.e., one doublet for the remaining backbone proton C4–H (7.87 ppm, **5.7**; 7.22 ppm, **5.8**) and a second doublet for the imidazolium proton C2–H (8.08 ppm, **5.7**; 8.13 ppm, **5.8**). Both hydrogen atoms show coupling with one another ($^{4}J_{H\text{-}H}$ = 1.5 Hz). Additional prove of the asymmetry in **5.7** and **5.8** are the resonances of the substituents at the nitrogen atoms, which show two separate sets of signals in the ^{1}H and ^{13}C{^{1}H} NMR spectra. The characteristic resonances of the methine protons of the *iso*-propyl groups were observed at 2.54 ppm and 2.80 ppm (**5.7**) and at 2.45 ppm and 2.94 ppm (**5.8**). The ^{13}C{^{1}H} NMR resonances for the NHC C2 carbon atom were shifted to 135.2 ppm (**5.7**) and 135.7 ppm (**5.8**), whereas the antimony bound carbon atom (C4) was observed at 146.5 ppm (**5.7**) and 151.1 ppm (**5.8**), respectively (Table 5.3).

Table 5.3: Selected ^{1}H NMR and ^{13}C{^{1}H} NMR chemical shifts (ppm) of the [a]NHC-adducts **5.7**-**5.10** recorded in CD_2Cl_2

	δ^{1}H (*i*Pr-C*H*)	δ^{1}H (SbCC*H*)	δ^{1}H (NC*H*N)	δ^{13}C (N*C*HN)	δ^{13}C (N*C*Sb)	δ^{13}C (NC*C*N)
5.7	2.54 2.80	7.87	8.08	135.2	146.5	136.4
5.8	2.45 2.94	7.22	8.13	135.7	151.1	132.8
5.9	2.33 2.43	7.65	9.13	141.2	139.2	133.1
5.10	2.45 2.51	7.72	8.68	139.9	139.4	133.1

Furthermore, crystals suitable for X-ray diffraction of **5.7** and **5.8** were obtained by diffusion of *n*-pentane into a saturated solution of the corresponding adduct in dichloromethane at 12 °C (Figure 5.3).

The compounds **5.7** and **5.8** crystallize in the monoclinic space groups $P2_1/c$ (**5.7**) and $C2/c$ (**5.8**). In analogy to the normal coordinated adducts **5.4a**-**5.6d**, the peripheries of the antimony centers of **5.7** and **5.8** adopt disphenoidal geometries. The $SbCl_2Ar$ moiety is coordinated to the backbone carbon atom C4 with bond lengths of 2.1639(18) Å (**5.7**) and 2.1582(18) Å/2.1545(18) Å (**5.8**).

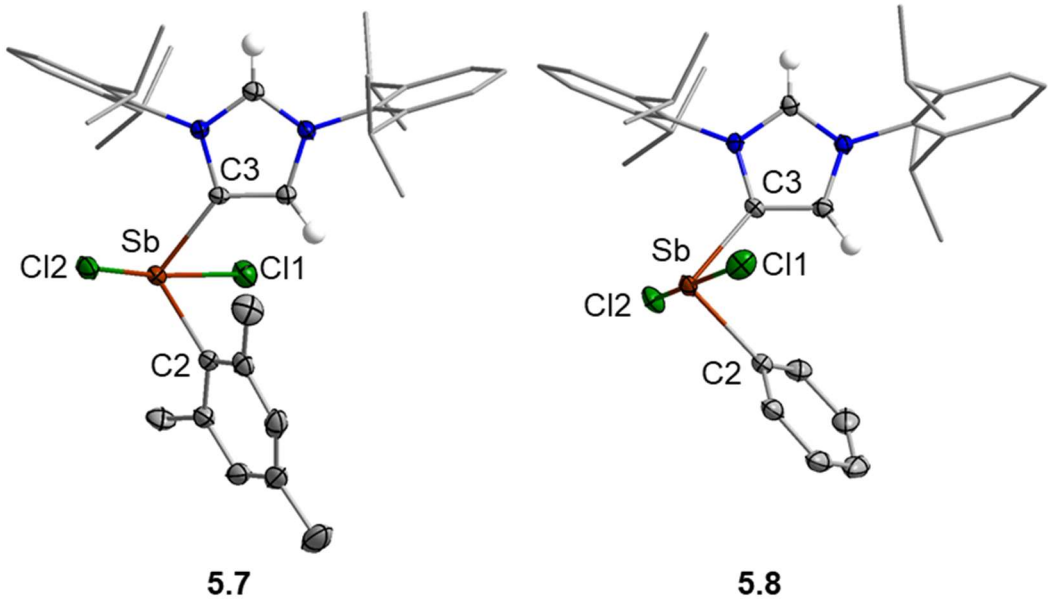

Figure 5.3: Molecular structures of $^{a}Dipp_2Im{\cdot}SbCl_2Mes$ (**5.7**) and $^{a}Dipp_2Im{\cdot}SbCl_2Ph$ (**5.8**) in the solid-state. Hydrogen atoms (except the imidazolium protons) and solvent molecules (**5.7**: benzene, **5.8**: toluene) are omitted for clarity. For compound **5.8**, only one of two independent molecules of the asymmetric unit is shown. Atomic displacement ellipsoids are set at 50 % probability. Selected bond lengths [Å] and angles [°]: **5.7**: Sb–C3, 2.1639(18); Sb–C2, 2.1716(19); Sb–Cl1, 2.6578(5); Sb–Cl2, 2.5752(5); C2–Sb–C3, 100.80(7); Cl1–Sb–Cl2, 169.969(15); **5.8** (molecule 1): Sb–C3, 2.1582(18); Sb–C2, 2.163(2); Sb–Cl1, 2.6093(5); Sb–Cl2, 2.5641(5); C2–Sb–C3, 93.16(7); Cl1–Sb–Cl2, 170.303(17); **5.8** (molecule 2): Sb–C3, 2.1545(18); Sb–C2, 2.1656(19); Sb–Cl1, 2.6627(5); Sb–Cl2, 2.5388(5); C2–Sb–C3, 95.39(7); Cl1–Sb–Cl2, 180.233(17).

Compared to the $Sb–C_{carbene}$ (C1) bond lengths found in the NHC-adducts, the distances Sb–C3 of the abnormal coordinated NHCs in **5.7** and **5.8** are notably shorter, which underscores an increased Sb–C bond strength and thus higher thermodynamic stability of these adducts. In contrast, the Sb–C2 distances of **5.7** (2.1716(19) Å) and **5.8** (2.163(2) Å; 2.1656(19) Å) are similar to the corresponding bond lengths of the

normal coordinated adducts (Table 5.2). The angles about the antimony center of **5.7** (C2–Sb–C3: 100.80(7)°; Cl1–Sb–Cl2: 169.969(15)°) and **5.8** (C2–Sb–C3: molecule 1, 93.16(7)°; molecule 2, 95.39(7)°; Cl1–Sb–Cl2: molecule 1, 170.303(17)°; molecule 2, 180.233(17)°) are only marginally affected by the coordination mode.

Chloride Abstraction from 7 and 8 by $AgBF_4$ and $GaCl_3$

For the synthesis of three-coordinate antimony cations we reacted **5.7** with the chloride abstracting agents $AgBF_4$ and $GaCl_3$. Driven by the precipitation of AgCl and the formation of $[GaCl_4]^-$ as counterion, these reactions afforded the imidazolium salts $[^aDipp_2Im{\cdot}SbClAr]^+[BF_4]^-$ (**5.9**) and $[^aDipp_2Im{\cdot}SbClAr]^+[GaCl_4]^-$ (**5.10**) in very good yields (**5.9**, 83 %; **5.10**, 91 %) (Scheme 5.2, bottom). The formation is evident from ^1H and $^{13}C\{^1H\}$ NMR data. Compared to the starting material **5.7** all resonances of **5.9** and **5.10** (Table 5.3) are shifted.

Single crystals suitable for X-Ray diffraction (Figure 5.4) were obtained for **5.9** and **5.10** by storing a concentrated dichloromethane solution at 6 °C.

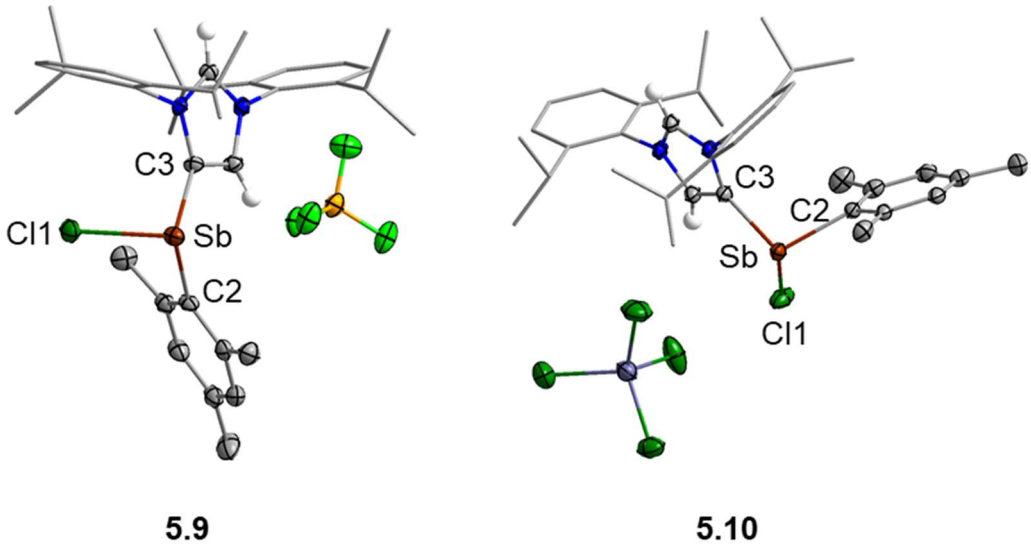

Figure 5.4: Molecular structures of $[^aDipp_2Im{\cdot}SbClMes]^+[BF_4]^-$ (**5.9**) and $[^aDipp_2Im{\cdot}SbClMes]^+[GaCl_4]^-$ (**5.10**) in the solid-state. Hydrogen atoms (except the imidazolium protons) and solvent molecules (**5.10**: CH_2Cl_2) are omitted for clarity. Atomic displacement ellipsoids are set at 50 % probability. Selected bond lengths [Å] and angles [°]: **5.9**: Sb–C3, 2.151(2); Sb–C2, 2.166(2); Sb–Cl1, 2.3971(6); C3–Sb–C2, 94.71(8); C3–Sb–Cl1, 96.59(6); C2–Sb–Cl1, 97.37(6); **5.10**: Sb–C3, 2.158(2); Sb–C2, 2.149(2); Sb–Cl1, 2.3563(6); C3–Sb–C2, 100.99(9); C3–Sb–Cl1, 91.26(7); C2–Sb–Cl1, 98.07(7).

The compounds **5.9** and **5.10** crystallize in the monoclinic space group $P2_1/c$ with one molecule in the asymmetric unit. In both structures the central atom Sb is surrounded by three substituents and adopts a pseudo tetrahedral geometry. The angles C2–Sb–C3, C2–Sb–Cl1 and C3–Sb–Cl1 range from 94.71(8)° to 100.99(9)°. There are no significant changes of the carbon antimony distances Sb–C2 (**5.9**, 2.166(2) Å; **5.10**, 2.149(2) Å; **5.7**, 2.1639(18) Å) and Sb–C3 (**5.9**, 2.151(2) Å; **5.10**, 2.158(2) Å; **5.7**, 2.1716(19) Å) upon chloride abstraction. However, the bond from Sb to chlorine Sb–Cl1 (**5.9**, 2.3971(6) Å; **5.10**, 2.3563(6) Å;) is significantly shortened in comparison to parent **5.7** (Sb1–Cl1, 2.6578(5) Å; Sb–Cl2, 2.5752(5) Å).

5.3 Conclusion

We present here a comprehensive study on synthesis, spectroscopy and molecular structures of NHC-stabilized antimony(III) adducts, which have been prepared by the reaction of different carbenes with the antimony compounds $SbCl_2R$ (R = Cl, Ph, Mes). The results obtained for the adducts NHC·$SbCl_2R$ (R = Cl, Ph, Mes) (**5.4a**-**5.6d**) give further insight into the bonding situation at antimony and the influence of different carbenes and NHC substitution pattern as well as different substituents at antimony on these adducts. Heating of the NHC adducts **5.6c** and **5.5c** or their precursors, respectively, led to isolation of the abnormally coordinated adducts $^{a}Dipp_2Im{\cdot}SbCl_2Ar$ (Ar = Mes (**5.7**), Ph (**5.8**)). Chloride abstraction from **5.7** by the *Lewis*-acids $GaCl_3$ and $AgBF_4$ afforded the ionic compounds $[^{a}Dipp_2Im{\cdot}SbClAr]^{+}[X]^{-}$ ($[X]^{-}$ = $[BF_4]^{-}$ (**5.9**); $[GaCl_4]^{-}$ (**5.10**)), which might be useful as precursors for the synthesis of other antimony (III) compounds with abnormally coordinated NHCs or novel, backbone Sb-substitutes NHCs. The variety of the NHC-stabilized antimony(III) compounds reported herein is a promising starting point for a further development of NHC antimony chemistry.

5.4 References

[1] a) P. P. Power, *Chem. Rev.* **1999**, *99*, 3463-3504; b) D. Martin, M. Melaimi, M. Soleilhavoup, G. Bertrand, *Organometallics* **2011**, *30*, 5304-5313; c) D. Martin, M. Soleilhavoup, G. Bertrand, *Chem. Sci.* **2011**, *2*, 389-399; d) C. D. Martin, M. Soleilhavoup, G. Bertrand, *Chem. Sci.* **2013**, *4*, 3020-3030; e) O. Back, M. Henry-Ellinger, C. D. Martin, D. Martin, G. Bertrand, *Angew. Chem. Int. Ed.* **2013**, *52*, 2939-2943; *Angew. Chem.* **2013**, *125*, 3011-3015; f) S. Bellemin-Laponnaz, S. Dagorne, *Chem. Rev.* **2014**, *114*, 8747-8774; g) Y. Wang, G. H. Robinson, *Inorg. Chem.* **2014**, *53*, 11815-11832; h) M. Soleilhavoup, G. Bertrand, *Acc. Chem. Res.* **2015**, *48*, 256-266; i) S. Würtemberger-Pietsch, U. Radius, T. B. Marder, *Dalton Trans.* **2016**, *45*, 5880-5895; j) M. Melaimi, R. Jazzar, M. Soleilhavoup, G. Bertrand, *Angew. Chem. Int. Ed.* **2017**, *56*, 10046-10068; *Angew. Chem.* **2017**, *129*, 10180-10203; k) U. S. D. Paul, U. Radius, *Eur. J. Inorg. Chem.* **2017**, 3362-3375; l) G. Guisado-Barrios, M. Soleilhavoup, G. Bertrand, *Acc. Chem. Res.* **2018**, *51*, 3236-3244; m) V. Nesterov, D. Reiter, P. Bag, P. Frisch, R. Holzner, A. Porzelt, S. Inoue, *Chem. Rev.* **2018**, *118*, 9678-9842; n) U. S. D. Paul, M. J. Krahfuss, U. Radius, *Chemie unserer Zeit* **2018**, *53*, 212-223; o) A. Doddi, M. Peters, M. Tamm, *Chem. Rev.* **2019**, *119*, 6994-7112; p) J. Lorkowski, M. Krahfuss, M. Kubicki, U. Radius, C. Pietraszuk, *Chem. Eur. J.* **2019**, *25*, 11365-11374; q) R. Jazzar, M. Soleilhavoup, G. Bertrand, *Chem. Rev.* **2020**, *120*, 4141-4168; r) S. C. Sau, P. K. Hota, S. K. Mandal, M. Soleilhavoup, G. Bertrand, *Chem. Soc. Rev.* **2020**, *49*, 1233-1252; s) M. Soleilhavoup, G. Bertrand, *Chem.* **2020**, *6*, 1275-1282; t) C. J. Carmalt, A. H. Cowley, *Adv. Inorg. Chem.* **2000**, *50*, 1-32; u) N. Kuhn, A. Al-Sheikh, *Coord. Chem. Rev.* **2005**, *249*, 829-857; v) C. E. Willans, *Organomet. Chem.* **2010**, *36*, 1-28; w) Y. Wang, G. H. Robinson, *Inorg. Chem.* **2011**, *50*, 12326-12337; x) D. P. Curran, A. Solovyev, M. Makhlouf Brahmi, L. Fensterbank, M. Malacria, E. Lacôte, *Angew. Chem. Int. Ed.* **2011**, *50*, 10294-10317; *Angew. Chem.* **2011**, *123*, 10476-10500; y) C. Fliedel, G. Schnee, T. Avilés, S. Dagorne, *Coord. Chem. Rev.* **2014**, *275*, 63-86; z) G. Prabusankar, A. Sathyanarayana, P. Suresh, C. N. Babu, K. Srinivas, B. P. R. Metla, *Coord.*

Chem. Rev. **2014**, *269*, 96−133; aa) K. C. Mondal, S. Roy, H. W. Roesky, *Chem. Soc. Rev.* **2016**, *45*, 1080-1111.

[2] a) M.-T. Lee, C.-H. Hu, *Organometallics* **2004**, *23*, 976-983; b) R. Dorta, E. D. Stevens, N. M. Scott, C. Costabile, L. Cavallo, C. D. Hoff, S. P. Nolan, *J. Am. Chem. Soc.* **2005**, *127*, 2485-2495; c) H. Jacobsen, A. Correa, C. Costabile, L. Cavallo, *J. Organomet. Chem.* **2006**, *691*, 4350-4358; d) S. Diez-Gonzalez, S. P. Nolan, *Coord. Chem. Rev.* **2007**, *251*, 874-883; e) R. Tonner, G. Heydenrych, G. Frenking, *Chem. Asian J.* **2007**, *2*, 1555-1567; f) R. A. Kelly III, H. Clavier, S. Giudice, N. M. Scott, E. D. Stevens, J. Bordner, I. Samardjiev, C. D. Hoff, L. Cavallo, S. P. Nolan, *Organometallics* **2008**, *27*, 202-210; g) N. M. Scott, H. Clavier, P. Mahjoor, E. D. Stevens, S. P. Nolan, *Organometallics* **2008**, *27*, 3181-3186; h) A. Poater, B. Cosenza, A. Correa, S. Giudice, F. Ragone, V. Scarano, L. Cavallo, *Eur. J. Inorg. Chem.* **2009**, 1759-1766; i) H. Clavier, S. P. Nolan, *Chem. Commun.* **2010**, *46*, 841-861; j) C. Lujan, S. P. Nolan, *J. Organomet. Chem.* **2011**, *696*, 3935-3938; k) J. Balogh, A. M. Z. Slawin, S. P. Nolan, *Organometallics* **2012**, *31*, 3259-3263; l) A. Collado, J. Balogh, S. Meiries, A. M. Z. Slawin, L. Falivene, L. Cavallo, S. P. Nolan, *Organometallics* **2013**, *32*, 3249-3252; m) A. Liske, K. Verlinden, H. Buhl, K. Schaper, C. Ganter, *Organometallics* **2013**, *32*, 5269-5272; n) D. J. Nelson, A. Collado, S. Manzini, S. Meiries, A. M. Z. Slawin, D. B. Cordes, S. P. Nolan, *Organometallics* **2014**, *33*, 2048-2058; o) S. V. C. Vummaleti, D. J. Nelson, A. Poater, A. Gomez-Suarez, D. B. Cordes, A. M. Z. Slawin, S. P. Nolan, L. Cavallo, *Chem. Sci.* **2015**, *6*, 1895-1904; p) M. Saab, D. J. Nelson, N. V. Tzouras, T. A. C. A. Bayrakdar, S. P. Nolan, F. Nahra, K. van Hecke, *Dalton Trans.* **2020**, *49*, 12068-12081.

[3] a) S. Pietsch, U. Paul, I. A. Cade, M. J. Ingleson, U. Radius, T. B. Marder, *Chem. Eur. J.* **2015**, *21*, 9018-9021; b) S. Würtemberger-Pietsch, H. Schneider, T. B. Marder, U. Radius, *Chem. Eur. J.* **2016**, *22*, 13032-13036; c) M. Eck, S. Würtemberger-Pietsch, A. Eichhorn, J. H. Berthel, R. Bertermann, U. S. D. Paul, H. Schneider, A. Friedrich, C. Kleeberg, U. Radius, T. B. Marder, *Dalton Trans.* **2017**, *46*, 3661-3680; d) A. F. Eichhorn, L. Kuehn, T. B. Marder, U. Radius, *Chem. Commun.* **2017**, *53*, 11694-11696; e) H. Schneider, A. Hock, R. Bertermann, U. Radius, *Chem. Eur. J.* **2017**, *23*, 12387-12398; f) A. Hock,

H. Schneider, M. J. Krahfuss, U. Radius, *Z. Anorg. Allg. Chem.* **2018**, *644*, 1243-1251; g) H. Schneider, A. Hock, A. D. Jaeger, D. Lentz, U. Radius, *Eur. J. Inorg. Chem.* **2018**, 4031-4043; h) L. Kuehn, M. Stang, S. Würtemberger-Pietsch, A. Friedrich, H. Schneider, U. Radius, T. B. Marder, *Faraday Discuss.* **2019**, *220*, 350-363; i) A. Hock, L. Werner, C. Luz, U. Radius, *Dalton Trans.* **2020**, *49*, 11108-11119; j) A. Hock, L. Werner, M. Riethmann, U. Radius, *Eur. J. Inorg. Chem.* **2020**, 4015-4023.

[4] a) D. Schmidt, J. H. Berthel, S. Pietsch, U. Radius, *Angew. Chem. Int. Ed.* **2012**, *51*, 8881-8885; *Angew. Chem.* **2012**, *124*, 9011-9015; b) P. Hemberger, A. Bodi, T. Gerber, M. Würtemberger, U. Radius, *Chem. Eur. J.* **2013**, *19*, 7090-7099; c) P. Hemberger, A. Bodi, J. H. Berthel, U. Radius, *Chem. Eur. J.* **2015**, *21*, 1434-1438; d) H. Schneider, D. Schmidt, U. Radius, *Chem. Eur. J.* **2015**, *21*, 2793-2797; e) H. Schneider, M. J. Krahfuß, U. Radius, *Z. Anorg. Allg. Chem.* **2016**, *642*, 1282-1286; f) A. F. Eichhorn, S. Fuchs, M. Flock, T. B. Marder, U. Radius, *Angew. Chem. Int. Ed.* **2017**, *56*, 10209-10213; *Angew. Chem.* **2017**, *129*, 10343-10347; g) U. S. D. Paul, U. Radius, *Chem. Eur. J.* **2017**, *23*, 3993-4009; h) H. C. Schmitt, M. Flock, E. Welz, B. Engels, H. Schneider, U. Radius, I. Fischer, *Chem. Eur. J.* **2017**, *23*, 3084-3090.

[5] a) H. Schneider, D. Schmidt, U. Radius, *Chem. Commun.* **2015**, *51*, 10138-10141; b) L. Werner, G. Horrer, M. Philipp, K. Lubitz, M. W. Kuntze-Fechner, U. Radius, *Z. Anorg. Allg. Chem.* **2021**, *647*, 881-895.

[6] a) J. I. Bates, P. Kennepohl, D. P. Gates, *Angew. Chem. Int. Ed.* **2009**, *48*, 9844-9847; *Angew. Chem.* **2009**, *121*, 10028-10031; b) J. J. Weigand, K.-O. Feldmann, F. D. Henne, *J. Am. Chem. Soc.* **2010**, *132*, 16321-16323; c) D. Mendoza-Espinosa, B. Donnadieu, G. Bertrand, *Chem. Asian J.* **2011**, *6*, 1099-1103; d) J. I. Bates, D. P. Gates, *Organometallics* **2012**, *31*, 4529-4536; e) F. D. Henne, E.-M. Schnöckelborg, K.-O. Feldmann, J. Grunenberg, R. Wolf, J. J. Weigand, *Organometallics* **2013**, *32*, 6674-6680; f) K. Schwedtmann, M. H. Holthausen, K.-O. Feldmann, J. J. Weigand, *Angew. Chem. Int. Ed.* **2013**, *52*, 14204-14208; *Angew. Chem.* **2013**, *125*, 14454-14458; g) A. Doddi, D. Bockfeld, A. Nasr, T. Bannenberg, P. G. Jones, M. Tamm, *Chem. Eur. J.* **2015**, *21*, 16178-16189; h) F. D. Henne, A. T. Dickschat, F. Hennersdorf, K.-O. Feldmann, J. J. Weigand, *Inorg. Chem.* **2015**, *54*, 6849-

6861; i) F. D. Henne, F. A. Watt, K. Schwedtmann, F. Hennersdorf, M. Kokoschka, J. J. Weigand, *Chem. Commun.* **2016**, *52*, 2023-2026; j) P. K. Majhi, K. C. Chow, T. H. Hsieh, E. G. Bowes, G. Schnakenburg, P. Kennepohl, R. Streubel, D. P. Gates, *Chem. Commun.* **2016**, *52*, 998-1001; k) K. Schwedtmann, R. Schoemaker, F. Hennersdorf, A. Bauza, A. Frontera, R. Weiss, J. J. Weigand, *Dalton Trans.* **2016**, *45*, 11384-11396; l) A. Beil, R. J. Gilliard, Jr., H. Grützmacher, *Dalton Trans.* **2016**, *45*, 2044-2052.; m) L. Dostal, *Coord. Chem. Rev.* **2017**, *353*, 142-158; n) T. Krachko, M. Bispinghoff, A. M. Tondreau, D. Stein, M. Baker, A. W. Ehlers, J. C. Slootweg, H. Grützmacher, *Angew. Chem. Int. Ed.* **2017**, *56*, 7948-7951; *Angew. Chem.* **2017**, *129*, 8056-8059.

[7] a) A. J. Arduengo III, J. C. Calabrese, A. H. Cowley, H. V. R. Dias, J. R. Goerlich, W. J. Marshall, B. Riegel, *Inorg. Chem.* **1997**, *36*, 2151-2158; b) A. J. Arduengo III, H. V. R. Dias, J. C. Calabrese, *Chem. Lett.* **1997**, *26*, 143-144; c) B. D. Ellis, C. A. Dyker, A. Decken, C. L. Macdonald, *Chem. Commun.* **2005**, 1965-1967; d) T. Böttcher, B. S. Bassil, L. Zhechkov, T. Heine, G.-V. Röschenthaler, *Chem. Sci.* **2013**, *4*, 77-83; e) A. Doddi, D. Bockfeld, T. Bannenberg, P. G. Jones, M. Tamm, *Angew. Chem. Int. Ed.* **2014**, *53*, 13568-13572; *Angew. Chem.* **2014**, *126*, 13786-13790; f) R. R. Rodrigues, C. L. Dorsey, C. A. Arceneaux, T. W. Hudnall, *Chem. Commun.* **2014**, *50*, 162-164; g) M. Bispinghoff, H. Grützmacher, *Chimia* **2016**, *70*, 279-283; h) M. Bispinghoff, A. M. Tondreau, H. Grützmacher, C. A. Faradji, P. G. Pringle, *Dalton Trans.* **2016**, *45*, 5999-6003; i) D. Bockfeld, A. Doddi, P. G. Jones, M. Tamm, *Eur. J. Inorg. Chem.* **2016**, 3704-3712; j) M. Cicac-Hudi, J. Bender, S. H. Schlindwein, M. Bispinghoff, M. Nieger, H. Grützmacher, D. Gudat, *Eur. J. Inorg. Chem.* **2016**, 649-658; k) A. Doddi, D. Bockfeld, M. K. Zaretzke, C. Kleeberg, T. Bannenberg, M. Tamm, *Dalton Trans.* **2017**, *46*, 15859-15864; l) S. Roy, K. C. Mondal, S. Kundu, B. Li, C. J. Schurmann, S. Dutta, D. Koley, R. Herbst-Irmer, D. Stalke, H. W. Roesky, *Chem. Eur. J.* **2017**, *23*, 12153-12157.

[8] a) J. D. Masuda, W. W. Schoeller, B. Donnadieu, G. Bertrand, *Angew. Chem. Int. Ed.* **2007**, *46*, 7052-7055; *Angew. Chem.* **2007**, *119*, 7182-7185; b) J. D. Masuda, W. W. Schoeller, B. Donnadieu, G. Bertrand, *J. Am. Chem. Soc.* **2007**, *129*, 14180-14181; c) Y. Wang, Y. Xie, P. Wei, R. B. King, H. F. Schaefer

III, P. v. R. Schleyer, G. H. Robinson, *J. Am. Chem. Soc.* **2008**, *130*, 14970-14971; d) O. Back, G. Kuchenbeiser, B. Donnadieu, G. Bertrand, *Angew. Chem. Int. Ed.* **2009**, *48*, 5530-5533; *Angew. Chem.* **2009**, *121*, 5638-5641; e) O. Back, B. Donnadieu, P. Parameswaran, G. Frenking, G. Bertrand, *Nature Chem.* **2010**, *2*, 369-373; f) Y. Wang, Y. Xie, M. Y. Abraham, R. J. Gilliard, P. Wei, H. F. Schaefer III, P. v. R. Schleyer, G. H. Robinson, *Organometallics* **2010**, *29*, 4778-4780; g) C. L. Dorsey, B. M. Squires, T. W. Hudnall, *Angew. Chem. Int. Ed.* **2013**, *52*, 4462-4465; *Angew. Chem.* **2013**, *125*, 4558-4561; h) M. H. Holthausen, S. K. Surmiak, P. Jerabek, G. Frenking, J. J. Weigand, *Angew. Chem. Int. Ed.* **2013**, *52*, 11078-11082; *Angew. Chem.* **2013**, *125*, 11284-11288; i) C. D. Martin, C. M. Weinstein, C. E. Moore, A. L. Rheingold, G. Bertrand, *Chem. Commun.* **2013**, *49*, 4486-4488; j) J. B. Waters, T. A. Everitt, W. K. Myers, J. M. Goicoechea, *Chem. Sci.* **2016**, *7*, 6981-6987; k) N. Hayakawa, K. Sadamori, S. Tsujimoto, M. Hatanaka, T. Wakabayashi, T. Matsuo, *Angew. Chem. Int. Ed.* **2017**, *56*, 5765-5769; Angew. Chem. **2017**, *129,* 5859-5863.

[9] a) M. Y. Abraham, Y. Wang, Y. Xie, P. Wei, H. F. Schaefer III, P. v. R. Schleyer, G. H. Robinson, *Chem. Eur. J.* **2010**, *16*, 432-435; b) N. Holzmann, G. Frenking, *Z. Naturforsch. A* **2014**, *69*, 385-395; c) J. W. Dube, Y. Zheng, W. Thiel, M. Alcarazo, *J. Am. Chem. Soc.* **2016**, *138*, 6869-6877; d) A. Doddi, M. Weinhart, A. Hinz, D. Bockfeld, J. M. Goicoechea, M. Scheer, M. Tamm, *Chem. Commun.* **2017**, *53*, 6069-6072; e) A. Doddi, D. Bockfeld, M. K. Zaretzke, T. Bannenberg, M. Tamm, *Chem. Eur. J.* **2019**, *25*, 13119-13123.

[10] a) A. Aprile, R. Corbo, K. V. Tan, D. J. Wilson, J. L. Dutton, *Dalton Trans.* **2014**, *43*, 764-768; b) B. Alič, A. Štefančiča, G. Tavčar, *Dalton Trans.* **2017**,*46*, 3338-3346; c) J. B. Waters, Q. Chen, T. A. Everitt, J. M. Goicoechea, *Dalton Trans.* **2017**, *46*, 12053-12066; d) G. Wang, L. A. Freeman, D. A. Dickie, R. Mokrai, Z. Benko, R. J. Gilliard Jr., *Inorg. Chem.* **2018**, *57*, 11687-11695; e) G. Wang, L. A. Freeman, D. A. Dickie, R. Mokrai, Z. Benko, R. J. Gilliard Jr., *Chem. Eur. J.* **2019**, *25*, 4335-4339; f) L. P. Ho, M. Tamm, *Dalton Trans.* **2021**, *50*, 1202-1205; g) M. M. Siddiqui, S. K. Sarkar, M. Nazish, M. Morganti, C. Köhler, J. Cai, L. Zhao, R. Herbst-Irmer, D. Stalke, G. Frenking, H. W. Roesky, *J. Am. Chem. Soc.* **2021**, *143*, 1301-1306; h) J. E. Walley, L. S. Warring, G. Wang,

D. A. Dickie, S. Pan, G. Frenking, R. J. Gilliard Jr., *Angew. Chem. Int. Ed.* **2021**, *60*, 6682-6690; *Angew. Chem.* **2021**, *133*, 6756-6764.

[11] A. Sidiropoulos, B. Osborne, A. N. Simonov, D. Dange, A. M. Bond, A. Stasch, C. Jones, *Dalton Trans.* **2014**, *43*, 14858-14864.

[12] R. Kretschmer, D. A. Ruiz, C. E. Moore, A. L. Rheingold, G. Bertrand, *Angew. Chem. Int. Ed.* **2014**, *53*, 8176-8179; *Angew. Chem*. **2014**, *126*, 8315-8318.

[13] a) L. P. Ho, A. Nasr, P. G. Jones, A. Altun, F. Neese, G. Bistoni, M. Tamm, *Chem. Eur. J.* **2018**, *24*, 18922-18932; b) O. Coughlin, T. Krämerband, S. L. Benjamin, *Dalton Trans.* **2020**, *49*, 1726-1730.

[14] a) C. L. Dorsey, R. M. Mushinski, T. W. Hudnall, *Chem. Eur. J.* **2014**, *20*, 8914-8917; b) J. Krüger, C. Wölper, L. John, L. Song, P. R. Schreiner, S. Schulz, *Eur. J. Inorg. Chem.* **2019**, 1669-1678.

[15] B. A. Chalmers, M. Bühl, K. S. Athukorala Arachchige, A. M. Slawin, P. Kilian, *Chem. Eur. J.* **2015**, *21*, 7520-7531.

[16] M. Ates, H. J. Breunig, A. Soltani-Neshan, M. Tegeler, *Z. Naturforsch. B* **1986**, *41*, 321-326.

[17] M. L. Green, G. Parkin, *Dalton Trans.* **2016**, *45*, 18784-18795.

[18] a) A. D. Becke, *Phys. Rev. A* **1988**, *38*, 3098-3100; b) C. Lee, W. Yang, R. G. Parr, *Phys. Rev. B*, **1988**, *37*, 785-789; c) A. D. Becke, *J. Chem. Phys.* **1993**, *98*, 5648-5652.

[19] a) A. Schäfer, H. Horn, R. Ahlrichs; *J. Chem. Phys.* **1992**, *97*, 2571; b) F. Weigend, M. Häser, H. Patzelt, R. Ahlrichs; *Chem. Phys. Letters* **1998**, *294*, 143; c) F. Weigend, R. Ahlrichs; *Phys. Chem. Chem. Phys.* **2005**, *7*, 3297; d) A. Hellweg, C. Hättig, S. Höfener, W. Klopper; *Theor. Chem. Acc.* **2007**, *117*, 587.

Chapter VI

A Versatile Route To Cyclic (Alkyl)(amino)carbene-stabilized Stibinidenes

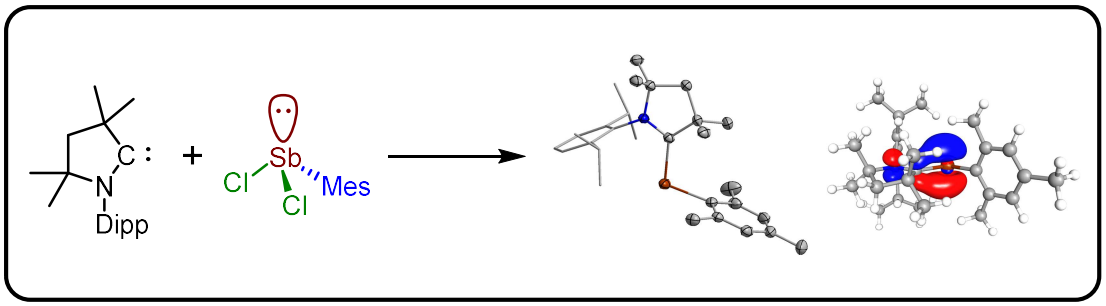

6 A Versatile Route To Cyclic (Alkyl)(amino)carbene-stabilized Stibinidenes

6.1 Introduction

The application of *N*-heterocyclic carbenes (NHCs)[1] and related molecules such as cyclic (alkyl)(amino)carbenes (cAACs)[2] in main group chemistry has led to impressive improvements in this field over the last decade. For example, significant progress has been achieved in the stabilization and isolation of *Lewis*-acid/base adducts with highly tunable NHC ligands in their stereo-electronic properties, in the chemistry of low-coordinate main group element compounds and in the substrate activation using low-valent main group element compounds.[3]

For group 15 elements, NHCs and related molecules have been applied especially in phosphorous chemistry for the synthesis of NHC-phosphenium salts and the synthesis of phosphino and phosphonio-substituted carbenes, for the preparation of carbene-stabilized main group diatomic and polyatomic allotropes and in the generation of carbene-stabilized phosphinides and in phosphinide transfer reactions using NHC-phosphinidenes.[4] Typical synthetic pathways to NHC-phosphinidenes (NHC·PR) are the reduction of adducts NHC·PCl_2R,[5] the cleavage of *cyclo*-phosphines $1/n(RP)_n$ with carbenes,[6] the dehydrogenative coupling of RPH_2 in the presence of NHCs[7], or the use of different other phosphinidene precursors.[8] This research also led to the development of related carbene-stabilized arsinidenes[6a, 5] as well as other arsenic compounds.[1h, 6]

Compared to the lighter group 15 homologues, the chemistry of low-valent NHC-stabilized antimony compounds is still in its infancy. However, it has been demonstrated previously that NHC- and cAAC-stabilized antimony(III) precursors are valuable starting materials for the development of antimony main group chemistry. The synthesis of the Sb(II) radical (cAAC^{Cy})·SbCl$_2^{\bullet}$ (cAAC^{Cy} = 2-azaspiro[4.5]dec-2-(2,6-di-*iso*-propylphenyl)-3,3-dimethyl-1-ylidene) (Scheme 6.1, **6.C**) was realized by reduction of (cAAC^{Cy})·SbCl$_3$ using one equivalent of KC$_8$. The reduction with two equivalents of KC$_8$ led to formation of the cAAC-stabilized stibinidene (cAAC^{Cy})·SbCl (Scheme 6.1, **6.B**) and reduction with three equivalents to the stiba-alkene dimer [(cAAC^{Cy})Sb]$_2$ (Scheme 6.1, **6.F**), respectively.[11] The first aryl-substituted carbene-stabilized stibinidene (DAC^{Mes})·SbPh (DAC^{Mes} = 1,3-dimesityl-5,5-dimethyl-4,6-dioxo-3,4,5,6-tetrahydro-pyrimidine-2-ylidene; Scheme 6.1, **6.A**) was prepared *via* reduction of (DAC^{Mes})·SbCl$_2$Ph.[12]

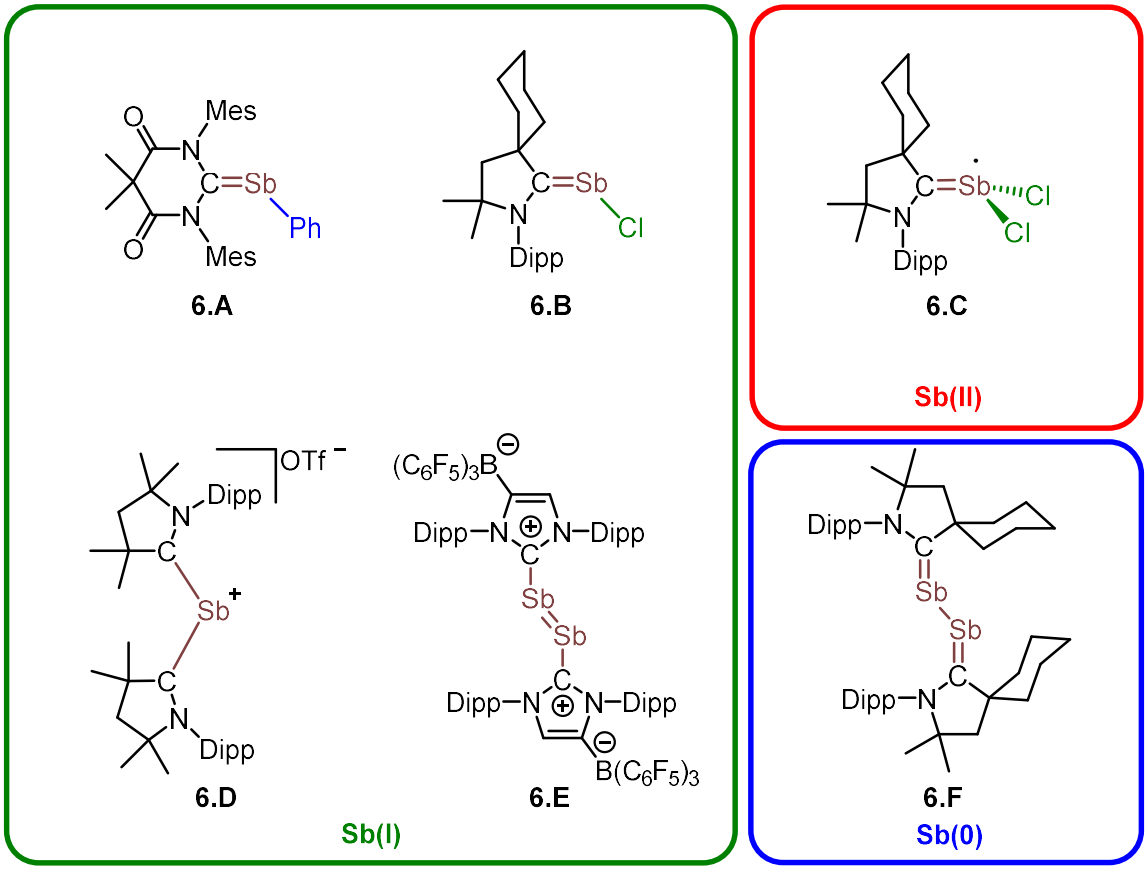

Scheme 6.1: Carbene-stabilized Sb(II), Sb(I) and Sb(0) compounds.

Furthermore, it was reported previously that the reduction of SbX_3 (X = F, Cl) with KC_8 in the presence of $cAAC^{Me}$ ($cAAC^{Me}$ = 1-(2,6-di-*iso*-propylphenyl)-3,3,5,5-tetramethyl-pyrrolidin-2-ylidene) and LiOTf (LiOTf = $LiCF_3SO_3$) in a molar ratio of 1:2:2:2 afforded $[(cAAC^{Me})_2Sb]^+[OTf]^-$ (Scheme 6.1, **6.D**) featuring an anionic, cAAC-stabilized antimony(I) center.[13] The NHC-stabilized distibene $[^a(B(C_5F_5)_3)\text{-}Dipp_2Im)\cdot Sb]_2$ ($Dipp_2Im$ = 1,3-di-(2,6-di-*iso*-propylphenyl)-imidazolin-2-ylidene) (Scheme 6.1, **6.E**) was synthesized *via* metallic reduction of $^a(B(C_5F_5)_3)\text{-}Dipp_2Im)\cdot SbCl_2$.[14]

We recently reported the synthesis and characterization of a number of carbene-stabilized antimony(III) compounds.[15] In course of these studies on *Lewis* acid/base adducts of NHCs and cAACs with the chlorostibanes $SbCl_3$ and $SbCl_2R$ (R = Ph and Mes) we observed that some adducts of sterical demanding carbenes with $SbCl_2Mes$ are quite unstable, most probably due to steric repulsion.[15] For the adduct $Mes_2Im\cdot SbCl_2Mes$ (Scheme 6.2, **6.G**; R_2Im = 1,3-di-organyl-imidazolin-2-ylidene; Mes = 2,4,6-trimethylphenyl) we observed a structural change in the solid-state geometry compared to adducts of sterically less demanding NHCs, for example $iPr_2Im^{Me}\cdot SbCl_2Mes$ (Scheme 6.2, **6.H**).[15] In these isomers the coordination site of the NHC ligand changes from an equatorial (**6.H**) into an axial position (**6.G**). We also demonstrated previously that $cAAC^{Me}\cdot SbCl_2Ph$ (Scheme 6.2, **6.I**) adopts a stable *Lewis*-acid/base adduct which features a solid-state structure similar to compound **6.H**. Herein we wish to report the different behavior on the reaction of two cAACs with $SbCl_2Mes$, which leads to a convenient synthesis of cAAC-stabilized stibinidenes cAAC·SbMes.

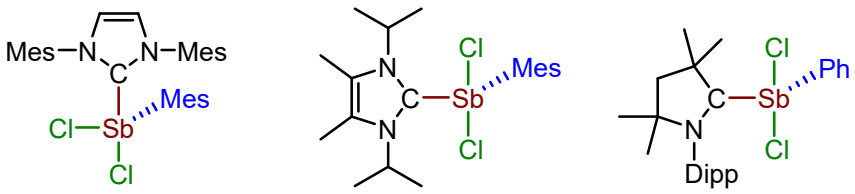

6.G **6.H** **6.I**

Scheme 6.2: Isomers of $NHC\cdot SbCl_2Ar$: $Dipp_2Im\cdot SbCl_2Mes$ (**6.G**), $iPr_2Im^{Me}\cdot SbCl_2Mes$ (**6.H**), and $cAAC^{Me}\cdot SbCl_2Ph$ (**6.I**)

6.2 Results and Discussion

The reaction of cAAC^{Me} and cAAC^{Cy} with $SbCl_2Mes$ in toluene at –78 °C leads to a pale-yellow slurry, which changes its color to orange-red upon raising the temperature to room temperature. Filtration of the resulting suspensions from a solvent mixture of hexane and toluene (ca. 3:1) separated a colorless precipitate, which consisted of the antimony(III) salts [cAAC^{Me}Cl]$^+$[$SbCl_3Mes$]$^-$ **6.1a** and [cAAC^{Cy}Cl]$^+$[$SbCl_3Mes$]$^-$ **6.1b**, respectively. The orange filtrate contained the cAAC-stabilized stibinidenes cAAC^{Me}·SbMes **6.2a** and cAAC^{Me}·SbMes **6.2b,** respectively. The latter compounds **6.2a** and **6.2b** were readily soluble in *n*-hexane and were isolated as orange solids in 44 % and 32% yield. However, these conversions were quantitative if the reaction was performed on NMR scale.

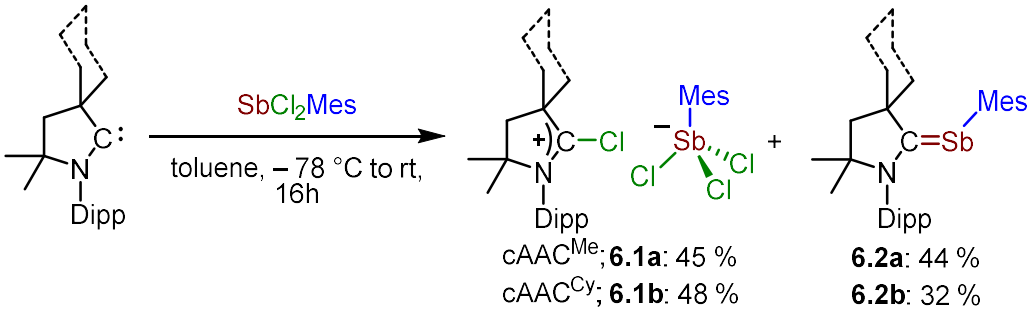

Scheme 6.3: The reaction of cAACs with $SbCl_2Mes$: Synthesis of the salts [cAAC^{Me}Cl]$^+$[$SbCl_3Mes$]$^-$ (**6.1a**) and [cAAC^{Cy}Cl]$^+$[$SbCl_3Mes$]$^-$ (**6.1b**), and the cAAC-stabilized stibinidenes cAAC^{Me}·SbMes (**6.2a**) and cAAC^{Cy}·SbMes (**6.2b**). Yields are based on a maximum of 50 % for **6.1** and 50 % for **6.2**.

All reaction products were characterized by ^{1}H NMR and ^{13}C{^{1}H} NMR spectroscopy, X-ray diffraction analysis and elemental analysis. The characteristic resonances in the ^{1}H NMR spectrum of **6.1a** (C*H*$_2$, 2.67 ppm; *i*Pr-C*H*, 2.46 ppm) and **6.1b** (C*H*$_2$, 2.66 ppm; *i*Pr-C*H*, 2.46 ppm) revealed almost identical chemical shifts for the [cAAC^{Me}Cl]$^{+}$ cation as reported previously for the gold salt [cAAC^{Ad}Cl]$^{+}$[AuCl$_4$]$^{-}$ (C*H*$_2$, 2.67 ppm; *i*Pr-C*H*, 2.45 ppm) of the related *N*-adamantyl substituted cation. The ^{13}C{^{1}H} NMR resonances of the carbon atoms attached to chlorine (former carbene carbon atom) of the [cAAC–Cl]$^{+}$ cation of **6.1a-b** (N*C*Cl: **6.1a**, 190.6 ppm; **6.1b**, 189.8 ppm) are very characteristic and were almost identical compared to the resonances reported for [cAAC^{Ad}Cl]$^{+}$[AuCl$_4$]$^{-}$ (N*C*Cl: 188.5 ppm).[16]

In addition, the ^{1}H NMR resonances of the mesityl group of compound **6.2a** (Mes-*p*-C*H*$_3$, 2.20 ppm; Mes-*o*-C*H*$_3$, 2.81 ppm; Mes-C*H*, 6.99 ppm) and **6.2b** (Mes-*p*-C*H*$_3$, 2.20 ppm; Mes-*o*-C*H*$_3$, 2.82 ppm; Mes-C*H*, 6.99 ppm) at the antimony center revealed a clear downfield shift compared to the starting material SbCl$_2$Mes (Mes-*p*-C*H*$_3$, 1.94 ppm; Mes-*o*-C*H*$_3$, 2.35 ppm; Mes-C*H*, 6.55 ppm). Furthermore, the characteristic septet of the cAAC methine protons (**6.2a**, *i*Pr-C*H*, 3.05 ppm; **6.2b**, *i*Pr-C*H*, 3.06 ppm) is shifted compared to either the free carbene (cAAC^{Me}: *i*Pr-C*H*, 3.13 ppm; cAAC^{Cy}: *i*Pr-C*H*, 3.15 ppm) or to the *Lewis*-acid/base adduct cAAC^{Me}·SbCl$_2$Ph (*i*Pr-C*H*, 3.25 ppm).[15] The ^{13}C{^{1}H} NMR resonances of the carbene carbon atom at 238.7 ppm and 239.4 ppm were also indicative for the formation of the cAAC-stabilized stibinidenes **6.2a** and **6.2b** (*cf.* cAAC^{Cy}·SbCl: 205.6 ppm in toluene-*d*$_8$,[11] DAC^{Mes}·SbPh: 205.6 ppm, C$_6$D$_6$)[12]). These resonances were remarkably shifted compared to free carbene (cAAC^{Me}: 313.6 ppm, and cAAC^{Cy}: 316.2 ppm), and also in a different region as compared to the chlorostibane(III) adduct cAAC^{Me}·SbCl$_2$Ph (225.8 ppm).[15]

Single crystals of **6.1a** and **6.1b** (Figure 6.1) suitable for X-ray diffraction analysis were obtained by slow evaporation of a saturated solution of these salts in dichloromethane at room temperature. The compounds **6.2a** and **6.2b** (Figure 6.2) were crystallized by storing at room temperature saturated solutions of these compounds in hexane at -30 °C. The compounds crystallize in the monoclinic space group $P2_1/n$ (**6.1** and **6.1b**) and in the triclinic space group $P\bar{1}$ (**6.2a** and **6.2b**), respectively, with one molecule in the asymmetric unit. The solid-state structures of **6.1a** and **6.1b** (Figure 6.1) feature separated [cAAC–Cl]$^+$ cations and [$SbCl_3Mes$]$^-$ counterions, the latter adopt disphenoidal geometries at the antimony(III) center. The antimony atom is substituted by two chlorine atoms in axial positions and a chlorine atom and the mesityl ligand in equatorial position.

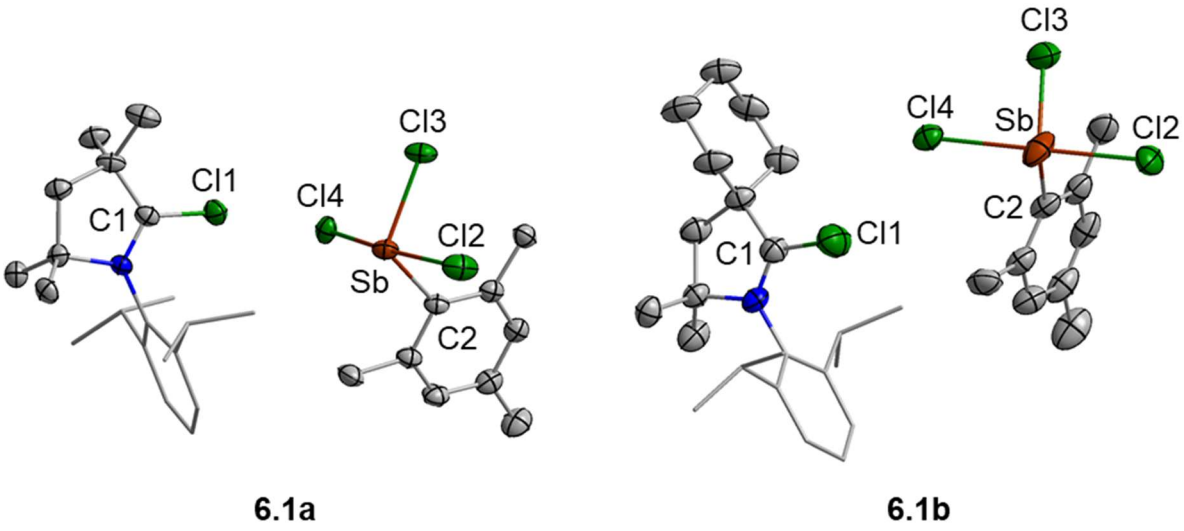

Figure 6.1: Molecular structures of [cAAC^{Me}Cl]$^+$[$SbCl_3Mes$]$^-$ (**6.1a**) and [cAAC^{Cy}Cl]$^+$[$SbCl_3Mes$]$^-$ (**6.1b**) in the solid-state. Hydrogen atoms were omitted for clarity. For **6.1a**, the chlorine atom Cl4 is disordered over two sites and the data reported correspond to the part resolved with 86 % occupancy. For **6.1b**, the "$SbCl_3$"-unit is disordered over two sites and the data reported correspond to the part with 72 % occupancy. Atomic displacement ellipsoids were set at the 50 % probability level. Selected bond lengths [Å] and angles [°]: **6.1a**: C1–Cl1, 1.659(3); Sb–C2, 2.159(2); Sb–Cl2, 2.5514(7); Sb–Cl3, 2.3766(6); Sb–Cl4, 2.4642(8), C2–Sb–Cl2, 89.00(7); C2–Sb–Cl3, 105.80(7); C2–Sb–Cl4, 82.30(8); Cl2–Sb–Cl3, 82.30(8); Cl3–Sb–Cl4, 84.73(3); Cl2–Sb–Cl4, 168.61(5); **6.1b**: C1–Cl1, 1.679(5); Sb–C2, 2.183(5); Sb–Cl2, 2.594(6); Sb–Cl3, 2.225(3); Sb–Cl4, 2.612(8), C2–Sb–Cl2, 90.4(2); C2–Sb–Cl3, 110.49(16); C2–Sb–Cl4, 87.6(2); Cl2–Sb–Cl3, 95.16(19); Cl3–Sb–Cl4, 83.8(2); Cl2–Sb–Cl4, 177.2(3).

The molecular structures of the cAAC-stabilized stibinidenes **6.2a** and **6.2b** (Figure 6.2) reveal two-coordinated antimony(I) atoms in which the cAAC and the mesityl substituent are bent with a C1–Sb–C2 angle of 100.82(9)° (**6.2a**) and 100.72(11)° (**6.2b**), respectively. The C3–C1–Sb–C2 torsion angle of **6.2a** (4.03(21)°) indicates planarity at the antimony center, whereas the structure of **6.2b** shows a slightly more distorted alignment with a torsion angle C3–C1–Sb–C2 of 14.34(30)°. This distortion is most probably due to the higher steric demand of cAAC^{Cy} compared to cAAC^{Me}. The Sb–C1 distances of 2.081(2) (**6.2a**) and 2.077(3) Å (**6.2b**) as well as the small distortion angles C3–C1–Sb–C2 at the Sb-C1 bond resembles those of other known stibaalkenes[17] as well as carbene-stabilized stibinidenes[11,12], which feature antimony carbon double bond character. To gain some insight into the bonding situation of **6.2a** and **6.2b**, we investigated the electronic structure of **6.2a** by using DFT calculations at the M06-2X/D3(BJ)//def2-TZVP(Sb)/def2-SVP(C,H,N,Cl)-level of theory. Geometry-optimized **6.2a** (Figure 6.3) closely resembles the essential features of the cAAC-stabilized stibinidene, as was found in the X-ray crystal structure of this compound, with a computed Sb–C1 distance of 2.077 Å (*cf.* exp: 2.081(2)), a C1–Sb–C2 angle of 100.1° (exp. 100.82(9)), and a torsion angle C3–C1–Sb–C2 of 7.2° (4.03(21)°).

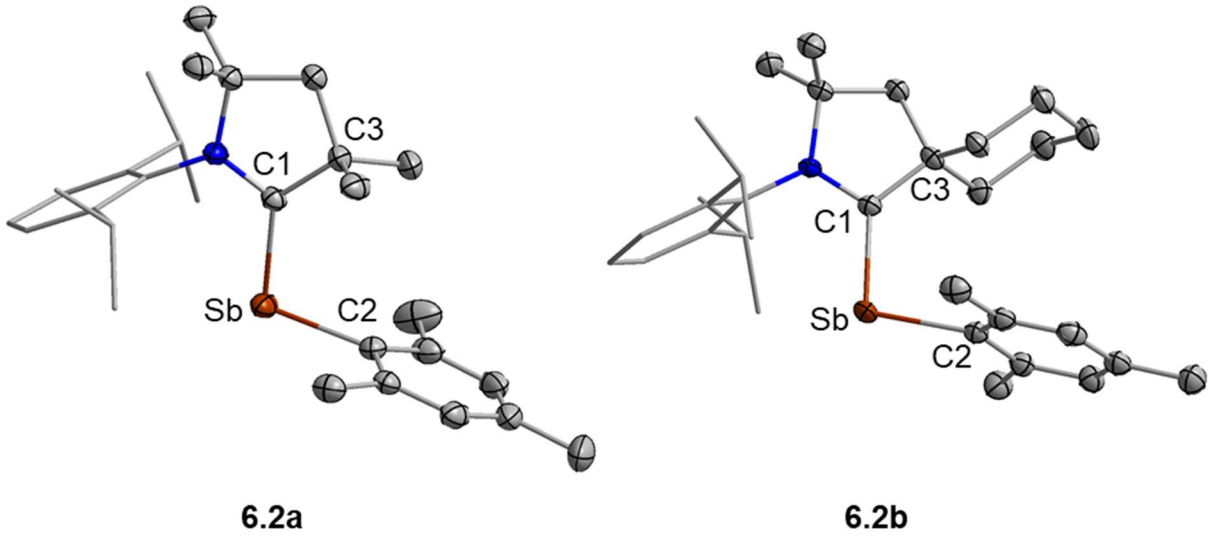

6.2a **6.2b**

Figure 6.2: Molecular structures of cAAC^{Me}·SbMes (**6.2a**) and cAAC^{Cy}·SbMes (**6.2b**) in the solid-state. Hydrogen atoms were omitted for clarity. Atomic displacement ellipsoids were set at the 50 % probability level. Selected bond lengths [Å] and angles [°]: **6.2a**: Sb–C1, 2.081(2); Sb–C2, 2.181(2); C1–Sb–C2, 100.82(9); C3–C1–Sb–C2, 4.03(21). **6.2b**: Sb–C1, 2.077(3); Sb–C2, 2.186(3); C1–Sb–C2, 100.72(11); C3–C1–Sb–C2, 14.34(30).

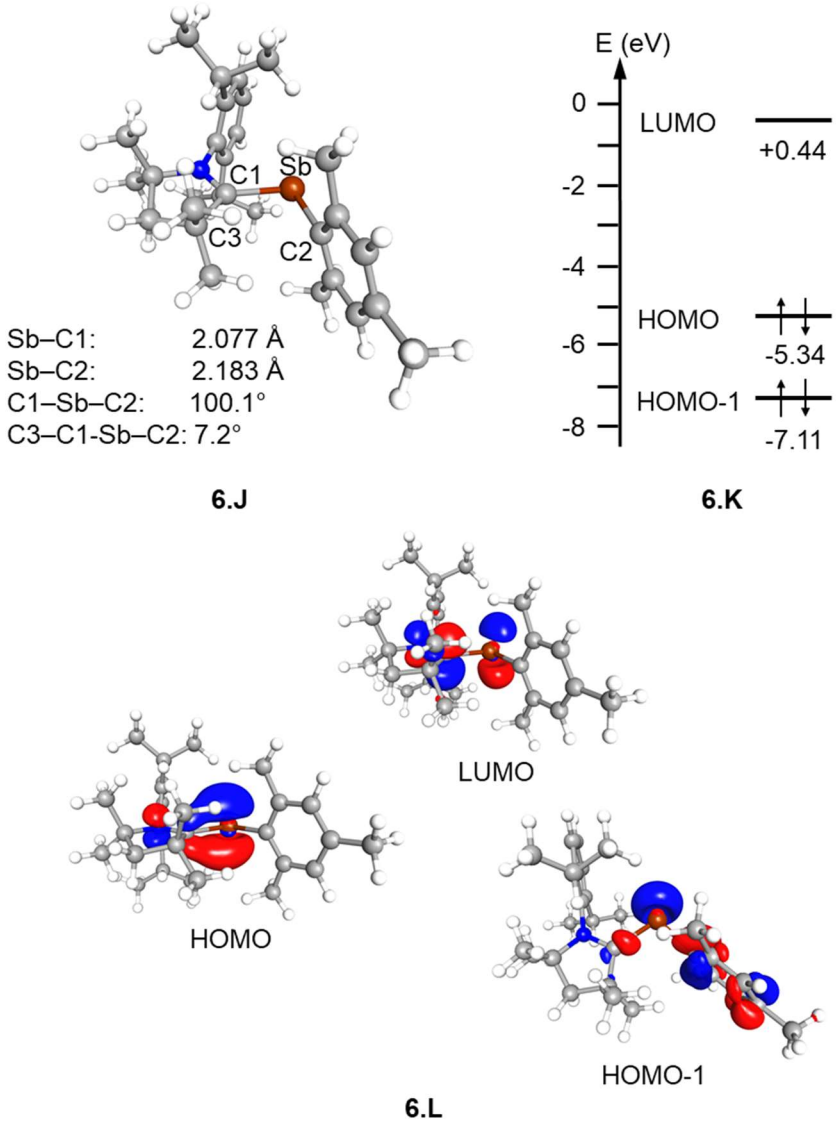

Figure 6.3: DFT-optimized (M06-2X/D3(BJ)//def2-TZVP(Sb)/def2-SVP(rest)) geometry of cAAC^{Me}·SbMes **6.2a** (**6.J**), orbital energies (**6.K**) and frontier orbitals (**6.L**) of **6.2a**.

Calculations of the relevant orbital energies revealed that the HOMO (Figure 6.3, **6.L**) is a Sb=C π-orbital located at the antimony(I) center, and the LUMO is the corresponding π–antibonding orbital. The Wiberg bond index calculated for the Sb=C(cAAC) bond is 1.389 ($d_{Sb\text{-}C}$ = 2.077 Å), much larger than the Wiberg bond index of 0.902 calculated for the Sb-C(Mes) bond ($d_{Sb\text{-}C}$ = 2.183 Å) or 0.713 calculated for cAAC^{Me}·$SbCl_2Mes$ ($d_{Sb\text{-}C(cAAC)}$ = 2.390 Å), which accounts for significant Sb=C(cAAC) double bond character. The HOMO-1 is distributed over the mesityl stibinidene unit with some localization at antimony and can thus be considered as a lone pair located at antimony.

Based on the isolated products and the experience we gathered on carbene adducts of antimony chlorides,[15] a mechanism was proposed for the reaction of cAAC^{Me} with $SbCl_2Mes$ (Scheme 6.4). In an initial step a *Lewis*-acid/base adduct is formed between the *Lewis*-base cAAC and *Lewis*-acidic $SbCl_2Mes$ to yield an adduct cAAC^{Me}·$SbCl_2Mes$. This adduct most probably adopts a structure in which the cAAC and one of the chloride substituents occupy axial positions, leading to a partially dissociated chloride substituents in *trans*-position to the excellent donor cAAC.[19] We have demonstrated previously on several occasions that these partially dissociated substituents can be easily transferred to *Lewis*-acids.[15,19] The Lewis-acid used here is $SbCl_2Mes$, and chloride transfer from cAAC^{Me}·$SbCl_2Mes$ to $SbCl_2Mes$ should form a contact ion pair [cAAC^{Me}·$SbClMes$]$^+$[$SbCl_3Mes$]$^-$ (**6.3**).

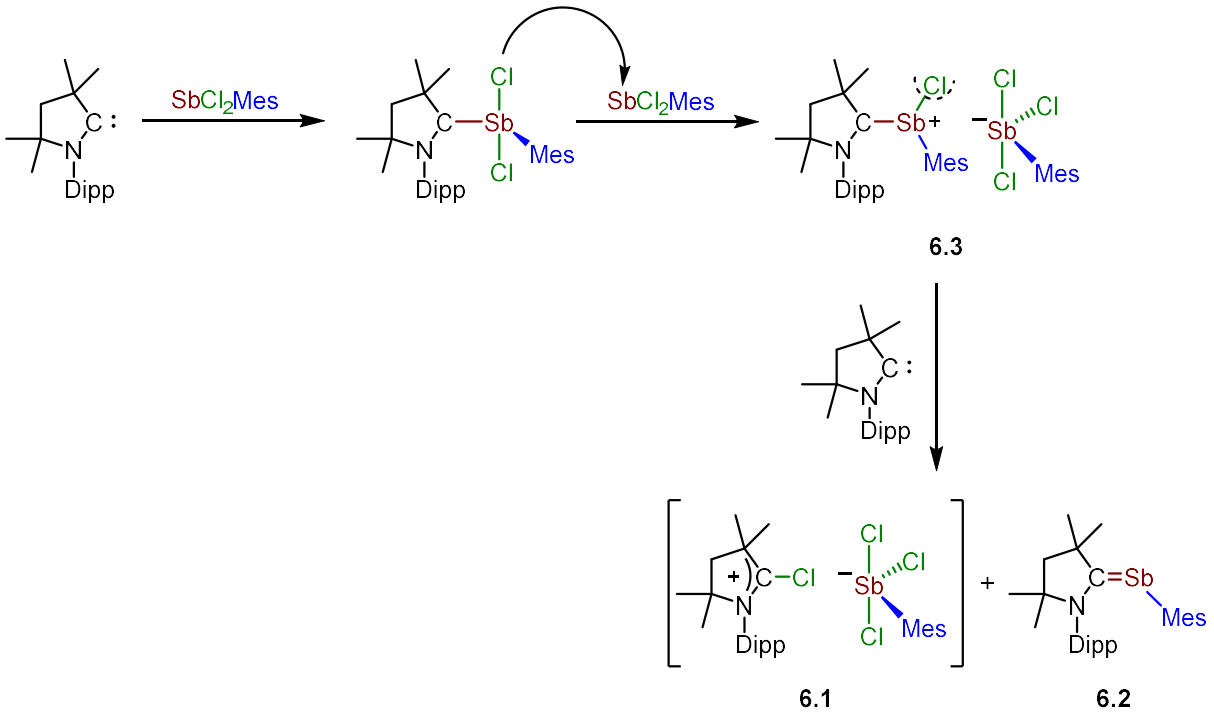

Scheme 6.4: Proposed mechanism for the formation of the compounds **6.1a** and **6.2a**.

The next step is chlorine abstraction from the cationic part of **6.3**, either by simple chloride transfer to the carbene carbon atom of the cAAC or by cAAC addition to cationic [cAAC^{Me}·$SbClMes$]$^+$ and subsequent elimination of [cAAC^{Me}Cl]$^+$, which leads to formation of the cAAC-stabilized stibinidene cAAC^{Me}·SbMes (**6.2a**) and the salt [cAAC^{Me}Cl]$^+$[$SbCl_3Mes$]$^-$ (**6.1a**). According to these steps, the reduction of the intermediate cAAC·$SbCl_2Mes$ initially formed to yield cAAC·SbMes is accomplished by

(i) transfer of "Cl^-" from cAAC·$SbCl_2Mes$ to $SbCl_2Mes$ (second step in Scheme 6.4) and (ii) formal transfer of "Cl^+" from $[cAAC^{Me}·SbClMes]^+$ to the cAAC, which makes in total the carbene carbon atom of $cAAC^{Me}$ the reducing reagent. The mechanism involving the addition of $cAAC^{Me}$ and subsequent elimination of $[cAAC^{Me}Cl]^+$ could be regarded as a reductive elimination at a main group element center.[20]

To support this mechanism, we reacted two equivalents $SbCl_2Mes$ with only one equivalent of $cAAC^{Me}$ in the hope to prevent the last step (i.e. "Cl^+" transfer). To our delight, if the reaction was performed in benzene at room temperature, compound **6.3** crystallized in low yield from the reaction mixture of the sluggish reaction. This salt crystallizes in the monoclinic space group $P2_1/c$ with one molecule in the asymmetric unit.

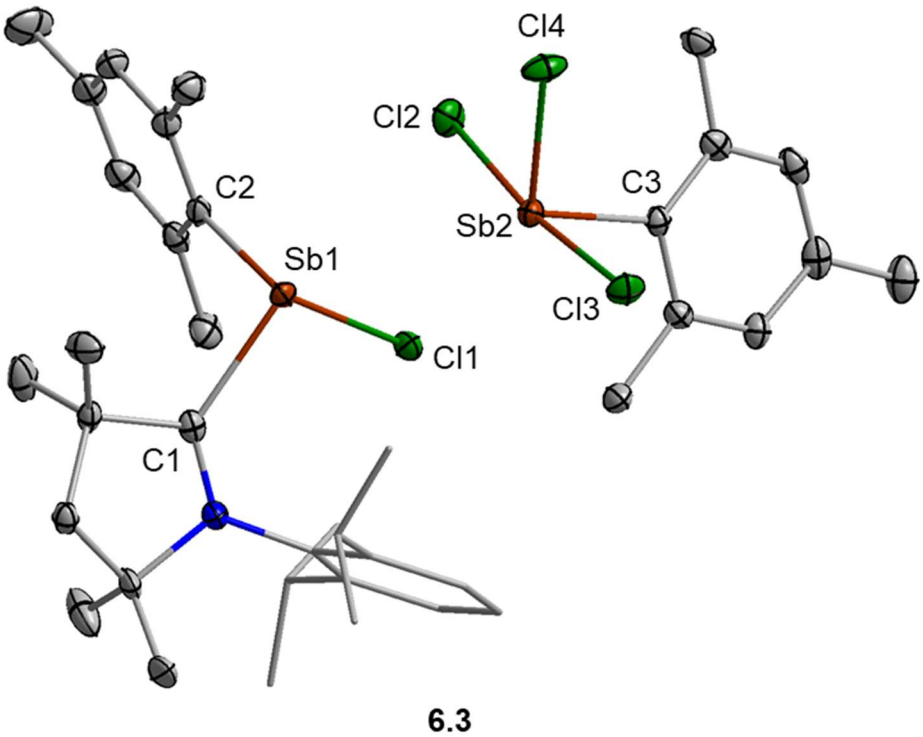

6.3

Figure 6.4: Molecular structure of $[cAAC^{Me}·SbClMes]^+[SbCl_3Mes]^-$ (**6.3**) in the solid-state. Hydrogen atoms and solvent molecules (benzene) were omitted for clarity. The "SbCl" unit in the $[cAAC^{Me}·SbClMes]^+$ cation is disordered over two sites and the data corresponding to the part with 93 % occupancy is shown. Atomic displacement ellipsoids were set at the 50 % probability level. Selected bond lengths [Å] and angles [°]: **6.3**: Sb1–C1, 2.258(3); Sb1–C2, 2.164(3); Sb1–Cl1, 2.3614(8); Sb2–C3, 2.161(3); Sb2–Cl2, 2.5898(7); Sb2–Cl3, 2.6285(7); Sb2–Cl4, 2.3742(7); C1–Sb1–C2, 96.44(10); C1–Sb–Cl1, 98.69(7); C2–Sb–Cl1, 101.24(8); Cl2–Sb2–C3, 89.27(7); Cl2–Sb2–Cl3, 172.78(2); Cl2–Sb2–Cl4, 88.05(2); Cl3–Sb2–C3, 89.17(7); Cl3–Sb2–Cl4, 85.57(2); Cl4–Sb–C3, 105.36(7).

The solid-state structure of **6.3** (Figure 6.4) reveals the salt $[cAAC^{Me}{\cdot}SbClMes]^+[SbCl_3Mes]^-$, in which the cation $[cAAC^{Me}{\cdot}SbClMes]^+$ adopts a three-coordinate pyramidal structure and the $[SbCl_3Mes]^-$ anion a four-coordinate disphenoidal geometry. The Sb1–C1 distance to the cAAC ligand of 2.258(3) Å is in the range of Sb-C distances observed previously for carben adducts of antimony(III) chlorides, for example 2.239(2) Å in $cAAC^{Me}{\cdot}SbCl_3$ or 2.243(3) Å in $cAAC^{Me}{\cdot}SbCl_2Ph$,[15] and is in line with a C-Sb single bond. Furthermore, it is worthy to note that the N*C*Sb $^{13}C\{^1H\}$ NMR resonance of **6.3** at 231.2 ppm (CD_2Cl_2) is located in-between the resonances observed for $cAAC^{Me}{\cdot}SbCl_2Ph$ (225.8 ppm) and for the stibinidenes **6.2a** and **6.2b** (**6.2a**, 238.7 ppm; **6.2b**, 239.4 ppm; C_6D_6). The isolation of compound **6.3** thus strongly supports the mechanism proposed in Scheme 6.4.

6.3 Conclusion

In conclusion, we report herein the quantitative synthesis of the cAAC-stabilized stibinidenes cAAC^{Me}·SbMes (**6.2a**) and cAAC^{Cy}·SbMes (**6.2b**) starting from $SbCl_2Mes$ and cAAC, which is accompanied with the 50 % formation of the salts $[cAAC^{Me}Cl]^+[SbCl_3Mes]^-$ (**6.1a**) and $[cAAC^{Cy}Cl]^+[SbCl_3Mes]^-$ (**6.1b**). The compounds were characterized by NMR- and IR spectroscopy, elemental analysis, and X-ray diffraction analysis. The bonding situation of **6.2a** was examined in some detail with the aid of DFT calculations, which accounts for an antimony carbene carbon double bond. A mechanism was proposed for this reaction which explains the reduction of the intermediate cAAC·$SbCl_2Mes$ initially formed with the cAAC carbene carbon atom to yield cAAC·SbMes (**6.2a**), i.e. the cAAC is used as the reducing reagent with oxidation of the carbene carbon atom. The important intermediate $[cAAC^{Me}·SbClMes]^+[SbCl_3Mes]^-$ (**6.3**) of this reaction sequence was isolated and structurally characterized. The procedure presented here is a convenient synthesis of cAAC-stabilized stibinidenes although one equivalent of cAAC and one equivalent of antimony is lost. We failed so far in the metallic reduction of **6.1**, which should – in principle – also afford cAAC-stabilized stibinidenes **6.2**. We also failed so far to replace $SbCl_2Mes$ as *Lewis*-acidic chloride acceptor, mainly because of the formation of stable adducts of the Lewis-acids then employed with the cAAC. However, the beauty of this reaction lies in a 100% conversion and the ease of the separation of **6.1** and **6.2**, which makes the further exploration of the chemistry of cAAC-stabilized stibinidenes convenient.

6.4 References

[1] a) W. A. Herrmann, C. Köcher, *Angew. Chem. Int. Ed.* **1997**, *36*, 2162-2187; *Angew. Chem.* **1997**, *109*, 2256-2282; b) D. Bourissou, O. Guerret, F. P. Gabbaï, G. Bertrand, *Chem. Rev.* **2000**, *100*, 39-91; c) S. P. Nolan, N-Heterocyclic Carbenes in Synthesis; Wiley-VCH, Weinheim, Germany, **2006**; d) F. E. Hahn, M. C. Jahnke, *Angew. Chem. Int. Ed.* **2008**, *47*, 3122-3172; *Angew. Chem.* **2008**, *120*, 3166-3216; e) T. Dröge, F. Glorius, *Angew. Chem. Int. Ed.* **2010**, *49*, 6940-6952; *Angew. Chem.* **2010**, *122*, 7094-7107; h) M. N. Hopkinson, C. Richter, M. Schedler, F. Glorius, *Nature* **2014**, *510*, 485-496.

[2] a) M. Melaimi, M. Soleilhavoup, G. Bertrand, *Angew. Chem. Int. Ed.* **2010**, *49*, 8810-8849; *Angew. Chem.* **2010**, *122*, 8992-9032; b) M. Melaimi, R. Jazzar, M. Soleilhavoup, G. Bertrand, *Angew. Chem. Int. Ed.* **2017**, *56*, 10046-10068; *Angew. Chem.* **2017**, *129*, 10180-10203; c) U. S. D. Paul, U. Radius, *Eur. J. Inorg. Chem.* **2017**, 3362-3375; d) U. S. D. Paul, M. J. Krahfuss, U. Radius, *Chem. Unserer Zeit* **2019**, *53*, 212-223.

[3] a) P. Power, *Nature* **2010**, *463*, 171-177; b) D. Martin, M. Soleilhavoup, G. Bertrand, *Chem. Sci.* **2011**, *2*, 389-399; c) Y. Wang, Gregory H. Robinson, *Dalton Trans.* **2012**, *41*, 337-345; d) C. D. Martin, M. Soleilhavoup, G. Bertrand, *Chem. Sci.* **2013**, *4*, 3020-3030; e) Y. Wang, G. H. Robinson, *Inorg. Chem.* **2014**, *53*, 11815-11832; f) T. Chu, G. I. Nikonov, *Chem Rev.* **2018**, *118*, 3608-3680; g) Y. Kim, E. Lee, *Chem. Eur. J.* **2018**, *24*, 19110-19121; h) V. V. Nesterov, D. Reiter, P. Bag, P. Frisch, R. Holzner, A. Porzelt, S. Inoue, *Chem. Rev.* **2018**, *118*, 9678-9842; i) A. Doddi, M. Peters, M. Tamm, *Chem. Rev.* **2019**, *119*, 6994−7112; j) S. Kundu, S. Sinhababu, V. Chandrasekhar, H. W. Roesky, *Chem. Sci.* **2019**, *10*, 4727-4741; k) M. M. D. Roy, A. A. Omaña, A. S. S. Wilson, M. S. Hill, S. Aldridge, E. Rivard, *Chem. Rev.* **2021**, *121*, 12784-12965.

[4] a) Y. Wang, G. H. Robinson, *Dalton Trans.* **2012**, *41*, 337-345; b) D. J. D. Wilson, J. L. Dutton, *Chem. Eur. J.* **2013**, *19*, 13626-13637; c) M. H. Holthausen, J. J. Weigand, *Chem. Soc. Rev.* **2014**, *43*, 6639-6657; d) A. Doddi, D. Bockfeld, M. K. Zaretzke, C. Kleeberg, T. Bannenberg, M. Tamm, *Dalton Trans.* **2017**, *46*, 15859-15864; e) L. Dostal, *Coord. Chem. Rev.* **2017**,

353, 142-158; f) J. E. Borger, A. W. Ehlers, J. C. Slootweg, K. Lammertsma, Chem. Eur. J. **2017**, *23*, 11738-11746; g) T. Krachko, J. C. Slootweg, *Eur. J. Inorg. Chem.* **2018**, *24*, 2734-2754; h) K. Schwedtmann, G. Zanoni, J. J. Weigand, *Chem. Asian J.* **2018**, *13*, 1388-1405;

[5] a) O. Back, M. Henry-Ellinger, C. D. Martin, D. Martin, G. Bertrand, *Angew. Chem. Int. Ed.* **2013**, *52*, 2939-2943; *Angew. Chem.* **2013**, *125*, 3011-3015; b) R. R. Rodrigues, C. L. Dorsey, C. A. Arceneaux, T. W. Hudnall, *Chem. Commun.* **2014**, *50*, 162-164; c) S. Roy, K. C. Mondal, S. Kundu, B. Li, C. J. Schurmann, S. Dutta, D. Koley, R. Herbst-Irmer, D. Stalke, H. W. Roesky, *Chem. Eur. J.* **2017**, *23*, 12153-12157; d) Y. Wang, Y. Xie, M. Y. Abraham, R. J. Gilliard, P. Wei, H. F. Schaefer III, P. v. R. Schleyer, G. H. Robinson, *Organometallics* **2010**, *29*, 4778-4780.

[6] a) A. J. Arduengo, J. C. Calabrese, A. H. Cowley, H. V. Dias, J. R. Goerlich, W. J. Marshall, B. Riegel, *Inorg. Chem.* **1997**, *36*, 2151-2158; b) A. J. Arduengo III, H. V. R. Dias, J. C. Calabrese, *Chem. Lett.* **1997**, *26*, 143-144; c) A. K. Adhikari, T. Grell, P. Lönnecke, E. Hey-Hawkins, *Eur. J. Inorg. Chem.* **2016**, 620-622; d) N. Hayakawa, K. Sadamori, S. Tsujimoto, M. Hatanaka, T. Wakabayashi, T. Matsuo, *Angew. Chem. Int. Ed.* **2017**, *56*, 5765-5769; *Angew. Chem.* **2017**, *129*, 5859-5863; e) T. Krachko, M. Bispinghoff, A. M. Tondreau, D. Stein, M. Baker, A. W. Ehlers, J. C. Slootweg, H. Grützmacher, *Angew. Chem. Int. Ed.* **2017**, *56*, 7948-7951; *Angew. Chem*. **2017**, *129*, 8056-8059.

[7] a) H. Schneider, D. Schmidt, U. Radius, *Chem. Commun.* **2015**, *51*, 10138-10141; b) M. Bispinghoff, H. Grützmacher, *Chimia* **2016**, *70*, 279-283; c) M. Bispinghoff, A. M. Tondreau, H. Grützmacher, C. A. Faradji, P. G. Pringle, *Dalton Trans.* **2016**, *45*, 5999-6003; d) L. Werner, G. Horrer, M. Philipp, K. Lubitz, M. W. Kuntze-Fechner, U. Radius, *Z. Anorg. Allg. Chem.* **2021**, 647, 881-895.

[8] a) F. E. Hahn, D. Le Van, M. C. Moyes, T. von Fehren, R. Fröhlich, E. U. Würthwein, *Angew. Chem. Int. Ed.* **2001**, *40*, 3144-3148; *Angew. Chem.* **2001**, *113*, 3241-3244; b) A. Doddi, D. Bockfeld, T. Bannenberg, P. G. Jones, M. Tamm, *Angew. Chem. Int. Ed.* **2014**, *53*, 13568-13572; *Angew. Chem.* **2014**, *126*, 13786-13790; c) M. Cicač-Hudi, J. Bender, S. H. Schlindwein, M.

Bispinghoff, M. Nieger, H. Grützmacher, D. Gudat, *Eur. J. Inorg. Chem.* **2016**, 649-658; d) D. Heift, Z. Benko, H. Grützmacher, *Dalton Trans.* **2014**, *43*, 5920-5928; e) Z. Li, X. Chen, Y. Li, C.-Y. Su, H. Grützmacher, *Chem. Commun.* **2016**, *52*, 11343-11346.

[9] a) A. Doddi, M. Weinhart, A. Hinz, D. Bockfeld, J. M. Goicoechea, M. Scheer, M. Tamm, *Chem. Commun.* **2017**, *53*, 6069-6072; b) S. Yao, Y. Grossheim, A. Kostenko, E. Ballestero-Martinez, S. Schutte, M. Bispinghoff, H. Grützmacher, M. Driess, *Angew. Chem. Int. Ed.* **2017**, *56*, 7465-7469; *Angew. Chem.* **2017**, *129*, 7573-7577; c) A. Hinz, M. M. Hansmann, G. Bertrand, J. M. Goicoechea, *Chem. Eur. J.* **2018**, *24*, 9514-9519; d) K. M. Melancon, M. B. Gildner, T. W. Hudnall, *Chem. Eur. J.* **2018**, *24*, 9264-9268; e) M. K. Sharma, S. Blomeyer, B. Neumann, H. G. Stammler, A. Hinz, M. van Gastel, R. S. Ghadwal, *Chem. Commun.* **2020**, *56*, 3575-3578; f) A. Schumann, J. Bresien, M. Fischer, C. Hering-Junghans, *Chem. Commun.* **2021**, *57*, 1014-1017; g) J. Krüger, C. Wölper, G. Haberhauer, S. Schulz, *Inorg. Chem.* **2022**, *61*, 597-604.

[10] a) M. Y. Abraham, Y. Wang, Y. Xie, R. J. Gilliard, Jr., P. Wei, B. J. Vaccaro, M. K. Johnson, H. F. Schaefer III, P. v. R. Schleyer, G. H. Robinson, *J. Am. Chem. Soc.* **2013**, *135*, 2486-2488; b) M. Donath, M. Bodensteiner, J. J. Weigand, *Chem. Eur. J.* **2014**, *20*, 17306-17310; c) J. W. Dube, Y. Zheng, W. Thiel, M. Alcarazo, *J. Am. Chem. Soc.* **2016**, *138*, 6869-6877; d) L. P. Ho, A. Nasr, P. G. Jones, A. Altun, F. Neese, G. Bistoni, M. Tamm, *Chem. Eur. J.* **2018**, *24*, 18922-18932; e) A. Doddi, D. Bockfeld, M. K. Zaretzke, T. Bannenberg, M. Tamm, *Chem. Eur. J.* **2019**, *25*, 13119-13123; f) L. P. Ho, M. K. Zaretzke, T. Bannenberg, M. Tamm, *Chem. Commun.* **2019**, *55*, 10709-10712; g) M. Piesch, S. Reichl, M. Seidl, G. Balázs, M. Scheer, *Angew. Chem. Int. Ed.* **2019**, *58*, 16563-16568; *Angew. Chem.* **2019**, *131*, 16716-16721; h) D. Bockfeld, M. Tamm, *Z. Anorg. Allg. Chem.* **2020**, *646*, 866-872.

[11] R. Kretschmer, D. A. Ruiz, C. E. Moore, A. L. Rheingold, G. Bertrand, *Angew. Chem. Int. Ed.* **2014**, *53*, 8176-8179; *Angew. Chem.* **2014**, *126*, 8315-8318.

[12] C. L. Dorsey, R. M. Mushinski, T. W. Hudnall, *Chem. Eur. J.* **2014**, *20*, 8914-8917.

[13] M. M. Siddiqui, S. K. Sarkar, M. Nazish, M. Morganti, C. Kohler, J. Cai, L. Zhao, R. Herbst-Irmer, D. Stalke, G. Frenking, H. W. Roesky, *J. Am. Chem. Soc.* **2021**, *143*, 1301-1306.

[14] L. P. Ho, A. Nasr, P. G. Jones, A. Altun, F. Neese, G. Bistoni, M. Tamm, *Chem. Eur. J.* **2018**, *24*, 18922-18932.

[15] M. S. M. Philipp, M. J. Krahfuss, K. Radacki, U. Radius, *Eur. J. Inorg. Chem.* **2021**, 4007-4019.

[16] A. S. Romanov, M. Bochmann, *Organometallics* **2015**, *34*, 2439-2454.

[17] a) P. B. Hitchcock, C. Jones, J. F. Nixon, *Angew. Chem. Int. Ed.* **1995**, *34*, 492-493; *Angew. Chem.* **1995**, *107*, 522-523; b) C. Jones, J. W. Steed, R. C. Thomas, *J. Chem. Soc., Dalton Trans.* **1999**, 1541-1542; c) C. Jones, *Coord. Chem. Rev.* **2001**, *215*, 151-169; d) P. C. Andrews, J. E. McGrady, P. J. Nichols, *Organometallics* **2004**, *23*, 446-453; e) J. Escudié, H. Ranaivonjatovo, *Organometallics* **2007**, *26*, 1542-1559.

[18] J. B. Waters, Q. Chen, T. A. Everitt, J. M. Goicoechea, *Dalton Trans.* **2017**, *46*, 12053-12066.

[19] a) U. S. D. Paul, U. Radius, *Chem. Eur. J.* **2017**, *23*, 3993-4009; b) H. Schneider, A. Hock, R. Bertermann, U. Radius, *Chem. Eur. J.* **2017**, *23*, 12387-12398; c) H. Schneider, A. Hock, A. D. Jaeger, D. Lentz, U. Radius, *Eur. J. Inorg. Chem.* **2018**, 4031-4043; d) A. Hock, L. Werner, C. Luz, U. Radius, *Dalton Trans.* **2020**, *49*, 11108-11119; e) A. Hock, L. Werner, M. Riethmann, U. Radius, *Eur. J. Inorg. Chem.* **2020**, 4015-4023; f) S. A. Föhrenbacher, V. Zeh, M. J. Krahfuss, N. Ignat'ev, M. Finze, U. Radius, *Eur. J. Inorg. Chem.* **2021**, 1941-1960.

[20] T. Chu, G. I. Nikonov, *Chem. Rev.* **2018***, 118*, 3608-3680.

7 Experimental Details

7.1 General procedures

All reactions and subsequent manipulations involving organometallic reagents were performed under an argon atmosphere by using standard Schlenk techniques or in a Glovebox (Innovative Technology Inc. and MBraun Uni Lab) as reported previously.[1] Argon was dried over silica gel and P_4O_{10}. All reactions were carried out in oven-dried glassware. Toluene, *n*-hexane, Et_2O, CH_2Cl_2 and THF were purified using a Pure-Solv 400 solvent purification system (Innovative Technology). Benzene was dried over sodium/ketyl. Deuterated solvents were purchased from Sigma-Aldrich and stored over molecular sieves (4 Å).

7.2 Starting materials

The carbenes Me_2Im^{Me},[2] iPr_2Im^{Me},[2] Mes_2Im,[3] $Dipp_2Im$,[4] *c*AAC^{Me}[5] and cAAC^{Cy}[5] were prepared according to published procedures. The starting materials $SbCl_2Ph$,[6] $SbMes_3$,[6-7] $SbCl_2Mes$,[6-7] 1,4-bis(trimethylsilyl)-1,4-dihydropyrazin,[8] $PbCl_2Ph_2$,[9] GeH_2Mes_2[10] and SnH_2Me_2[11] (Caution: SnH_2Me_2 (bp. 35 °C) is volatile and toxic[12, 13]) were synthesized according to literature procedures. All other reagents were purchased from Sigma-Aldrich, ABCR or the chemical distribution center of the University of Würzburg used without further purification.

7.3 Analytical Methods

Elemental analysis

Elemental analyses (C, H, N, S) were performed in the micro-analytical laboratory of the University of Würzburg with an Elementar vario micro cube and are reported in wt%.

7.4 Spectroscopic methods

IR spectroscopy

Infrared spectra were recorded on solid samples at room temperature on a Bruker Alpha FT-IR spectrometer using an ATR unit and are reported in cm^{-1}. In dependence of the intensity of the vibration bands the following abbreviations were used: very strong (vs), strong (s), middle (m), weak (w) and very weak (vw).

NMR spectroscopy

NMR spectra were recorded at 298 K using Bruker Avance III Nanobay 400 (^{1}H: 400.5 MHz; $^{13}C\{^{1}H\}$: 100.7 MHz, ^{207}Pb: 83.8 MHz, ^{119}Sn: 149.3 MHz), Bruker Avance Neo I 500 (^{1}H: 500.1 MHz, $^{13}C\{^{1}H\}$: 125.8 MHz, ^{207}Pb: 104.8 MHz, ^{119}Sn: 186.5 MHz) and Bruker Avance Neo I 600 (^{1}H: 600.2 MHz) spectrometers. Assignment of the NMR data was supported by ^{1}H-^{1}H, ^{1}H-^{13}C, and ^{1}H-^{207}Pb correlation experiments. ^{13}C NMR spectra were broad-band proton-decoupled ($^{13}C\{^{1}H\}$). Assignment of the ^{13}C NMR data was supported by ^{13}C,^{1}H correlation experiments.^{1}H and $^{13}C\{^{1}H\}$ NMR chemical shifts are listed in parts per million (ppm). The ^{1}H NMR shifts were referenced *via* residual proton resonances of the corresponding deuterated solvent C_6D_5H (^{1}H: δ = 7.16 ppm, C_6D_6), C_7D_7H (^{1}H: δ = 2.08, 6.97, 7.01, 7.09 ppm, toluene-d_8), $CDHCl_2$ (^{1}H: δ = 5.32, CD_2Cl_2), $CHCl_3$ (^{1}H: δ = 7.26, $CDCl_3$), and d_7-THF (^{1}H: δ = 3.58, 1.72, THF-d_8). ^{13}C NMR spectra are reported relative to TMS using the carbon resonances of the deuterated solvent C_6D_6 (^{13}C: δ = 128.06 ppm), toluene-d_8 (^{13}C: δ = 20.43, 125.13, 127.96, 128.87, 137.48 ppm), CD_2Cl_2 (^{13}C: δ = 53.84), $CDCl_3$ (^{13}C: δ = 77.16) and THF-d_8 (^{13}C: δ = 67.21, 25.31).[14] ^{207}Pb NMR spectra are reported relative to $Pb(CH_3)_4$. Coupling constants are quoted in Hertz (Hz). ^{119}Sn NMR and $^{119}Sn\{^{1}H\}$ NMR spectra are reported relative to $SnMe_4$. The solid-state ^{1}H DP/MAS,$^{13}C\{^{1}H\}$ CP/MAS and $^{119}Sn\{^{1}H\}$ CP/MAS NMR spectra were recorded at 22 °C with a Bruker Avance Neo 400 WB NMR spectrometer with bottom layer rotors of ZrO_2 (open diameter 4 mm) loaded with approximately 100 mg of the sample (^{1}H, 400.1 MHz; $^{13}C\{^{1}H\}$, 100.6 MHz; ^{119}Sn, 149.2 MHz; DP = direct polarization; CP = cross polarization, MAS = magic-angle spinning). The chemical shifts were calibrated by setting the ^{13}C low-field signal of adamantine to δ = 38.48 ppm according to the IUPAC recommendations[15] with

$\Xi[^{13}C]$ = 25.145020 MHz and $\Xi[^{119}Sn]$ = 37.290632 MHz.[15] Coupling constants are quoted in Hertz. ^{1}H DOSY measurements of Compound **3.9** and **3.10** in toluene-d_8 were performed at 298.15 K in 5 mm NMR tubes on a Bruker Avance Neo I 600 NMR spectrometer equipped with a 5 mm TBO iProbe with *z*-axis gradient coil capable of producing pulsed magnetic field gradients of 50.5 G/cm. Temperature calibration was performed with a standard sample of 4% CH_3OH in CD_3OD. The gradient coil was calibrated to 5.002 G/mm at 298.15 K using a “Doped Water” NMR sample (0.1 mg $GdCl_3$/ml D_2O + 1 % H_2O + 0.1 % $^{13}CH_3OH$, 40 mm filling height). Data were acquired and processed using the Bruker software Topspin 4.1.4. The DOSY data were recorded with the stimulated echo BPP-LED pulse sequence (longitudinal eddy current delay sequence with bipolar gradient pulse pairs for diffusion and additional spoil gradients). The diffusion time Δ (**3.9** and **3.10**: 50 ms) was kept constant in each DOSY experiment while the ‘smoothed square’ diffusion gradients were incremented from 2 % to 98 % of maximum gradient strength in 24 linear steps. One component fittings of the gradient strength dependence of the signal areas were performed by a Levenberg-Marquardt algorithm incorporated in the Bruker software Topspin 4.1.4. For multiplicities, the following abbreviations are used: s = singlet, d = doublet, t = triplet, sept = septet, m = multiplet, br = broad.

7.5 Synthetic Procedures for Chapter II

Synthesis of Me_2Im^{Me}·$GeCl_2Me_2$ (2.1a)

$GeCl_2Me_2$ (140 µL, 210 mg, 1.21 mmol, 1.0 eq) was added dropwise to a solution of Me_2Im^{Me} (150 mg, 1.97 mmol, 1.0 eq) in *n*-hexane (7 mL) and stirred at room temperature for 30 minutes. The resulting precipitate was isolated by filtration, washed with *n*-hexane (3 x 5 mL) and dried *in vacuo* to yield **2.1a** (313 mg, 1.05 mmol, 87 %) as a colorless solid. Crystals suitable for single crystal X-ray diffraction were obtained by storing a benzene solution of **2.1a** at 6 °C.

^{1}H NMR (500.1 MHz, C_6D_6, 298 K): δ = 0.97 (s, 6 H, CC*H*$_3$), 1.96 (s, 6 H, GeC*H*$_3$), 3.20 (s, 6 H, NC*H*$_3$).

^{13}C{^{1}H} NMR (125.8 MHz, C_6D_6, 298 K): δ = 7.6 (C*C*H$_3$), 20.7 (Ge*C*H$_3$), 33.3 (N*C*H$_3$), 125.2 (N*CC*N), 155.8 (NCGe).

Elemental analysis (%) calcd. For $C_9H_{18}Cl_2GeN_2$ [297.79 g/mol]: C, 36.30; H, 6.09; N, 9.41; found: C, 37.65; H, 6.61; N, 10.07.

IR (cm^{-1}): 3155 (vw), 2979 (w), 2935 (s), 2843 (w), 2790 (w), 1769 (vw), 1650 (m), 1637 (m), 1581 (s), 1486 (m), 1447 (s), 1411 (m), 1401 (m), 1374 (w), 1341 (vw), 1318 (vw), 1244 (m), 1219 (m), 1149 (w), 1114 (vw), 1096 (w), 1045 (w), 994 (w), 890 (m), 852 (vs), 796 (m), 753 (m), 671 (vw), 630 (s), 587 (m), 571 (m), 531 (vw), 508 (vw).

Synthesis of *i*Pr_2Im^{Me}·$GeCl_2Me_2$ (2.1b)

$GeCl_2Me_2$ (91.2 µL, 137 mg, 788 µmol, 1.0 eq) was added dropwise to a solution of *i*Pr_2Im^{Me} (142 mg, 788 µmol, 1.0 eq) in *n*-hexane (7 mL) and stirred at room temperature for 30 minutes. The resulting precipitate was isolated by filtration, washed with *n*-hexane (3 x 5 mL) and dried *in vacuo* to yield **2.1b** (215 mg, 468 µmol, 60 %) as a colorless solid. Crystals suitable for single crystal X-ray diffraction were obtained by storing a benzene solution of **2.1b** at 6 °C.

^{1}H NMR (500.1 MHz, C_6D_6, 298 K): δ = 1.17 (d, 12 H, $^{3}J_{H\text{-}H}$ = 7.0 Hz, *i*Pr-C*H*$_3$), 1.38 (s, 6 H, C*H*$_3$CCC*H*$_3$), 1.97 (s, 6 H, GeC*H*$_3$), 5.39 (sept, 2 H, $^{3}J_{H\text{-}H}$ = 7.0 Hz, *i*Pr-C*H*).

^{13}C{^{1}H} NMR (125.8 MHz, C_6D_6, 298 K): δ = 9.9 (NC*C*H$_3$), 21.0 (*i*Pr-*C*H$_3$), 22.1 (Ge*C*H$_3$), 52.3 (*i*Pr-*C*H), 125.8 (N*CC*N), 157.5 (N*C*N).

Elemental analysis (%) calcd. For $C_{13}H_{26}Cl_2GeN_2$ [353.90 g/mol]: C, 44.12; H, 7.41; N, 7.92; found: C, 44.20; H, 7.51; N, 7.97.

IR (cm^{-1}): 2996 (vw), 2972 (w), 2938 (w), 2880 (vw), 1629 (w), 1550 (vw), 1464 (m), 1439 (m), 1412 (s), 1391 (m), 1370 (m), 1338 (w), 1309 (vw), 1241 (w), 1219 (s), 1173 (vw), 1139 (vw), 1112 (m), 1083 (m), 1030 (vw), 931 (w), 903 (vw), 885 (vw), 853 (s), 842 (vs), 794 (m), 775 (m), 753 (m), 664 (vw), 628 (m), 590 (m), 543 (m), 437 (vw), 409 (vw).

Synthesis of Dipp$_2$Im·GeCl$_2$Me$_2$ (2.1c)

$GeCl_2Me_2$ (45.4 µL, 68.4 mg, 394 µmol, 1.0 eq) was added dropwise to a solution of Dipp$_2$Im (153 mg, 394 µmol, 1.0 eq) in *n*-hexane (7 mL) and stirred at room temperature for 30 minutes. The resulting precipitate was isolated by filtration, washed with *n*-hexane (3 x 5 mL) and dried *in vacuo* to yield **2.1c** (171 mg, 373 µmol, 95 %) as a colorless solid. Crystals suitable for single crystal X-ray diffraction were obtained by storing a benzene solution of **2.1c** at 6 °C.

^{1}H NMR (500.1 MHz, C_6D_6, 298 K): δ = 0.95 (d, 12 H, $^{3}J_{H\text{-}H}$ = 6.9 Hz, *i*Pr-C*H*$_3$), 1.03 (s, 6 H, GeC*H*$_3$), 1.57 (d, 12 H, $^{3}J_{H\text{-}H}$ = 6.9 Hz, *i*Pr-C*H*$_3$), 3.45 (sept, 4 H, $^{3}J_{H\text{-}H}$ = 6.9 Hz, *i*Pr-C*H*), 6.50 (s, 2 H, C*H*C*H*), 7.13 (m, 4 H, Dipp-*m*-C*H*), 7.19 (m, 2 H, Dipp-*p*-C*H*).

^{13}C{^{1}H} NMR (125.8 MHz, C_6D_6, 298 K): δ = 20.7 (Ge*C*H$_3$), 23.0 (*i*Pr-*C*H$_3$), 26.8 (*i*Pr-*C*H$_3$), 29.2 (*i*Pr-*C*H), 124.1 (*C*H*C*H), 124.7 (Dipp-*m*-*C*H), 132.0 (Dipp-*p*-*C*H), 132.9 (Dipp-*i*-*C*), 147.6 (Dipp-*o*-*C*), 160.5 (N*C*N).

Elemental analysis (%) calcd. For $C_{29}H_{42}Cl_2GeN_2$ [562.20 g/mol]: C, 61.96; H, 7.53; N, 4.98; found: C, 62.08; H, 7.66; N, 5.04.

IR (cm^{-1}): 3161 (vw), 3111 (vw), 3077 (w), 2965 (m), 2930 (w), 2868 (w), 1644 (vw), 1588 (vw), 1558 (vw), 1535 (w), 1464 (m), 1441 (m), 1418 (m), 1385 (m), 1363 (m), 1330 (m), 1307 (vw), 1269 (vw), 1252 (vw), 1238 (vw), 1210 (m), 1182 (w), 1146 (vw), 1122 (m), 1101 (w), 1059 (m), 948 (w), 932 (m), 848 (vw), 802 (s), 771 (s), 758 (vs), 730 (vw), 709 (w), 636 (m), 582 (w), 548 (vw), 462 (w), 439 (vw).

Synthesis of $Me_2Im^{Me}{\cdot}SnCl_2Me_2$ (2.2a)

A solution of $SnCl_2Me_2$ (265 mg, 1.21 mmol, 1.0 eq) and Me_2Im^{Me} (150 mg, 1.21 mmol, 1.0 eq) in *n*-hexane (10 mL) was stirred at room temperature overnight. The resulting precipitate was isolated by filtration, washed with *n*-hexane (3 x 5 mL) and dried *in vacuo* yield **2.2a** (324 mg, 942 µmol, 78 %) as a colorless solid.

^{1}H NMR (500.1 MHz, C_6D_6, 298 K): δ = 0.96 (s, 6 H, CCH_3), 1.55 (s, 6 H, $^3J_{H\text{-}119Sn}$ = 84.9 Hz, $^3J_{H\text{-}119Sn}$ = 81.0 Hz, SnCH_3), 3.14 (s, 6 H, NCH_3).

^{13}C{^{1}H} NMR (125.8 MHz, C_6D_6, 298 K): δ = 7.7 (CCH_3), 12.0 (GeCH_3), 34.0 (NCH_3), 125.8 (NCCN), 160.0 (NCSn).

^{119}Sn{^{1}H} NMR (186.5 MHz, C_6D_6, 298 K): δ = −222.5.

Elemental analysis (%) calcd. For $C_9H_{18}Cl_2N_2Sn$ [343.87 g/mol]: C, 31.44; H, 5.28; N, 8.15; found: C, 31.44; H, 5.32; N, 8.09.

IR (cm^{-1}): 2995 (vw), 2956 (vw), 2922 (vw), 2869 (vw), 1650 (m), 1577 (vw), 1542 (vw), 1483 (w), 1474 (w), 1445 (s), 1408 (m), 1398 (s), 1374 (w), 1230 (w), 1195 (vw), 1142 (vw), 1102 (vw), 1044 (vw), 978 (vw), 849 (s), 795 (vs), 745 (s), 661 (vw), 623 (vw), 561 (s), 528 (m), 459 (vw).

Synthesis of *i*Pr$_2$Im^{Me}·SnCl$_2$Me$_2$ (2.2b)

A solution of $SnCl_2Me_2$ (183 mg, 832 µmol, 1.0 eq) and *i*Pr$_2$Im^{Me} (150 mg, 832 µmol, 1.0 eq) in *n*-hexane (10 mL) was stirred at room temperature overnight. The resulting precipitate was isolated by filtration, washed with *n*-hexane (3 x 5 mL) and dried *in vacuo* to yield **2.2b** (273 mg, 682 µmol, 82 %) as a colorless solid. Crystals suitable for single crystal X-ray diffraction were obtained by slow evaporation of a benzene solution of **2.2b** at room temperature.

^{1}H NMR (500.1 MHz, C_6D_6, 298 K): δ = 1.15 (d, 12 H, $^3J_{H\text{-}H}$ = 7.0 Hz, *i*Pr-C*H*$_3$), 1.39 (s, 6 H, CC*H*$_3$), 1.52 (s, 6 H, $^3J_{H\text{-}119Sn}$ = 82.7 Hz, $^3J_{H\text{-}119Sn}$ = 79.0 Hz, SnC*H*$_3$), 5.25 (sept, 2 H, $^3J_{H\text{-}H}$ = 7.0 Hz, *i*Pr-C*H*).

^{13}C{^{1}H} NMR (125.8 MHz, C_6D_6, 298 K): δ = 9.8 (NC*C*H$_3$), 12.8 (Sn*C*H$_3$), 21.3 (*i*Pr-*C*H$_3$), 54.0 (*i*Pr-*C*H), 126.3 (N*CC*N), 162.6 (N*C*N).

^{119}Sn{^{1}H} NMR (186.5 MHz, C_6D_6, 298 K): δ = −227.8.

Elemental analysis (%) calcd. For $C_{13}H_{26}Cl_2N_2Sn$ [399.98 g/mol]: C, 39.04; H, 6.55; N, 7.00; found: C, 38.65; H, 6.58; N, 6.83.

IR (cm^{-1}): 3013 (vw), 2978 (w), 2938 (vw), 2912 (vw), 2879 (vw), 1628 (w), 1557 (vw), 1461 (m), 1440 (m), 1405 (s), 1390 (m), 1373 (s), 1337 (m), 1308 (vw), 1221 (s), 1186 (w), 1171 (vw), 1141 (m), 1111 (m), 1080 (vw), 1026 (vw), 907 (w), 887 (vw), 796 (vs), 766 (s), 693 (vw), 620 (vw), 556 (s), 524 (m), 458 (vw), 424 (w).

Synthesis of Dipp$_2$Im·SnCl$_2$Me$_2$ (2.2c)

A solution of $SnCl_2Me_2$ (113 mg, 515 µmol, 1.0 eq) and Dipp$_2$Im (200 mg, 515 µmol, 1.0 eq) in *n*-hexane (10 mL) was stirred at room temperature overnight. The resulting precipitate was isolated by filtration, washed with *n*-hexane (3 x 5 mL) and dried *in vacuo* to yield **2.2c** (237 mg, 390 µmol, 76 %) as a colorless solid. Crystals suitable for single crystal X-ray diffraction were obtained by slow evaporation of a benzene solution of **2.2c** at room temperature.

^{1}H NMR (500.1 MHz, C_6D_6, 298 K): δ = 0.57 (s, 6 H, $^{2}J_{H\text{-}119Sn}$ = 84.2 Hz, $^{2}J_{H\text{-}119Sn}$ = 88.1 Hz, SnCH_3), 0.95 (d, 12 H, $^{3}J_{H\text{-}H}$ = 7.0 Hz, *i*Pr-CH_3), 1.57 (d, 12 H, $^{3}J_{H\text{-}H}$ = 7.0 Hz, *i*Pr-CH_3), 3.31 (sept, 4 H, $^{3}J_{H\text{-}H}$ = 6.9 Hz, *i*Pr-C*H*), 6.54 (s, 2 H, C*H*C*H*), 7.14 (m, 4 H, Dipp-*m*-C*H*), 7.20 (m, 2 H, Dipp-*p*-C*H*).

^{13}C{^{1}H} NMR (125.8 MHz, C_6D_6, 298 K): δ = 11.9 (Ge*C*H$_3$), 23.1 (*i*Pr-*C*H$_3$), 26.8 (*i*Pr-*C*H$_3$), 29.2 (*i*Pr-*C*H), 124.6 (*C*H*C*H), 124.7 (Dipp-*m*-*C*H), 132.0 (Dipp-*p*-*C*H), 133.3 (Dipp-*i*-*C*), 147.4 (Dipp-*o*-*C*), 165.9 (N*C*N).

^{119}Sn{^{1}H} NMR (186.5 MHz, C_6D_6, 298 K): δ = −217.6.

Elemental analysis (%) calcd. For $C_{29}H_{42}Cl_2N_2Sn$ [608.28 g/mol]: C, 57.26; H, 6.96; N, 4.61; found: C, 56.82; H, 7.03; N, 4.46.

IR (cm^{-1}): 3160 (vw), 3115 (w), 3082 (w), 2964 (m), 2928 (m), 2868 (w), 1638 (vw), 1529 (vw), 1557 (w), 1537 (vw), 1463 (m), 1441 (m), 1415 (m), 1385 (m), 1363 (m), 1352 (w), 1329 (m), 1305 (w), 1269 (w), 1253 (w), 1211 (m), 1183 (w), 1147 (vw), 1118 (m), 1102 (w), 1059 (m), 949 (w), 932 (w), 902 (vw), 874 (vw), 802 (vs), 768 (s), 757 (vs), 703 (w), 631 (w), 565 (m), 527 (w), 459 (w), 438 (vw).

Synthesis of Me_2Im^{Me}·$GeCl_4$ (2.3)

$GeCl_4$ (200 µL, 376 mg, 1.76 mmol, 1.0 eq) was added dropwise to a solution of Me_2Im^{Me} (218 mg, 1.76 mmol, 1.0 eq) in *n*-hexane (7 mL) at −78 °C. The solution was warmed to room temperature and stirred overnight. A precipitate formed during that time was isolated by filtration, washed with Et_2O (5 mL) and *n*-hexane (5 mL) and dried *in vacuo* to yield **2.3** (473 mg, 1.40 mmol, 80 %) as a colorless solid. Crystals suitable for single crystal X-ray diffraction were obtained by slow evaporation of a concentrated toluene solution of **2.3** at room temperature.

^{1}H NMR (500.1 MHz, C_6D_6, 298 K): δ = 0.80 (s, 6 H, NCH_3), 3.28 (s, 6 H, CCH_3).

^{13}C{^{1}H} NMR (125.8 MHz, C_6D_6, 298 K): δ = 7.3 (C*C*H$_3$), 33.5 (NC*C*H$_3$), 125.0 (N*C*CN), 153.6 (N*C*N)*. * The resonance at 153.6 ppm was detected in the corresponding ^{1}H,^{13}C{^{1}H} HMBC spectrum.

IR (cm^{-1}): 3156 (vw), 3082 (vw), 2976 (m), 2930 (m), 2865 (w), 2785 (vw), 1640 (s), 1579 (m), 1537 (vw), 1486 (m), 1446 (vs), 1404 (s), 1372 (m), 1338 (w), 1267 (vw), 1230 (w), 1206 (w), 1110 (w), 1096 (w), 1044 (w), 1007 (vw), 966 (vw), 937 (vw), 847 (vs), 756 (m), 712 (w), 664 (vw), 629 (w), 605 (vw), 569 (m), 539 (vw), 506 (vw), 473 (vw), 415 (vw).

Synthesis of *i*Pr$_2$Im^{Me}·SnCl$_4$·THF (2.4)

$SnCl_4$ (130 µL, 289 mg, 1.11 mmol, 1.0 eq) was added dropwise to a solution of *i*Pr$_2$Im^{Me} (200 mg, 2.63 mmol, 1.0 eq) in THF (10 mL) and stirred at room temperature for one hour. The reaction mixture was filtered, and the filtrate layered with *n*-hexane (10 mL). The product crystallized after one week at −30 °C and the micro crystalline solid was isolated by filtration and dried *in vacuo* to yield **2.4** (1.13 g, 2.26 mmol, 85 %) as a colorless solid. Crystals suitable for single crystal X-ray diffraction were obtained by layering a concentrated solution of **2.4** in THF with *n*-hexane and storing at −30 °C.

^{1}H NMR (400.5 MHz, C_6D_6, 298 K): δ = 1.12 (d, 12 H, $^3J_{H\text{-}H}$ = 7.0 Hz, *i*Pr-C*H*$_3$), 1.29 (s, 6 H, C*H*$_3$CCC*H*$_3$), 1.40 (m, 4 H, OC*H*$_2$C*H*$_2$), 3.78 (m, 4 H, OC*H*$_2$), 5.67 (sept, 2 H, $^3J_{H\text{-}H}$ = 7.0 Hz, *i*Pr-C*H*).

^{13}C{^{1}H} NMR (100.7 MHz, C_6D_6, 298 K): δ = 9.7 (NC*C*H$_3$), 21.2 (*i*Pr-*C*H$_3$), 25.6 (O*C*H$_2$*C*H$_2$), 54.6 (*i*Pr-*C*H), 68.5 (O*C*H$_2$), 126.8 (N*CC*N), 160.1 (N*C*N).

^{119}Sn{^{1}H} NMR (149.3 MHz, C_6D_6, 298 K): δ = −446.5 (br).

Elemental analysis (%) calcd. For $C_{15}H_{28}Cl_4N_2Osn$ + C_4H_8O [585.02 g/mol]: C, 39.01; H, 6.20; N, 4.79; found: C, 37.96; H, 5.95; N, 6.90.

IR (cm^{-1}): 3144 (vw), 2987 (w), 2976 (w), 2938 (w), 2877 (vw), 1636 (w), 1551 (vw), 1444 (m), 1385 (m), 1367 (vs), 1283 (vw), 1204 (s), 1163 (w), 1141 (m), 1114 (m), 1070 (w), 1014 (w), 968 (vw), 932 (vw), 901 (w), 882 (vw), 853 (w), 833 (w), 754 (m), 677 (vw), 650 (vw), 585 (vw), 541 (m), 506 (vw), 464 (vw), 432 (m)

Synthesis of [^{a}Dipp$_2$Im·GeClMe$_2$]$^+$[Cl]$^-$ (2.5)

$GeCl_2Me_2$ (59.6 µL, 89.4 mg, 515 µmol, 1.0 eq) was added to a solution of $Dipp_2Im$ (200 mg, 515 µmol, 1.0 eq) in benzene (10 mL) and refluxed overnight. The resulting precipitate was isolated by filtration, washed with *n*-hexane (3 x 5 mL) and dried *in vacuo* to yield **2.5** (205 mg, 365 µmol, 71 %) as a colorless solid. Crystals of **2.5** suitable for X-ray diffraction were obtained by cooling the saturated refluxing benzene solution of this compound to room temperature.

^{1}H NMR (400.5 MHz, CD_2Cl_2, 298 K): δ = 0.76 (s, 6 H, GeCH_3), 1.28 (d, 6 H, $^3J_{H-H}$ = 6.9 Hz, *i*Pr-CH_3), 1.29 (d, 6 H, $^3J_{H-H}$ = 6.9 Hz, *i*Pr-CH_3), 1.30 (d, 6 H, $^3J_{H-H}$ = 6.9 Hz, *i*Pr-CH_3), 1.35 (d, 6 H, $^3J_{H-H}$ = 6.9 Hz, *i*Pr-CH_3), 2.41 (sept, 2 H, $^3J_{H-H}$ = 6.9 Hz, *i*Pr-CH), 2.44 (sept, 2 H, $^3J_{H-H}$ = 6.9 Hz, *i*Pr-CH), 7.40 (d, 2 H, $^3J_{H-H}$ = 7.9 Hz, Dipp-*m*-CH), 7.43 (d, 2 H, $^3J_{H-H}$ = 7.9 Hz, Dipp-*m*-CH), 7.62 (t, 1 H, $^3J_{H-H}$ = 7.9 Hz, Dipp-*p*-CH), 7.66 (t, 1 H, $^3J_{H-H}$ = 7.9 Hz, Dipp-*p*-CH), 7.68 (s, 1 H, NCHCGe), 12.2 (s, 1 H, NCHN).

^{13}C{^{1}H} NMR (100.7 MHz, CD_2Cl_2, 298 K): δ = 5.3 (GeCH$_3$), 22.3 (*i*Pr-CH$_3$), 23.9 (*i*Pr-CH$_3$), 24.9 (*i*Pr-CH$_3$), 26.6 (*i*Pr-CH$_3$), 29.6 (*i*Pr-CH), 29.7 (*i*Pr-CH), 125.0 (Dipp-*m*-CH), 125.1 (Dipp-*m*-CH), 130.4 (Dipp-*i*-*C*), 131.0 (Dipp-*i*-*C*), 132.0 (NCHCGe), 132.4 (Dipp-*p*-CH), 132.9 (Dipp-*p*-CH), 136.8 (NCGe), 145.1 (NCHN), 145.6 (Dipp-*o*-*C*), 146.0 (Dipp-*o*-*C*).

Elemental analysis (%) calcd. For $C_{29}H_{42}Cl_2GeN_2$ [562.20 g/mol]: C, 61.96; H, 7.53; N, 4.98; found: C, 62.34; H, 7.97; N, 4.74.

IR (cm^{-1}): 3151 (vw), 3076 (w), 2962 (s), 2929 (m), 2868 (m), 2827 (m), 2753 (s), 1888 (vw), 1644 (vw), 1588 (vw), 1545 (w), 1531 (m), 1496 (w), 1463 (s), 1443 (w), 1419 (w), 1386 (m), 1365 (m), 1330 (m), 1301 (w), 1259 (w), 1204 (m), 1183 (m), 1106 (w), 1059 (s), 951 (m), 935 (m), 853 (m), 810 (vs), 773 (s), 759 (vs), 739 (vs), 709 (w), 698 (m), 685 (m), 637 (m), 582 (vw), 538 (vs), 522 (w), 466 (vs), 443 (m).

Synthesis of cAAC^{Me}·GeCl$_2$Me$_2$ (2.6)

$GeCl_2Me_2$ (250 µL, 563 mg, 1.97 mmol, 1.0 eq) was added dropwise to a solution of cAAC^{Me} (342 mg, 1.97 mmol, 1.0 eq) in *n*-hexane (7 mL) and the resulting solution was stirred at room temperature for 30 minutes. A precipitate formed during that time was isolated by filtration, washed with *n*-hexane (3 x 5 mL) and dried *in vacuo* to yield **2.6** (798 mg, 1.74 mmol, 88 %) as a colorless solid. Crystals suitable for single crystal X-ray diffraction were obtained by storing a solution of **2.6** in benzene at 6 °C.

^{1}H NMR (500.1 MHz, toluene-d_8, 233 K): δ = 0.81 (s, 3 H, GeCH_3), 0.94 (s, 6 H, NC(CH_3)$_2$), 1.04 (d, 6 H, $^3J_{H-H}$ = 6.7 Hz, *i*Pr-CH_3), 1.28 (s, 2 H, CH_2), 1.64 (d, 6 H, $^3J_{H-H}$ = 6.7 Hz, *i*Pr-CH_3), 1.75 (s, 6 H, NCC(CH_3)$_2$), 1.97 (s, 3 H, GeCH_3), 3.23 (sept, 2 H, $^3J_{H-H}$ = 6.7 Hz, *i*Pr-CH), 6.94 (m, 2 H, Dipp-*m*-CH), 6.98 (m, 1 H, Dipp-*p*-CH).

^{13}C{^{1}H} NMR (125.8 MHz, toluene-d_8, 233 K): δ = 15.0 (GeCH$_3$), 25.2 (GeCH$_3$), 27.0 (*i*Pr-CH$_3$), 28.2 (NC(CH$_3$)$_2$), 28.3 (*i*Pr-CH$_3$), 29.2 (*i*Pr-CH), 32.1 (NCC(CH$_3$)$_2$), 51.5 (CH$_2$), 54.4 (NCC(CH$_3$)$_2$), 82.1 (NC(CH$_3$)$_2$), 126.5 (Dipp-*m*-CH), 130.7 (Dipp-*p*-CH), 132.5 (Dipp-*i*-C), 147.0 (Dipp-*o*-C), 214.1 (NCGe).

Elemental analysis (%) calcd. For $C_{22}H_{37}Cl_2GeN$ [459.08 g/mol]: C, 57.56; H, 8.12; N, 3.05; found: C, 58.21; H, 8.47; N, 3.15.

IR (cm^{-1}): 3079 (vw), 2986 (m), 2970 (m), 2933 (m), 2868 (m), 2823 (m), 1638 (m), 1592 (vw), 1525 (vw), 1465 (s), 1390 (w), 1377 (m), 1369 (m), 1359 (w), 1343 (m), 1270 (w), 1257 (w), 1246 (w), 1205 (w), 1171 (vw), 1135 (w), 1110 (w), 1053 (m), 950 (w), 933 (vw), 901 (m), 883 (m), 844 (s), 811 (vs), 788 (s), 768 (s), 717 (vw), 676 (w), 652 (m), 630 (w), 607 (w), 592 (w), 559 (w), 517 (vw), 489 (w), 425 (vw).

Synthesis of cAAC^{Me}·$SnCl_2Me_2$ (2.7)

A solution of $SnCl_2Me_2$ (154 mg, 701 µmol, 1.0 eq) and cAAC^{Me} (200 mg, 701 µmol, 1.0 eq) in *n*-hexane (10 mL) was stirred at room temperature overnight. A precipitate formed during that time was isolated by filtration, washed with *n*-hexane (3 x 5 mL) and dried *in vacuo* to yield **2.7** (240 mg, 475 µmol, 68 %) as a colorless solid. Crystals suitable for single crystal X-ray diffraction were obtained by slow evaporation of a benzene solution of **2.7** at room temperature.

^{1}H NMR (500.1 MHz, toluene-d_8, 233 K): δ = 0.42 (s, 3 H, overlapping broad satellites, SnCH_3), 0.82 (s, 6 H, NC(CH_3)$_2$), 1.04 (d, 6 H, $^3J_{H\text{-}H}$ = 6.7 Hz, *i*Pr-CH_3), 1.21 (s, 2 H, CH_2), 1.60 (d, 6 H, $^3J_{H\text{-}H}$ = 6.7 Hz, *i*Pr-CH_3), 1.66 (s, 3 H, overlapping broad satellites, SnCH_3), 1.70 (s, 6 H, NCC(CH_3)$_2$), 3.06 (sept, 2 H, $^3J_{H\text{-}H}$ = 6.7 Hz, *i*Pr-CH), 6.91 (m, 2 H, Dipp-*m*-CH), 6.97 (m, 1 H, Dipp-*p*-CH).

^{13}C{^{1}H} NMR (125.8 MHz, toluene-d_8, 233 K): δ = 5.9 (SnCH$_3$), 18.6 (SnCH$_3$), 26.2 (*i*Pr-CH$_3$), 28.6 (NC(CH$_3$)$_2$), 29.0 (*i*Pr-CH), 29.1 (*i*Pr-CH$_3$), 31.0 (NCC(CH$_3$)$_2$), 50.0 (CH$_2$), 55.7 (NCC(CH$_3$)$_2$), 83.4 (NC(CH$_3$)$_2$), 126.4 (Dipp-*m*-CH), 130.7 (Dipp-*p*-CH), 132.6 (Dipp-*i*-C), 146.6 (Dipp-*o*-C), 226.3 (NCSn).

^{119}Sn{^{1}H} NMR (186.5 MHz, toluene-d_8, 233 K): δ = −214.1.

Elemental analysis (%) calcd. For $C_{22}H_{37}Cl_2NSn$ [505.16 g/mol]: C, 52.31; H, 7.38; N, 2.77; found: C, 52.22; H, 7.45; N, 2.61.

IR (cm^{-1}): 2964 (m), 2930 (m), 2872 (w), 1643 (vw), 1587 (vw), 1529 (m), 1458 (m), 1390 (m), 1375 (m), 1346 (w), 1324 (w), 1265 (w), 1207 (w), 1188 (m), 1181 (m), 1160 (vw), 1128 (w), 1107 (w), 1053 (w), 1015 (vw), 997 (vw), 973 (vw), 930 (vw), 879 (vw), 809 (vs), 775 (vs), 610 (w), 556 (s), 521 (m), 492 (vw), 433 (vw), 412 (vw).

Synthesis of cAAC^{Me}·$GeCl_2Ph_2$ (2.8)

A solution of $GeCl_2Ph_2$ (147 µL, 209 mg, 0.70 mmol, 1.0 eq) in *n*-hexane (5 mL) was added to a solution of cAAC^{Me} (200 mg, 0.70 mmol, 1.0 eq) in *n*-hexane (5 mL) at −78 °C and was stirred overnight whilst warming to room temperature. A precipitate formed during that time was isolated by filtration, washed with *n*-hexane (2 x 5 mL) and dried *in vacuo* to yield **2.8** (281 mg, 482 µmol, 69 %) as a colorless solid. Partial decomposition of the compound in solution was observed. Crystals suitable for single crystal X-ray diffraction were obtained by storing a benzene solution of **2.8** at 6 °C.

^{1}H NMR (500.1 MHz, C_6D_6, 298 K): δ = 0.99 (d, 6 H, $^3J_{H\text{-}H}$ = 6.5 Hz, *i*Pr-CH_3), 1.18 (s, 6 H, NC(CH_3)$_2$), 1.30 (d, 6 H, $^3J_{H\text{-}H}$ = 6.5 Hz, *i*Pr-CH_3), 1.45 (s, 2 H, CH_2), 1.70 (s, 6 H, NCC(CH_3)$_2$), 3.31 (sept, 2 H, $^3J_{H\text{-}H}$ = 6.5 Hz, *i*Pr-C*H*), 6.88 (br, 3 H, Ph-C*H*), 7.00 (d, 2 H, $^3J_{H\text{-}H}$ = 7.7 Hz, Dipp-*m*-C*H*), 7.13 (t, 1 H, $^3J_{H\text{-}H}$ = 7.7 Hz, Dipp-*p*-C*H*), 7.31 (br, 2 H, Ph-C*H*), 7.42 (br, 2 H, Ph-C*H*), 7.55 (m, 1 H, Ph-C*H*), 9.37 (br, 2 H, Ph-C*H*).

^{13}C{^{1}H} NMR (125.8 MHz, C_6D_6, 298 K): δ = 25.7 (*i*Pr-*C*H_3), 28.0 (NC(*C*H_3)$_2$), 28.2 (*i*Pr-*C*H_3), 29.2 (*i*Pr-*C*H), 32.9 (NCC(*C*H_3)$_2$), 52.4 (*C*H_2), 55.1 (NC*C*(CH$_3$)$_2$), 82.7 N*C*(CH$_3$)$_2$), 126.9 (Dipp-*m*-*C*H), 127.0 (Ph-*C*H), 128.2 (Ph-*C*H), 129.2 (Ph-*C*H), 130.8 (Dipp-*p*-*C*H), 131.8 (Ph-*C*H), 133.0 (Ph-*C*H), 134.5 (Dipp-*i*-*C*), 135.4 (Ph-*C*H), 138.0 (Ph-*C*H), 141.0 (Ph-i-*C*), 145.0 (Ph-i-*C*), 147.9 (Dipp-*o*-*C*), 213.0 (N*C*Ge).

Elemental analysis (%) calcd. For $C_{22}H_{37}Cl_2GeN$ [459.08 g/mol]: C, 65.90; H, 7.09; N, 2.40; found: C, 65.44; H, 7.34; N, 2.34.

IR (cm^{-1}): 3050 (vw), 2970 (m), 2931 (m), 2870 (w), 1683 (vw), 1639 (vw), 1584 (vw), 1513 (m), 1471 (m), 1456 (m), 1431 (m), 1391 (m), 1376 (w), 1367 (w), 1346 (vw), 1322 (w), 1302 (w), 1265 (w), 1205 (vw), 1182 (m), 1158 (vw), 1127 (w), 1097 (w), 1082 (w), 1072 (m), 1054 (w), 1026 (w), 999 (w), 932 (vw), 911 (vw), 874 (vw), 810 (m), 778 (w), 747 (s), 736 (vs), 692 (vs), 674 (m), 610 (vw), 564 (w), 519 (vw), 503 (vs), 475 (s), 461 (s), 437 (vw), 416 (vw).

Synthesis of [cAAC^{Me}·GeMe$_3$]$^+$[Cl]$^-$ (2.9)

GeClMe$_3$ (100 µL, 124 mg, 809 µmol, 1.5 eq) was added dropwise to a solution of cAAC^{Me} (154 mg, 515 µmol, 1.0 eq) in THF (3 mL) and stirred at room temperature for 2 h. The reaction mixture was left standing at room temperature over night and **2.9** crystallized out of solution. The solvent was decanted, and the solid material dried *in vacuo* to yield **2.9** (215 mg, 468 µmol, 60 %) as a colorless microcrystalline solid. Partial decomposition of the compound in solution was observed. Crystals suitable for single crystal X-ray diffraction were obtained by storing a concentrated THF solution of **2.9** at room temperature.

^{1}H NMR (400.5 MHz, CD_2Cl_2, 298 K): δ = 0.35 (s_{br}, 9 H, Ge(C*H*$_3$)$_3$), 1.20 (d, 6 H, $^3J_{H\text{-}H}$ = 6.7 Hz, *i*Pr-C*H*$_3$), 1.35 (d, 6 H, $^3J_{H\text{-}H}$ = 6.7 Hz, *i*Pr-C*H*$_3$), 1.59 (s, 6 H, NCC(C*H*$_3$)$_2$), 1.67 (s, 6 H, NC(C*H*$_3$)$_2$), 2.48 (s, 2 H, C*H*$_2$), 2.74 (sept, 2 H, $^3J_{H\text{-}H}$ = 6.7 Hz, *i*Pr-C*H*), 7.41 (d, 2 H, $^3J_{H\text{-}H}$ = 7.8 Hz, Dipp-*m*-C*H*), 7.59 (t, 2 H, $^3J_{H\text{-}H}$ = 7.8 Hz, Dipp-*p*-C*H*).

^{13}C{^{1}H} NMR (100.7 MHz, CD_2Cl_2, 298 K): δ = 2.4 (Ge(*C*H$_3$)$_3$), 24.8 (*i*Pr-*C*H$_3$), 25.8 (*i*Pr-*C*H$_3$), 28.6 (NC(*C*H$_3$)$_2$), 29.2 (NCC(*C*H$_3$)$_2$), 29.4 (*i*Pr-*C*H), 50.0 (*C*H$_2$), 56.7 (NC*C*(CH$_3$)$_2$), 86.4 (N*C*(CH$_3$)$_2$), 126.9 (Dipp-*m*-*C*H), 131.9 (Dipp-*i*-*C*), 132.3 (Dipp-*p*-*C*H), 145.1 (Dipp-*o*-*C*), 222.9 (N*C*Ge).

Elemental analysis (%) calcd. For $C_{23}H_{40}ClGeN$ [438.66 g/mol]: C, 62.98; H, 9.19; N, 3.19; found: C, 62.53; H, 9.35; N, 3.28.

IR (cm^{-1}): 2967 (s), 2930 (m), 2867 (m), 2823 (m), 1638 (m), 1590 (vw), 1561 (vw), 1465 (s), 1440 (m), 1391 (w), 1378 (m), 1368 (m), 1359 (m), 1342 (m), 1325 (w), 1256 (w), 1239 (w), 1205 (m), 1174 (vw), 1135 (m), 1110 (vw), 1053 (m), 1000 (vw), 972 (vw), 949 (m), 901 (w), 841 (m), 811 (vs), 797 (s), 767 (m), 754 (w), 676 (w), 652 (vw), 608 (s), 559 (m), 517 (vw), 489 (w), 469 (vw), 446 (vw), 426 (vw), 409 (vw).

Synthesis of $[cAAC^{Me}Cl]^+[GeCl_3]^-$ (2.10)

A solution of $cAAC^{Me}$ (1.00 g, 3.50 mmol, 1.0 eq) in Et_2O (15 mL) was added to a solution of $GeCl_4$ (400 µL, 751 mg, 3.50 mmol, 1.0 eq) in Et_2O (15 mL) at −78 °C. The reaction mixture was allowed to warm to room temperature over a period of 2 h. The resulting precipitate was isolated by filtration, washed with Et_2O (5 mL) and *n*-hexane (2 x 5 mL) and dried *in vacuo* to yield **2.10** (1.53 g, 3.06 mmol, 87 %) as a colorless solid. Crystals suitable for single crystal X-ray diffraction were obtained by slow evaporation of a dichloromethane solution of **2.10** at room temperature.

^{1}H NMR (500.1 MHz, CD_2Cl_2, 298 K): δ = 1.20 (d, 6 H, $^3J_{H-H}$ = 6.6 Hz, *i*Pr-CH_3), 1.39 (s, 6 H, NC(CH_3)$_2$), 1.64 (s, 2 H, CH_2), 1.77 (s, 6 H, NCC(CH_3)$_2$), 2.48 (sept, 2 H, $^3J_{H-H}$ = 6.6 Hz, *i*Pr-C*H*), 2.76 (d, 6 H, $^3J_{H-H}$ = 6.6 Hz, *i*Pr-CH_3), 7.47 (d, 2 H, $^3J_{H-H}$ = 7.9 Hz, Dipp-*m*-C*H*), 7.66 (t, 1 H, $^3J_{H-H}$ = 7.9 Hz, Dipp-*p*-C*H*).

^{13}C{^{1}H} NMR (125.8 MHz, CD_2Cl_2, 298 K): δ = 23.4 (*i*Pr-*C*H$_3$), 26.3 (*i*Pr-*C*H$_3$), 28.4, (NCC(*C*H$_3$)$_2$), 29.0 (NC(*C*H$_3$)$_2$), 30.4 (*i*Pr-*C*H), 48.2 (*C*H$_2$), 51.7 (N*C*(CH$_3$)$_2$) 84.5 (NC*C*(CH$_3$)$_2$), 126.9 (Dipp-*m*-*C*H), 127.6 (Dipp-*i*-*C*), 133.2 (Dipp-*p*-*C*H), 144.7 (Dipp-*o*-*C*), 190.6 (N*C*Cl).

Elemental analysis (%) calcd. For $C_{20}H_{31}Cl_4GeN$ [499.91 g/mol]: C, 48.05; H, 6.25; N, 2.80; found: C, 48.07; H, 6.21; N, 2.70.

IR (cm^{-1}): 3003 (vw), 2974 (m), 2932 (w), 2872 (w), 1606 (vs), 1596 (w), 1460 (m), 1440 (m), 1379 (m), 1366 (m), 1335 (w), 1315 (vw), 1266 (w), 1206 (vw), 1183 (w), 1169 (w), 1134 (s), 1114 (m), 1061 (m), 1053 (m), 1014 (vw), 972 (vw), 955 (vw), 929 (w), 870 (w), 818 (vs), 795 (vw), 743 (m), 711 (vw), 700 (vw), 633 (vw), 610 (m), 567 (m), 506 (w), 494 (m), 426 (w).

Synthesis of [cAAC^{Me}Cl]$^{+}$[SnCl$_3$]$^{-}$ (2.11) and cAAC^{Me}·SnCl$_4$ (2.12)

A solution of cAAC^{Me} (1.00 g, 3.50 mmol, 1.0 eq) in Et_2O (15 mL) was added to a solution of $SnCl_4$ (409 µL, 913 mg, 3.50 mmol, 1.0 eq) in Et_2O (15 mL) at −78 °C. The reaction mixture was allowed to warm to room temperature overnight. All volatile material of the resulting suspension were removed *in vacuo* and the remaining solid was washed with benzene (3 x 8 mL). The solid was dried *in vacuo* to yield **2.11** (729 mg, 1.34 mmol, 38 %) as a colorless solid. Crystals suitable for single crystal X-ray diffraction were obtained by slow diffusion of *n*-hexane into a saturated dichloromethane solution of **2.11** at room temperature. Removing all volatile materials of the filtrate *in vacuo* afforded **2.12** (841 mg, 1.54 mmol, 44 %) as a colorless solid. Crystals suitable for single crystal X-ray diffraction were obtained by slow evaporation of a saturated benzene solution of **2.12** at room temperature.

2.11: **^{1}H NMR** (500.1 MHz, CD_2Cl_2, 298 K): δ = 1.20 (d, 6 H, $^{3}J_{H\text{-}H}$ = 6.7 Hz, *i*Pr-CH_3), 1.39 (d, 6 H, $^{3}J_{H\text{-}H}$ = 6.7 Hz, *i*Pr-CH_3), 1.64 (s, 6 H, NC(CH_3)$_2$), 1.77 (s, 6 H, NCC(CH_3)$_2$), 2.48 (sept, 2 H, $^{3}J_{H\text{-}H}$ = 6.7 Hz, *i*Pr-CH), 2.79 (s, 2 H, CH_2), 7.46 (d, 2 H, $^{3}J_{H\text{-}H}$ = 7.8 Hz, Dipp-*m*-CH), 7.66 (t, 1 H, $^{3}J_{H\text{-}H}$ = 7.8 Hz, Dipp-*p*-CH).

^{13}C{^{1}H} NMR (125.8 MHz, CD_2Cl_2, 298 K): δ = 23.5 (*i*Pr-*C*H$_3$), 26.3 (*i*Pr-*C*H$_3$), 28.4 (NCC(*C*H$_3$)$_2$), 29.1 (NC(*C*H$_3$)$_2$), 30.4 (*i*Pr-*C*H), 48.2 (*C*H$_2$), 51.8 (NC*C*(CH$_3$)$_2$), 84.6 N*C*(CH$_3$)$_2$), 126.9 (Dipp-*m*-*C*H), 127.7 (Dipp-*i*-*C*), 133.2 (Dipp-*p*-*C*H), 144.7 (Dipp-*o*-*C*), 190.6 (N*C*Cl).

^{119}Sn{^{1}H} NMR (186.5 MHz, CD_2Cl_2, 298 K): δ = −34.8.

Elemental analysis (%) calcd. For $C_{20}H_{31}Cl_4NSn$ [545.99 g/mol]: C, 44.00; H, 5.72; N, 2.57; found: C, 44.20; H, 6.05; N, 2.31.

IR (cm^{-1}): 2969 (s), 2930 (m), 2871 (w), 1643 (vw), 1605 (vs), 1584 (w), 1458 (s), 1440 (m), 1378 (m), 1366 (m), 1335 (w), 1265 (w), 1205 (w), 1183 (w), 1168 (w), 1129 (s), 1113 (m), 1059 (m), 973 (vw), 955 (vw), 928 (w), 896 (vw), 869 (vw), 815 (vs), 768 (vw), 743 (w), 710 (vw), 675 (vw), 652 (vw), 632 (vw), 609 (w), 566 (w), 507 (vw), 493 (w), 425 (w).

2.12: **^{1}H NMR** (500.1 MHz, C_6D_6, 298 K): δ = 1.32 (d, 6 H, $^{3}J_{H\text{-}H}$ = 6.5 Hz, *i*Pr-CH_3), 1.41 (d, 6 H, $^{3}J_{H\text{-}H}$ = 6.5 Hz, *i*Pr-CH_3), 1.53 (s, 6 H, $^{4}J_{H\text{-}117Sn}$ = 7.7 Hz overlapped by $^{4}J_{H\text{-}119Sn}$ = 7.7 Hz, NCC(CH_3)$_2$), 1.99 (s, 6 H, NC(CH_3)$_2$), 2.28 (s, 2 H, CH_2), 2.85 (sept, 2 H, $^{3}J_{H\text{-}H}$ = 6.6 Hz, *i*Pr-C*H*), 7.40 (d, 2 H, $^{3}J_{H\text{-}H}$ = 7.9 Hz, Dipp-*m*-C*H*), 7.55 (t, 1 H, $^{3}J_{H\text{-}H}$ = 7.9 Hz, Dipp-*p*-C*H*).

^{13}C{^{1}H} NMR (125.8 MHz, C_6D_6, 298 K): δ = 26.4 (*i*Pr-*C*H$_3$), 28.3 (*i*Pr-*C*H$_3$), 29.6 (*i*Pr-*C*H), 29.8 (NCC(*C*H$_3$)$_2$), 31.0 (NC(*C*H$_3$)$_2$), 51.1 (*C*H$_2$), 55.1 (NC*C*(CH$_3$)$_2$), 87.1 (N*C*(CH$_3$)$_2$), 127.0 (Dipp-*m*-*C*H), 131.5 (Dipp-*i*-*C*), 131.8 (Dipp-*p*-*C*H), 146.7 (Dipp-*o*-*C*), 218.9 (N*C*Sn).

^{119}Sn{^{1}H} NMR (186.5 MHz, C_6D_6, 298 K): δ = −406.3.

Elemental analysis (%) calcd. For $C_{20}H_{31}Cl_4NSn$ [545.99 g/mol]: C, 44.00; H, 5.72; N, 2.57; found: C, 43.76; H, 5.72; N, 2.43.

IR (cm^{-1}): 2971 (m), 2932 (m), 2871 (w), 1644 (vw), 1604 (m), 1583 (vw), 1550 (w), 1456 (s), 1390 (m), 1374 (m), 1342 (w), 1329 (w), 1266 (w), 1197 (w), 1179 (w), 1126 (m), 1105 (m), 1053 (m), 1013 (vw), 970 (vw), 930 (w), 873 (vw), 809 (vs), 773 (m), 738 (vw), 712 (vw), 677 (vw), 649 (vw), 631 (vw), 608 (w), 558 (w), 493 (w), 426 (vw), 412 (vw).

Synthesis of Me_2Im^{Me}·$SnMe_2$ (2.13)

A suspension of Me_2Im^{Me}·$SnCl_2Me_2$ (**2.2a**) (15.0 mg, 43.6 µmol, 1.0 eq) and KC_8 (24.0 mg, 175 µmol, 4.0 eq) in C_6D_6 (0.6 mL) was stirred for 2 d. The reaction mixture was then filtered and all volatile material of the filtrate was removed *in vacuo* to yield **2.13** (8.00 mg, 29.3 µmol, 67 %) as a colorless solid. Crystals suitable for single crystal X-ray diffraction were obtained by slow evaporation of a concentrated toluene solution of **2.13** at room temperature.

^{1}H NMR (500.1 MHz, C_6D_6, 298 K): δ = 0.73 (s, 6 H, overlapping broad satellites, SnCH_3), 1.31 (s, 6 H, NCCH_3), 3.19 (s, 6 H, NCH_3).

$^{13}C\{^1H\}$ NMR (125.8 MHz, C_6D_6, 298 K): δ = 0.5 (Sn*C*H_3), 8.3 (C*C*H_3), 34.4 (N*C*H_3), 124.2 (N*C*CH_3), 183.4 (N*C*N).

$^{119}Sn\{^1H\}$ NMR (186.5 MHz, C_6D_6, 298 K): δ = −83.3.

Elemental analysis (%) calcd. For $C_9H_{18}SnN_2$ [272.97 g/mol]: C, 39.60; H, 6.65; N, 10.26; found: C, 36.93; H, 6.40; N, 8.91. After several attempts, this is the best result so far. This may be due to the high air sensitivity of **2.13**.

IR (cm^{-1}): 2977 (w), 2947 (m), 2919 (m), 1897 (m), 1855 (w), 1784 (vw), 1688 (w), 1662 (m), 1649 (m), 1598 (w), 1574 (w), 1455 (m), 1431 (s), 1396 (m), 1374 (s), 1366 (s), 1309 (w), 1226 (w), 1194 (w), 1122 (vw), 1095 (vw), 965 (m), 844 (m), 754 (s), 732 (s), 712 (m), 664 (w), 569 (s), 549 (s), 515 (w), 475 (vw), 449 (vs).

Synthesis of cAAC^{Me}·$SnMe_2$·$SnCl_2Me_2$ (2.14)

Route A: A suspension of **2.7** (200 mg, 396 µmol, 1.0 eq) and KC_8 (401 mg, 2.97 mmol, 7.5 eq) in toluene (15 mL) was sonicated for 7 min (until the color of the solution was deep red). The suspension was further stirred at 0 °C for 15 min. After cooling to −78 °C, the dark red suspension was filtrated at −78 °C through a pad of celite pad into precooled (−78 °C) $SnCl_2Me_2$ (87.0 mg, 396 µmol, 1.0 eq). The red solution was allowed to warm to 0 °C and stirred for 2 h. The color changed to pale yellow. Removing all volatiles *in vacuo* afforded a pale-yellow oil. Washing with *n*-hexane (3 x 10 mL) and subsequently removing all volatile materials *in vacuo* yielded **2.14** (188 mg, 287 µmol, 73 %) as a colorless solid. In some instances, the product had to be recrystallized for further purification by storing a saturated dichloromethane solution of **2.14** at −30 °C for several days. Crystals suitable for single crystal X-ray diffraction were obtained by storing a concentrated toluene solution of **2.14** at −30 °C. Route B: A solution of **2.7** (20 mg, 39.6 µmol, 1.0 eq), $SnCl_2Me_2$ (8.70 mg, 39.6 µmol, 1.0 eq), and 1,4-bis(trimethylsilyl)-1,4-dihydropyrazin (8.70 mg, 39.6 µmol, 1.0 eq) in C_6D_6 (0.6 mL) was heated to 65 °C for 1 d. Cooling the reaction mixture to room temperature and storage of the solution for several hours led to the formation of colorless crystals, which were separated from the solution, washed with *n*-hexane

(2 x 1 mL) and dried *in vacuo* to yield **2.14** (21.0 mg, 32.1 µmol, 81 %) as a colorless crystalline solid. Partial decomposition of the compound in solution was observed.

^{1}H NMR (500.1 MHz, CD_2Cl_2, 298 K): δ = 0.24 (br, 6 H, SnCH_3), 0.96 (s, 6 H, satellites overlapping: $^{3}J_{H\text{-}117Sn}$ = $^{3}J_{H\text{-}119Sn}$ = 11.3 Hz, $^{2}J_{H\text{-}117Sn}$ = 64.9 Hz, $^{2}J_{H\text{-}119Sn}$ = 67.8 Hz, Sn-CH_3), 1.24 (d, 6 H, $^{3}J_{H\text{-}H}$ = 6.6 Hz, *i*Pr-CH_3), 1.32 (d, 6 H, $^{3}J_{H\text{-}H}$ = 6.6 Hz, *i*Pr-CH_3), 1.49 (s, 6 H, NC(CH_3)$_2$), 1.78 (s_{br}, 6 H, NCC(CH_3)$_2$), 2.22 (s, 2 H, CH_2), 3.05 (br, 2 H, *i*Pr-CH), 7.40 (d, 2 H, $^{3}J_{H\text{-}H}$ = 7.9 Hz, Dipp-*m*-CH), 7.54 (d, 1 H, $^{3}J_{H\text{-}H}$ = 7.9 Hz, Dipp-*p*-CH).

^{13}C{^{1}H} NMR (125.8 MHz, CD_2Cl_2, 298 K): δ = −9.5 (Sn*C*H_3), 24.3 (*i*Pr-*C*H_3), 27.4 (*i*Pr-*C*H_3), 28.8 (NCC(*C*H_3)$_2$), 29.1 (NC(*C*H_3)$_2$ overlapped by *i*Pr-*C*H), 49.5 (*C*H_2), 57.7 (NC*C*(CH$_3$)$_2$), 85.2 (N*C*(CH$_3$)$_2$), 126.7 (Dipp-*m*-*C*H), 131.6 (Dipp-*p*-*C*H), 133.2 (Dipp-*i*-*C*), 146.1 (Dipp-*o*-*C*), 237.9 (N*C*Sn). One of the Sn*C*H$_3$-resonances could not be observed due to the broadening.

^{119}Sn{^{1}H} NMR (186.5 MHz, CD_2Cl_2, 298 K): δ = −120.6 (s, $^{1}J_{119Sn\text{-}117Sn}$ = 9492 Hz, $^{1}J_{119Sn\text{-}119Sn}$ = 9910 Hz, C*Sn*Me$_2$), −127.1 ($^{1}J_{119Sn\text{-}117Sn}$ = 9492 Hz, $^{1}J_{119Sn\text{-}119Sn}$ = 9910 Hz, *Sn*Cl$_2$Me$_2$).

Elemental analysis (%) calcd. for $C_{24}H_{43}Cl_2NSn_2$ + C_6H_6 [732.05 g/mol]: C, 49.22; H, 6.75; N, 1.91; found: C, 49.16; H, 6.70; N, 1.92.

IR (cm^{-1}): 3008 (vw), 2966 (m), 2926 (w), 2868 (w), 2280 (vw), 1589 (vw) 1541 (w), 1457 (w), 1385 (w), 1366 (vw), 1345 (w), 1326 (vw), 1269 (vw), 1250 (w), 1196 (w), 1181 (w), 1125 (vw), 1110 (vw), 1053 (vw), 1008 (vw), 993 (vw), 932 (vw), 876 (m), 818 (s), 778 (s), 761 (vw), 671 (vw), 608 (vw), 590 (vw), 566 (vw), 541 (m), 525 (m), 505 (vs), 431 (vw).

7.6 Synthetic Procedures for Chapter III

Synthesis of cAAC^{Me}H–GeHMes$_2$ (3.1)

A solution of GeH_2Mes_2 (110 mg, 351 µmol, 1.0 eq) and cAAC^{Me} (100 mg, 351 µmol, 1.0 eq) in toluene (10 mL) was stirred at 85 °C overnight. After removing all volatiles *in vacuo*, *n*-hexane (10 mL) was added to the remaining solid. The resulting suspension was filtered, and the filtrate subsequently concentrated to a volume of 5 mL. Storing the concentrated solution at −30 °C for 2 weeks yielded **3.1** (162 mg, 468 µmol, 77 %) as a colorless solid. Crystals suitable for single crystal X-ray diffraction were obtained by slow evaporation of a concentrated toluene solution of **3.1** at room temperature.

^{1}H NMR (500.1 MHz, C_6D_6, 298 K): δ = 0.60 (d, 3 H, $^3J_{H\text{-}H}$ = 6.9 Hz, *i*Pr-C*H*$_3$), 0.92 (s, 3 H, NC(C*H*$_3$)$_2$), 1.14 (d, 3 H, $^3J_{H\text{-}H}$ = 6.9 Hz, *i*Pr-C*H*$_3$), 1.27 (d, 3 H, $^3J_{H\text{-}H}$ = 6.9 Hz, *i*Pr-C*H*$_3$), 1.28 (s, 3 H, NC(C*H*$_3$)$_2$), 1.43 (d, 3 H, $^3J_{H\text{-}H}$ = 6.9 Hz, *i*Pr-C*H*$_3$), 1.56 (s, 3 H, NCC(C*H*$_3$)$_2$), 1.71 (s, 3 H, NCC(C*H*$_3$)$_2$), 1.72 (d, 1 H, $^2J_{H\text{-}H}$ = 12.4 Hz, C*H*$_2$), 1.74 (br, 3 H, Mes-*o*-C*H*$_3$), 1.97 (s, 3 H, Mes-*p*-C*H*$_3$), 2.07 (s, 3 H, Mes-*p*-C*H*$_3$), 2.23 (d, 1 H, $^2J_{H\text{-}H}$ = 12.4 Hz, C*H*$_2$), 2.36 (br, 3 H, Mes-*o*-C*H*$_3$), 2.46 (br, 3 H, Mes-*o*-C*H*$_3$), 2.83 (br, 3 H, Mes-*o*-C*H*$_3$), 3.39 (sept, 2 H, $^3J_{H\text{-}H}$ = 6.9 Hz, *i*Pr-C*H*), 4.08 (sept, 2 H, $^3J_{H\text{-}H}$ = 6.9 Hz, *i*Pr-C*H*), 4.66 (d, 1 H, $^3J_{H\text{-}H}$ = 6.6 Hz, NC*H*N), 5.95 (d, 1 H, $^3J_{H\text{-}H}$ = 6.6 Hz, Ge*H*), 6.57 (br, 3 H, Mes-C*H* overlapped by Mes-C*H*), 6.87 (br, 1 H, Mes-C*H*), 6.95 (dd, 1 H, $^3J_{H\text{-}H}$ = 7.6 Hz, $^4J_{H\text{-}H}$ = 1.9 Hz, Dipp-*m*-C*H*), 7.09 (dd, 1 H, $^3J_{H\text{-}H}$ = 7.6 Hz, $^4J_{H\text{-}H}$ = 1.9 Hz, Dipp-*m*-C*H*), 7.15 (t, 2 H, $^3J_{H\text{-}H}$ = 7.6 Hz, Dipp-*p*-C*H*).

^{13}C{^{1}H} NMR (125.8 MHz, C_6D_6, 298 K): δ = 20.8 (Mes-*p*-*C*H$_3$), 21.0 (Mes-*p*-*C*H$_3$), 22.6 (*i*Pr-*C*H$_3$), 23.5 (Mes-*o*-*C*H$_3$), 24.2 (Mes-*o*-*C*H$_3$), 24.8 (*i*Pr-*C*H$_3$), 24.9 (Mes-*o*-*C*H$_3$), 25.3 (Mes-*o*-*C*H$_3$), 25.5 (*i*Pr-*C*H$_3$), 27.5 (*i*Pr-*C*H$_3$), 27.9 (*i*Pr-*C*H), 28.07 (NC(*C*H$_3$)$_2$), 28.09 (*i*Pr-*C*H), 29.7 (NCC(*C*H$_3$)$_2$), 32.2 (NCC(*C*H$_3$)$_2$), 33.1 (NC(*C*H$_3$)$_2$), 44.3 (N*C*(CH$_3$)$_2$), 60.5 (*C*H$_2$), 64.2 (NC*C*(CH$_3$)$_2$), 75.0 (N*C*Ge), 124.6 (Dipp-*m*-*C*H), 125.4 (Dipp-*m*-*C*H), 127.1 (Dipp-*p*-*C*H), 128.8 (Mes-*m*-*C*H), 129.5 (Mes-*m*-*C*H), 135.6 (Mes-*i*-*C*), 137.6 (Mes-*p*-*C*), 137.7 (Mes-*p*-*C*), 140.7 (Mes-*i*-*C*), 142.0 (Mes-*o*-*C*), 142.8 (Mes-*o*-*C*), 143.8 (Mes-*p*-*C*), 143.9 (Mes-*o*-*C*), 144.4 (Mes-*o*-*C*), 149.5 (Dipp-*o*-*C*), 152.4 (Dipp-*o*-*C*).

Elemental analysis (%) calcd. for $C_{38}H_{55}GeN$ [598.50 g/mol]: C, 76.26; H, 9.26; N, 2.34; found: C, 76.52; H, 9.26; N, 2.43.

IR ([cm^{-1}]): 3019 (vw), 3001 (w), 2991 (w), 2967 (m), 2938 (m), 2910 (m), 2869 (w), 2056 (Ge-H, m), 1601 (w), 1552 (vw), 1468 (m), 1449 (m), 1436 (s), 1410 (w), 1366 (m), 1313 (m), 1248 (w), 1194 (m), 1175 (w), 1165 (w), 1123 (w), 1096 (vw), 1064 (m), 1048 (w), 1030 (w), 1014 (w), 958 (vw), 926 (w), 907 (vw), 888 (vw), 850 (m), 842 (m), 806 (vs), 769 (vs), 704 (m), 672 (vw), 635 (vw), 600 (w), 583 (m), 566 (w), 550 (m), 539 (m), 496 (vw), 476 (vw), 444 (w), 420 (vw).

Synthesis of Me_2Im^{Me}·$GeMes_2$ (3.2)

A solution of GeH_2Mes_2 (126 mg, 403 µmol, 1.0 eq) in benzene (5 mL) was added to a solution of Me_2Im^{Me} (100 mg, 805 µmol, 2.0 eq) in benzene (5 mL) and the resulting mixture was heated for 10 d at 65 °C with stirring. All volatiles (including the side product $Me_2Im^{Me}H_2$) were removed *in vacuo* to yield **3.2** (148 mg, 340 µmol, 84 %) as a colorless solid. Crystals suitable for single crystal X-ray diffraction were obtained by slow evaporation of a concentrated toluene solution of **3.2** at room temperature.

^{1}H NMR (500.1 MHz, C_6D_6, 298 K): δ = 1.13 (s, 6 H, NCC*H*$_3$), 2.30 (s, 6 H, Mes-*p*-C*H*$_3$), 2.63 (s, 6 H, Mes-*o*-C*H*$_3$), 3.05 (s, 6 H, NC*H*$_3$), 6.97 (4 H, Mes-*m*-C*H*).

^{13}C{^{1}H} NMR (125.8 MHz, C_6D_6, 298 K): δ = 8.0 (C*C*H$_3$), 21.3 (Mes-*p*-*C*H$_3$), 25.6 (Mes-*o*-*C*H$_3$), 32.9 (N*C*H$_3$), 124.8 (N*C*CH$_3$), 128.6 (Mes-*m*-*C*H), 134.8 (Mes-*p*-*C*), 144.5 (Mes-*o*-*C*), 151.3 (Mes-*i*-*C*), 175.4 (N*C*N).

Elemental analysis (%) calcd. for $C_{25}H_{34}GeN_2$ [435.19 g/mol]: C, 69.00; H, 7.88; N, 6.44; found: C, 66.38; H, 7.73; N, 5.89. After several attempts, this is the best result so far, which may be due to the high sensitivity of **3.2**.

Synthesis of cAAC^{Me}H–SnHMe$_2$ (3.3)

A solution of SnH_2Me_2 (288 mg, 1.91 mmol, 1.0 eq) in *n*-hexane (5 mL) was added to a solution of cAAC^{Me} (546 mg, 351 µmol, 1.0 eq) in *n*-hexane (5 mL) at −78 °C and the reaction was allowed to warm over a period of 2 h. Removing all volatiles *in vacuo* yielded **3.3** (162 mg, 468 µmol, 77 %) as a colorless solid. Crystals suitable for single crystal X-ray diffraction were obtained by slow evaporation of a concentrated toluene solution of **3.3** at room temperature.

^{1}H NMR (500.1 MHz, C_6D_6, 298 K): δ = −0.28 (d, 3 H, $^3J_{H\text{-}H}$ = 2.6 Hz, $^2J_{H\text{-}117Sn}$ = 52.2 Hz, $^2J_{H\text{-}119Sn}$ = 54.2 Hz, Sn-CH_3), 0.07 (d, 3 H, $^3J_{H\text{-}H}$ = 2.6 Hz, $^2J_{H\text{-}117Sn}$ = 49.5 Hz, $^2J_{H\text{-}117Sn}$ = 51.5 Hz, Sn-CH_3), 1.07 (s, 3 H, NCC(CH_3)$_2$), 1.11 (s, 3 H, NCC(CH_3)$_2$), 1.21 (d, 3 H, $^3J_{H\text{-}H}$ = 6.7 Hz, *i*Pr-CH_3), 1.22 (d, 3 H, $^3J_{H\text{-}H}$ = 6.7 Hz, *i*Pr-CH_3), 1.27 (d, 6 H, $^3J_{H\text{-}H}$ = 6.7 Hz, *i*Pr-CH_3), 1.33 (s, 3 H, NC(CH_3)$_2$), 1.48 (s, 3 H, NC(CH_3)$_2$), 1.78 (d, 1 H, $^2J_{H\text{-}H}$ = 12.5 Hz, CH_2), 1.82 (d, 1 H, $^2J_{H\text{-}H}$ = 12.5 Hz, CH_2), 3.38 (sept, 1 H, $^3J_{H\text{-}H}$ = 6.9 Hz, *i*Pr-C*H*), 4.00 (sept, 1 H, $^3J_{H\text{-}H}$ = 6.9 Hz, *i*Pr-C*H*), 4.02 (d, 1 H, $^3J_{H\text{-}H}$ = 3.9 Hz, overlapping satellites: $^2J_{H\text{-}117Sn}$ = 30.5 Hz, $^2J_{H\text{-}119Sn}$ = 30.5 Hz, NC*H*N), 5.02 (dsept, 1 H, $^3J_{H\text{-}H}$ = 2.6 Hz, $^3J_{H\text{-}H(NCHN)}$ = 3.9 Hz, $^1J_{H\text{-}117Sn}$ = 1588 Hz, $^1J_{H\text{-}119Sn}$ = 1661 Hz, Sn*H*), 7.06 (t, 1 H, $^3J_{H\text{-}H}$ = 4.7 Hz, Dipp-*p*-C*H*), 7.14 (d, 2 H, $^3J_{H\text{-}H}$ = 4.7 Hz, Dipp-*m*-C*H*).

^{13}C{^{1}H} NMR (125.8 MHz, C_6D_6, 298 K): δ = −10.6 (Sn*C*H$_3$), −10.3 (Sn*C*H$_3$), 24.7 (*i*Pr-*C*H$_3$), 25.7 (*i*Pr-*C*H$_3$), 25.9 (*i*Pr-*C*H$_3$), 26.0 (*i*Pr-*C*H$_3$), 27.1 (*i*Pr-*C*H), 29.2 (NCC(*C*H$_3$)$_2$), 29.4 (NCC(*C*H$_3$)$_2$), 29.6 (*i*Pr-*C*H), 30.6 (NC(*C*H$_3$)$_2$), 31.9 (NC(*C*H$_3$)$_2$), 41.1 (NC*C*(CH$_3$)$_2$), 58.6 (*C*H$_2$), 63.9 (N*C*(CH$_3$)$_2$), 72.0 (N*C*HN), 125.1 (Dipp-*m*-*C*H), 125.6 (Dipp-*p*-*C*H), 127.2 (Dipp-*m*-*C*H), 140.9 (Dipp-*i*-*C*H), 151.4 (Dipp-*o*-*C*), 151.5 (Dipp-*o*-*C*).

^{119}Sn{^{1}H} NMR (186.5 MHz, C_6D_6, 298 K): δ = −139.6 (s).

^{119}Sn NMR (186.5 MHz, C_6D_6, 298 K): δ = −139.6 (dm, $^1J_{H\text{-}119Sn}$ = 1661 Hz).

Elemental analysis (%) calcd. for $C_{22}H_{39}NSn$ [436.27 g/mol]: C, 60.57; H, 9.01; N, 3.21; found: C, 60.94; H, 9.41; N, 3.17.

IR ([cm^{-1}]): 3051 (vw), 2962 (m), 2938 (m), 2935 (m), 2866 (m), 2754 (w), 1805 (Sn−H, s), 1573 (vw), 1458 (m), 1436 (m), 1383 (m), 1364 (m), 1324 (w), 1310 (w), 1288 (w), 1257 (w), 1249 (w), 1210 (m), 1173 (vw), 1156 (m), 1105 (w), 1070 (vw), 1045 (w), 1012 (vw), 953 (vw), 927 (vw), 884 (vw), 810 (m), 772 (s), 707 (w), 685 (w), 654 (m), 607 (vw), 595 (vw), 573 (m), 557 (w), 509 (vs), 468 (w), 437 (w), 407 (vw).

Synthesis of $Me_2Im^{Me}{\cdot}SnMe_2$ (3.4)

A solution of SnH_2Me_2 (282 mg, 1.87 mmol, 1.0 eq) in toluene (5 mL) was added to a solution of Me_2Im^{Me} (465 mg, 3.74 mmol, 2.0 eq) in toluene (5 mL) at −78 °C and the resulting mixture was allowed to warm to room temperature over a period of 2 h. All volatiles (including the side product $Me_2Im^{Me}H_2$) were removed *in vacuo* to yield **3.4** (340 mg, 1.25, mmol, 67 %) as a yellow solid. Crystals suitable for single crystal X-ray diffraction were obtained by slow evaporation of a concentrated toluene solution of **3.4** at room temperature.

^{1}H NMR (500.1 MHz, C_6D_6, 298 K): δ = 0.73 (s, 6 H, overlapping broad satellites, SnC*H*$_3$), 1.31 (s, 6 H, NCC*H*$_3$), 3.19 (s, 6 H, NC*H*$_3$).

^{13}C{^{1}H} NMR (125.8 MHz, C_6D_6, 298 K): δ = 0.5 (Sn*C*H$_3$), 8.3 (C*C*H$_3$), 34.4 (N*C*H$_3$), 124.2 (N*C*CH$_3$), 183.4 (N*C*N).

^{119}Sn{^{1}H} NMR (186.5 MHz, C_6D_6, 298 K): δ = −83.3.

Elemental analysis (%) calcd. for $C_9H_{18}SnN_2$ [272.97 g/mol]: C, 39.60; H, 6.65; N, 10.26; found: C, 36.93; H, 6.40; N, 8.91. After several attempts, this is the best result so far, which may be due to the high air sensitivity of **3.4**.

IR ([cm^{-1}]): 2977 (w), 2947 (m), 2919 (m), 1897 (m), 1855 (w), 1784 (vw), 1688 (w), 1662 (m), 1649 (m), 1598 (w), 1574 (w), 1455 (m), 1431 (s), 1396 (m), 1374 (s), 1366 (s), 1309 (w), 1226 (w), 1194 (w), 1122 (vw), 1095 (vw), 965 (m), 844 (m), 754 (s), 732 (s), 712 (m), 664 (w), 569 (s), 549 (s), 515 (w), 475 (vw), 449 (vs).

Synthesis of $(SnMe_2)_n$ (3.5)

Route A: A solution of SnH_2Me_2 (317 mg, 2.10 mmol, 1.0 eq) in toluene (10 mL) was added to a solution of $Dipp_2Im$ (817 mg, 2.10 mmol, 1.0 eq) in toluene (10 mL) at −78 °C and the resulting mixture was allowed to warm to room temperature overnight. All volatiles were removed *in vacuo* to obtain a yellow solid. The crude product was washed with *n*-hexane (3 x 12 mL) to remove the $Dipp_2ImH_2$, yielding **3.5** (120 mg, 223 µmol, 63 %) as a yellow solid. *Route B*: A solution of SnH_2Me_2 (313 mg, 2.08 mmol, 1.0 eq) in toluene (10 mL) was added to a solution of Me_2Im^{Me} (206 mg, 1.66 mmol, 0.8 eq) in toluene (10 mL) at −78 °C and the resulting mixture was allowed to warm to room temperature overnight. All volatiles (including the side product $Me_2Im^{Me}H_2$ and excess SnH_2Me_2) were removed *in vacuo* to yield **3.5** (224 mg, 1.51 mmol, 91 %) as a yellow solid.

^{1}H NMR (500.1 MHz, C_6D_6, 298 K): δ = 0.53 (m).

^{13}C{^{1}H} NMR (125.8 MHz, C_6D_6, 298 K): δ = −12.3.

^{119}Sn{^{1}H} NMR (186.5 MHz, C_6D_6, 298 K): δ = −246.4 ($(SnMe_2)_{7/8}$), −244.6 ($(SnMe_2)_{7/8}$), −242.7 ($(SnMe_2)_6$).

^{1}H DP/MAS NMR solid-state (400.1 MHz, 295 K, ν_{Mas} = 14.8 kHz): δ = 0.92 (s_{br}).

^{13}C{^{1}H} CP/MAS NMR solid-state (100.6 MHz, 295 K, ν_{Mas} = 13.5 kHz, contact time: 2.00 ms): δ = −10.4 (s).

^{119}Sn{^{1}H} CP/MAS NMR solid-state (149.2 MHz, 295 K, ν_{Mas} = 14.8 kHz, contact time: 5.00 ms): δ = −226.0 (CSA: δ_{11} = −110.35, δ_{22} = −233.27, δ_{33} = −337.02)

NMR spectra after heating the mixture of the cyclomers:

^{1}H NMR (500.1 MHz, C_6D_6, 298 K): δ = 0.53 (m) 0.64 (m).

^{119}Sn{^{1}H} NMR (186.5 MHz, C_6D_6, 298 K): δ = −246.4 ($(SnMe_2)_{7/8}$), −244.6 ($(SnMe_2)_{7/8}$), −242.7 ($(SnMe_2)_6$), −232.4.

Elemental analysis (%) calcd. for n x C_2H_6Sn [n x 148.78 g/mol]: C, 16.15; H, 4.07; found: C, 18.75; H, 4.12. After several attempts, this is the best result, which is attributed to the high sensitivity of **5**.

IR ([cm^{-1}]): 2966 (w), 2905 (m), 2330 (w), 1670 (vw), 1532 (vw), 1457 (w), 1385 (vw), 1367 (vw), 1328 (vw), 1254 (vw), 1204 (vw), 1182 (m), 1056 (m), 1034 (m), 953 (vw), 936 (vw), 768 (s), 702 (vs), 510 (vs), 493 (vs).

7.7 Synthetic Procedures for Chapter IV

Synthesis of $Me_2Im^{Me}{\cdot}PbI_2$ (4.1)

A suspension of Me_2Im^{Me} (200 mg, 1.61 mmol, 1.0 eq) and PbI_2 (742 mg, 1.61 mmol, 1.0 eq) in THF (10 mL) was stirred at room temperature overnight. The resulting precipitate was isolated by filtration, washed with Et_2O (1 x 5 mL) and *n*-hexane (2 x 5 mL) and dried *in vacuo* to yield **4.1** (571 mg, 976 µmol, 61 %) as a colorless solid.

^{1}H NMR (400.5 MHz, $CDCl_3$, 298 K): δ = 2.24 (s, 6 H, CC*H*$_3$), 3.90 (s, 6 H, NC*H*$_3$).

^{13}C{^{1}H} NMR (100.7 MHz, $CDCl_3$, 298 K): δ = 8.6 (C*C*H$_3$), 34.1 (N*C*H$_3$), 126.8, (*C*CH$_3$), 137.5 (N*C*N). The resonance at 137.5 ppm was detected in the HMBC NMR spectrum of compound **4.1**.

Elemental analysis (%) calcd. for $C_7H_{12}I_2N_2Pb$ [585.20 g/mol]: C, 14.37; H, 2.07; N, 4.79; found: C, 13.88; H, 2.18; N, 4.72.

IR ([cm^{-1}]): 3495 (w), 3151 (w), 3076 (w), 3026 (m), 2978 (m), 2945 (w), 2918 (w), 1855 (w), 1637 (m), 1575 (vs), 1473 (w), 1442 (s), 1435 (s), 1414 (m), 1378 (m), 1341 (m), 1258 (w), 1206 (s), 1153 (vw), 1134 (vw), 1104 (w), 1034 (w), 965 (vw), 842 (w), 828 (m), 797 (w), 731 (m), 721 (vw), 615 (s), 565 (vw), 526 (vw), 489 (vw), 444 (vw), 410 (vw).

Synthesis of *i*Pr$_2$Im^{Me}·PbI$_2$ (4.2)

A suspension of *i*Pr$_2$Im^{Me} (80.0 mg, 444 µmol, 1.0 eq) and PbI$_2$ (205 mg, 444 µmol, 1.0 eq) in THF (25 mL) was stirred at room temperature overnight. The resulting precipitate was collected by filtration, washed with Et$_2$O (1 x 5 mL) and *n*-hexane (2 x 5 mL) and dried *in vacuo* to yield **4.2** (90.0 mg, 140 µmol, 32 %) as a yellow solid. Crystals suitable for single crystal X-ray diffraction were obtained by slow evaporation of a THF solution of **4.2** at room temperature.

^{1}H NMR (400.5 MHz, $CDCl_3$, 298 K): δ = 1.71 (d, 12 H, $^3J_{H\text{-}H}$ = 6.8 Hz, *i*Pr-C*H*$_3$), 2.29 (s, 6 H, C*H*$_3$CCC*H*$_3$), 4.58 (sept, 2 H, $^3J_{H\text{-}H}$ = 6.8 Hz, *i*Pr-C*H*).

^{13}C{^{1}H} NMR (100.7 MHz, $CDCl_3$, 298 K): δ = 9.1 (NC*C*H$_3$), 23.1 (*i*Pr-*C*H$_3$), 51.5 (*i*Pr-*C*H), 126.1, (N*C*CH$_3$), 133.6 (N*C*N). The resonance at 133.6 ppm was detected in the HMBC NMR spectrum of the compound.

Elemental analysis (%) calcd. for $C_{11}H_{20}I_2N_2Pb$ [641.30 g/mol]: C, 20.60; H, 3.14; N, 4.37; found: C, 19.59; H, 2.98; N, 3.81.

IR ([cm^{-1}]): 3058 (w), 3036 (vw), 3008 (vw), 2981 (vw), 2964 (vw), 2930 (vw), 2867 (vw), 1955 (vw),1875 (vw), 1819 (vw), 1680 (vw), 1568 (m), 1474 (m), 1427 (s), 1382 (w), 1367 (w), 1327 (w), 1297 (w), 1259 (w), 1185 (vw), 1151 (vw), 1096 (vw), 1060 (m), 1015 (m), 995 (s), 908 (vw), 852 (vw), 801 (vw), 723 (vs), 693 (vs), 616 (vw), 511 (vw), 447 (m), 439 (vs).

Synthesis of Dipp$_2$Im·PbI$_2$ (4.3)

A suspension of Dipp$_2$Im (600 mg, 1.54 mmol, 1.0 eq) and PbI$_2$ (712 mg, 1.54 mmol, 1.0 eq) in THF (10 mL) was stirred at room temperature overnight. The resulting precipitate was isolated by filtration, washed with Et$_2$O (1 x 5 mL) and *n*-hexane (2 x 5 mL) and dried *in vacuo* to yield **4.3** (483 mg, 568 µmol, 37 %) as a colorless solid.

^{1}H NMR (400.5 MHz, C_6D_6, 298 K): δ = 1.00 (d, 12 H, $^3J_{H\text{-}H}$ = 6.9 Hz, *i*Pr-C*H*$_3$), 1.40 (d, 12 H, $^3J_{H\text{-}H}$ = 6.9 Hz, *i*Pr-C*H*$_3$), 2.81 (sept, 2 H, $^3J_{H\text{-}H}$ = 6.8 Hz, *i*Pr-C*H*), 6.52 (s, 2H,

NC*H*), 7.11 (d, 4 H, $^{3}J_{H\text{-}H}$ = 7.8 Hz, Dipp-*m*-C*H*$_3$), 7.25 (d, 2 H, $^{3}J_{H\text{-}H}$ = 7.8 Hz, Dipp-*p*-C*H*$_3$).

^{13}C{^{1}H} NMR (100.7 MHz, C_6D_6, 298 K): δ = 24.0 (*i*Pr-*C*H$_3$), 25.4 (*i*Pr-*C*H$_3$), 29.0 (*i*Pr-*C*H), 124.3 (N*C*H), 124.6 (Dipp-*m*-*C*H$_3$), 130.9 (Dipp-*p*-*C*H$_3$), 135.6 (Dipp-*i*-*C*), 145.9 (Dipp-*o*-*C*H$_3$). (N*C*N) was not observed.

Elemental analysis (%) calcd. for $C_{27}H_{36}I_2N_2Pb$ [849.61 g/mol]: C, 38.17; H, 4.27; N, 3.30; found: C, 38.15; H, 4.44; N, 3.13.

IR ([cm^{-1}]): 3135 (vw), 3067 (vw), 2961 (m), 2923 (m), 2867 (w), 1588 (vw), 1532 (m), 1458 (m), 1403 (w), 1386 (m), 1365 (m), 1326 (m), 1302 (vw), 1276 (vw), 1255 (vw), 1200 (w), 1180 (w), 1099 (w), 1058 (m), 937 (w), 906 (vw), 805 (s), 757 (vs), 681 (w), 633 (vw), 569 (vw), 538 (vw), 517 (vw), 442 (w).

Synthesis of cAAC^{Me}·PbI$_2$ (4.4)

A suspension of cAAC^{Me} (1.00 g, 3.50 mmol, 1.0 eq) and PbI_2 (1.61 g, 3.50 mmol, 1.0 eq) in THF (15 mL) was stirred at room temperature overnight. The resulting precipitate was isolated by filtration, washed with Et_2O (1 x 5 mL) and *n*-hexane (2 x 5 mL) and dried *in vacuo* to yield **4.4** (1.53 g, 3.06 mmol, 87 %) as a colorless solid. Crystals suitable for single crystal X-ray diffraction were obtained by slow evaporation of a dichloromethane solution of **4.4** at room temperature.

^{1}H NMR (500.1 MHz, THF-*d*$_8$, 298 K): δ = 1.33 (d, 6 H, $^{3}J_{H\text{-}H}$ = 6.7 Hz, *i*Pr-C*H*$_3$), 1.34 (d, 6 H, $^{3}J_{H\text{-}H}$ = 6.7 Hz, *i*Pr-C*H*$_3$), 1.48 (s, 6 H, NCC(C*H*$_3$)$_2$), 1.88 (s, 6 H, NC(C*H*$_3$)$_2$), 2.19 (s, 2 H, C*H*$_2$), 2.93 (sept, 2 H, $^{3}J_{H\text{-}H}$ = 6.7 Hz, *i*Pr-C*H*), 7.441 (d, 2 H, $^{3}J_{H\text{-}H}$ = 8.1 Hz, Dipp-*m*-C*H*), 7.442 (d, 2 H, $^{3}J_{H\text{-}H}$ = 7.4 Hz, Dipp-*m*-C*H*), 7.53 (dd, 1 H, $^{3}J_{H\text{-}H}$ = 7.4 Hz, $^{3}J_{H\text{-}H}$ = 8.1 Hz, Dipp-*p*-C*H*).

^{13}C{^{1}H} NMR (125.8 MHz, THF-*d*$_8$, 298 K): δ = 24.4 (*i*Pr-*C*H$_3$), 28.5 (*i*Pr-*C*H$_3$), 28.8, (NCC(*C*H$_3$)$_2$), 29.2 (*i*Pr-*C*H), 32.0 (NC(*C*H$_3$)$_2$), 51.5 (*C*H$_2$), 63.8 (N*C*(CH$_3$)$_2$) 84.9 (NC*C*(CH$_3$)$_2$), 126.9 (Dipp-*m*-*C*H), 131.5 (Dipp-*p*-*C*H), 133.4 (Dipp-*i*-*C*), 146.6 (Dipp-*o*-*C*H). (N*C*N) was not observed.

Elemental analysis (%) calcd. for $C_{20}H_{31}I_2NPb$ [746.48 g/mol]: C, 32.18; H, 4.19; N, 1.88; found: C, 31.96; H, 4.02; N, 1.86.

IR ([cm^{-1}]): 1962 (m), 2925 (w), 2865 (w), 1632 (m), 1584 (w), 1449 (m), 1386 (w), 1365 (m), 1336 (m), 1261 (m), 1237 (w), 1200 (w), 1183 (w), 1164 (vw), 1125 (m), 1102 (m), 1052 (m), 1042 (m), 1025 (m), 982 (vw), 954 (vw), 929 (m), 912 (w), 896 (w), 808 (vs), 764 (m), 716 (vw), 702 (vw), 672 (vw), 650 (w), 605 (w), 570 (vw), 556 (w), 511 (w), 481 (w), 460 (vw), 419 (vw).

Synthesis of $Me_2Im^{Me}{\cdot}PbCl_2Ph_2$ (4.5)

A suspension of $PbCl_2Ph_2$ (348 mg, 805 µmol, 1.0 eq) and Me_2Im^{Me} (100 mg, 805 µmol, 1.0 eq) in THF (10 mL) was stirred at room temperature overnight. All volatiles were removed *in vacuo* to yield **4.5** (341 mg, 613 µmol, 76 %) as an off-white solid. Crystals suitable for single crystal X-ray diffraction were obtained by slow evaporation of a toluene solution of **4.5** at room temperature.

^{1}H NMR (500.1 MHz, C_6D_6, 298 K): δ = 0.90 (s, 6 H, CC*H*$_3$), 3.11 (s, 6 H, NC*H*$_3$), 7.12 (tm, 2 H, $^3J_{H\text{-}H}$ = 7.4 Hz, Ph-*p*-C*H*), 7.36 (tm, 4 H, $^3J_{H\text{-}H}$ = 8.0 Hz, $^4J_{H\text{-}207Pb}$ = 65.8 Hz, Ph-*m*-C*H*), 9.26 (dm, 4 H, $^3J_{H\text{-}H}$ = 8.0 Hz, $^3J_{H\text{-}207Pb}$ = 174.2 Hz, Ph-*o*-C*H*).

^{13}C{^{1}H} NMR (125.8 MHz, C_6D_6, 298 K): δ = 7.7 (C*C*H$_3$), 34.9 (N*C*H$_3$), 125.7 (N*C*CN), 130.1 ($^4J_{13C\text{-}207Pb}$ = 35.1 Hz, Ph-*p*-*C*H), 130.4 ($^3J_{13C\text{-}207Pb}$ = 166.2 Hz, Ph-*m*-*C*H), 137.0 ($^2J_{13C\text{-}207Pb}$ = 123.1 Hz, Ph-*o*-*C*H), 157.4 ($^1J_{13C\text{-}207Pb}$ = 1147.1 Hz, Ph-*i*-*C*), 175.9 (N*C*Pb).

^{207}Pb NMR (104.8 MHz, C_6D_6, 298 K): δ = –394.0.

Elemental analysis (%) calcd. for $C_{19}H_{22}Cl_2N_2Pb$ + 0.5 (C_6H_6) [595.56 g/mol]: C, 44.37; H, 4.23; N, 4.70; found: C, 44.51; H, 4.25; N, 4.56.

IR ([cm^{-1}]): 3054 (w), 3042 (w), 1984 (vw), 2954 (vw), 2922 (vw), 1638 (w), 1567 (m), 1472 (m), 1433 (m), 1396 (w), 1372 (vw), 1328 (vw), 1307 (vw), 1260 (vw), 1230 (vw), 1205 (vw), 1177 (w), 1155 (vw), 1105 (vw), 1053 (w), 1035 (w), 1014 (m), 993 (m), 843 (m), 739 (vs), 683 (vs), 649 (w), 615 (w), 568 (vw), 539 (vw), 507 (w), 444 (s).

Synthesis of *i*Pr$_2$Im^{Me}·PbCl$_2$Ph$_2$ (4.6)

A suspension of $PbCl_2Ph_2$ (120 mg, 277 µmol, 1.0 eq) and *i*Pr$_2$Im^{Me} (50.0 mg, 277 µmol, 1.0 eq) in THF (10 mL) was stirred at room temperature overnight. All volatiles were removed *in vacuo* to yield **4.6** (130 mg, 212 µmol, 77 %) as a colorless solid. Crystals suitable for single crystal X-ray diffraction were obtained by slow evaporation of a benzene solution of **4.6** at room temperature.

^{1}H NMR (400.5 MHz, C_6D_6, 298 K): δ = 1.05 (d, 12 H, $^3J_{H\text{-}H}$ = 7.0 Hz, *i*Pr-C*H*$_3$), 1.35 (s, 6 H, CC*H*$_3$), 5.27 (sept, 2 H, $^3J_{H\text{-}H}$ = 7.0 Hz, *i*Pr-C*H*), 7.08 (tm, 2 H, $^3J_{H\text{-}H}$ = 7.3 Hz, $^5J_{H\text{-}207Pb}$ = 30.7 Hz, Ph-*p*-C*H*), 7.32 (tm, 4 H, $^3J_{H\text{-}H}$ = 8.0 Hz, $^4J_{H\text{-}207Pb}$ = 65.3 Hz, Ph-*m*-C*H*), 9.19 (m, 4 H, $^3J_{H\text{-}H}$ = 8.0 Hz, $^3J_{H\text{-}207Pb}$ = 172.2 Hz, Ph-*o*-C*H*).

^{13}C{^{1}H} NMR (100.7 MHz, C_6D_6, 298 K): δ = 9.8 (C*C*H$_3$), 21.2 (*i*Pr-*C*H$_3$), 54.7 (*i*Pr-*C*H), 126.2 (N*CC*N), 129.9 ($^4J_{13C\text{-}207Pb}$ = 34.2 Hz, Ph-*p*-*C*H), 130.3 ($^3J_{13C\text{-}207Pb}$ = 164.2 Hz, Ph-*o*-*C*H), 136.5 ($^2J_{13C\text{-}207Pb}$ = 122.4 Hz, Ph-*m*-*C*H), 158.3 ($^1J_{13C\text{-}207Pb}$ = 1122.3 Hz, Ph-*i*-*C*), 179.1 (N*C*Pb).

^{207}Pb NMR (83.8 MHz, C_6D_6, 298 K): δ = –397.3.

Elemental analysis (%) calcd. for $C_{23}H_{30}Cl_2N_2Pb$ [612.61 g/mol]: C, 45.09; H, 4.94; N, 4.57; found: C, 45.21; H, 5.23; N, 4.64.

IR ([cm^{-1}]): 3053 (w), 2974 (w), 2935 (vw), 2874 (vw), 1626 (vw), 1567 (m), 1473 (m), 1434 (s), 1406 (m), 1391 (m), 1372 (m), 1336 (w), 1308 (vw), 1293 (vw), 1219 (m), 1191 (w), 1177 (w), 1137 (w), 1110 (w), 1076 (vw), 1054 (vw), 1015 (w), 993 (m), 928 (vw), 906 (vw), 886 (vw), 857 (vw), 763 (vw), 744 (vs), 735 (vs), 691 (m), 647 (vw), 541 (ww), 487 (vw), 448 (vs), 421 (vw).

Synthesis of Dipp$_2$Im·PbCl$_2$Ph$_2$ (4.7)

A suspension of $PbCl_2Ph_2$ (111 mg, 257 µmol, 1.0 eq) and *i*Pr$_2$Im^{Me} (100 mg, 257 µmol, 1.0 eq) in THF (10 mL) was stirred at room temperature overnight. All volatiles were removed *in vacuo* to yield **4.7** (193 mg, 235 µmol, 91 %) as an off-white solid. Crystals suitable for single crystal X-ray diffraction were obtained by storing a benzene solution of **4.7** at 6 °C.

^{1}H NMR (400.5 MHz, C_6D_6, 298 K): δ = 0.95 (d, 12 H, $^3J_{H\text{-}H}$ = 6.9 Hz, *i*Pr-C*H*$_3$), 1.49 (d, 12 H, $^3J_{H\text{-}H}$ = 6.9 Hz, *i*Pr-C*H*$_3$), 3.47 (sept, 2 H, $^3J_{H\text{-}H}$ = 6.9 Hz, *i*Pr-C*H*), 6.53 (s, 2 H, NC*H*), 6.88 (tm, 2 H, $^3J_{H\text{-}H}$ = 6.9 Hz, Ph-*p*-C*H*), 6.90 (m, 4 H, Dipp-*m*-C*H*), 6.99 (m, 6 H, Dipp-*p*-C*H* overlapped by Ph-*m*-C*H*), 8.26 (dm, 4 H, $^3J_{H\text{-}H}$ = 6.9 Hz, $^3J_{H\text{-}^{207}Pb}$ = 184.1 Hz, Ph-*o*-C*H*).

^{13}C{^{1}H} NMR (100.7 MHz, C_6D_6, 298 K): δ = 22.9 (*i*Pr-*C*H$_3$), 26.8 (*i*Pr-*C*H$_3$), 29.0 (*i*Pr-*C*H), 124.4 (N*CC*N), 124.9 (Dipp-*m*-*C*H), 128.8 (Ph-*p*-*C*H), 129.1 (Ph-*m*-*C*H), 131.7 (Dipp-*p*-*C*H), 133.9 (Dipp-*i*-*C*), 136.3 ($^2J_{^{13}C\text{-}^{207}Pb}$ = 127.3 Hz, Ph-*o*-*C*H), 146.9 (Dipp-*o*-*C*), 158.9 (Ph-*i*-*C*), 180.2 (N*C*Pb).

^{207}Pb NMR (104.8 MHz, C_6D_6, 298 K): δ = –397.2.

Elemental analysis (%) calcd. for $C_{39}H_{46}Cl_2N_2Pb$ [820.91 g/mol]: C, 57.06; H, 5.65; N, 3.41; found: C, 57.10; H, 5.67; N, 3.16.

IR ([cm^{-1}]): 3173 (vw), 3144 (vw), 3051 (w), 2964 (m), 2931 (w), 2867 (w), 1590 (vw), 1568 (w), 1537 (vw), 1473 (m), 1463 (m), 1433 (m), 1414 (w), 1385 (w), 1363 (w), 1329 (w), 1298 (vw), 1271 (vw), 1255 (vw), 1207 (w), 1184 (w), 1111 (w), 1061 (w), 1013 (w), 993 (m), 947 (vw), 932 (vw), 800 (m), 755 (s), 728 (vs), 687 (s), 632 (vw), 542 (vw), 520 (vw), 504 (vw), 443 (s).

Synthesis of cAAC^{Me}·$PbCl_2Ph_2$ (4.8)

A suspension of $PbCl_2Ph_2$ (151 mg, 350 µmol, 1.0 eq) and cAAC^{Me} (100 mg, 350 µmol, 1.0 eq) in benzene (15 mL) was stirred at room temperature for three hours. The resulting precipitate was removed by filtration. All volatiles of the filtrate were removed *in vacuo* to yield **4.8** (231 mg, 322 µmol, 92 %) as a pale-yellow solid. Crystals suitable for single crystal X-ray diffraction were obtained by storing a benzene solution of **4.8** at 6 °C.

^{1}H NMR (500.1 MHz, toluene-d_8, 233 K): δ = 0.93 (d, 6 H, $^3J_{H\text{-}H}$ = 6.5 Hz, *i*Pr-CH_3), 1.08 (s, 6 H, NC(CH_3)$_2$), 1.23 (s, 2 H, CH_2), 1.53 (d, 6 H, $^3J_{H\text{-}H}$ = 6.5 Hz, *i*Pr-CH_3), 1.60 (s, 6 H, NCC(CH_3)$_2$), 3.12 (sept, 2 H, $^3J_{H\text{-}H}$ = 6.5 Hz, *i*Pr-CH), 6.76 (d, 2 H, $^3J_{H\text{-}H}$ = 7.8 Hz, Dipp-*m*-CH), 6.88 (t, 1 H, $^3J_{H\text{-}H}$ = 7.3 Hz, Ph-*p*-CH), 6.89 (t, 1 H, $^3J_{H\text{-}H}$ = 7.8 Hz, Dipp-*p*-CH), 6.94 (t, 2 H, $^3J_{H\text{-}H}$ = 7.9 Hz, Ph-*m*-CH), 7.06 (t, 1 H, $^3J_{H\text{-}H}$ = 7.3 Hz, Ph-*p*-CH), 7.32 (t, 2 H, $^3J_{H\text{-}H}$ = 7.9 Hz, $^4J_{H\text{-}207Pb}$ = 61.4 Hz, Ph-*m*-CH), 7.64 (d, 2 H, $^3J_{H\text{-}H}$ = 7.9 Hz, $^3J_{H\text{-}207Pb}$ = 168.7 Hz, Ph-*o*-CH), 9.41 (d, 2 H, $^3J_{H\text{-}H}$ = 7.9 Hz, $^3J_{H\text{-}207Pb}$ = 168.7 Hz, Ph-*o*-CH).

^{13}C{^{1}H} NMR (125.8 MHz, toluene-d_8, 233 K): δ = 25.6 (*i*Pr-*C*H$_3$), 27.9 (*i*Pr-*C*H$_3$), 28.0 (NCC(*C*H$_3$)$_2$), 29.0 (*i*Pr-*C*H), 30.6 (NC(*C*H$_3$)$_2$), 50.7 (*C*H$_2$), 57.5 (NC*C*(CH$_3$)$_2$), 84.6 N*C*(CH$_3$)$_2$), 126.0 (Dipp-*m*-*C*H), 128.8 (Ph-*p*-*C*H), 129.0 (Ph-*m*-*C*H), 129.7 (Ph-*p*-*C*H), 130.1 (Ph-*m*-*C*H), 130.7 (Dipp-*p*-*C*H), 134.5 (Dipp-*i*-*C*), 135.9 (Ph-*o*-*C*H), 137.0 (Ph-*o*-*C*H), 146.3 (Dipp-*o*-*C*), 159.8 (Ph-*i*-*C*), 160.2 (Ph-*i*-*C*), 241.2 (N*C*Pb).

^{207}Pb NMR (104.6 MHz, toluene-d_8, 233 K): δ = –401.7.

Elemental analysis (%) calcd. for $C_{32}H_{41}Cl_2NPb$ [717.79 g/mol]: C, 53.55; H, 5.76; N, 1.95; found: C, 53.04; H, 5.84; N, 1.89.

IR ([cm^{-1}]): 3055 (vw), 2956 (s), 2927 (s), 2865 (m), 1679 (vw), 1642 (vw), 1566 (w), 1456 (m), 1435 (s), 1382 (m), 1366 (m), 1335 (m), 1323 (m), 1260 (m), 1238 (w), 1208 (m), 1177 (w), 1144 (m), 1108 (w), 1050 (m), 1014 (m), 992 (w), 974 (w), 957 (m), 940 (vs), 898 (m), 887 (w), 841 (vw), 813 (m), 775 (m), 724 (vs), 681 (m), 652 (vw), 623 (vw), 608 (vw), 595 (vw), 573 (vw), 544 (m), 505 (w), 484 (w), 444 (vs).

Synthesis of Me_2Im^{Me}·$PbPh_2$ (4.9)

A suspension of $PbCl_2Ph_2$ (174 mg, 403 µmol, 1.0 eq), Me_2Im^{Me} (50.0 mg, 403 µmol, 1.0 eq) and KC_8 (217 mg, 1.61 mmol, 4.0 eq) in benzene (15 mL) was stirred at room temperature overnight. The reaction mixture was filtrated over a pad of celite. All volatiles of the filtrate were removed *in vacuo* to yield **4.9** (123 mg, 253 µmol, 63 %) as a yellow solid. Crystals suitable for single crystal X-ray diffraction were obtained by slow evaporation of a saturated toluene solution of **4.9** at room temperature.

^{1}H NMR (500.1 MHz, C_6D_6, 298 K): δ = 1.20 (s, 6 H, CC*H*$_3$), 3.01 (s, 6 H, NC*H*$_3$), 7.24 (m, 2 H, Ph-*p*-C*H*), 7.50 (m, 4 H, Ph-*m*-C*H*), 8.35 (m, 4 H, $^3J_{H\text{-}207Pb}$ = 24.0 Hz, Ph-*o*-C*H*).

^{13}C{^{1}H} NMR (125.8 MHz, C_6D_6, 298 K): δ = 8.3 (C*C*H$_3$), 35.7 (N*C*H$_3$), 124.9 (N*C*CN), 125.6 (Ph-*p*-*C*H), 129.8 ($^3J_{13C\text{-}207Pb}$ = 29.6 Hz, Ph-*m*-*C*H), 139.9 ($^2J_{13C\text{-}207Pb}$ = 57.8 Hz, Ph-*o*-*C*H), 190.5 (N*C*N), 195.9 ($^1J_{13C\text{-}207Pb}$ = 1059.2 Hz, Ph-*i*-*C*).

^{207}Pb NMR (104.8 MHz, C_6D_6, 298 K): δ = 1402.8.

Elemental analysis (%) calcd. for $C_{19}H_{22}N_2Pb$ [485.60 g/mol]: C, 47.00; H, 4.57; N, 5.77; found: C, 47.82; H, 4.73; N, 5.87.

IR ([cm^{-1}]): 3118 (vw), 3045 (vw), 3029 (w), 2995 (w), 2979 (w), 2945 (m), 2919 (m) (m), 2852 (w), 2569 (vw), 1943 (vw), 1865 (vw), 1815 (vw), 1754 (vw), 1658 (w), 1562 (w), 1466 (w), 1429 (m), 1421 (s), 1396 (w), 1379 (m), 1364 (m), 1323 (w), 1292 (w), 1249 (w), 1224 (vw), 1184 (w), 1149 (vw), 1125 (vw), 1088 (vw), 1052 (m), 1031 (vw), 1009 (w), 993 (m), 900 (vw), 841 (m), 719 (vs), 702 (vs), 634 (m), 568 (w), 547 (w), 501 (vw), 443 (m), 435 (m).

Synthesis of *i*Pr_2Im^{Me}·$PbPh_2$ (4.10)

A suspension of $PbCl_2Ph_2$ (240 mg, 555 µmol, 1.0 eq), *i*Pr_2Im^{Me} (100.0 mg, 555 µmol, 1.0 eq) and KC_8 (225 mg, 1.66 mmol, 1.0 eq) in benzene (10 mL) was stirred at room temperature overnight. The reaction mixture was filtrated over a pad of celite. All volatiles of the filtrate were removed *in vacuo*. The resulting pale yellow oil was

suspended in *n*-hexane. All volatiles were removed *in vacuo* to yield **4.10** (35.0 mg, 64.6 µmol, 12 %) as a yellow solid. Crystals suitable for single crystal X-ray diffraction were obtained by slow evaporation of a benzene solution of **4.10** at room temperature.

^{1}H NMR (400.5 MHz, C_6D_6, 298 K): δ = 0.93 (d, 12 H, $^{3}J_{H\text{-}H}$ = 6.7 Hz, *i*Pr-C*H*$_3$), 1.49 (s, 6 H, CC*H*$_3$), 5.11 (sept, 2 H, $^{3}J_{H\text{-}H}$ = 6.7 Hz, *i*Pr-C*H*), 7.24 (m, 2 H, Ph-*p*-C*H*), 7.52 (m, 4 H, Ph-*m*-C*H*), 8.34 (m, 4 H, $^{3}J_{H\text{-}207Pb}$ = 26.6 Hz, Ph-*o*-C*H*).

^{13}C{^{1}H} NMR (100.7 MHz, C_6D_6, 298 K): δ = 9.8 (C*C*H$_3$), 21.9 (*i*Pr-*C*H$_3$), 54.2 (*i*Pr-*C*H), 125.3 (N*CC*N), 125.7 (Ph-*p*-*C*H), 129.7 ($^{3}J_{13C\text{-}207Pb}$ = 30.6 Hz, Ph-*m*-*C*H), 139.7 ($^{2}J_{13C\text{-}207Pb}$ = 56.5 Hz, Ph-*o*-*C*H), 198.3 (Ph-*i*-*C*). (N*C*N) was not observed.

Elemental analysis (%) calcd. for $C_{23}H_{30}N_2Pb$ [541.71 g/mol]: C, 51.00; H, 5.58; N, 5.17; found: C, 50.41; H, 5.58; N, 4.99.

IR ([cm^{-1}]): 3119 (vw), 3040 (m), 3018 (w), 2980 (m), 2937 (m), 2875 (w), 1938 (vw), 1874 (vw), 1809 (vw), 1629 (vw), 1562 (w), 1461 (m), 1441 (m), 1429 (m), 1419 (m), 1390 (w), 1363 (s), 1319 (w), 1294 (w), 1280 (w), 1249 (w), 1214 (m), 1167 (vw), 1131 (m), 1106 (m), 1066 (vw), 1050 (m), 1018 (w), 1010 (w), 994 (m), 904 (w), 885 (vw), 777 (vw), 747 (w), 718 (vs), 700 (vs), 632 (w), 541 (w), 493 (vw), 442 (s), 408 (vw).

7.8 Synthetic Procedures for Chapter V

General procedure for the adducts NHC·SbCl$_3$ (5.4a-5.6d)

A solution of $SbCl_2R$ (R = Cl, Ph, Mes) in 5 mL Et_2O (**5.4a**-**e**, **5.6a**-**d**) or 5 mL toluene (**5.5a**-**e**) was added at –78 °C *via* a cannula to a suspension of the corresponding NHC (1.0 eq) in 5 mL of the same solvent. The reaction mixture was allowed to warm to room temperature overnight. The resulting colorless precipitate was isolated by filtration, washed with *n*-hexane (2 x 5 mL) and dried *in vacuo*.

Synthesis of Me_2Im^{Me}·$SbCl_3$ (5.4a)

$SbCl_3$ (100 mg, 371 µmol) was reacted with Me_2Im^{Me} (46.0 mg, 371 µmol). Recrystallization *via* diffusion of *n*-hexane into a solution of the crude product in THF yielded **5.4a** (107 mg, 272 µmol, 73 %) as colorless crystals. Crystals of **5.4a** suitable for single crystal X-ray diffraction were grown by layering a THF solution of **5.4a** with *n*-hexane and storing at room temperature.

^{1}H NMR (400.5 MHz, THF-d_8, 298 K): δ = 2.24 (s, 6 H, CCH_3), 4.03 (s, 6 H, NCH_3).

^{13}C{^{1}H} NMR (100.7 MHz, THF-d_8, 298 K): δ = 8.5 (NCCH$_3$), 35.3 (NCH$_3$), 128.7 (NCCN), 162.5 (NCN).

Elemental analysis (%) calcd. for $C_7H_{12}Cl_3N_2Sb$ [352.30 g/mol]: C, 23.87; H, 3.43; N, 7.95 found: C, 23.94; H, 3.39; N, 7.68.

IR ([cm^{-1}]): 3146 (vw), 3067 (w), 2984 (vw), 2957 (w), 2925 (w), 2863 (vw), 1682 (vw), 1642 (m), 1573 (m), 1472 (s), 1442 (vs), 1391 (s), 1368 (s), 1261 (m), 1229 (m), 1205 (m), 1127 (m), 1095 (m), 1056 (m), 1032 (m), 867 (vw), 841 (vs), 801 (m), 745 (vs), 701 (m), 621 (w), 591 (vw), 567 (m), 505 (vw), 464 (vw).

Synthesis of *i*Pr_2Im^{Me}·$SbCl_3$ (5.4b)

$SbCl_3$ (127 mg, 555 µmol) was reacted with *i*Pr_2Im^{Me} (100 mg, 555 µmol) to yield **5.4b** (145 mg, 354 µmol, 64 %) as a colorless solid. Crystals of **5.4b** suitable for single crystal X-ray diffraction were grown by storing a saturated benzene solution of **5.4b** at 6 °C.

^{1}H NMR (500.1 MHz, C_6D_6, 298 K): δ = 1.13 (d, 12 H, $^3J_{H\text{-}H}$ = 6.9 Hz, *i*Pr-CH_3), 1.32 (s, 6 H, CH_3CCCH_3), 5.45 (sept, 2 H, $^3J_{H\text{-}H}$ = 6.9 Hz, *i*Pr-CH).

^{13}C{^{1}H} NMR (125.8 MHz, C_6D_6, 298 K): δ = 9.8 (NCCH$_3$), 21.3 (*i*Pr-CH$_3$), 53.5 (*i*Pr-CH), 127.1 (NCCN), 164.3 (NCN).

Elemental analysis (%) calcd. for $C_{11}H_{20}Cl_3N_2Sb$ [408.41 g/mol]: C, 32.35; H, 4.94; N, 6.86; found: C, 33.19; H, 5.23; N, 7.05.

IR ([cm^{-1}]): 3010 (vw), 2979 (w), 2944 (w), 2926 (w), 2876 (w), 1623 (w), 1595 (w), 1552 (w), 1448 (s), 1438 (s), 1381 (vs), 1372 (vs), 1344 (m), 1315 (w), 1291 (w), 1228 (vw), 1204 (m), 1167 (w), 1138 (w), 1110 (m), 1073 (vw), 1027 (m), 1004 (vw), 974 (vw), 952 (vw), 936 (vw), 898 (w), 886 (vw), 858 (s), 760 (w), 747 (m), 706 (w), 688 (vw), 648 (vw), 580 (w), 548 (m), 540 (w), 497 (vw), 431 (w), 412 (vw).

Synthesis of Dipp$_2$Im·SbCl$_3$ (5.4c)

$SbCl_3$ (766 mg, 1.97 mmol) was reacted with $Dipp_2Im$ (450 mg, 1.97 mmol) to give **5.4c** (930 mg, 1.51 mmol, 76 %) as a colorless solid. Crystals of **5.4c** suitable for single crystal X-ray diffraction were grown by storing a saturated benzene solution of **5.4c** at 6 °C.

^{1}H NMR (500.1 MHz, C_6D_6, 298 K): δ = 0.93 (d, 12 H, $^3J_{H\text{-}H}$ = 6.7 Hz, *i*Pr-C*H*$_3$), 1.55 (d, 12 H, $^3J_{H\text{-}H}$ = 6.7 Hz, *i*Pr-C*H*$_3$), 3.25 (sept, 4 H, $^3J_{H\text{-}H}$ = 6.7 Hz, *i*Pr-C*H*), 6.47 (s, 2 H, C*H*C*H*), 7.11 (d, 4 H, Dipp-*m*-C*H*), 7.19 (d, 1 H, $^3J_{H\text{-}H}$ = 7.1 Hz, Dipp-*p*-C*H*), 7.21 (d, 2 H, $^3J_{H\text{-}H}$ = 7.1 Hz, Dipp-*p*-C*H*).

^{13}C{^{1}H} NMR (125.8 MHz, C_6D_6, 298 K): δ = 23.1 (*i*Pr-*C*H$_3$), 26.7 (*i*Pr-*C*H$_3$), 29.3 (*i*Pr-C*H*), 124.7 (Dipp-*m*-*C*H), 125.4 (*C*H*C*H) 132.1 (Dipp-*i*-*C*), 132.2 (Dipp-*p*-*C*H), 147.0 (Dipp-*o*-*C*), 165.7 (N*C*N).

Elemental analysis (%) calcd. for $C_{27}H_{36}Cl_3N_2Sb$ [616.71 g/mol]: C, 52.59; H, 5.88; N, 4.54; found: C, 52.69; H, 5.89; N, 4.38.

IR ([cm^{-1}]): 3159 (w), 3124 (w), 3083 (w), 3032 (vw), 2964 (s), 2929 (m), 2869 (m), 1632 (vw), 2586 (vw), 1555 (w), 1538 (w), 1462 (s), 1439 (s), 1418 (m), 1384 (m), 1362 (m), 1328 (m), 1309 (w), 1268 (w), 1254 (w), 1208 (m), 1182 (m), 1146 (w), 1116 (m), 1100 (w), 1060 (m), 1043 (w), 948 (w), 933 (w), 903 (vw), 884 (vw), 867 (vw), 802 (vs), 769 (s), 756 (vs), 698 (m), 681 (w), 630 (w), 581 (vw), 544 (vw), 518 (vw), 459 (w), 436 (w), 416 (vw).

Synthesis of $Mes_2Im{\cdot}SbCl_3$ (5.4d)

$SbCl_3$ (100 mg, 438 µmol) was reacted with Mes_2Im (133 mg, 438 µmol) to yield **5.4d** (184.6 mg, 345 µmol, 79 %) as a colorless solid. Crystals of **5.4d** suitable for single crystal X-ray diffraction were grown by storing a saturated toluene solution of **5.4d** at −30 °C.

^{1}H NMR (400.5 MHz, C_6D_6, 298 K): δ = 2.04 (s, 6 H, Mes-*p*-C*H*$_3$), 2.32 (s, 12 H, Mes-*o*-C*H*$_3$), 5.95 (s, 2 H, C*H*C*H*), 6.68 (s, 4 H, Mes-C*H*).

^{13}C{^{1}H} NMR (100.7 MHz, C_6D_6, 298 K): δ = 19.1 (Mes-*o*-*C*H$_3$), 21.1 (Mes-*p*-*C*H$_3$), 124.2 (*C*H*C*H), 129.9 (Mes-*m*-*C*H), 131.8 (Mes-*i*-*C*), 136.3 (Mes-*o*-*C*), 141.2 (Mes-*p*-*C*), 164.1 (N*C*N).

Elemental analysis (%) calcd. for $C_{21}H_{24}Cl_3N_2Sb$ [532.55 g/mol]: C, 47.36; H, 4.54; N, 5.26; found: C, 47.51; H, 4.96; N, 5.45.

IR ([cm^{-1}]): 3170 (vw), 3147 (w), 3108 (w), 3079 (w), 3022 (m), 2971 (m), 2950 (m), 2916 (m), 1860 (m), 2786 (w), 2761 (w), 1607 (m), 1538 (s), 1481 (s), 1456 (m), 1446 (m), 1411 (w), 1380 (m), 1335 (vw), 1318 (vw), 1296 (vw), 1254 (vw), 1229 (vs), 1163 (w), 1117 (w), 1097 (w), 1076 (w), 1059 (m), 1036 (m), 966 (vw), 932 (m), 902 (vw), 854 (vs), 812 (vw), 756 (s), 736 (w), 726 (m), 698 (s), 678 (s), 589 (w), 570 (s), 551 (w), 502 (w), 453 (vw), 423 (vw).

Synthesis of $cAAC^{Me}{\cdot}SbCl_3$ (5.4e)

$SbCl_3$ (200 mg, 1.61 mmol) was reacted with $cAAC^{Me}$ (367 mg, 1.61 mmol) to yield **5.4e** (386 mg, 1.10 mmol, 68 %) as a colorless solid. Crystals of **5.4e** suitable for single crystal X-ray diffraction were grown by storing a saturated benzene solution of **5.4e** at room temperature.

^{1}H NMR (400.5 MHz, C_6D_6, 298 K): δ = 1.06 (s, 6 H, NC(C*H*$_3$)$_2$), 1.14 (d, 6 H, $^3J_{H\text{-}H}$ = 6.8 Hz, *i*Pr-C*H*$_3$), 1.32 (d, 6 H, $^3J_{H\text{-}H}$ = 6.8 Hz, *i*Pr-C*H*$_3$), 1.50 (s, 2 H, C*H*$_2$), 1.60 (s, 6 H, NCC(C*H*$_3$)$_2$), 3.11 (sept, 2 H, $^3J_{H\text{-}H}$ = 6.5 Hz, *i*Pr-C*H*), 7.08 (m, 2 H, Dipp-*m*-C*H*), 7.16 (m, 1 H, Dipp-*p*-C*H*).

$^{13}C\{^1H\}$ NMR (100.7 MHz, C_6D_6, 298 K): δ = 23.7 (*i*Pr-*C*H_3), 26.3 (*i*Pr-*C*H_3), 28.6 (NC(*C*H_3)$_2$), 29.2 (NCC(*C*H_3)$_2$), 29.3 (*i*Pr-*C*H), 51.1 (*C*H_2), 58.5 (NC*C*(C*H*$_3$)$_2$), 82.7 N*C*(C*H*$_3$)$_2$), 124.8 (Dipp-*m*-*C*H), 129.3 (Dipp-*p*-*C*H), 135.9 (Dipp-*i*-*C*), 146.3 (Dipp-*o*-*C*), 231.0 (N*C*Sb). The resonance at 231.0 ppm could not be observed in the $^{13}C\{^1H\}$ NMR Spektrum but *via* $^{13}C\{^1H\}$ HMBC NMR.

Elemental analysis (%) calcd. for $C_{20}H_{31}Cl_3NSb$ [513.59 g/mol]: C, 46.77; H, 6.08; N, 2.73; found: C, 47.47; H, 6.06; N, 2.31.

IR ([cm^{-1}]): 3073 (vw), 2971 (m), 2931 (m), 2871 (w), 1639 (vw), 1587 (vw), 1522 (m), 1457 (s), 1388 (m), 1372 (m), 1347 (m), 1324 (w), 1317 (w), 1271 (w), 1206 (w), 1183 (m), 1160 (w), 1127 (m), 1105 (m), 1054 (m), 1016 (vw), 993 (w), 971 (w), 953 (w), 932 (m), 876 (w), 837 (vw), 813 (vs), 773 (s), 697 (m), 675 (w), 652 (vw), 630 (vw), 609 (m), 560 (m), 492 (m), 432 (vw), 408 (vw).

Synthesis of Me_2Im^{Me}·$SbCl_2Ph$ (5.5a)

$SbCl_2Ph$ (150 mg, 438 µmol) was reacted with Me_2Im^{Me} (69.0 mg, 438 µmol). Recrystallization by diffusion of *n*-hexane into a dichloromethane solution of the crude product yielded **5.5a** (158 mg, 401 µmol, 72 %) as colorless crystals. Crystals of **5.5a** suitable for single crystal X-ray diffraction were grown by layering a THF solution of **5.5a** with *n*-hexane and storing at room temperature.

^1H NMR (400.5 MHz, THF-d_8, 298 K): δ = 2.18 (s_{br}, 6 H, CC*H*$_3$) 3.28 (br, 3 H, NC*H*$_3$), 4.00 (br, 3 H, NC*H*$_3$), 7.33 (m, 1 H, Ph-*p*-CH), 7.39 (m, 2 H, Ph-*m*-C*H*), 8.54 (m, 2 H, Ph-*o*-C*H*).

$^{13}C\{^1H\}$ NMR (100.7 MHz, THF-d_8, 298 K): δ = 8.5 (NC*C*H$_3$), 35.5 (N*C*H$_3$), 128.0 (N*CC*N), 129.0 (Ph-*m*-*C*H), 129.8 (Ph-*p*-*C*H), 137.9 (Ph-*o*-*C*H), 144.2 (Ph-*i*-*C*), 157.7 (N*C*N).

Elemental analysis (%) calcd. for $C_{13}H_{17}Cl_2N_2Sb$ [393.95 g/mol]: C, 39.63; H, 4.35; N, 7.11; found: C, 40.23; H, 4.47; N, 6.43.

IR ([cm^{-1}]): 3064 (vw), 3047 (vw), 3035 (vw), 2986 (vw), 2953 (w), 2919 (vw), 1647 (m), 1575 (w), 1474 (m), 1433 (s), 1397 (m), 1373 (m), 1330 (vw), 1303 (vw), 1264 (vw), 1229 (w), 1205 (vw), 1184 (vw), 1160 (vw), 1105 (vw), 1061 (m), 1018 (vw), 997 (m), 977 (vw), 912 (vw), 847 (m), 763 (vs), 692 (s), 654 (w), 623 (vw), 595 (vw), 569 (w), 562 (w), 455 (s).

Synthesis of *i*Pr$_2$Im^{Me}·SbCl$_2$Ph (5.5b)

SbCl$_2$Ph (80.0 mg, 297 µmol) was reacted with *i*Pr$_2$Im^{Me} (53.5 mg, 297 µmol) to yield **5.5b** (101 mg, 224 µmol, 76 %) as a colorless solid. Crystals of **5.5b** suitable for single crystal X-ray diffraction were grown by storing a saturated benzene solution of **5.5b** at room temperature.

^{1}H NMR (500.1 MHz, C$_6$D$_6$, 298 K): δ = 0.86 (d, 6 H, $^3J_{H\text{-}H}$ = 6.6 Hz, *i*Pr-C*H*$_3$), 1.21 (d, 6 H, $^3J_{H\text{-}H}$ = 6.6 Hz, *i*Pr-C*H*$_3$), 1.33 (s, 3 H, C*H*$_3$), 1.37 (s, 3 H, C*H*$_3$), 5.08 (sept$_{br}$, 1 H, $^3J_{H\text{-}H}$ = 6.6 Hz, *i*Pr-C*H*), 5.57 (sept$_{br}$, 1 H, $^3J_{H\text{-}H}$ = 6.6 Hz, *i*Pr-C*H*), 7.17 (m, 1 H, Ph-*p*-C*H*), 7.34 (m, 2 H, Ph-*m*-C*H*), 9.19 (m, 2 H, Ph-*o*-C*H*).

^{13}C{^{1}H} NMR (125.8 MHz, C$_6$D$_6$, 298 K): δ = 9.6 (NC(*C*H$_3$)C(*C*H$_3$)), 9.9 (NC(*C*H$_3$)C(*C*H$_3$)), 20.9 (*i*Pr-*C*H$_3$), 21.2 (*i*Pr-*C*H$_3$), 52.8 (*i*Pr-*C*H), 55.2 (*i*Pr-*C*H), 126.3 (N*C*CN), 126.8 (NC*C*N), 129.1 (Ph-*m*-*C*H), 129.7 (Ph-*p*-*C*H), 137.2 (Ph-*o*-*C*H), 143.8 (Ph-*i*-*C*H), 161.3 (N*C*N).

Elemental analysis (%) calcd. for C$_{17}$H$_{25}$Cl$_2$N$_2$Sb [450.06 g/mol]: C, 45.37; H, 5.60; N, 6.22; found: C, 45.50; H, 5.63; N, 6.15.

IR ([cm^{-1}]): 3044 (vw), 2999 (w) 2970 (w), 2934 (w), 2875 (vw), 1627 (w), 1477 (w) 1460 (w), 1428 (m), 1400 (m), 1369 (m), 1335 (w), 1305 (vw), 1218 (m), 1186 (w), 1171 (w), 1139 (m), 1109 (m), 1076 (w), 1059 (m), 1018 (w), 998 (w), 905 (w), 885 (vw), 854 (vw), 764 (w), 742 (vs), 696 (s), 648 (w), 540 (w), 452 (m), 427 (w).

Synthesis of Dipp$_2$Im·SbCl$_2$Ph (5.5c)

$SbCl_2Ph$ (50.0 mg, 185 µmol) was reacted with $Dipp_2Im$ (72.0 mg, 185 µmol) to yield **5.5c** (83.5 mg, 127 µmol, 68 %) as a colorless solid.

^{1}H NMR (500.1 MHz, C_6D_6, 298 K): δ = 0.92 (s_{br}, 12 H, *i*Pr-C*H*$_3$), 1.50 (s_{br}, 12 H, *i*Pr-C*H*$_3$), 3.30 (sept, 4 H, $^3J_{H\text{-}H}$ = 6.7 Hz, *i*Pr-C*H*), 6.49 (s, 2 H, C*H*C*H*), 6.91 (m, 3 H, Ph-*p*/*m*-C*H*), 7.05 (br, 6 H, Dipp-*p*/*m*-C*H*), 8.32 (m, 2 H, Dipp-*o*-C*H*).

^{1}H NMR (500.1 MHz, toluene-d_8, 258 K): δ = 0.86 (br, 6 H, *i*Pr-C*H*$_3$), 0.95 (br, 6 H, *i*Pr-C*H*$_3$), 1.32 (br, 6 H, *i*Pr-C*H*$_3$), 1.63 (br, 6 H, *i*Pr-C*H*$_3$), 3.21 (br, 2 H, *i*Pr-C*H*), 3.28 (br, 2 H, *i*Pr-C*H*), 6.34 (br, 2 H, C*H*C*H*), 6.74 (br, 2 H, Dipp-*p*-C*H*), 6.89 (m, 3 H, overlap of Ph-*m*-C*H and* Ph-p-C*H*), 6.95 (br, 1 H, Dipp-*p*-C*H*), 7.07 (br, 2 H, Dipp-*m*-C*H*), 7.16 (br, 1 H, Dipp-*p*-C*H*), 8.29 (m, 2 H, Ph-*o*-C*H*).

^{13}C{^{1}H} NMR (125.8 MHz, C_6D_6, 298 K): δ = 23.0 (*i*Pr-*C*H$_3$), 26.6 (*i*Pr-*C*H$_3$), 29.1 (*i*Pr-*C*H), 124.5 (Dipp-*m*-*C*H), 125.5 (N*CC*N), 127.5, (Ph-*p*-*C*H), 128.3 (Ph-*m*-*C*H), 131.8 (Dipp-*p*-*C*H), 133.3 (Dipp-*i*-*C*), 137.4 (Ph-*o*-*C*H), 142.6 (Ph-*i*-*C*), 146.7 (Dipp-*o*-*C*), 162.0 (N*C*N).

^{13}C{^{1}H} NMR (125.8 MHz, toluene-d_8, 258 K): δ = 22.9 (*i*Pr-*C*H$_3$), 26.1 (*i*Pr-*C*H$_3$), 26.8 (*i*Pr-*C*H$_3$), 28.7 (*i*Pr-*C*H), 29.2 (*i*Pr-*C*H), 124.1 (N*CC*N), 124.4 (Dipp-*m*-*C*H), 125.8 (N*CC*N), 127.5 (Ph-*p*/*m*-*C*H), 128.2 (Ph-*p*/*m*-*C*H), 131.3 (Dipp-*p*-*C*H), 132.0 (Dipp-*p*-*C*H), 132.5 (Dipp-*i*-*C*), 133.3 (Dipp-*i*-*C*), 137.2 (Ph-*o*-*C*H), 141.7 (Ph-*i*-*C*), 145.6 (Dipp-*o*-*C*), 146.8 (Dipp-*o*-*C*), 162.1 (N*C*N).

Elemental analysis (%) calcd. for $C_{33}H_{41}Cl_2N_2Sb$ [658.37 g/mol]: C, 60.20; H, 6.28; N, 4.26; found: C, 61.73; H, 6.53; N, 3.86.

IR ([cm^{-1}]): 3243 (vw), 3159 (w), 3123 (w), 3080 (w), 3031 (vw), 2965 (s), 2929 (m), 2870 (w), 1714 (vw), 1588 (m), 1538 (m), 1463 (m), 1440 (w), 1417 (m), 1385 (m), 1363 (m), 1328 (w), 1309 (w), 1256 (m), 1205 (w), 1182 (vw), 1146 (w), 1116 (m), 1101 (m), 1060 (m), 1043 (w), 1022 (w), 949 (w), 934 (w), 884 (vw), 864 (vw), 828 (vw), 802 (s), 769 (m), 756 (vs), 705 (s), 682 (w), 630 (w), 580 (vw), 570 (vw), 543 (vw), 518 (vw), 507 (vw), 483 (vw), 459 (w), 438 (w), 415 (vw).

Synthesis of $Mes_2Im{\cdot}SbCl_2Ph$ (5.5d)

$SbCl_2Ph$ (300 mg, 1.11 mmol) was reacted with Mes_2Im (339 mg, 1.11 mmol) to yield **5.5d** (439 mg, 0.76 mmol, 69 %) as a colorless solid. Crystals of **5.5d** suitable for single crystal X-ray diffraction were grown by storing a saturated benzene solution of **5.5d** at 6 °C.

^{1}H NMR (500.1 MHz, C_6D_6, 298 K): δ = 1.92 (s_{br}, 3 H, Mes-*p*-C*H*$_3$) 2.02 (s_{br}, 3 H, Mes-*p*-C*H*$_3$), 2.15 (s_{br}, 6 H, Mes-*o*-C*H*$_3$), 2.42 (s_{br}, 6 H, Mes-*o*-C*H*$_3$), 5.84 (d_{br}, 2 H, C*H*C*H*), 6.23 (s_{br}, 2 H, Mes-C*H*), 6.74 (s_{br}, 2 H, Mes-C*H*), 6.97 (m, 3 H, overlap of Ph-*p*-C*H* and Ph-*m*-C*H*), 8.66 (m, 2 H, Ph-*o*-C*H)*.

^{13}C{^{1}H} NMR (125.8 MHz, C_6D_6, 298 K): δ = 18.8 (Mes-*p*-*C*H$_3$), 19.7 (Mes-*o*-*C*H$_3$), 21.0 (Mes-*o*-*C*H$_3$), 123.2 (N*CC*N), 124.1 (N*CC*N), 127.6 (Ph-*p*/*m*-*C*H), 129.1 (Mes-*m*-*C*H), 129.9 (Mes-*m*-*C*H), 132.9 (Mes-*o*-*C*), 135.7 (Mes-*p*-*C*), 136.4 (Mes-*p*-*C*), 137.0 (Ph-*o*-*C*H), 140.1 (Mes-*o*-*C*), 141.0 (Ph-*i*-*C*), 161.0 (N*C*N).

Elemental analysis (%) calcd. for $C_{27}H_{29}Cl_2N_2Sb$ [574.20 g/mol]: C, 56.48; H, 5.09; N, 4.88; found: C, 55.96; H, 5.05; N, 4.83.

IR ([cm^{-1}]): 3153 (w), 3128 (w), 3087 (vw), 3055 (w), 3045 (w), 2976 (w), 2919 (w), 2861 (w), 2736 (vw), 1820 (vw), 1765 (vw), 1727 (vw), 1698 (vw), 1608 (m), 1576 (w), 1556 (w), 1478 (s), 1464 (m), 1429 (m), 1413 (m), 1378 (m), 1299 (m), 1230 (s), 1195 (w), 1168 (w), 1157 (vw), 1120 (m), 1095 (w), 1056 (m), 1038 (m), 998 (w), 976 (vw), 931 (m), 901 (w), 880 (vw), 863 (m), 847 (s), 759 (s), 728 (vs), 697 (m), 690 (s), 670 (vw), 641 (w), 593 (w), 577 (w), 565 (w), 500 (vw), 480 (w), 449 (m), 421 (vw).

Synthesis of $cAAC^{Me}{\cdot}SbCl_2Ph$ (5.5e)

$SbCl_2Ph$ (100 mg, 371 µmol) was reacted with $cAAC^{Me}$ (106 mg, 371 µmol) to give **5.5e** (169 mg, 304 µmol, 82 %) as a colorless solid. Crystals of **5.5e** suitable for single crystal X-ray diffraction were grown by storing a saturated benzene solution of **5.5e** at room temperature.

^{1}H NMR (500.1 MHz, C_6D_6, 298 K): δ = 1.04 (d, 6 H, $^{3}J_{H\text{-}H}$ = 6.6 Hz, *i*Pr-C*H*$_3$), 1.12 (s, 6 H, NC(C*H*$_3$)$_2$), 1.32 (s, 2 H, C*H*$_2$), 1.45 (s, 6 H NCC(C*H*$_3$)$_2$), 1.72 (d, 6 H, $^{3}J_{H\text{-}H}$ = 6.6 Hz, *i*Pr-C*H*$_3$), 3.25 (sept, 2 H, $^{3}J_{H\text{-}H}$ = 6.6 Hz, *i*Pr-C*H*), 7.10 (m, 3 H, overlap of Dipp-*m*-C*H* and Ph-*p*-C*H*), 7.15 (t_{br}, 1 H, $^{3}J_{H\text{-}H}$ = 7.6 Hz, Ph-*p*-C*H*), 7.32 (t_{br}, 2 H, $^{3}J_{H\text{-}H}$ = 7.6 Hz, Ph-*m*-C*H*), 9.27 (br, 2 H, Ph-*o*-C*H*).

^{13}C{^{1}H} NMR (125.8 MHz, C_6D_6, 298 K): δ = 26.1 (*i*Pr-*C*H$_3$), 27.3 (*i*Pr-*C*H$_3$), 27.7 (NC(*C*H$_3$)$_2$), 29.2 (*i*Pr-*C*H), 31.0 (NCC(*C*H$_3$)$_2$), 51.2 (*C*H$_2$), 59.9 (N*C*(CH$_3$)$_2$) 82.4 (NC*C*(CH$_3$)$_2$), 126.4 (Dipp-*m*-*C*H), 128.8 (Ph-*m*-*C*H), 129.6 (Dipp-*p*-*C*H), 131.3 (Ph-*p*-*C*H), 133.7 (Dipp-*i*-*C*), 138.1 (Ph-*o*-*C*H), 144.2 (Ph-*i*-*C*), 146.8 (Dipp-*o*-C), 225.8 (N*C*Sb).

Elemental analysis (%) calcd. for $C_{26}H_{36}Cl_2NSb$ [555.24 g/mol]: C, 56.24; H, 6.54; N, 2.77; found: C, 55.13; H, 6.63; N, 2.59.

IR ([cm^{-1}]): 3148 (vw), 2971 (m), 2930 (w), 2869 (vw), 1644 (vw), 1587 (vw), 1513 (m), 1468 (m), 1456 (m), 1431 (m), 1392 (m), 1378 (w), 1366 (m), 1347 (w), 1318 (w), 1266 (w), 1222 (vw), 1205 (w), 1183 (m), 1158 (w), 1129 (m), 1105 (w), 1057 (m), 1019 (vw), 999 (w), 973 (vw), 927 (w), 877 (vw), 861 (vw), 826 (vw), 808 (s), 771 (s), 743 (vs), 696 (s), 648 (vw), 608 (w), 591 (vw), 562 (w), 549 (vw), 492 (w), 456 (m), 433 (vw).

Synthesis of Me_2Im^{Me}·$SbCl_2Mes$ (5.6a)

$SbCl_2Mes$ (225 mg, 722 µmol) was reacted with Me_2Im^{Me} (89.6 mg, 722 µmol). Recrystallization by diffusion of *n*-hexane into a dichloromethane solution of the crude product yielded **5.6a** (249 mg, 506 µmol, 70 %) as colorless crystals. Crystals of **5.6a** suitable for single crystal X-ray diffraction were grown by layering a THF solution of **5.6a** with *n*-hexane and storing at room temperature.

^{1}H NMR (400.5 MHz, $CDCl_3$, 298 K): δ = 2.23 (s, 6 H, Mes-*o*-C*H*$_3$) 2.27 (s, 3 H, Mes-*p*-C*H*$_3$), 2.65 (s_{br}, 6 H, NCC*H*$_3$), 3.90 (s_{br}, 6 H, NC*H*$_3$), 6.94 (s, 2 H, Mes-C*H*).

^{13}C{^{1}H} NMR (100.7 MHz, $CDCl_3$, 298 K): δ = 9.3 (Mes-o-*C*H$_3$), 21.1 (Mes-*p*-*C*H$_3$), 24.8 (NC*C*H$_3$), 36.5 (N*C*H$_3$), 128.2 (Mes-*p*-*C*), 130.0 (Mes-*m*-*C*H), 139.9 (Mes-*o*-*C*), 143.2 (Mes-*i*-*C*), 144.2 (N*CC*N), 155.7 (N*C*N).

Elemental analysis (%) calcd. for $C_{16}H_{23}Cl_2N_2Sb$ [436.03 g/mol]: C, 44.07; H, 5.32; N, 6.42; found: C, 43.70; H, 5.33; N, 6.35.

IR ([cm^{-1}]): 3047 (vw), 2986 (vw), 2955 (w), 2919 (m), 2860 (vw), 2736 (vw), 1770 (vw), 1644 (m), 1596 (w), 1555 (w), 1473 (s), 1436 (vs), 1402 (m), 1393 (m), 1385 (m), 1371 (s), 1291 (m), 1262 (w), 1228 (m), 1112 (w), 1057 (w), 1033 (m), 924 (vw), 906 (w), 870 (s), 845 (s), 802 (w), 743 (m), 708 (m), 660 (vw), 623 (vw), 583 (w), 569 (m), 552 (m), 541 (w), 498 (vw).

Synthesis of *i*Pr$_2$Im^{Me}·SbCl$_2$Mes (5.6b)

$SbCl_2Mes$ (800 mg, 2.57 mmol) was reacted with *i*Pr$_2$Im^{Me} (463 mg, 2.57 mmol) to yield **5.6b** (960 mg, 1.95 mmol, 76 %) as a colorless solid. Crystals of **5.6b** suitable for single crystal X-ray diffraction were grown by storing a saturated benzene solution of **5.6b** at room temperature.

^{1}H NMR (500.1 MHz, C_6D_6, 298 K): δ = 1.22 (d, 12 H, $^3J_{H\text{-}H}$ = 6.8 Hz, *i*Pr-C*H*$_3$), 1.44 (s, 6 H, Mes-*o*-C*H*$_3$), 2.13 (s, 3 H, Mes-*p*-C*H*$_3$), 2.92 (s_{br}, 6 H, Mes-*o*-C*H*$_3$), 5.55 (br, 2 H, *i*Pr-C*H*), 6.84 (s_{br}, 2 H, Mes-C*H*).

^{13}C{^{1}H} NMR (125.8 MHz, C_6D_6, 298 K): δ = 10.1 (NC*C*H$_3$), 21.0 (Mes-*p*-*C*H$_3$), 22.0 (*i*Pr-*C*H$_3$), 27.1 (Mes-*o*-*C*H$_3$), 54.7 (*i*Pr-*C*H), 128.4 (N*C*C*N*), 130.1 (Mes-*m*-*C*H), 139.4 (Mes-*p*-*C*), 144.6 (Mes-*i*-*C*), 145.3 (Mes-*o*-*C*), 158.4 (N*C*N).

Elemental analysis (%) calcd. for $C_{20}H_{31}Cl_2N_2Sb$ [492.14 g/mol]: C, 48.81; H, 6.35; N, 5.69; found: C, 48.46; H, 6.28; N, 5.54.

IR ([cm^{-1}]): 3010 (w), 2979 (m), 2945 (m), 2926 (m), 2882 (w), 2732 (vw), 1623 (w), 1595 (w), 1552 (w), 1448 (s), 1438 (s), 1381 (vs), 1372 (vs), 1345 (m), 1290 (w), 1237 (w), 1205 (m), 1167 (w), 1138 (w), 1110 (m), 1073 (vw), 1026 (m), 1004 (vw), 974 (vw), 952 (vw), 937 (vw), 898 (w), 886 (vw), 858 (m), 760 (w), 747 (m), 706 (w), 688 (w), 648 (vw), 579 (w), 548 (m), 540 (w), 497 (vw), 466 (vw), 430 (w), 411 (vw).

Synthesis of Dipp$_2$Im·SbCl$_2$Mes (5.6c)

SbCl$_2$Mes (666 mg, 2.57 mmol) was reacted with Dipp$_2$Im (830 mg, 2.57 mmol) to yield **5.6c** (1.10 g, 1.43 mmol, 67 %) as a colorless solid.

^{1}H NMR (400.5 MHz, C_6D_6, 298 K): δ = 0.94 (d, 12 H, $^3J_{H\text{-}H}$ = 6.8 Hz, *i*Pr-C*H*$_3$), 1.26 (d, 12 H, $^3J_{H\text{-}H}$ = 6.8 Hz, *i*Pr-C*H*$_3$), 1.98 (s, 3 H, Mes-*p*-C*H*$_3$), 2.37 (s, 6 H, Mes-*o*-C*H*$_3$), 2.92 (sept, 4 H, $^3J_{H\text{-}H}$ = 6.8 Hz, *i*Pr-C*H*), 6.54 (s, 2 H, C*H*C*H*), 6.56 (s, 2 H, Mes-*m*-C*H*), 7.04 (d, 4 H, $^3J_{H\text{-}H}$ = 7.8 Hz, Dipp-*m*-C*H*), 7.20 (t, 2 H, $^3J_{H\text{-}H}$ = 7.8 Hz, Dipp-*p*-C*H*).

^{13}C{^{1}H} NMR (100.7 MHz, C_6D_6, 298 K): δ = 21.0 (Mes-*p*-*C*H$_3$), 22.8 (*i*Pr-*C*H$_3$), 23.1 (Mes-*o*-*C*H$_3$), 26.3 (*i*Pr-*C*H$_3$), 29.1 (*i*Pr-*C*H), 124.6 (Dipp-*m*-*C*H), 124.9 (*C*H*C*H), 130.3 (Mes-*m*-*C*H), 131.2 (Dipp-*p*-*C*H), 135.0 (Dipp-*i*-*C*)*, 138.9 (Mes-*p*-*C*)*, 143.6 (Mes-*o*-*C*), 146.4 (Dipp-*o*-*C*), 150.5 (Mes-*i*-*C*)*. The resonances at 135.0 ppm, 138.9 ppm and 150.5 ppm could not be observed in the ^{13}C{^{1}H} NMR Spektrum but *via* ^{13}C{^{1}H} HMBC NMR. No Signal was detected for (N*C*N).

Elemental analysis (%) calcd. for $C_{36}H_{47}Cl_2N_2Sb$ [700.45 g/mol]: C, 61.73; H, 6.76; N, 4.00; found: C, 61.31; H, 6.71; N, 3.82.

IR ([cm^{-1}]): 3163 (vw), 3059 (vw), 2961 (m), 2925 (w), 2864 (w), 1596 (w), 1556 (w), 1538 (w), 1462 (m), 1456 (m), 1442 (m), 1386 (m), 1361 (w), 1323 (w), 1291 (w), 1275 (w), 1256 (w), 1202 (w), 1179 (w), 1148 (vw), 1114 (w), 1088 (m), 1058 (m), 1036 (m), 935 (w), 884 (vw), 845 (w), 808 (m), 756 (s), 702 (vw), 682 (vs), 636 (w), 580 (w), 540 (w), 519 (vw), 456 (w), 441 (w), 416 (w).

Synthesis of Mes$_2$Im·SbCl$_2$Mes (5.6d)

SbCl$_2$Mes (100 mg, 321 µmol) was reacted with Mes$_2$Im (97.6 mg, 321 µmol) to yield **5.6d** (151 mg, 245 µmol, 76 %) as a colorless solid. Crystals of **5.6d** suitable for single crystal X-ray diffraction were grown by storing a saturated benzene solution of **5.6d** at room temperature.

^{1}H NMR (500.1 MHz, CD_2Cl_2, 298 K): δ = 2.00 (s_{br}, 12 H, Mes-*o*-C*H*$_3$), 2.21 (br, 9 H, overlap of Sb-Mes-*p*-C*H*$_3$ and Mes-*p*-C*H*$_3$), 2.36 (s_{br}, 6 H, Mes-*o*-C*H*$_3$), 6.55 (s_{br}, 2 H, Sb-Mes-C*H*), 6.88 (s_{br}, 4 H, Mes-C*H*), 7.13 (s_{br}, 2 H, C*H*C*H*).

^{13}C{^{1}H} NMR (125.8 MHz, CD_2Cl_2, 298 K): δ = 18.1 (Mes-*o*-*C*H$_3$), 21.1 (Sb-Mes-*o*-*C*H$_3$), 21.3 (Mes-*p*-*C*H$_3$), 23.0, (Sb-Mes-*p*-*C*H$_3$), 124.4 (N*CC*N), 129.7 (Mes-*C*H), 129.8 (Sb-Mes-*o*-*C*), 130.1 (Sb-Mes-*C*H), 133.9 (Mes-*o*-*C*), 135.2 (Mes-*i*-*C*), 138.8 (Sb-Mes-*i*-*C*), 140.4 (Mes-*p*-*C*), 145.7 (Sb-Mes-*p*-*C*), 174.0 (N*C*N).

Elemental analysis (%) calcd. for $C_{30}H_{35}Cl_2N_2Sb$ [616.28 g/mol]: C, 58.47; H, 5.72; N, 4.55; found: C, 57.09; H, 5.92; N, 4.47. After several attempts this is the best result so far.

IR ([cm^{-1}]): 3109 (vw), 3067 (vw) 3013 (w), 2947 (m), 2915 (m), 2858 (m), 2736 (vw), 1597 (w) 1538 (s) 1480 (s), 1444 (s), 1405 (m), 1377 (m), 1336 (vw), 1319 (vw), 1288 (w), 1258 (vw),1227 (s), 1161 (w), 1092 (w), 1058 (m), 1032 (m), 966 (vw), 930 (w), 840 (vs), 754 (m), 724 (m), 702 (s), 674 (vs), 569 (vs), 550 (m), 542 (m), 498 (vw), 453 (vw).

Synthesis of ^{a}Dipp$_2$Im·SbCl$_2$Mes (5.7)

Procedure A: A solution of **5.6c** (100 mg, 143 µmol) in benzene (5 mL) was refluxed for 24 h. After cooling to room temperature all volatiles were removed *in vacuo* to yield **5.7** (98.3 mg, 140 µmol, 98 %) as a colorless solid. Procedure B: A solution of $SbCl_2Mes$ (225 mg, 722 µmol) and $Dipp_2Im$ (280 mg, 722 µmol, 1.0 eq) in benzene (5 mL) was refluxed for 24 hours. After cooling to room temperature *n*-hexane (7 mL) was added. The resulting precipitate was isolated by filtration, washed with *n*-hexane (2 x 4 mL) and dried *in vacuo* to give **5.7** (451 mg, 644 µmol, 89 %) as a colorless solid. Crystals of **5.7** suitable for single crystal X-ray diffraction were grown by diffusion of *n*-pentane into a dichloromethane solution of **5.7** and storing at 12 °C.

^{1}H NMR (500.1 MHz, CD_2Cl_2, 298 K): δ = 1.14 (d, 6 H, $^{3}J_{H\text{-}H}$ = 6.9 Hz, *i*Pr-C*H*$_3$), 1.22 (d, 6 H, $^{3}J_{H\text{-}H}$ = 6.9 Hz, *i*Pr-C*H*$_3$), 1.26 (d, 6 H, $^{3}J_{H\text{-}H}$ = 6.9 Hz, *i*Pr-C*H*$_3$), 1.50 (d, 6 H, $^{3}J_{H\text{-}H}$ = 6.9 Hz, *i*Pr-C*H*$_3$), 2.24 (s, 3 H, Mes-*p*-C*H*$_3$), 2.54 (sept, 2 H, $^{3}J_{H\text{-}H}$ = 6.9 Hz, *i*Pr-

C*H*), 2.69 (s, 6 H, Mes-*o*-C*H*$_3$), 2.80 (sept, 2 H, $^3J_{H\text{-}H}$ = 6.9 Hz, *i*Pr-C*H*), 6.89 (s_{br}, 1 H, Mes-C*H*), 7.37 (d, $^3J_{H\text{-}H}$ = 7.7 Hz, 2 H, Dipp-*m*-C*H*), 7.41 (d, 2 H, $^3J_{H\text{-}H}$ = 7.7 Hz, Dipp-*m*-C*H*), 7.58 (t, 1 H, $^3J_{H\text{-}H}$ = 7.7 Hz, Dipp-*p*-C*H*), 7.61 (t, 1 H, $^3J_{H\text{-}H}$ = 7.7 Hz, Dipp-*p*-C*H*), 7.87 (m, 1 H, SbCC*H*), 8.08 (m, 1 H, NC*H*N).

^{13}C{^{1}H} NMR (125.8 MHz, CD_2Cl_2, 298 K): δ = 21.0 (Mes-*p*-CH_3), 22.5 (*i*Pr-CH_3), 24.4 (*i*Pr-CH_3), 24.5 (*i*Pr-CH_3), 24.8 (Mes-*o*-CH_3), 26.9 (*i*Pr-CH_3), 29.3 (*i*Pr-C*H*), 29.6 (*i*Pr-C*H*), 124.9 (Dipp-*m*-C*H*), 125.1 (Dipp-*m*-C*H*), 129.8 (Mes-C*H*), 130.0 (Dipp-*i*-C), 131.5 (Dipp-*i*-C), 132.1 (Dipp-*p*-C*H*), 132.3 (Dipp-*p*-C*H*), 135.2 (NC*H*N), 136.4 (SbC*C*HN), 139.1, (Mes-*o*-C), 143.4 (Mes-*p*-C), 145.8 (Dipp-*p*-C*H*), 146.3 (Dipp-*o*-C), 146.5 (NCSb), 147.6 (Mes-*i*-C).

Elemental analysis (%) calcd. for $C_{36}H_{47}Cl_2N_2Sb$ [700.45 g/mol]: C, 61.73; H, 6.76; N, 4.00; found: C, 61.74; H, 6.52; N, 4.00.

IR ([cm^{-1}]): 3148 (vw), 3090 (w), 3060 (w), 3015 (vw), 2959 (s), 2925 (m), 2867 (m), 1707 (vw), 1660 (vw), 1597 (w), 1540 (m), 1488 (m), 1462 (s), 1442 (m), 1385 (m), 1364 (m), 1350 (w), 1327 (m), 1289 (w), 1275 (w), 1255 (w), 1199 (w), 1183 (m), 1147 (m), 1108 (s), 1058 (m), 1042 (m), 978 (w), 957 (vw), 935 (w), 922 (vw), 908 (vw), 858 (w), 841 (m), 802 (vs), 754 (vs), 703 (vw), 688 (w), 672 (m), 637 (vw), 580 (w), 540 (w), 518 (vw), 472 (vw), 451 (w), 438 (w), 420 (w).

Synthesis of ^{a}Dipp$_2$Im·SbCl$_2$Ph (5.8)

Procedure A: A solution of **5.5c** (60 mg, 143 µmol) in benzene (5 mL) was refluxed for 24 h. After cooling to room temperature all volatiles were removed *in vacuo* to yield **5.8** (57.1 mg, 140 µmol, 95 %) as a colorless solid. Procedure B: A solution of $SbCl_2Ph$ (70.0 mg, 259 µmol) and $Dipp_2Im$ (101 mg, 259 µmol, 1.0 eq) in benzene (5 mL) was refluxed for 24 h. After cooling to room temperature *n*-hexane (7 mL) was added. The resulting precipitate was isolated by filtration, washed with *n*-hexane (2 x 4 mL) and dried *in vacuo* to yield **5.8** (147 mg, 223 µmol, 86 %) as a colorless solid. Crystals of **5.8** suitable for single crystal X-ray diffraction were grown by diffusion of *n*-pentane into a concentrated CH_2Cl_2 of **5.8** solution at 12 °C.

^{1}H NMR (500.1 MHz, CD_2Cl_2, 298 K): δ = 1.11 (d, 6 H, $^{3}J_{H-H}$ = 6.9 Hz, *i*Pr-CH_3), 1.20 (d, 6 H, $^{3}J_{H-H}$ = 6.9 Hz, *i*Pr-CH_3), 1.21 (d, 6 H, $^{3}J_{H-H}$ = 6.9 Hz, *i*Pr-CH_3), 1.49 (d, 6 H, $^{3}J_{H-H}$ = 6.9 Hz, *i*Pr-CH_3), 2.45 (sept, 2 H, $^{3}J_{H-H}$ = 6.9 Hz, *i*Pr-C*H*), 2.94 (sept, 2 H, $^{3}J_{H-H}$ = 6.9 Hz, *i*Pr-C*H*), 7.22 (d, 1 H, $^{4}J_{H-H}$ = 1.5 Hz, SbCC*H*), 7.31 (m, 1 H, Ph-*p*-C*H*), 7.33 (d, 2 H, $^{3}J_{H-H}$ = 7.9 Hz, Dipp-*m*-C*H*), 7.38 (m, 2 H, Ph-*m*-C*H*), 7.44 (d, 2 H, $^{3}J_{H-H}$ = 7.9 Hz, Dipp-*m*-C*H*), 7.55 (t, 1 H, Dipp-*p*-C*H*), 7.64 (t, 1 H, Dipp-*p*-C*H*), 8.13 (d, 1 H, $^{4}J_{H-H}$ = 1.5 Hz, NC*H*N), 8.27 (m, 2 H, Ph-*o*-C*H*).

^{13}C{^{1}H} NMR (125.8 MHz, CD_2Cl_2, 298 K): δ = 22.9 (*i*Pr-*C*H_3), 24.3 (*i*Pr-*C*H_3), 24.5 (*i*Pr-*C*H_3), 26.9 (*i*Pr-*C*H_3), 29.3 (*i*Pr-*C*H), 29.4 (*i*Pr-*C*H), 125.0 (Dipp-*m*-*C*H), 125.1 (Dipp-*m*-*C*H), 128.5 (Ph-*m*-*C*H), 129.1 (Ph-*p*-*C*H), 130.2 (Dipp-*i*-*C*), 131.5 (Dipp-*i*-*C*), 132.3 (Dipp-*p*-*C*H), 132.4 (Dipp-*p*-*C*H), 132.8 (N*C*HCSb), 135.7 (N*C*HN), 137.0 (Ph-*m*-*C*H), 145.7 (Dipp-*o*-*C*), 146.5 (Dipp-*o*-*C*), 148.1 (Ph-*i*-*C*), 151.1 (N*C*Sb).

Elemental analysis (%) calcd. for $C_{33}H_{41}Cl_2N_2Sb$ [658.37 g/mol]: C, 60.20; H, 6.28; N, 4.26; found: C, 61.08; H, 7.02; N, 4.71.

IR ([cm^{-1}]): 3148 (vw), 3091 (w), 3062 (w), 3014 (vw), 2959 (s), 2925 (m), 2867 (m), 1714 (vw), 1661 (vw), 1598 (w), 1540 (m), 1488 (m), 1462 (s), 1442 (m), 1385 (m), 1364 (m), 1350 (w), 1327 (m), 1289 (w), 1275 (w), 1255 (w), 1199 (m), 1183 (m), 1147 (vw), 1108 (m), 1059 (s), 1042 (m), 978 (w), 957 (vw), 935 (w), 923 (vw), 908 (vw), 858 (w), 841 (m), 802 (vs), 754 (vs), 703 (vw), 688 (vw), 672 (m), 637 (vw), 581 (w), 540 (w), 517 (vw), 472 (vw), 452 (w), 437 (w), 420 (vw).

Synthesis of [^{a}Dipp$_2$Im·SbClMes]$^{+}$[BF$_4$]$^{-}$ (5.9)

A solution of **5.7** (225 mg, 321 µmol) and $AgBF_4$ (63.5 mg, 321 µmol, 1.0 eq) in CH_2Cl_2 (5 mL) was stirred for 15 min. The resulting precipitate was isolated by filtration and washed with dichloromethane (2 x 3 mL). All volatiles were removed *in vacuo* to yield **5.9** (177 mg, 267 µmol, 83 %) as a colorless solid. Crystals suitable for single crystal X-Ray diffraction were obtained by storing a concentrated dichloromethane solution of **5.9** at 6 °C.

^{1}H NMR (500.1 MHz, CD_2Cl_2, 298 K): δ = 1.03 (b, 6 H, $^{3}J_{H\text{-}H}$ = 6.7 Hz, *i*Pr-CH_3), 1.13 (d, 6 H, $^{3}J_{H\text{-}H}$ = 6.7 Hz, *i*Pr-CH_3), 1.24 (d, 6 H, $^{3}J_{H\text{-}H}$ = 6.7 Hz, *i*Pr-CH_3), 1.28 (d, 6 H, $^{3}J_{H\text{-}H}$ = 6.9 Hz, *i*Pr-CH_3), 2.25 (s, 3 H, Mes-*p*-CH_3), 2.33 (m, 8 H, overlap of Mes-*o*-CH_3 and *i*Pr-C*H*), 2.43 (sept, 2 H, $^{3}J_{H\text{-}H}$ = 6.7 Hz, *i*Pr-C*H*), 6.92 (s, 2 H, Mes-C*H*), 7.36 (d, 2 H, $^{3}J_{H\text{-}H}$ = 7.7 Hz, Dipp-*m*-C*H*), 7.40 (d, 2 H, $^{3}J_{H\text{-}H}$ = 7.7 Hz, Dipp-*m*-C*H*), 7.64 (t, 1 H, $^{3}J_{H\text{-}H}$ = 7.7 Hz, Dipp-*p*-C*H*), 7.65 (d, 1 H, $^{4}J_{H\text{-}H}$ = 1.4 Hz, NC*H*N), 7.66 (t, 1 H, Dipp-*p*-C*H*), 9.13 (d, 1 H, $^{4}J_{H\text{-}H}$ = 1.4 Hz, NC*H*CSb).

^{13}C{^{1}H} NMR (125.8 MHz, CD_2Cl_2, 298 K): δ = 21.3 (Mes-*p*-CH_3), 21.7 (*i*Pr-CH_3), 23.9 (Mes-*o*-CH_3), 24.27 (*i*Pr-CH_3), 24.32 (*i*Pr-CH_3), 26.3 (*i*Pr-CH_3), 29.6 (*i*Pr-C*H*), 29.9 (*i*Pr-C*H*), 125.2 (Dipp-*m*-C*H*), 125.6 (Dipp-*m*-C*H*), 129.9 (Dipp-*i*-*C*), 130.2 (Dipp-*i*-*C*), 130.8 (Mes-*m*-C*H*), 132.7 (Dipp-*p*-C*H*), 133.1 (N*C*HCSb), 133.5 (Dipp-*p*-C*H*), 138.0 (Mes-*i*-*C*), 139.2 (N*C*Sb), 141.2 (N*C*HN), 143.1 (Mes-*o*-*C*), 145.4 (Dipp-*o*-*C*), 145.5 (Dipp-*o*-*C*), 145.9 (Mes-*p*-*C*).

Elemental analysis (%) calcd. for $C_{36}H_{47}ClBF_4N_2Sb$ [751.80 g/mol]: C, 57.51; H, 6.30; N, 4.72; found: C, 57.16; H, 6.69; N, 3.91.

IR ([cm^{-1}]): 3116 (w), 3067 (vw), 3024 (vw), 2965 (m), 2928 (m), 2870 (w), 1597 (w), 1540 (m), 1496 (w), 1462 (m), 1387 (w), 1366 (m), 1330 (m), 1288 (w), 1256 (w), 1207 (m), 1185 (m), 1082 (s), 1057 (s), 1037 (s), 1008 (vs), 978 (m), 958 (m), 937 (m), 884 (w), 847 (m), 802 (s), 756 (s), 732 (w), 703 (w), 671 (m), 636 (vw), 580 (w), 542 (w), 518 (m), 451 (w), 431 (w).

Synthesis of [^{a}Dipp$_2$Im·SbClMes]$^{+}$[GaCl$_4$]$^{-}$ (5.10)

A solution of **5.7** (100 mg, 143 µmol) and $GaCl_3$ (25.1 mg, 143 µmol, 1.0 eq) in dichloromethane (5 mL) was stirred for 24 h. All volatiles were removed *in vacuo* to yield **5.10** (114 mg, 130 µmol, 91 %) as an off-white solid. Crystals suitable for single crystal X-Ray diffraction were obtained by storing a concentrated dichloromethane solution of **5.10** at 6 °C.

^{1}H NMR (500.1 MHz, CD_2Cl_2, 298 K): δ = 0.50 (d, 3 H, $^{3}J_{H\text{-}H}$ = 6.8 Hz, *i*Pr-CH_3), 1.05 (d, 3 H, $^{3}J_{H\text{-}H}$ = 6.8 Hz, *i*Pr-CH_3), 1.19 (d, 3 H, $^{3}J_{H\text{-}H}$ = 6.8 Hz, *i*Pr-CH_3), 1.25 (d, 3 H, $^{3}J_{H\text{-}}$

$_H$ = 6.8 Hz, *i*Pr-C*H*$_3$), 1.26 (d, 3 H, $^3J_{H-H}$ = 6.8 Hz, *i*Pr-C*H*$_3$), 1.28 (d, 3 H, $^3J_{H-H}$ = 6.8 Hz, *i*Pr-C*H*$_3$), 1.34 (d, 3 H, $^3J_{H-H}$ = 6.8 Hz, *i*Pr-C*H*$_3$), 1.49 (d, 3 H, $^3J_{H-H}$ = 6.8 Hz, *i*Pr-C*H*$_3$), 2.04 (sept, 1 H, $^3J_{H-H}$ = 6.8 Hz, *i*Pr-C*H*), 2.26 (s, 3 H, Mes-*p*-C*H*$_3$), 2.30 (s, 6 H, Mes-*o*-C*H*$_3$), 2.31 (sept, 1 H, $^3J_{H-H}$ = 6.8 Hz, *i*Pr-C*H*), 2.45 (sept, 1 H, $^3J_{H-H}$ = 6.8 Hz, *i*Pr-C*H*), 2.51 (sept, 1 H, $^3J_{H-H}$ = 6.8 Hz, *i*Pr-C*H*), 6.94 (s, 2 H, Mes-C*H*), 7.27 (dd, 1 H, $^3J_{H-H}$ = 7.9 Hz, $^4J_{H-H}$ = 1.2 Hz, Dipp-*m*-C*H*), 7.45 (m, 2 H, Dipp-*m*-C*H*), 7.51 (dd, 1 H, $^3J_{H-H}$ = 7.9 Hz, $^4J_{H-H}$ = 1.2 Hz, Dipp-*m*-C*H*), 7.67 (t, 1 H, $^3J_{H-H}$ = 7.9 Hz, Dipp-*p*-C*H*), 7.70 (t, 1 H, $^3J_{H-H}$ = 7.9 Hz, Dipp-*p*-C*H*), 7.72 (d, 1 H, $^4J_{H-H}$ = 1.5 Hz, NC*H*CS*b*), 8.68 (d, 1 H, $^4J_{H-H}$ = 1.5 Hz, NC*H*N).

^{13}C{^{1}H} NMR (125.8 MHz, CD_2Cl_2, 298 K): δ = 20.6 (*i*Pr-*C*H$_3$), 21.3 (Mes-*p*-*C*H$_3$), 22.6 (*i*Pr-*C*H$_3$), 23.7 (Mes-*o*-*C*H$_3$), 24.2 (*i*Pr-*C*H$_3$), 24.2 (*i*Pr-*C*H$_3$), 24.5 (*i*Pr-*C*H$_3$), 24.9 (*i*Pr-*C*H$_3$), 26.5 (*i*Pr-*C*H$_3$), 26.9 (*i*Pr-*C*H$_3$), 29.7 (*i*Pr-*C*H), 29.9 (*i*Pr-*C*H), 30.1 (*i*Pr-*C*H), 125.5 (Dipp-*m*-*C*H), 125.6 (Dipp-*m*-*C*H), 125.9 (Dipp-*m*-*C*H), 126.1 (Dipp-*m*-*C*H), 129.5 (Dipp-*i*-*C*), 129.7 (Dipp-*i*-*C*), 131.0 (Mes-*m*-*C*H), 133.1 (N*C*HCSb), 133.2 (Dipp-*p*-*C*H), 134.0 (Dipp-*p*-*C*H), 136.8 (Mes-*i*-*C*), 139.4 (N*C*Sb), 139.9 (N*C*HN), 143.7 (Mes-*o*-*C*), 145.2 (Dipp-*o*-*C*), 145.3 (Dipp-*o*-*C*), 145.5 (Dipp-*o*-*C*), 145.8 (Dipp-*o*-*C*), 146.0 (Mes-*p*-*C*).

Elemental analysis (%) calcd. for $C_{36}H_{47}Cl_5GaN_2Sb$ [876.52 g/mol]: C, 49.33; H, 5.41; N, 3.20; found: C, 48.63; H, 5.64; N, 3.34.

IR ([cm^{-1}]): 3148 (vw), 3111 (m), 3069 (vw), 3028 (vw), 2964 (s), 2928 (m), 2871 (m), 1715 (vw), 1660 (vw), 1596 (w), 1541 (m), 1501 (w), 1477 (w), 1463 (s), 1442 (s), 1389 (m), 1367 (m), 1351 (w), 1329 (m), 1289 (w), 1276 (w), 1256 (w), 1202 (m), 1182 (m), 1149 (vw), 1093 (m), 1070 (m), 1061 (m), 1034 (w), 959 (vw), 937 (w), 860 (s), 803 (vs), 755 (s), 705 (vw), 681 (vw), 670 (m), 638 (vw), 579 (w), 542 (m), 519 (vw), 493 (vw), 451 (vw), 435 (vw), 420 (w).

7.9 Synthetic Procedures for Chapter VI

Synthesis of [cAAC^{Me}Cl]$^+$[SbCl$_3$Mes]$^-$ (6.1a) and cAAC^{Me}·SbMes (6.2a)

A solution of $SbCl_2Mes$ (983 mg, 3.15 mmol, 1 eq) in toluene (22 mL) was added under vigorous stirring at −78 °C to a solution of cAAC^{Me} (106 mg, 371 µmol, 1 eq) in toluene (22 mL). The suspension was stirred for three hours at −78 °C with subsequent warming to room temperature over 17 hours. The orange-red suspension was concentrated to a volume of 15 mL and hexane (50 mL) was added. The resulting suspension was filtered and washed with *n*-hexane (2 x 15 mL) to yield **6.1a** (949 mg, 1.42 mmol, 45 %) as an off-white solid. Crystals of **6.1a** suitable for X-ray diffraction analysis were grown by slow evaporation of a saturated solution of **6.1a** in dichloromethane at room temperature. Removal of all volatile material of the filtrate afforded **6.2a** (722 mg, 1.37 mmol, 44 %) as an orange solid. However, it was found that such good yields could only be obtained if these conditions were strictly kept, otherwise increased decomposition was observed. In some instances, the product had to be recrystallized for further purification by storing a saturated and filtrated hexane solution of **6.2a** at −30 °C for several days. These crystals are typically also suitable for X-ray diffraction analysis.

[cAAC^{Me}Cl]$^+$[SbCl$_3$Mes]$^-$ (6.1a):

^{1}H NMR (400.5 MHz, CD_2Cl_2, 298 K): δ = 1.19 (d, 6 H, $^3J_{H\text{-}H}$ = 6.8 Hz, *i*Pr-CH_3), 1.38 (d, 6 H, $^3J_{H\text{-}H}$ = 6.8 Hz, *i*Pr-CH_3), 1.59 (s, 6 H, NC(CH_3)$_2$), 1.71 (s, 6 H, NCC(CH_3)$_2$), 2.22 (s, 3 H, Mes-*p*-CH_3), 2.46 (sept, 2 H, $^3J_{H\text{-}H}$ = 6.8 Hz, *i*Pr-C*H*), 2.67 (s, 2 H, CH_2), 2.71 (s, 6 H, Mes-*o*-CH_3), 6.82 (s, 2 H, Mes-C*H*), 7.46 (d, 2 H, $^3J_{H\text{-}H}$ = 7.8 Hz, Dipp-*m*-C*H*), 7.67 (t, 1 H, $^3J_{H\text{-}H}$ = 7.8 Hz, Dipp-*p*-C*H*).

^{13}C{^{1}H} NMR (100.7 MHz, CD_2Cl_2, 298 K): δ = 21.1 (Mes-*p*-CH_3), 22.5 (Mes-*o*-CH_3), 23.4 (*i*Pr-CH_3), 26.3 (*i*Pr-CH_3), 28.3 (NC(CH_3)$_2$), 28.9 (NCC(CH_3)$_2$), 30.4 (*i*Pr-C*H*), 48.0 (CH_2), 51.6 (NC*C*(CH$_3$)$_2$), 84.4 (N*C*(CH$_3$)$_2$), 126.9 (Mes-*m*-C*H*), 127.6 (Dipp-*i*-*C*), 130.3 (Dipp-*m*-C*H*), 133.2 (Dipp-*p*-C*H*), 138.6 (Mes-*p*-*C*), 143.0 (Mes-*o*-*C*), 144.7 (Dipp-*o*-*C*), 155.2 (Mes-*i*-*C*), 190.6 (N*C*Cl).

Elemental analysis (%) calcd. for $C_{29}H_{42}Cl_4NSb$ [668.22 g/mol]: C, 52.13; H, 6.34; N, 2.10; found: C, 52.33; H, 6.39; N, 2.01.

IR ([cm^{-1}]): 3005 (vw), 2973 (m), 2931 (m), 2867 (w), 1644 (vw), 1602 (s) 1582 (w), 1463 (s), 1454 (s), 1391 (m), 1384 (m), 1372 (m), 1346 (w), 1336 (w), 1287 (w), 1265 (m), 1202 (w), 1178 (w), 1164 (w), 1133 (s), 1108 (m), 1061 (m), 1052 (m), 1034 (m), 969 (vw), 933 (w), 910 (vw), 890 (w), 868 (w), 848 (m), 808 (vs), 793 (m), 765 (vw), 737 (m), 704 (w), 652 (vw), 630 (vw), 609 (vw), 577 (w), 563 (w), 543 (w), 493 (w), 425 (vw), 416 (vw).

cAAC^{Me}·SbMes (6.2a):

^{1}H NMR (500.1 MHz, C_6D_6, 298 K): δ = 1.05 (s, 6 H, NCC(CH_3)$_2$), 1.24 (d, 6 H, $^3J_{H-H}$ = 6.8 Hz, *i*Pr-CH_3), 1.28 (s, 6 H, NC(CH_3)$_2$), 1.69 (s, 2 H, CH_2), 1.77 (d, 6 H, $^3J_{H-H}$ = 6.8 Hz, *i*Pr-CH_3), 2.20 (s, 3 H, Mes-*p*-CH_3), 2.81 (s, 6 H, Mes-*o*-CH_3), 3.05 (sept, 2 H, $^3J_{H-H}$ = 6.8 Hz, *i*Pr-C*H*), 6.99 (s_{br}, 2 H, Mes-C*H*), 7.159 (d, 1 H, $^3J_{H-H}$ = 8.4 Hz, Dipp-*m*-C*H*, overlapped with C_6D_5H), 7.160 (d, 1 H, $^3J_{H-H}$ = 6.9 Hz, Dipp-*m*-C*H*, overlapped with C_6D_5H), 7.67 (dd, 1 H, $^3J_{H-H}$ = 6.9 Hz, $^3J_{H-H}$ = 8.4 Hz, Dipp-*p*-C*H*).

^{13}C{^{1}H} NMR (125.8 MHz, C_6D_6, 298 K): δ = 21.2 (Mes-*p*-*C*H_3), 25.3 (*i*Pr-*C*H_3), 28.8 (*i*Pr-*C*H_3), 29.0 (*i*Pr-*C*H), 29.1 (NCC(*C*H_3)$_2$), 31.0 (NC(*C*H_3)$_2$), 31.3 (Mes-*o*-*C*H_3), 55.7 (*C*H_2), 55.9 (N*C*(CH$_3$)$_2$) 71.5 (NC*C*(CH$_3$)$_2$), 126.4 (Dipp-*m*-*C*H), 127.6 (Mes-*m*-*C*H), 129.4 (Dipp-*p*-*C*H), 136.1 (Dipp-*i*-*C*), 137.3 (Mes-*p*-*C*), 138.5 (Mes-*i*-*C*), 146.2 (Mes-*o*-*C*), 148.0 (Dipp-*o*-*C*), 238.6 (N*C*Sb).

Elemental analysis (%) calcd. for $C_{29}H_{42}NSb$ [526.42 g/mol]: C, 66.17; H, 8.04; N, 2.66; found: C, 66.40; H, 8.17; N, 2.54.

IR ([cm^{-1}]): 3058 (vw), 2960 (s), 2926 (s), 2864 (m), 1678 (m), 1590 (vw), 1441 (m), 1382 (m), 1366 (m), 1336 (vs), 1254 (m), 1234 (w), 1203 (s), 1178 (m), 1137 (s), 1109 (m), 1050 (m), 1012 (m), 975 (w), 957 (w), 939 (m), 899 (w), 847 (m), 805 (s), 776 (m), 751 (w), 698 (w), 638 (vw), 608 (vw), 574 (m), 550 (w), 540 (w), 479 (vw), 447 (w), 431 (vw), 408 (vw).

Synthesis of [cAAC^{Cy}Cl]$^+$[SbCl$_3$Mes]$^-$ (1b) and cAAC^{Cy}·SbMes (2b)

A solution of $SbCl_2Mes$ (192 mg, 614 µmol, 1 eq) in toluene (7 mL) was added under vigorous stirring at −78 °C to a solution of cAAC^{Cy} (200 mg, 614 µmol, 1 eq) in toluene (7 mL). The suspension was stirred for three hours at −78 °C with subsequent warming to room temperature over 17 hours. The orange suspension was concentrated to a volume of 5 mL and hexane (15 mL) was added. The resulting suspension was filtered and washed with *n*-hexane (3 x 10 mL) to yield **6.1b** (211 mg, 298 µmol, 48 %) as an off-white solid. In some instances, the product had to be purified by slow diffusion of n-hexane into a saturated solution of the compound in THF at room temperature which afforded **6.1b** (46.0 mg, 65.0 µmol, 11 %) as a colorless crystalline solid. These crystals were also suitable for X-ray diffraction analysis. Removal of all volatile material of the filtrate afforded **6.2b** (126 mg, 198 µmol, 32 %) as an orange solid. It was found that such good yields could only be obtained if the conditions mentioned here were strictly kept, otherwise increased decomposition was observed. In some instances, the product had to be recrystallized for further purification by storing a saturated and filtrated solution of **6.2b** in hexane at −30 °C for several days. These crystals of **6.2b** were also suitable for X-ray diffraction analysis.

[cAAC^{Cy}Cl]$^+$[SbCl$_3$Mes]$^-$ (6.1b):

^{1}H NMR (400.5 MHz, CD_2Cl_2, 258 K): δ = 1.18 (d, 6 H, $^3J_{H\text{-}H}$ = 6.7 Hz, *i*Pr-CH_3), 1.38 (d, 6 H, $^3J_{H\text{-}H}$ = 6.7 Hz, *i*Pr-CH_3), 1.40 (m, 1 H, Cy-CH_2), 1.50 (m, 2 H, Cy-CH_2), 1.59 (s, 6 H, NC(CH_3)$_2$), 1.86 (m, 2 H, Cy-CH_2), 1.97 (m, 4 H, Cy-CH_2, overlapped with m, 1 H, Cy-CH_2), 2.23 (s, 3 H, Mes-*p*-CH_3), 2.46 (sept, 2 H, $^3J_{H\text{-}H}$ = 6.7 Hz, *i*Pr-CH), 2.66 (s, 2 H, CH_2), 2.71 (s, 6 H, Mes-*o*-CH_3), 6.82 (s, 2 H, Mes-CH), 7.46 (d, 2 H, $^3J_{H\text{-}H}$ = 7.8 Hz, Dipp-*m*-CH), 7.65 (t, 1 H, $^3J_{H\text{-}H}$ = 7.8 Hz, Dipp-*p*-CH).

^{13}C{^{1}H} NMR (100.7 MHz, CD_2Cl_2, 298 K): δ = 21.1 (Mes-*p*-CH_3), 21.4 (Cy-CH_2 overlapped with Cy-CH_2), 22.6 (Mes-*o*-CH_3), 23.4 (*i*Pr-CH_3), 24.5 (Cy-CH_2), 26.3 (*i*Pr-CH_3), 29.4 (NCC(CH_3)$_2$), 30.4 (*i*Pr-CH), 35.8 (Cy-CH_2), 44.1 (CH_2), 56.3 (NCCCy), 83.8 (NC(CH$_3$)$_2$), 126.9 (Mes-*m*-CH), 127.6 (Dipp-*i*-C), 130.3 (Dipp-*m*-CH), 133.1 (Dipp-*p*-CH), 138.7 (Mes-*p*-C), 143.1 (Mes-*o*-C), 144.7 (Dipp-*o*-C), 154.9 (Mes-*i*-C), 189.8 (NCCl).

Elemental analysis (%) calcd. for $C_{32}H_{46}Cl_4NSb$ [708.26 g/mol]: C, 54.27; H, 6.55; N, 1.98; found: C, 54.07; H, 6.54; N, 1.97.

IR ([cm^{-1}]): 2969 (m), 2930 (s), 2858 (m), 1724 (vw), 1680 (vw), 1641 (vw), 1600 (s), 1581 (m), 1463 (s), 1446 (vs), 1388 (m), 1374 (m), 1346 (w), 1320 (w), 1288 (w), 1270 (w), 1247(m), 1205 (w), 1180 (w), 1158 (w), 1132 (s), 1118 (m), 1053 (m), 1029 (w), 1014 (w), 991 (vw), 935 (m), 873 (vw), 848 (m), 807 (s), 781 (vw), 765 (vw), 735 (w), 705 (w), 688 (vw), 650 (vw), 630 (vw), 592 (w), 579 (w), 562 (w), 553 (w), 542 (w), 529 (w), 490 (w), 422 (w).

cAAC^{Me}·SbMes (6.2b):

^{1}H NMR (400.5 MHz, C_6D_6, 298 K): δ = 0.63 (m, 1 H, Cy-CH_2), 1.06 (s, 6 H, NC(CH_3)$_2$), 1.10 (m, 2 H, Cy-CH_2), 1.26 (d, 6 H, $^3J_{H\text{-}H}$ = 6.7 Hz, *i*Pr-CH_3), 1.14 (m, 1 H, Cy-CH_2 overlapped with m, 1 H, Cy-CH_2), 1.68 (m, 2 H, Cy-CH_2), 1.78 (s, 2 H, CH_2), 1.79 (d, 6 H, $^3J_{H\text{-}H}$ = 6.7 Hz, *i*Pr-CH_3), 2.02 (m, 2 H, Cy-CH_2) 2.20 (s, 3 H, Mes-*p*-CH_3), 2.82 (s, 6 H, Mes-*o*-CH_3), 3.06 (sept, 2 H, $^3J_{H\text{-}H}$ = 6.7 Hz, *i*Pr-C*H*), 6.99 (s_{br}, 2 H, Mes-C*H*), 7.17 (d, 1 H, $^3J_{H\text{-}H}$ = 8.7 Hz, Dipp-*m*-C*H*, overlapped with C_6D_5H), 7.17 (d, 1 H, $^3J_{H\text{-}H}$ = 6.7 Hz, Dipp-*m*-C*H*, overlapped with C_6D_5H), 7.67 (dd, 1 H, $^3J_{H\text{-}H}$ = 6.7 Hz, $^3J_{H\text{-}H}$ = 8.7 Hz, Dipp-*p*-C*H*).

^{13}C{^{1}H} NMR (125.8 MHz, C_6D_6, 298 K): δ = 21.2 (Mes-*p*-*C*H_3), 23.3 (Cy-*C*H_2), 25.4 (*i*Pr-*C*H_3), 25.8 (Cy-*C*H_2), 28.9 (*i*Pr-*C*H_3), 29.0 (*i*Pr-*C*H), 29.6 (NC(*C*H_3)$_2$), 31.3 (Mes-*o*-*C*H_3), 37.9 (Cy-*C*H_2),49.6 (*C*H_2), 60.9 (N*C*(CH$_3$)$_2$) 71.9 (NC*C*Cy), 126.4 (Dipp-*m*-*C*H), 127.6 (Mes-*m*-*C*H), 129.4 (Dipp-*p*-*C*H), 136.1 (Dipp-*i*-*C*), 137.2 (Mes-*p*-*C*), 139.2 (Mes-*i*-*C*), 146.1 (Mes-*o*-*C*), 148.0 (Dipp-*o*-*C*), 239.4 (N*C*Sb).

Elemental analysis (%) calcd. for $C_{32}H_{46}NSb$ [566.49 g/mol]: C, 67.85; H, 8.19; N, 2.47; found: C, 67.56; H, 8.33; N, 2.38.

IR ([cm^{-1}]): 3053 (vw), 2963 (s), 2921 (s), 2861 (m), 1678 (m), 1589 (vw), 1463 (m), 1441 (m), 1382 (m), 1362 (m), 1347 (s), 1336 (vs), 1285(w), 1259 (m), 1241 (m), 1227 (m), 1202 (w), 1175 (s), 1153 (m), 1112 (s), 1096 (s), 1050 (s), 1039 (m), 1015 (m), 933 (m), 889 (w), 846 (m), 805 (vs), 777 (m), 766 (w), 699 (w), 638 (vw), 614 (vw), 600 (vw), 579 (vw), 563 (vw), 549, 530 (vw), 477 (vw), 455 (vw), 430 (vw), 411 (vw).

Synthesis of $[cAAC^{Me}{\cdot}SbClMes]^{+}[SbCl_3Mes]^{-}$ (6.3)

A mixture of $cAAC^{Me}$ (10.0 mg, 35.0 µmol, 1 eq) and $SbCl_2Mes$ (21.9 mg, 70.1 µmol, 2 eq) was suspended at room temperature in C_6D_6 (0.6 mL). After a few minutes a yellow oil precipitates which contains a mixture of compounds. At the layer between oil and solvent compound **6.3** crystallizes after 1−3 days. The solvent and residual oil was removed and the crystalline solid was washed with toluene (2 x 1 mL) to yield **6.3** (7.60 mg, 1.42 mmol, 24 %) as a colorless crystalline solid. These crystals were suitable for X-ray diffraction analysis.

^{1}H NMR (500.1 MHz, CD_2Cl_2, 258 K): δ = 1.05 (br, 6 H, Mes-*p*-CH_3), 1.25 (d, 6 H, $^{3}J_{H\text{-}H}$ = 6.3 Hz, *i*Pr-CH_3), 1.61 (s, 6 H, NCC(CH_3)$_2$), 1.72 (s, 6 H, NC(CH_3)$_2$), 2.20 (s, 3 H, Mes-*p*-CH_3), 2.25 (d, 6 H, $^{3}J_{H\text{-}H}$ = 6.3 Hz, *i*Pr-CH_3), 2.27 (s, 3 H, Mes-*p*-CH_3), 2.42 (sept, 2 H, $^{3}J_{H\text{-}H}$ = 6.3 Hz, *i*Pr-C*H*), 2.49 (s, 2 H, CH_2), 2.66 (s, 6 H, Mes-*o*-CH_3), 6.82 (s, 2 H, Mes-C*H*), 6.98 (s, 2 H, Mes-C*H*), 7.34 (d, 2 H, $^{3}J_{H\text{-}H}$ = 7.8 Hz, Dipp-*m*-C*H*), 7.60 (t, 1 H, $^{3}J_{H\text{-}H}$ = 7.8 Hz, Dipp-*p*-C*H*).

^{13}C{^{1}H} NMR (125.8 MHz, CD_2Cl_2, 258 K): δ = 20.9 (Mes-*p*-CH_3), 21.0 (*i*Pr-CH_3), 22.2 (Mes-*o*-CH_3), 24.0 (Mes-*o*-CH_3), 26.1 (Mes-*p*-CH_3, overlapped by NCC(CH_3)$_2$), 27.3 (*i*Pr-CH_3), 28.3 (NC(CH_3)$_2$), 29.4 (*i*Pr-C*H*), 52.9 (CH_2), 57.9 (NCC(CH$_3$)$_2$), 86.1 (NC(CH$_3$)$_2$), 127.3 (Dipp-*m*-CH), 129.9 (Mes-CH_2), 130.2 (Mes-CH_2), 131.7 (Dipp-*i*-C), 132.8 (Dipp-*p*-C), 138.7 (Mes-*p*-C), 140.7 (Mes-*i*-C), 142.6 (Mes-*o*-C), 143.6 (Mes-*p*-C), 144.1 (Dipp-*o*-C), 144.9 (Dipp-*o*-C), 153.4 (Mes-*i*-C), 231.2 (NCSb).

Elemental analysis (%) calcd. for $C_{38}H_{53}Cl_4NSb_2$ + (C_6H_6) [987.28 g/mol]: C, 53.53; H, 6.02; N, 1.42; found: C, 53.14; H, 5.96; N, 1.35.

IR ([cm^{-1}]): 3002 (vw), 2967 (m), 2927 (w), 2867 (w), 1644 (vw), 1595 (w), 1555 (vw), 1526 (w), 1458(m), 1447 (m), 1389 (w), 1373 (m), 1329 (w), 1312 (vw), 1292 (w), 1265 (vw), 1242 (vw), 1203 (vw), 1181 (w), 1121 (w), 1106 (w), 1089 (vw), 1049 (w), 1030 (w), 1010 (vw), 971 (vw), 927 (vw), 874 (vw), 852 (m), 807 (s), 770 (m), 737 (vw), 702 (vw), 672 (vw), 630 (vw), 608 (vw), 593 (vw), 580 (w), 563 (w), 553 (w), 541 (w), 504 (vs), 432 (vw).

7.10 References

[1] J. H. J. Berthel, L. Tendera, M. W. Kuntze-Fechner, L. Kuehn, U. Radius, *Eur. J. Inorg. Chem.* **2019**, 3061-3072.

[2] a) N. Kuhn, T. Kratz, *Synthesis* **1993**, *1993*, 561-562; b) T. Schaub, M. Backes, U. Radius, *Organometallics* **2006**, *25*, 4196-4206; c) T. Schaub, U. Radius, A. Brucks, M. P. Choules, M. T. Olsen, T. B. Rauchfuss, *Inorg. Synth.* **2011**, 78-91.

[3] A. J. Arduengo III, H. V. R. Dias, R. L. Harlow, M. Kline, *J. Am. Chem. Soc.* **1992**, *114*, 5530-5534.

[4] a) X. Bantreil, S. P. Nolan, *Nat. Protoc.* **2011**, *6*, 69-77; b) L. Jafarpour, E. D. Stevens, S. P. Nolan, *J. Organomet. Chem.* **2000**, *606*, 49-54.

[5] V. Lavallo, Y. Canac, C. Prasang, B. Donnadieu, G. Bertrand, *Angew. Chem. Int. Ed.* **2005**, *44*, 5705-5709; *Angew. Chem.* **2005**, *117*, 5851-5855.

[6] B. A. Chalmers, M. Bühl, K. S. Athukorala Arachchige, A. M. Slawin, P. Kilian, *Chem. Eur. J.* **2015**, *21*, 7520-7531.

[7] M. Ates, H. J. Breunig, A. Soltani-Neshan, M. Tegeler, *Z. Naturforsch. B* **1986**, *41*, 321-326.

[8] R. A. Sulzbach, A. F. M. Iqbal, *Angew. Chem. Int. Ed.* **1971**, *10*, 127; *Angew. Chem.* **1971**, *4*, 145.

[9] H. Gilman, J. D. Robinson, *J. Am. Chem. Soc.* **1929**, *51*, 3112-3114.

[10] J. A. Cooke, C. E. Dixon, M. R. Netherton, G. M. Kollegger, R. M. Baines, *Synth. React. Inorg. Met.-Org. Chem.* **1996**, *26*, 1205-1217.

[11] A. G. Hernan, P. N. Horton, M. B. Hursthouse, J. D. Kilburn, *J. Organomet. Chem.* **2006**, *691*, 1466-1475.

[12] J. E. Griffiths, *Inorg. Chem.* **2002**, *2*, 375-377.

[13] a) A. E. Finholt, A. C. Bond, K. E. Wilzbach, H. I. Schlesinger, *J. Am. Chem. Soc.* **2002**, *69*, 2692-2696; b) F. Paneth, G. Joachimoglu, *Chem. Ber.* **2006**, *57*, 1925-1930.

[14] G. R. Fulmer, A. J. M. Miller, N. H. Sherden, H. E. Gottlieb, A. Nudelman, B. M. Stoltz, J. E. Bercaw, K. I. Goldberg, *Organometallics* **2010**, *29*, 2176-2179.

[15] R. K. Harris, E. D. Becker, S. M. C. De Menezes, R. Goodfellow, P. Granger, *Pure Appl. Chem.* **2001**, *73*, 1795-1818.

8 Crystallographic Details

8.1 Collection parameters

Crystal data were collected on a Bruker X8 Apex-2 diffractometer with a CCD area detector and graphite monochromated Mo-Kα radiation on a Rigaku XtaLAB Synergy-DW diffractometer with an Hy-Pix-6000HE detector and monochromated CuKα radiation equipped with an Oxford Cryo 800 cooling unit or a Rigaku XtaLAB Synergy-R diffractometer with a HPA area detector and multi-layer mirror monochromated Cu-Kα radiation. The crystals were immersed in a film of perfluoropoly-ether oil on a glass fiber MicroMount^{TM} (MiTeGen) and data were collected at 100 K. The images were processed with the Bruker or Crysalis software packages and equivalent reflections were merged. Corrections for Lorentz-polarization effects and absorption were performed if necessary and the structures were solved by direct methods. Subsequent difference Fourier syntheses revealed the positions of all other non-hydrogen atoms. The structures were solved by using the ShelXTL software package.[1] All non-hydrogen atoms were refined anisotropically. Hydrogen atoms were assigned to idealized positions and were included in structure factors calculations. The Diamond software was used for graphical representation.

The crystallographic data (cif-files) of the published compounds were uploaded to the **C**ambridge **C**rystallographic **D**ata **C**entre (CCDC) and can be obtained free of charge from *via* www.ccdc.cam.ac.uk/data_request/cif.

[1] G. M. Sheldrick, *Acta Crystallogr. Sect. C: Cryst. Struct. Commun.* **2015**, *71*, 3-8.

8.2 Crystallographic data

8.2.1 Crystallographic Data of Chapter II

Crystallographic data (excluding structure factors) for the structures reported in Chapter II have been deposited with the Cambridge Crystallographic Data Centre as supplementary publication no.s CCDC 2184111 (**2.2b**), 21841112 (**2.2c**), 2184113 (**2.1a**), 2184114 (**2.4**), 2184115 (**2.1b**), 2184116 (**2.1c**), 2184117 (**2.7**), 2184118 (**2.10**), 2184119 (**2.9**), 2184120 (**2.5**), 2184121 (**2.3**), 2184122 (**2.13**), 2184123 (**2.14**), 2184124 (**2.8**), 2184125 (**2.12**), 2184126 (**2.11**), 2184127 (**2.6**).

8.2.2 Crystallographic Data of Chapter III

Crystallographic data (excluding structure factors) for the structures reported in Chapter III have been deposited with the Cambridge Crystallographic Data Centre as supplementary publication no.s CCDC 2195878 (**3.3**), CCDC 2195879 (**3.1**), CCDC 2195880 (**3.2**).

8.2.3 Crystallographic Data of Chapter IV

Crystallographic data (excluding structure factors) for the structures reported in Chapter IV have been deposited with the Cambridge Crystallographic Data Centre as supplementary publication no.s CCDC 2193317 (**4.2**), CCDC 2193318 (**4.5**), CCDC 2193319 (**4.8**), CCDC 2193320 (**4.10**), CCDC 2193321 (**4.9**), CCDC 2193322 (**4.6**), CCDC 2193323 (**4.4**), and CCDC 2193324 (**4.7**).

8.2.4 Crystallographic Data of Chapter V

Crystallographic data (excluding structure factors) for the structures reported in Chapter V have been deposited with the Cambridge Crystallographic Data Centre as supplementary publication no.s CCDC 2098205 (**5.5a**), CCDC 2098206 (**5.4e**), CCDC 2098207 (**5.4a**), CCDC 2098208 (**5.5b**), CCDC 2098209 (**5.6a**), CCDC 2098210 (**5.4b**), CCDC 2098211 (**5.4c**), CCDC 2098212 (**5.4d**), CCDC 2098213 (**5.5.6b**), CCDC 2098214 (**5.5d**), CCDC 2098215 (**5.5e**), CCDC 2098216 (**5.7**), CCDC 2098217 (**5.6d**), CCDC 2098218 (**5.10**), CCDC 2098219 (**5.9**), CCDC 2098220 (**5.8**).

8.2.5 Crystallographic Data of Chapter VI

Crystallographic data (excluding structure factors) for the structures reported in Chapter VI have been deposited with the Cambridge Crystallographic Data Centre as supplementary publication no.s CCDC 2154795 (**6.1a**), CCDC 2154792 (**6.1b**), CCDC 2154796 (**6.2a**), CCDC 2154793 (**6.2b**), CCDC 2154794 (**6.3**).

9 Computational Details

9.1 Computational Details of Chapter III

Calculations were carried out using the TURBOMOLE V7.2 2017 program suite, a development of the University of Karlsruhe and the Forschungszentrum Karlsruhe GmbH, 1989-2007, TURBOMOLE GmbH, since 2007; available from http://www.turbomole.org.[1] Geometry optimizations and frequency calculations were performed using (RI-)DFT calculations[2-3] on a m4 grid employing the M06-2x[4] functional and a def2-TZVP basis set for Si and Ge and def2-SVP basis sets for C, H, N and Cl atoms.[5] The resulting energies (Figure 2) were calculated using the same functional but a def2-TZVPP basis set[5] for all atoms.

9.2 Computational Details of Chapter V

The calculations were carried out using the TURBOMOLE V7.5.1 suite of programs.[6] Geometry optimizations were performed using (RI-)DFT calculations[2] on the B3LYP/def2-SV(P) level of theory.[5e, 7-8]

9.3 Computational Details of Chapter VI

The calculations were carried out using the TURBOMOLE V7.5.1 suite of programs.[6] Geometry optimizations were performed using (RI-)DFT calculations[2] on a m4 grid employing the D3BJ[9] dispersion-corrected M06-2x[10] functional and a def2-TZVP basis set for Sb and def2-SVP basis sets for C, H, N and Cl atoms.[8a, 11] Wiberg bond indices[12] have been evaluated from the DFT ground state electron density.

9.4 References

[1] S. G. Balasubramani; G. P. Chen; S. Coriani; M. Diedenhofen; M. S. Frank; Y. J. Franzke; F. Furche; R. Grotjahn; M. E. Harding; C. Hättig; A. Hellweg; B. Helmich- Paris; C. Holzer; U. Huniar; M. Kaupp; A. Marefat Khah; S. Karbalaei Khani; T. Müller; F. Mack; B. D. Nguyen; S. M. Parker; E. Perlt; D. Rappoport; K. Reiter; S. Roy; M. Rückert; G. Schmitz; M. Sierka; E. Tapavicza; D. P. Tew; C. van Wüllen; V. K. Voora; F. Weigend; A. Wodyński; J. M. Yu. *J. Chem. Phys.* **2020**, *152*, 184107.

[2] a) M. Häser, R. Ahlrichs, *J. Comput. Chem.* **1989**, *10*, 104-111; b) O. Treutler, R. Ahlrichs, *J. Chem. Phys. C.* **1995**, *102*, 346-354; c) K. Eichkorn, O. Treutler, H. Öhm, M. Häser, R. Ahlrichs, Chem. Phys. Lett. **1995**, *242*, 652-660; d) K. Eichkorn, F. Weigend, O. Treutler, R. Ahlrichs, *Theor. Chem. Acc.* **1997**, *97*, 119-124; e) M. v. Arnim, R. Ahlrichs, *J. Comp. Chem.* **1998**, *19*, 1746-1757; f) F. Weigend, *Phys. Chem. Chem. Phys.* **2002**, *4*, 4285-4291; g) M. Sierka, A. Hogekamp R. Ahlrichs, *J. Chem. Phys.* **2003**, *118*, 9136-9148; h) P. Deglmann, K. May, F. Furche, R. Ahlrichs, *Chem. Phys. Lett.* **2004**, *384*, 103-107; i) R. Ahlrichs, Phys. Chem. Chem. Phys. **2004**, *6*, 5119-5121.

[3] a) P. Deglmann, F. Furche, R. Ahlrichs, *Chem. Phys. Lett.* **2002**, *362*, 511-518; b) P. Deglmann, F. Furche, *J. Chem. Phys.* **2002**, *117*, 9535.

[4] Y. Zhao, D. Truhlar, *Theor. Chem. Acc.* **2008**, *120*, 215–241.

[5] a) H. Horn, R. Ahlrichs, *J. Chem. Phys.* **1992**, *97*, 2571-2577; b) A. Schäfer, C. Huber, R. Ahlrichs, *J. Chem. Phys.* **1994**, *100*, 5829-5835. c) K. Eichkorn, O. Treutler, H. Öhm, M. Häser R. Ahlrichs, *Chem. Phys. Let.* **1995**, *242*, 652-660; d) K. Eichkorn, F. Weigend, O. Treutler, R. Ahlrichs, *Theor. Chem. Acc.* **1997**, *97*, 119-124; e) F. Weigend, R. Ahlrichs, *Phys. Chem. Chem. Phys.* **2005**, *7*, 3297-3305; f) F. Weigend, *Phys. Chem. Chem. Phys.* **2006**, *8*, 1057-1065.

[6] a) R. Ahlrichs, M. Bär, M. Häser, H. Horn, C. Kölmel, *Chem. Phys. Lett.* **1989**, *162*, 165-169; b) F. Furche, R. Ahlrichs, C. Hättig, W. Klopper, M. Sierka, F. Weigend, *Wiley Interdiscip. Rev.-Comput. Mol. Sci.* **2014**, *4*, 91-100.

[7] a) A. D. Becke, *Phys. Rev. A* **1988**, *38*, 3098-3100; b) C. Lee, W. Yang, R. G. Parr, *Phys. Rev. B*, **1988**, *37*, 785-789; c) A. D. Becke, *J. Chem. Phys.* **1993**, *98*, 5648-5652.

[8] a) A. Schäfer, H. Horn, R. Ahlrichs; *J. Chem. Phys.* **1992**, *97*, 2571-2577; b) F. Weigend, M. Häser, H. Patzelt, R. Ahlrichs; *Chem. Phys. Letters* **1998**, *294*, 143; c) A. Hellweg, C. Hättig, S. Höfener, W. Klopper; *Theor. Chem. Acc.* **2007**, *117*, 587.

[9] a) S. Grimme, J. Antony, S. Ehrlich, H. Krieg, *J. Chem. Phys.* **2010**, *132*, 154104; b) S. Grimme, S. Ehrlich, L. Goerigk, *J. Comput. Chem.* **2011**, *32*, 1456-1465.

[10] Y. Zhao, D. G. Truhlar, *Theor. Chem. Acc.* **2007**, *120*, 215-241.

[11] F. Weigend, *Phys. Chem. Chem. Phys.* **2006**, *8*, 1057-1065.

[12] K. A. Wiberg, *Tetrahedron* **1968**, *24*, 1083-1096.

10 Summary

This thesis reports on synthesis and reactivity of new NHC- and cAAC-stabilized *Lewis*-acid/*Lewis*-base adducts of group 14 and group 15 element compounds. Since this field of chemistry offers a variety of reactivities and new classes of compounds, Chapter I gives an general introduction into this field.

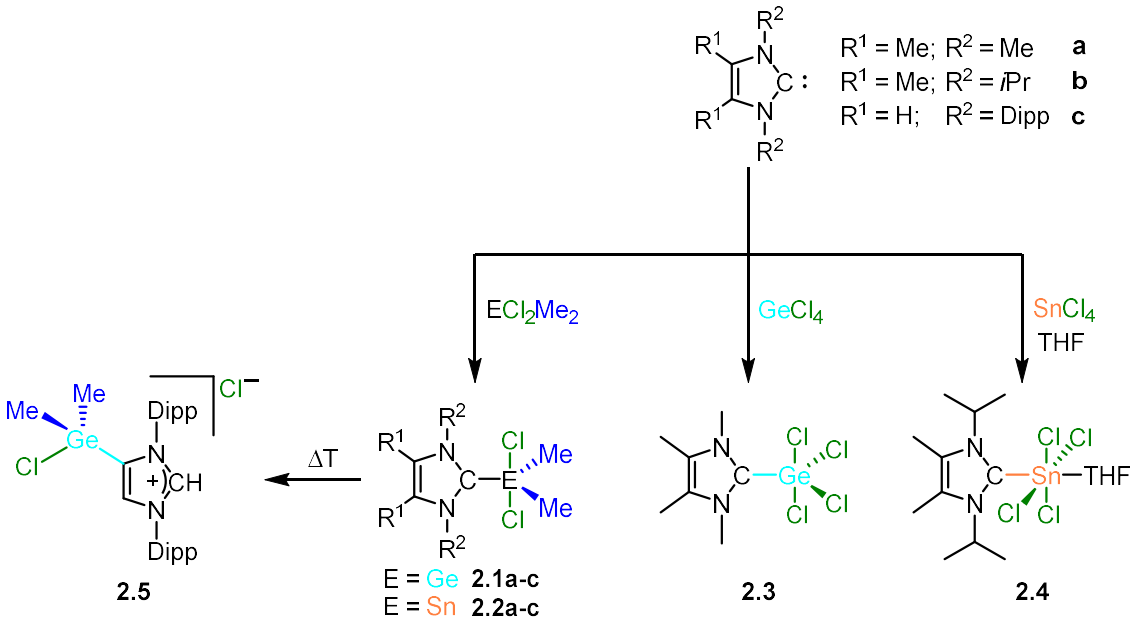

Scheme 10.1: Synthesis of NHC-stabilized germanium and tin chloride compounds **2.1**-**2.4** as well as thermal induced isomerization of **2.1c** to **2.5**.

NHC-stabilized element chloride adducts are suitable starting materials for the synthesis of the low-valent and thus highly reactive main-group element compounds, Chapter II examines the reactivity of NHCs and cAAC^{Me} towards various germanium and tin chlorides. The reaction of ECl_2Me_2 (E = Ge, Sn) with the NHCs Me_2Im^{Me} (**a**), iPr_2Im^{Me} (**b**) and $Dipp_2Im$ (**c**) led to formation of the adducts NHC·ECl_2Me_2 (**2.1a**-**2.2c**, Scheme 10.1), respectively. In addition, the reaction of Me_2Im^{Me} with $GeCl_4$ yielded the trigonal bipyramidal adduct Me_2Im^{Me}·$GeCl_4$ (**2.3**, Scheme 10.1). In contrast, the reaction of iPr_2Im^{Me} with $SnCl_4$ in THF afforded iPr_2Im^{Me}·$SnCl_4$·THF (**2.4**, Scheme 10.1) with an octahedral coordination environment. Thermal treatment of the sterically demanding NHC adduct **2.1c** yielded the abnormally coordinated adduct salt $[^aDipp_2Im·GeClMe_2]^+[Cl]^-$ (**2.5**, Scheme 10.1).

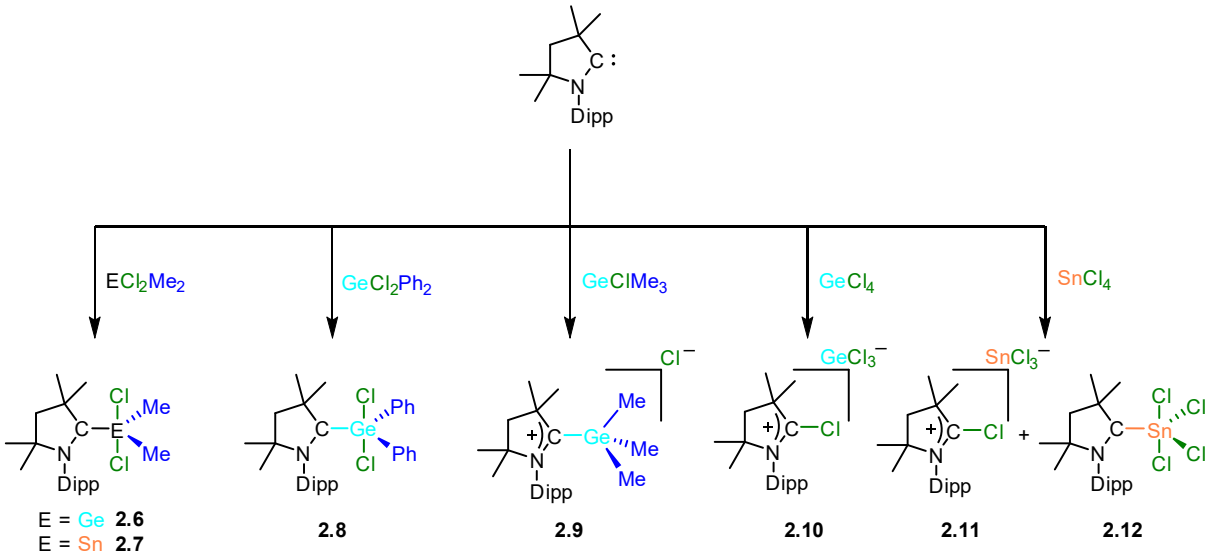

Scheme 10.2: Synthesis of cAAC^{Me} adducts (**2.6-2.9**, **2.12**) and salts (**2.10**, **2.11**) with different germanium and tin chloride compounds.

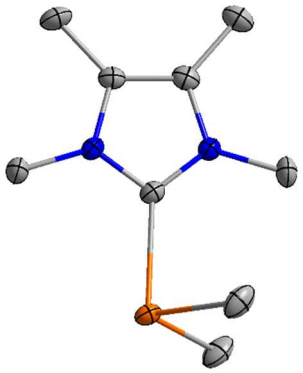

2.13

Figure 10.1: Molecular structure of **2.13.**

Analogously to the syntheses of **2.1a-2.2c**, the reaction of cAAC^{Me} with ECl_2Me_2 (E = Ge, Sn) and $GeCl_2Ph_2$ afforded the adducts cAAC^{Me}·$GeCl_2Me_2$ (**2.6**, Scheme 10.2), cAAC^{Me}·$SnCl_2Me_2$ (**2.7**, Scheme 10.2) and cAAC^{Me}·$GeCl_2Ph_2$ (**2.8**, Scheme 10.2), respectively. In contrast, the formation of the salts $[cAAC^{Me}GeMe_3]^+[Cl]^-$ (**2.9**, Scheme 10.2) and $[cAAC^{Me}Cl]^+[GeCl_3]^-$ (**2.10**, Scheme 10.2) was observed for the reaction of cAAC^{Me} with $GeClMe_3$ and $GeCl_4$, respectively. For the reaction with $SnCl_4$, both the isostructural salt $[cAAC^{Me}Cl]^+[SnCl_3]^-$ (**2.11**, Scheme 10.2) and the adduct cAAC^{Me}·$SnCl_4$ (**2.12**, Scheme 10.2) were obtained. Since the compounds **2.1a-2.12** may be reduced to form low-valent compounds, the adduct **2.2a** was treated with KC_8 to isolate the stannylene Me_2Im^{Me}·$SnMe_2$ (**2.13**, Figure 10.1). In contrast, reductions of $SnCl_2Me_2$ in the presence of iPr_2Im^{Me} or $Dipp_2Im$ as well as reductions of their adducts **2.2b** and **2.2c** have been unsuccessful. However, the reduction of **2.7** resulted in an unstable

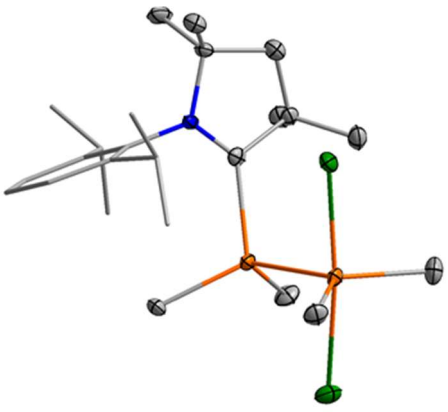

2.14

Figure 10.2: Molecular structure of cAAC^{Me}·$SnMe_2$·$SnMe_2Cl_2$ (**2.14**).

stannylene, which could be stabilized by an additional equivalent of $SnCl_2Me_2$ to afford $cAAC^{Me}{\cdot}SnMe_2{\cdot}SnMe_2Cl_2$ (**2.14**, Figure 10.2).

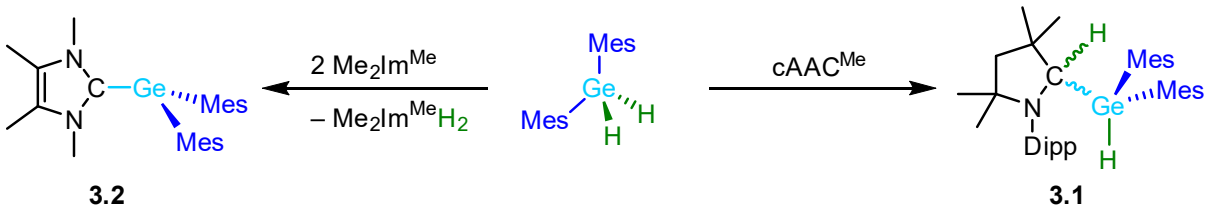

Scheme 10.3: Reaction of $cAAC^{Me}$ and Me_2Im^{Me} with GeH_2Mes_2.

The compounds **2.1a**-**2.12** were investigated as starting materials for the synthesis of the corresponding carbene-stabilized hydride compounds by chlorine/hydrogen exchange with hydrogenation agents. However, the hydrogenation of **2.1a**-**2.12** was unsuccessful, but the reactivity of carbenes towards selected tetrelanes is reported in Chapter III. The reaction of GeH_2Mes_2 with $cAAC^{Me}$ resulted in the insertion of the carbene carbon atom into one Ge–H bond and the subsequent isolation of $cAAC^{Me}H$–$GeHMes_2$ (**3.1**, Scheme 10.3, Figure 10.3). However, the reaction of GeH_2Mes_2 with two equivalents of Me_2Im^{Me} at elevated temperatures yielded the literature known NHC-stabilized germylene $Me_2Im^{Me}{\cdot}GeMes_2$ (**3.2**, Scheme 10.3) by dehydrogenation of GeH_2Mes_2 and formation of $NHCH_2$.

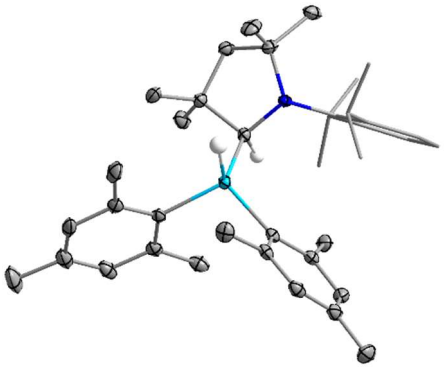

3.1

Figure 10.3: Molecular structure of $cAAC^{Me}H$–$GeHMes_2$ (**3.1**).

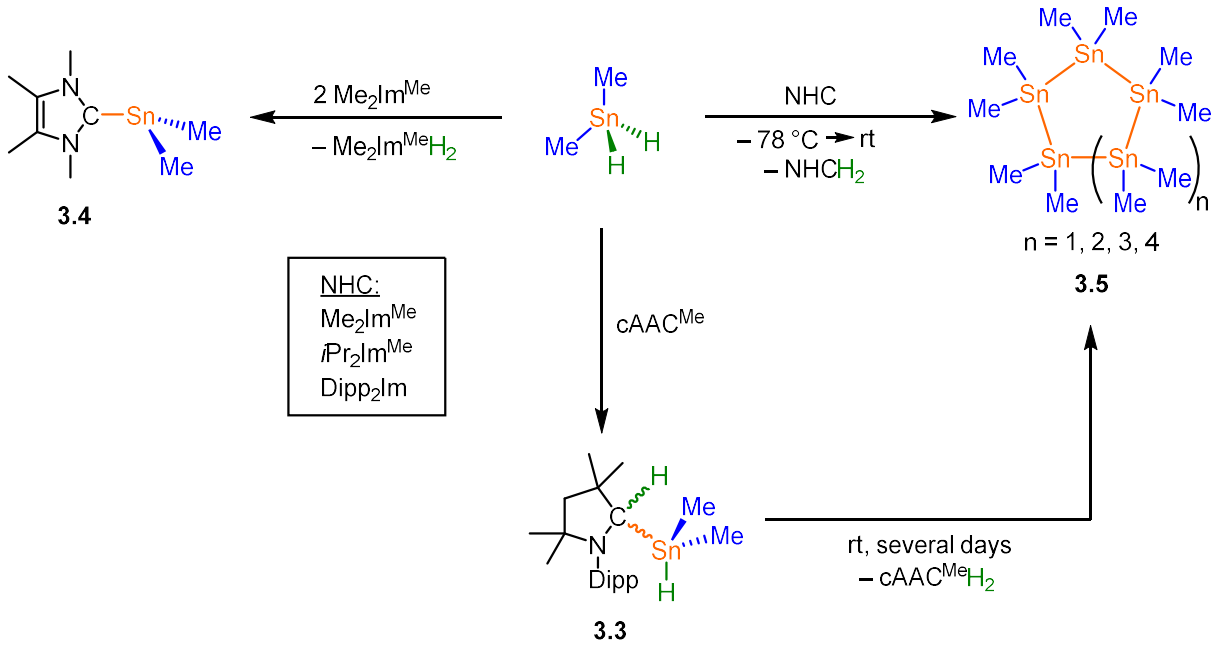

Scheme 10.4: Reaction of the NHCs Me_2Im^{Me}, iPr_2Im^{Me}, $Dipp_2Im$ and $cAAC^{Me}$ with SnH_2Me_2.

As with the synthesis of **3.1**, the reaction of SnH_2Me_2 with $cAAC^{Me}$ afforded the insertion product $cAAC^{Me}H–SnHMe_2$ (**3.3**, Scheme 10.4). Furthermore, the NHC mediated dehydrogenation of SnH_2Me_2 led to the NHC-stabilized stannylene $Me_2Im^{Me}{\cdot}SnMe_2$ (**3.4**, Scheme 10.4). Reacting the sterically more demanding NHCs iPr_2Im^{Me} and $Dipp_2Im$ as well as just one equivalent of Me_2Im^{Me} with SnH_2Me_2 at low temperatures gave rise to the dehydrogenative coupling of the *in situ* formed $\{SnMe_2\}$ moieties selectively to form one tin oligomer $(SnMe_2)_n$ (**3.5**, Scheme 10.4) as a yellow solid, which is supposed to be the *cyclo*-pentamer. In solution, the tin *cyclo*-oligomers $(SnMe_2)_n$ (n = 6, 7, 8) were observed *via* NMR. In addition, compound **3.3** was completely transformed into the same tin cyclomers after a few days in solution. Thermal treatment of **3.3** or **3.5** as well as the reaction of the NHCs with SnH_2Me_2 at room temperature, also led to the formation of the tin cyclomers $(SnMe_2)_n$ (n = 6, 7, 8) and additional formation of another oligomer, proposed to be the *cyclo*-pentamer. Thus, it can be assumed that compound **3.3** represents an intermediate in the DHC of SnH_2Me_2.

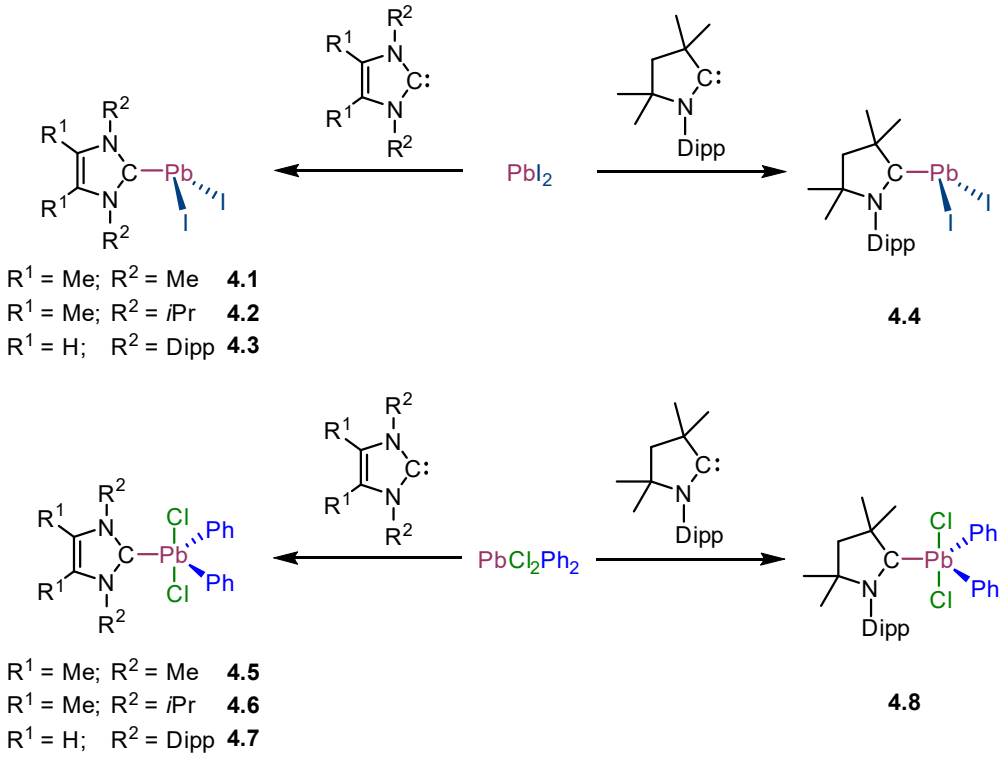

Scheme 10.5: Synthesis of NHC and cAAC-supported PbI_2 (**4.1**-**4.4**) and $PbCl_2Ph_2$ (**4.5**-**4.7**) adducts.

The large variety of new compounds of the elements germanium and tin inspired the investigations into similar lead compounds. Thus, in Chapter IV the NHCs and $cAAC^{Me}$ were treated with PbI_2 affording the plumbylenes $Me_2Im^{Me}{\cdot}PbI_2$ (**4.1**), $iPr_2Im^{Me}{\cdot}PbI_2$ (**4.2**), $Dipp_2Im{\cdot}PbI_2$ (**4.3**) and $cAAC^{Me}{\cdot}PbI_2$ (**4.4**), respectively (Scheme 10.5, top). Since arylation of the lead(II) compounds **4.1**-**4.4** has so far been unsuccessful, another reaction pathway was chosen. The Pb(IV) adducts $NHC{\cdot}PbCl_2Ph_2$ (**4.5**-**4.7**) and $cAAC^{Me}{\cdot}PbCl_2Ph_2$ (**4.8**) were synthesized by reaction of the precursor $PbCl_2Ph_2$ and the corresponding carbenes (Scheme 10.5, bottom). Further reduction of **4.5** and **4.6** with KC_8 yielded the corresponding NHC-stabilized diaryl substituted plumbylenes $Me_2Im^{Me}{\cdot}PbPh_2$ (**4.9**, Figure 10.4) and $iPr_2Im^{Me}{\cdot}PbPh_2$ (**4.10**). NMR spectroscopic studies suggest coexistence of the respective NHC and a $\{PbPh_2\}$ moiety in solution.

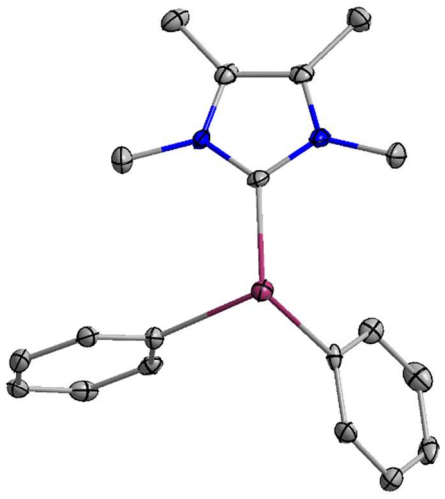

4.9

Figure 10.4: Molecular structure of $Me_2Im^{Me}{\cdot}PbPh_2$ (**4.9**).

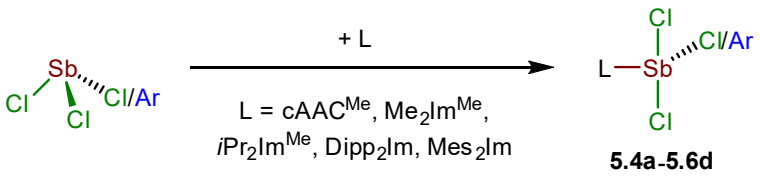

Scheme 10.6: Synthesis of NHC- and cAAC^{Me}-stabilized $SbCl_3$ (**5.4a-e**), $SbCl_2Ph$ (**5.5a-e**) and $SbCl_2Mes$ (**5.6a-d**) adducts.

In addition to the chemistry with heavy group 14 elements, the reactivity and synthesis of NHC- and cAAC-stabilized compounds of the heavy group 15 element antimony were reported in Chapter V. The adducts NHC·$SbCl_2R$ (R = Cl, Ph, Mes) (**5.4a-5.6d**) were prepared by reaction of the antimony compounds $SbCl_2R$ (R = Cl, Ph, Mes) with the corresponding carbenes (L) (Scheme 10.6). The data obtained for **5.4a-5.6d** give further insight into the bonding situation at antimony and how the use of a variety of carbenes, with differing substitution patterns, on top of different substituents affects the chemistry of these adducts. Thermal treatment of Dipp$_2$Im·$SbCl_2$Mes (**5.6c**) and Dipp$_2$Im·$SbCl_2$Ph (**5.5c**) or their precursors led to a change in coordination and consequently to the abnormally coordinated adducts ^{a}Dipp$_2$Im·$SbCl_2$Ar (Ar = Mes (**5.7**), Ph (**5.8**)), respectively. Chloride abstraction from **5.7** by the *Lewis*-acids $GaCl_3$ and $AgBF_4$ afforded the ionic compounds $[^a\text{Dipp}_2\text{Im}\cdot\text{SbClMes}]^+[X]^-$ ($[X]^- = [BF_4]^-$ (**5.9**, Figure 10.5); $[GaCl_4]^-$ (**5.10**)).

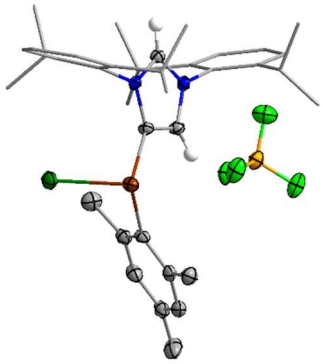

5.9

Figure 10.5: Molecular structures of $[^a\text{Dipp}_2\text{Im}\cdot\text{SbClMes}]^+[BF_4]^-$ (**5.9**).

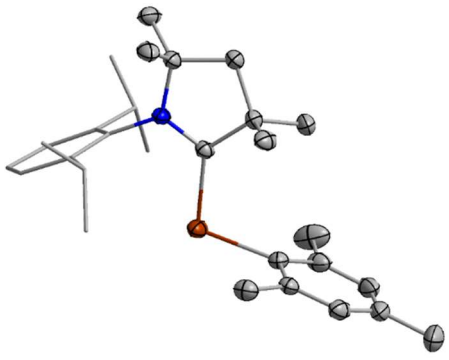

6.2a

Figure 10.6: Molecular structure of cAAC^{Me}·SbMes (**6.2a**).

The range of antimony adducts synthesized in Chapter V is in opposition to in the reactivity of cAACs towards $SbCl_2Mes$, which was investigated in further detail in Chapter VI. The investigations showed that the reaction of $SbCl_2Mes$ with cAAC^{Me} and cAAC^{Cy} leads to the cAAC-stabilized stibinidenes cAAC^{Me}·SbMes (**6.2a**, Figure 10.6) and cAAC^{Cy}·SbMes (**6.2b**), respectively. This reaction is accompanied by the 50 % formation of the salts [cAAC^{Me}Cl]$^+$[$SbCl_3Mes$]$^-$ (**6.1a**) and [cAAC^{Cy}Cl]$^+$[$SbCl_3Mes$]$^-$ (**6.1b**), respectively. The bonding situation of **6.2a** was examined in some detail with the aid of DFT calculations, which confirms an antimony carbene carbon double bond.

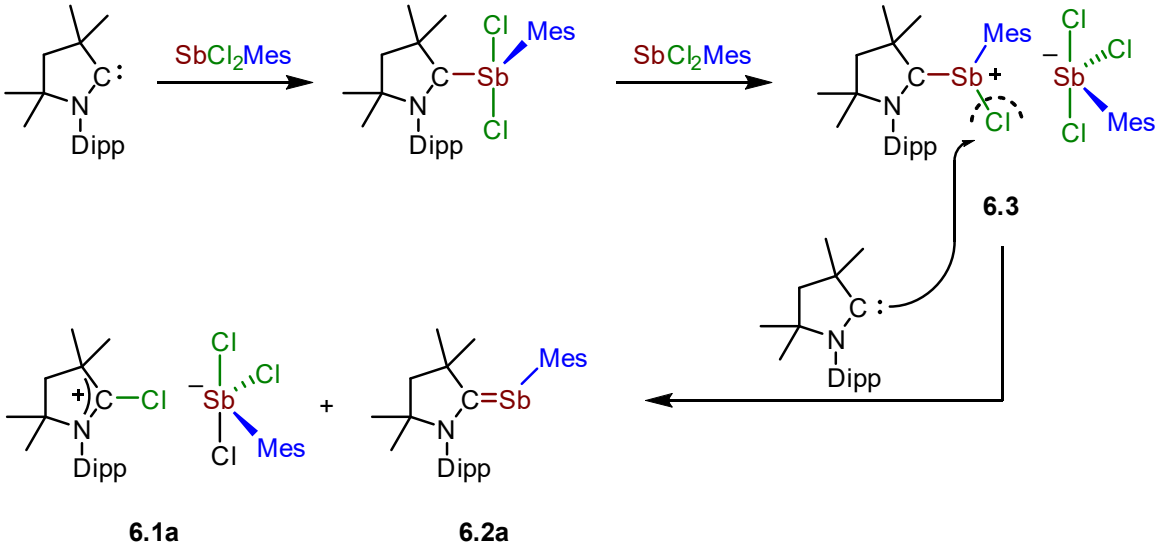

Scheme 10.7: Proposed mechanism with the intermediate **6.3** for the formation of the compounds **6.1a** and **6.2a**.

A mechanism was proposed for this reaction which explains the reduction of the intermediate [cAAC^{Me}·SbClMes]$^+$[$SbCl_3Mes$]$^-$ (**6.3**) with the carbene carbon atom acting as a reducing reagent, yielding the stibinidene cAAC^{Me}·SbMes (**6.2a**, Scheme 10.7). To corroborate this mechanism, the key intermediate [cAAC^{Me}·SbClMes]$^+$[$SbCl_3Mes$]$^-$ (**6.3**) of this reaction sequence was isolated by reaction of cAAC^{Me} with two equivalents of $SbCl_2Mes$.

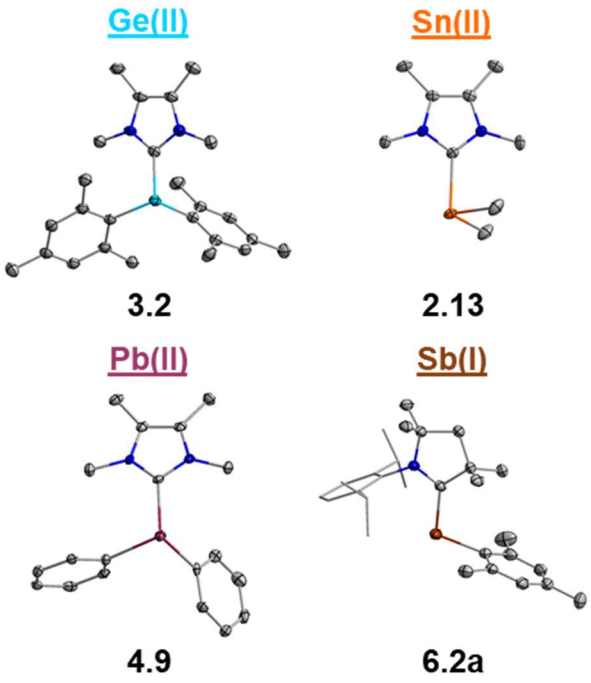

Figure 10.7: Molecular structures of the low-valent compounds **3.2**, **2.13**, **4.9** and **6.2a.**

In the course of this work, the syntheses and reactivities of NHC- and cAAC-stabilized group 14 and group 15 element compounds were investigated in detail and various reduction pathways to low-valent compounds of each element (Figure 10.7) were established. Remarkable differences in reactivity between the NHCs and cAACs could be observed. For GeH_2Mes_2, complete reduction to the corresponding NHC-stabilized germylene was observed with Me_2Im^{Me}, while only insertion into a Ge–H bond was obtained with cAAC. For stannanes, the dehydrogenative coupling of $\{SnMe_2\}$ moieties was also observed for both carbene types. For antimony, the first known metal-free and carbene-mediated reduction of Sb(III) to Sb(I) could be realized under mild conditions and in quantitative yields.

11 Zusammenfassung

In der vorliegenden Arbeit wird die Synthese und Reaktivität neuer NHC- und cAAC-stabilisierter *Lewis*-Säure/*Lewis*-Base-Addukte von Verbindungen mit Elementen der Gruppen 14 und 15 beschrieben. Da dieses Feld der Chemie eine breite Spanne an Reaktivitäten und neuen Verbindungsklassen aufweist, bietet Kapitel I eine allgemeine Übersicht des derzeitigen Kenntnisstandes in diesem Gebiet.

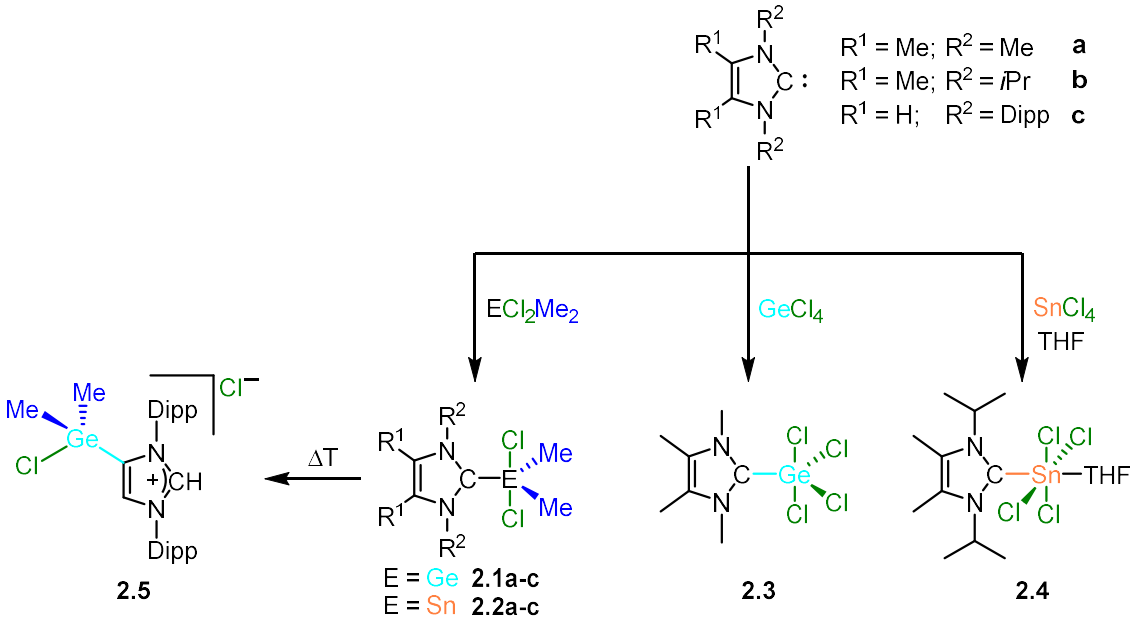

Schema 11.1: Synthese der NHC-stabilisierten Germanium- und Zinnchloridverbindungen **2.1-2.4** sowie die thermisch induzierte Isomerisierung von **2.1c** zu **2.5**.

NHC-stabilisierte Elementchlorid-Addukte sind geeignete Ausgangsmaterialien für die Synthese von niedervalenten und häufig hochreaktiven Hauptgruppenelementverbindungen. In Kapitel II wird über die Reaktivität von NHCs und cAAC^{Me} gegenüber verschiedenen Germanium- und Zinnchloriden berichtet. Die Reaktion von ECl_2Me_2 (E = Ge, Sn) mit den freien NHCs Me_2Im^{Me} (**a**), iPr_2Im^{Me} (**b**) und $Dipp_2Im$ (**c**) führte je zur Bildung des entsprechenden Addukts NHC·ECl_2Me_2 (**2.1a-2.2c**, Schema 11.1). Darüber hinaus lieferte die Reaktion von Me_2Im^{Me} mit $GeCl_4$ das trigonal-bipyramidale Addukt Me_2Im^{Me}·$GeCl_4$ (**2.3**, Schema 11.1). Im Gegensatz dazu ergab die Reaktion von iPr_2Im^{Me} mit $SnCl_4$ in THF das Addukt iPr_2Im^{Me}·$SnCl_4$·THF (**2.4**, Schema 11.1) mit einer oktaedrischen Koordinationsumgebung. Die thermische Belastung des sterisch anspruchsvollen NHC-Addukts **2.1c** führte über einen

Koordinationswechsel zum abnormal koordinierten Adduktsalz [^{a}Dipp$_2$Im·GeClMe$_2$]$^+$[Cl]$^-$ (**2.5**, Schema 11.1).

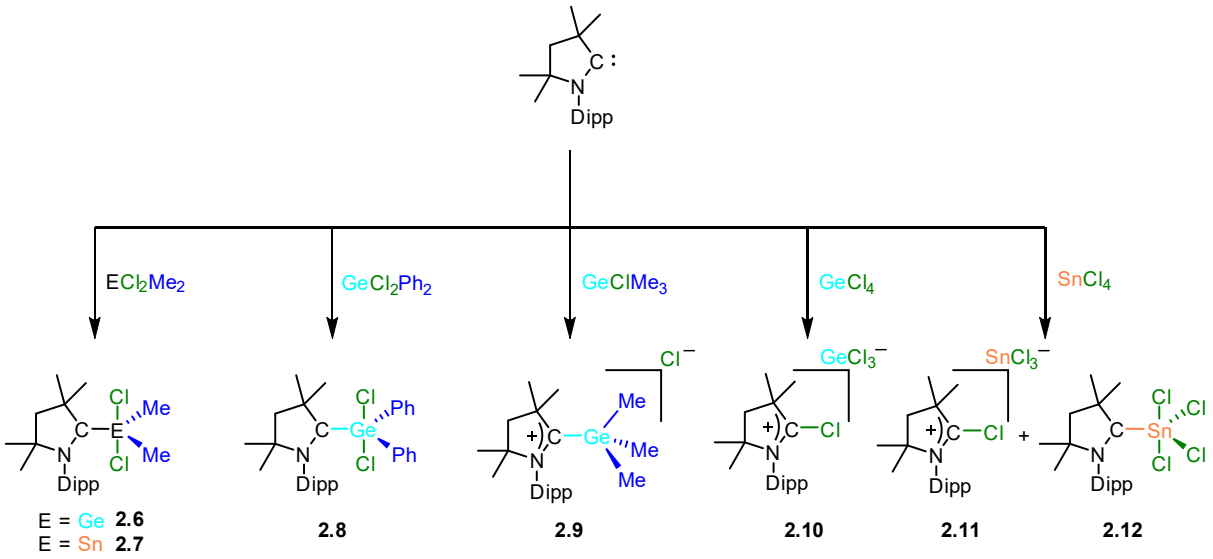

Schema 11.2: Synthese der cAAC^{Me}-Addukte **2.6-2.9** und **2.12** sowie der Salze **2.10** und **2.11** ausgehend von verschiedenen Germanium- und Zinnchloridverbindungen.

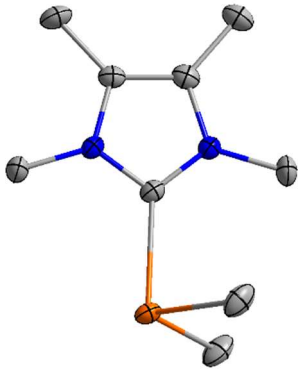

2.13

Abbildung 11.1: Molekülstruktur von **2.13**.

Analog zu den Synthesen der Verbindungen **2.1a-2.2c**, führten die Reaktionen von cAAC^{Me} mit ECl$_2$Me$_2$ (E = Ge, Sn) bzw. GeCl$_2$Ph$_2$ zur Biildung der Addukte cAAC^{Me}·GeCl$_2$Me$_2$ (**2.6**, Schema 11.2), cAAC^{Me}·SnCl$_2$Me$_2$ (**2.7**, Schema 11.2) bzw. cAAC^{Me}·GeCl$_2$Ph$_2$ (**2.8**, Schema 11.2). Im Vergleich dazu wurde für die Reaktion von cAAC^{Me} mit GeClMe$_3$ oder GeCl$_4$ die Bildung der entsprechenden Salze [cAAC^{Me}GeMe$_3$]$^+$[Cl]$^-$ (**2.9**, Schema 11.2) und [cAAC^{Me}Cl]$^+$[GeCl$_3$]$^-$ (**2.10**, Schema 11.2) beobachtet. Für die Reaktion mit SnCl$_4$ konnte sowohl das isostrukturelle Salz [cAAC^{Me}Cl]$^+$[SnCl$_3$]$^-$ (**2.11**, Schema 11.2), als auch das Addukt cAAC^{Me}·SnCl$_4$ (**2.12**, Schema 11.2) erhalten werden. Da die Verbindungen **2.1a-2.12** potentiell zu entsprechenden niedervalenten Verbindungen reduziert werden können, wurde **2.2a**

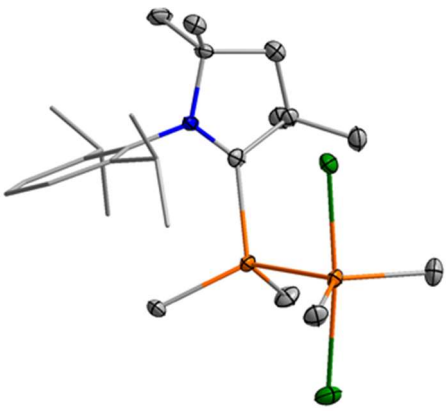

2.14

Abbildung 11.2: Molekülstruktur von cAAC^{Me}·SnMe$_2$·SnMe$_2$Cl$_2$ (**2.14**).

mit KC_8 umgesetzt, wodurch $Me_2Im^{Me}{\cdot}SnMe_2$ (**2.13**, Abbildung 11.1) als Reduktionsprodukt isoliert wurde. Allerdings blieben sowohl die Reduktionsversuche von $SnCl_2Me_2$ in Anwesenheit von iPr_2Im^{Me} oder $Dipp_2Im$ als auch der Addukte **2.2b** und **2.2c** erfolglos. Die Reduktion von **2.7** führte zu einem instabilen Stannylen, welches durch ein weiteres Äquivalent $SnCl_2Me_2$ stabilisiert und als $cAAC^{Me}{\cdot}SnMe_2{\cdot}SnMe_2Cl_2$ (**2.14**, Abbildung 11.2) isoliert werden konnte.

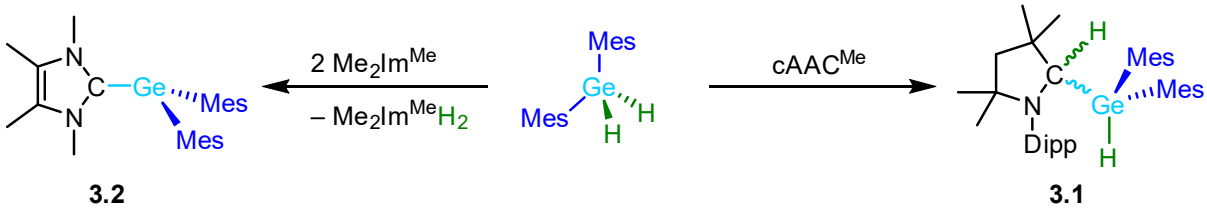

Schema 11.3: Reaktionen von $cAAC^{Me}$ und Me_2Im^{Me} mit GeH_2Mes_2.

Die Verbindungen **2.1a-2.12** wurden bezüglich Chlor/Wasserstoff-Austauschreaktionen durch Hydrierungsmitteln untersucht wodurch entsprechende Carben-stabilisierte Hydridverbindungen erhalten werden könnten. Jedoch blieb die Hydrierung der Verbindungen **2.1a-2.12** erfolglos, weshalb auch die Reaktivität von NHCs und $cAAC^{Me}$ gegenüber verschiedenen Tetrel-Wasserstoffverbindungen untersucht und in Kapitel III beschrieben wurde. Die Reaktion von GeH_2Mes_2 mit $cAAC^{Me}$ resultierte in der Insertion des Carbenkohlenstoffatoms in eine Ge–H-Bindung, wodurch $cAAC^{Me}H–GeHMes_2$ (**3.1**, Schema 11.3, Abbildung 11.3) als Reaktionsprodukt erhalten wurde. Die Umsetzung von GeH_2Mes_2 mit zwei Äquivalenten Me_2Im^{Me} bei erhöhten Temperaturen führte jedoch unter Wasserstoffabspaltung in Form von $NHCH_2$ zum NHC-stabilisierten Germylen $Me_2Im^{Me}{\cdot}GeMes_2$ (**3.2**, Schema 11.3).

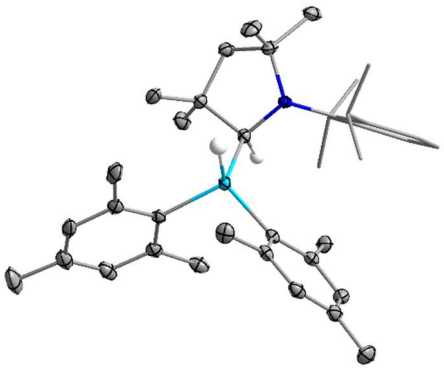

3.1

Abbildung 11.3: Molekülstruktur von $cAAC^{Me}H–GeHMes_2$ (**3.1**).

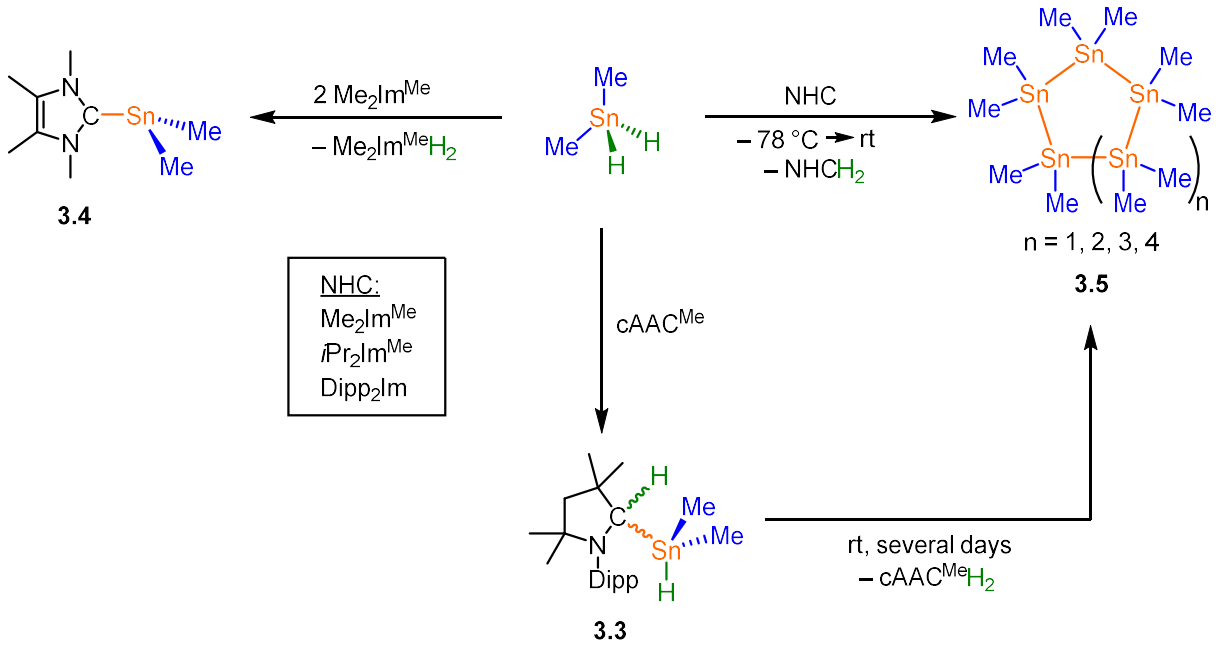

Schema 11.4: Reaktionen der NHCs Me_2Im^{Me}, iPr_2Im^{Me}, $Dipp_2Im$ und von $cAAC^{Me}$ mit SnH_2Me_2.

Wie schon bei der Synthese von Verbindung **3.1** beobachtet, führte auch die Reaktion von SnH_2Me_2 mit $cAAC^{Me}$ zur Insertion und dem entsprechenden Produkt $cAAC^{Me}H$–$SnHMe_2$ (**3.3**, Schema 11.4). Darüber hinaus wurde die NHC-vermittelte Dehydrierung von SnH_2Me_2 und die Bildung des NHC-stabilisierten Stannylens $Me_2Im^{Me}{\cdot}SnMe_2$ (**3.4**, Scheme 11.4) beobachtet. Die Umsetzungen der sterisch anspruchsvolleren NHCs iPr_2Im^{Me} und $Dipp_2Im$, sowie die Umsetzung nur eines Äquivalents an Me_2Im^{Me} mit SnH_2Me_2 bei niedrigen Temperaturen, resultierten in der Dehydrokupplung der *in situ* gebildeten {$SnMe_2$}-Einheiten. So wurde selektiv ein Zinnoligomer $(SnMe_2)_n$ (**3.5**, Schema 11.4), vermutlich das *cyclo*-Pentamer, als gelber Feststoff erhalten. In Lösung konnten die Zinn-*cyclo*-Oligomere $(SnMe_2)_n$ (n = 6, 7, 8) NMR-spektroskopisch beobachtet werden. Zudem wurde Verbindung **3.3** nach einigen Tagen in Lösung vollständig in die gleichen Zinn-*cyclo*-Oligomere umgewandelt. Die thermische Belastung von **3.3** oder **3.5**, sowie die Umsetzung der NHCs mit SnH_2Me_2 bei Raumtemperatur führten ebenfalls zur Bildung der Zinn-*cyclo*-Oligomere $(SnMe_2)_n$ (n = 6, 7, 8) sowie eines weiteren Oligomers, bei dem es sich vermutlich um das *cyclo*-Pentamer handelt. Daher kann davon ausgegangen werden, dass Verbindung **3.3** eine Zwischenstufe in der Dehydrokupplung von SnH_2Me_2 darstellt.

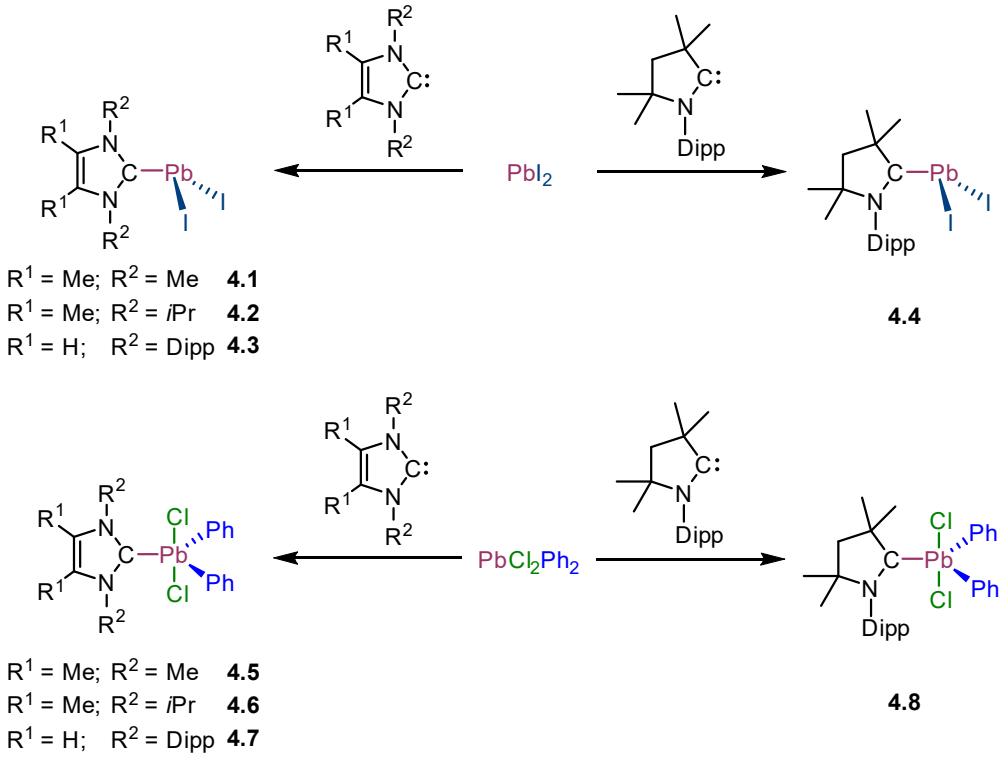

R^1 = Me; R^2 = Me **4.1**
R^1 = Me; R^2 = *i*Pr **4.2**
R^1 = H; R^2 = Dipp **4.3**

4.4

R^1 = Me; R^2 = Me **4.5**
R^1 = Me; R^2 = *i*Pr **4.6**
R^1 = H; R^2 = Dipp **4.7**

4.8

Schema 11.5: Synthese der NHC- und cAAC-Addukte von PbI_2 (**4.1-4.4**) und $PbCl_2Ph_2$ (**4.5-4.7**).

Die große Vielfalt an neuen Verbindungen der Elemente Germanium und Zinn führte auch zur Untersuchung ähnlicher Bleiverbindungen. So wurden in Kapitel IV verschiedene NHCs, sowie $cAAC^{Me}$ mit PbI_2 reagiert, um das jeweilige Plumbylen $Me_2Im^{Me}{\cdot}PbI_2$ (**4.1**), $iPr_2Im^{Me}{\cdot}PbI_2$ (**4.2**), $Dipp_2Im{\cdot}PbI_2$ (**4.3**) oder $cAAC^{Me}{\cdot}PbI_2$ (**4.4**) zu erhalten (Schema 11.5, oben). Da Arylierungsversuche der erhaltenen Pb(II)-Verbindungen **4.1-4.4** erfolglos blieben, wurde ein alternativer Reaktionspfad gewählt. Hierfür wurden zuerst die Pb(IV)-Addukte $NHC{\cdot}PbCl_2Ph_2$ (**4.5-4.7**) und $cAAC^{Me}{\cdot}PbCl_2Ph_2$ (**4.8**) aus der Reaktion von $PbCl_2Ph_2$ mit dem jeweiligen Carben synthetisiert (Schema 11.5, unten). Anschließende Reduktion von **4.5** und **4.6** mit KC_8 führte zu den NHC-stabilisierten diarylsubstituierten Plumbylenen $Me_2Im^{Me}{\cdot}PbPh_2$ (**4.9**, Abbildung 11.4) und $iPr_2Im^{Me}{\cdot}PbPh_2$ (**4.10**). NMR spektroskopische Untersuchungen in Lösung sprechen für eine Koexistenz von NHC und $\{PbPh_2\}$.

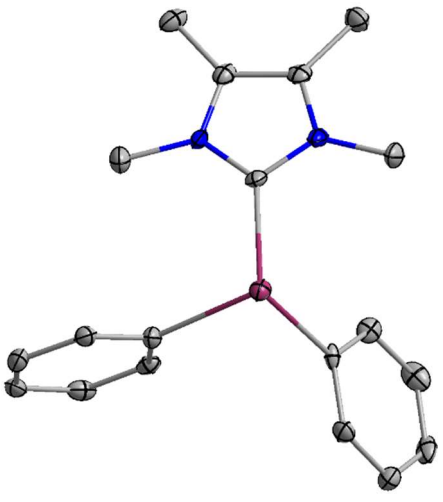

4.9

Abbildung 11.4: Molekülstruktur von $Me_2Im^{Me}{\cdot}PbPh_2$ (**4.9**).

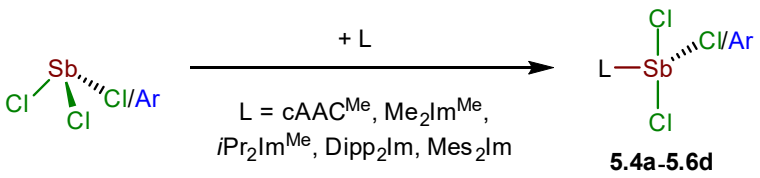

Schema 11.6: Synthese der NHC- und cAAC^{Me}-Addukte von $SbCl_3$ (**5.4a-e**), $SbCl_2Ph$ (**5.5a-e**) und $SbCl_2Mes$ (**5.6a-d**).

Zusätzlich zur Chemie der höheren Homologen der Gruppe 14 wurde in Kapitel V über die Synthese und Reaktivität von NHC- und cAAC-stabilisierten Verbindungen des schweren Gruppe-15-Elements Antimon berichtet. Die Addukte NHC·$SbCl_2R$ (R = Cl, Ph, Mes) (**5.4a-5.6d**) wurden durch Reaktion der Antimonverbindungen $SbCl_2R$ (R = Cl, Ph, Mes) mit den entsprechenden Carbenen (L) dargestellt (Schema 11.6). Die für **5.4a-5.6d** erhaltenen Daten geben einen Einblick in die Bindungssituation am Antimon, sowie über den Einfluss verschiedener Carbene mit unterschiedlichen Substitutionsmustern und variierender Substituenten am Antimon auf die Chemie der entsprechenden Addukte. Beispielsweise führte die thermische Belastung von $Dipp_2Im$·$SbCl_2Mes$ (**5.6c**) oder $Dipp_2Im$·$SbCl_2Ph$ (**5.5c**) bzw. der Kombination ihrer Vorstufen zu den jeweiligen abnormal koordinierten Addukten $^{a}Dipp_2Im$·$SbCl_2Ar$ (Ar = Mes (**5.7**), Ph (**5.8**)). Die Chloridabstraktion von **5.7** durch die *Lewis*-Säuren $GaCl_3$ und $AgBF_4$ lieferte die ionischen Verbindungen $[^{a}Dipp_2Im·SbClMes]^+[X]^-$ ($[X]^- = [BF_4]^-$ (**5.9**, Abbildung 11.5); $[GaCl_4]^-$ (**5.10**)).

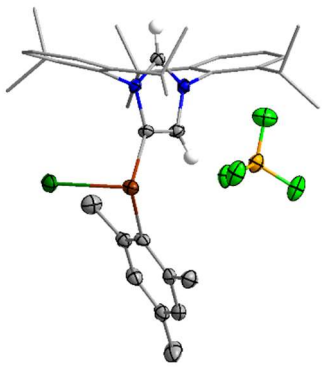

5.9

Abbildung 11.5: Molekülstruktur von $[^{a}Dipp_2Im·SbClMes]^+[BF_4]^-$ (**5.9**).

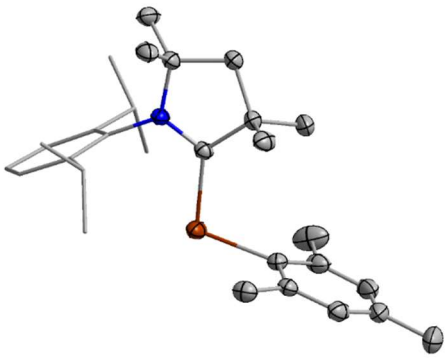

6.2a

Abbildung 11.6: Molekülstruktur von cAAC^{Me}·SbMes (**6.2a**).

Im Vergleich zur Reihe der, in Kapitel V beschriebenen Carben-Antimon-Addukte wurde für die Umsetzung von cAACs mit $SbCl_2Mes$ eine andere Reaktivität beobachtet. Die, in Kapitel VI beschriebenen Untersuchungen zeigten, dass die Reaktionen von $SbCl_2Mes$ mit cAAC^{Me} bzw. cAAC^{Cy} zu den cAAC-stabilisierten Stibinidenen cAAC^{Me}·SbMes (**6.2a**, Abbildung 11.6) bzw. cAAC^{Cy}·SbMes (**6.2b**) führte. Die Reaktionen gehen mit einer 50 %igen Bildung der Salze [cAAC^{Me}Cl]$^+$[$SbCl_3Mes$]$^-$ (**6.1a**) bzw. [cAAC^{Cy}Cl]$^+$[$SbCl_3Mes$]$^-$ (**6.1b**) einher. Die Bindungssituation von **6.2a** wurde mit Hilfe von DFT-Rechnungen näher untersucht, welche eine Sb=C$_{Carben}$-Doppelbindung bestätigen.

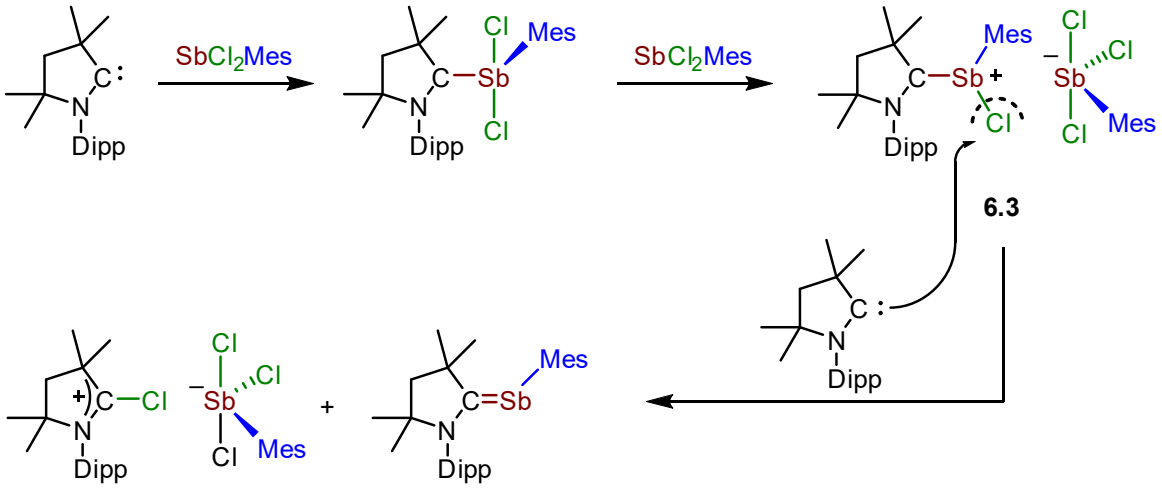

Schema 11.7: Postulierter Mechanismus für die Bildung der Verbindungen **6.1a** und **6.2a** über das Zwischenprodukt **6.3**.

Für diesen Reaktionstyp wurde ein Mechanismus über die Reduktion des Zwischenprodukts [cAAC^{Me}·SbClMes]$^+$[$SbCl_3Mes$]$^-$ (**6.3**) hin zum Stibiniden cAAC^{Me}·SbMes (**6.2a**, Schema 11.7) postuliert, wobei das Carben-Kohlenstoffatom als Reduktionsmittel fungiert. Um diesen Mechanismus zu bestätigen, wurde das Schlüsselintermediat [cAAC^{Me}·SbClMes]$^+$[$SbCl_3Mes$]$^-$ (**6.3**) dieser Reaktionsfolge durch Reaktion von cAAC^{Me} mit zwei Äquivalenten $SbCl_2Mes$ gezielt isoliert.

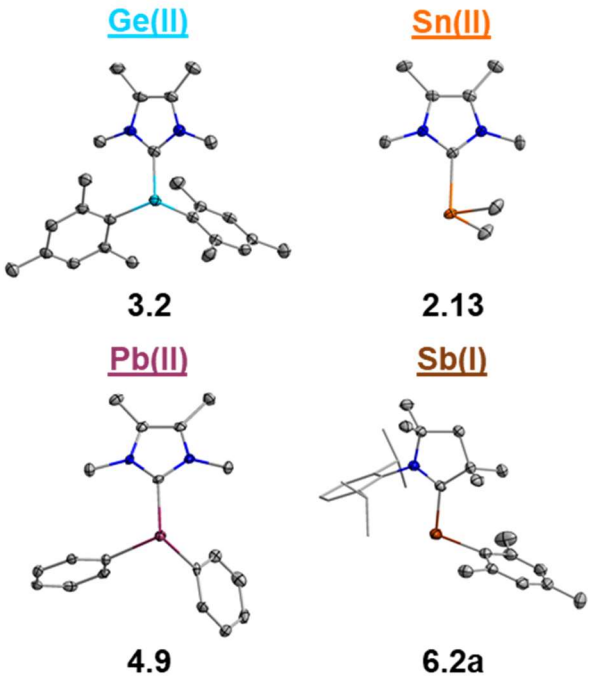

Abbildung 11.7: Molekülstrukturen der niedervalenten Verbindungen **3.2**, **2.13**, **4.9** und **6.2a**.

Im Rahmen dieser Arbeit wurden die Synthesen und Reaktivitäten von NHC- und cAAC-stabilisierten Verbindungen von Gruppe 14 und 15 Elementen eingehend untersucht und verschiedene Reduktionswege zu niederwertigen Verbindungen der einzelnen Elemente (Abbildung 11.7) etabliert. Zudem konnten bemerkenswerte Unterschiede in der Reaktivität zwischen NHCs und cAACs festgestellt werden. Für GeH_2Mes_2 konnte mit Me_2Im^{Me} beispielsweise eine vollständige Reduktion zum entsprechenden NHC-stabilisierten Germylen beobachtet werden, während $cAAC^{Me}$ in eine Ge–H-Bindung insertierte. Zudem wurde für SnH_2Me_2 die Dehydrokupplung von $\{SnMe_2\}$-Einheiten durch beide Carbenarten beobachtet. In der Chemie des Antimons konnte zudem die erste bekannte metallfreie und Carben-vermittelte Reduktion von Sb(III) zu Sb(I) unter milden Bedingungen und in quantitativen Ausbeuten realisiert werden.

12 Appendix

12.1 Abbreviations

Substituents

^{a}	abnormal or backbone-coordinated
Ar	aryl
Ar*	2,6-bis(diphenylmethyl)-4-methylphenyl
Ar^{F}	3,5-$(CF_3)_2C_6H_3$
Ar^{Mes}	2,6-dimesitylphenyl
Ar^{Trip}	2,6-bis(2,4,6-tri-*iso*-propylphenyl)phenyl
Cy	cyclohexyl
Cp*	1,2,3,4,5-pentamethyl-*cyclo*-penta-dienyl
Dipp	2,6-di-*iso*-propylphenyl
DMB	2,3-dimethylbut-2-enyl
DMP	2,3-dihydro-1,3-di-3'-methoxypropyl
Et	ethyl
*i*Pr	*iso*-propyl
*n*Pr	*n*-propyl
Me	methyl
Mes	mesityl
Neop	neopentyl
Ph	phenyl
Pin	pinacol
Pn	pnictogen

R^F	$C(CF_3)_3$
^{s}	saturated backbone
Tbb	2,6-$(CH(SiMe_3)_2)_2$-4-(*t*Bu)C_6H_2
*t*Bu	*tert*-butyl
Trip	2,4,6-tri-*iso*-propylphenyl
TMS	trimethylsilyl

Solvents and reagents

B_2pin_2	bis(pinacolato)diboron
C_6D_6	deuterated benzene
DCM	dichloromethane
Et_2O	diethyl ether
*n*BuLi	*n*-butyllithium
OTf	trifluoromethanesulfonate
THF	tetrahydrofuran

***N*-Heterocyclic Carbenes and Cyclic (Alkyl)(amino)carbenes**

cAAC	Cyclic (Alkyl)(amino)carbene
$cAAC^{Me}$	1-(2,6-di-*iso*-propylphenyl)-3,3,5,5-tetramethyl-pyrrolidin-2-ylidene
$cAAC^{Et}$	1-(2,6-di-*iso*-propylphenyl)-3,3-diethyl-5,5-dimethyl-pyrrolidin-2-ylidene
$cAAC^{Cy}$	2-azaspiro[4.5]dec-2-(2,6-di-*iso*-propylphenyl)-3,3-dimethyl-1-ylidene
DAC^{Mes}	1,3-dimesityl-5,5-dimethyl-4,6-dioxo-3,4,5,6-tetrahydro-pyrimidin-2-ylidene
$Dipp_2Im$	1,3-(2,6-di-*iso*-propylphenyl)imidazolin-2-ylidene

6-Dipp$_2$Im	1,3-bis(2,6-di-iso-propylphenyl)-4,5,6-hexahydropyrimi-din-2-yliden
^{s}Dipp$_2$Im	1,3-(2,6-di-*iso*-propylphenyl)imidazolidine-2-ylidene
*i*Pr$_2$Im	1,3-di-*iso*-propylimidazolin-2-ylidene
*i*Pr$_2$Im^{Me}	1,3-di-*iso*-propyl-4,5-dimethylimidazolin-2-ylidene
Me$_2$Im^{Me}	1,3,4,5-tetramethylimidazolin-2-ylidene
^{s}Me$_2$ImF$_2$	2,2-difluoro-1,3-dimethylimidazolidine
Mes$_2$Im	1,3-dimesitylimidazolin-2-ylidene
Neop$_2$Im$^{(C6H4)}$	1,3-di-neopentylbenz-imidazolin-2-ylidene
NHDC	:C[N(2,6-*i*Pr$_2$C$_6$H$_3$)]$_2$(CH)C:
NHO	*N*-heterocyclic olefin
NHPb	*N*-heterocyclic plumbylene
*n*Pr$_2$Im	1,3-di-*n*-propylimidazolin-2-ylidene
N-*t*BuIm	1-*tert*-butyl-3-boryl-imidazolin-2-ylidene
R$_2$Im^{Me}	1,3-di-organyl-4,5-dimethyl-imidazolin-2-ylidene
*t*Bu$_2$Im	1,3-di-*tert*-butylimidazolin-2-ylidene

Analytical abbreviations

CSD	Cambridge Structural Database
d	doublet (in NMR spectroscopy); days
DFT	density functional theory
DOSY	diffusion ordered spectroscopy
eq.	equivalent
h	hour
HMBC	heteronuclear multiple bond correlation
HMQC	heteronuclear multiple quantum correlation

HSQC	heteronuclear single quantum correlation
m	multiplet (in NMR spectroscopy)
min	minute
NMR	nuclear magnetic resonance
q	quartet (in NMR spectroscopy)
rt	room temperature
s	singlet (in NMR spectroscopy)
sec	second
sept	septet (in NMR spectroscopy)
t	triplet (in NMR spectroscopy)

Symbols and non-SI-units

Å	Ångström, 1 Å = 10^{-10} m
J	J-coupling constant in NMR spectroscopy, [Hz]
ppm	parts per million
Z	number of molecules per unit cell
δ	chemical shift in NMR spectroscopy, [ppm]
ν	frequency, [s^{-1}]

12.2 List of compounds

Chapter II:

2.1a $Me_2Im^{Me}{\cdot}GeCl_2Me_2$

2.1b $iPr_2Im^{Me}{\cdot}GeCl_2Me_2$

2.1c $Dipp_2Im{\cdot}GeCl_2Me_2$

2.2a $Me_2Im^{Me}{\cdot}SnCl_2Me_2$

2.2b $iPr_2Im^{Me}{\cdot}SnCl_2Me_2$

2.2c $Dipp_2Im{\cdot}SnCl_2Me_2$

2.3 $Me_2Im^{Me}{\cdot}GeCl_4$

2.4 $iPr_2Im^{Me}{\cdot}SnCl_4{\cdot}THF$

2.5 $[^aDipp_2Im{\cdot}GeClMe_2]^+[Cl]^-$

2.6 $cAAC^{Me}{\cdot}GeCl_2Me_2$

2.7 $cAAC^{Me}{\cdot}SnCl_2Me_2$

2.8 $cAAC^{Me}{\cdot}GeCl_2Ph_2$

2.9 $[cAAC^{Me}{\cdot}GeMe_3]^+[Cl]^-$

2.10 $[cAAC^{Me}Cl]^+[GeCl_3]^-$

2.11 $[cAAC^{Me}Cl]^+[SnCl_3]^-$

2.12 $cAAC^{Me}{\cdot}SnCl_4$

2.13 $Me_2Im^{Me}{\cdot}SnMe_2$

2.14 $cAAC^{Me}{\cdot}SnMe_2{\cdot}SnCl_2Me_2$

Chapter III:

3.1 cAAC^{Me}H–GeHMes$_2$

3.2 Me$_2$Im^{Me}·GeMes$_2$

3.3 cAAC^{Me}H–SnHMe$_2$

3.4 Me$_2$Im^{Me}·SnMe$_2$

Chapter IV:

4.1 Me$_2$Im^{Me}·PbI$_2$

4.2 *i*Pr$_2$Im^{Me}·PbI$_2$

4.3 Dipp$_2$Im·PbI$_2$

4.4 cAAC^{Me}·PbI$_2$

4.5 Me$_2$Im^{Me}·PbCl$_2$Ph$_2$

4.6 *i*Pr$_2$Im^{Me}·PbCl$_2$Ph$_2$

4.7 Dipp$_2$Im·PbCl$_2$Ph$_2$

4.8 cAAC^{Me}·PbCl$_2$Ph$_2$

4.9 Me$_2$Im^{Me}·PbPh$_2$

4.10 *i*Pr$_2$Im^{Me}·PbPh$_2$

Chapter V:

5.4a Me$_2$Im^{Me}·SbCl$_3$

5.4b *i*Pr$_2$Im^{Me}·SbCl$_3$

5.4c Dipp$_2$Im·SbCl$_3$

5.4d Mes$_2$Im·SbCl$_3$

5.4e cAAC^{Me}·SbCl$_3$

5.5a Me$_2$Im^{Me}·SbCl$_2$Ph

5.5b ***i*Pr$_2$Im^{Me}·SbCl$_2$Ph**

5.5c **Dipp$_2$Im·SbCl$_2$Ph**

5.5d **Mes$_2$Im·SbCl$_2$Ph**

5.5e **cAAC^{Me}·SbCl$_2$Ph**

5.6a **Me$_2$Im^{Me}·SbCl$_2$Mes**

5.6b ***i*Pr$_2$Im^{Me}·SbCl$_2$Mes**

5.6c **Dipp$_2$Im·SbCl$_2$Mes**

5.6d **Mes$_2$Im·SbCl$_2$Mes**

5.7 **^{a}Dipp$_2$Im·SbCl$_2$Mes**

5.8 **^{a}Dipp$_2$Im·SbCl$_2$Ph**

5.9 **[^{a}Dipp$_2$Im·SbClMes]$^+$[BF$_4$]$^-$**

5.10 **[^{a}Dipp$_2$Im·SbClMes]$^+$[GaCl$_4$]$^-$**

Chapter VI:

6.1a **[cAAC^{Me}Cl]$^+$[SbCl$_3$Mes]$^-$**

6.1b **[cAAC^{Cy}Cl]$^+$[SbCl$_3$Mes]$^-$**

6.2a **cAAC^{Me}·SbMes**

6.2b **cAAC^{Cy}·SbMes**

6.3 **[cAAC^{Me}·SbClMes]$^+$[SbCl$_3$Mes]$^-$**

12.3 Erklärung zur Autorenschaft

Julius-Maximilians-
UNIVERSITÄT
WÜRZBURG

Fakultät für
CHEMIE UND
PHARMAZIE

Erklärung zur Autorenschaft

N-Heterocyclic Carbenes and Cyclic (Alkyl)(amino)carbenes as Ligands for p-Block Element Compounds, N-Heterocyclic Carbene and Cyclic (Alkyl)(amino)carbene Adducts of Germanium(IV) and Tin(IV) Chlorides and Organyl Chlorides, Michael S. M. Philipp, Rüdiger Bertermann, Udo Radius*, *European Journal of Inorganic Chemistry*, **2022**, e202200429, DOI: 10.1002/ejic.202200429.

Detaillierte Darstellung der Anteile an der Veröffentlichung (in %)
Angabe Autoren/innen (ggf. Haupt- / Ko- / korrespondierende/r Autor/in) mit Vorname Nachname (Initialen)

Michael S. M. Philipp (MP), Rüdiger Bertermann (RB), Udo Radius (UR)

Autor	MP	RB	UR	Σ in Prozent
Konzept	5%	0%	5%	10%
Synthese	30%	0%	0%	30%
Analytik	17.5%	10%	0%	27.5%
Verfassen der Veröffentlichung	12.5%	0%	5%	17.5%
Korrektur der Veröffentlichung	5%	0%	5%	10%
Koordination der Veröffentlichung	0%	0%	5%	5%
Summe	70%	10%	20%	100%

Julius-Maximilians-
UNIVERSITÄT
WÜRZBURG

Fakultät für
CHEMIE UND
PHARMAZIE

Erklärung zur Autorenschaft

N-Heterocyclic Carbenes and Cyclic (Alkyl)(amino)carbenes as Ligands for p-Block Element Compounds, Activation of Ge–H and Sn–H bonds with N-Heterocyclic Carbenes and a Cyclic (Alkyl)(amino)carbene, Michael S. M. Philipp, Rüdiger Bertermann, Udo Radius*, **2022**, Submitted Manuscript.

Detaillierte Darstellung der Anteile an der Veröffentlichung (in %)
Angabe Autoren/innen (ggf. Haupt- / Ko- / korrespondierende/r Autor/in) mit Vorname Nachname (Initialen)

Michael S. M. Philipp (MP), Rüdiger Bertermann (RB), Udo Radius (UR)

Autor	MP	RB	UR	∑ in Prozent
Konzept	5%	0%	5%	10%
Synthese	30%	0%	0%	30%
Analytik	17.5%	10%	0%	27.5%
Verfassen der Veröffentlichung	12.5%	0%	5%	17.5%
Korrektur der Veröffentlichung	5%	0%	5%	10%
Koordination der Veröffentlichung	0%	0%	5%	5%
Summe	70	10%	20%	100%

Julius-Maximilians-
UNIVERSITÄT
WÜRZBURG

Fakultät für
CHEMIE UND
PHARMAZIE

Erklärung zur Autorenschaft

N-Heterocyclic Carbenes and Cyclic (Alkyl)(amino)carbenes as Ligands for p-Block Element Compounds, N-Heterocyclic carbene and cyclic (alkyl)(amino)carbene adducts of plumbanes and plumbylenes, Michael S. M. Philipp, Rüdiger Bertermann, Udo Radius*, *Dalton Transactions*, **2022**, Accepted Manuscript, DOI: 10.1039/D2DT02462D.

Detaillierte Darstellung der Anteile an der Veröffentlichung (in %)
Angabe Autoren/innen (ggf. Haupt- / Ko- / korrespondierende/r Autor/in) mit Vorname Nachname (Initialen)

Michael S. M. Philipp (MP), Rüdiger Bertermann (RB), Udo Radius (UR)

Autor	MP	RB	UR	∑ in Prozent
Konzept	5%	0%	5%	10%
Synthese	25%	0%	0%	25%
Analytik	17.5%	12.5%	0%	30%
Verfassen der Veröffentlichung	12.5%	0%	5%	17.5%
Korrektur der Veröffentlichung	5%	2.5%	5%	12.5%
Koordination der Veröffentlichung	0%	0%	5%	5%
Summe	65%	15%	20%	100%

Julius-Maximilians-
UNIVERSITÄT
WÜRZBURG

Fakultät für
CHEMIE UND
PHARMAZIE

Erklärung zur Autorenschaft

N-Heterocyclic Carbenes and Cyclic (Alkyl)(amino)carbenes as Ligands for p-Block Element Compounds, N-Heterocyclic Carbene and Cyclic (Alkyl)(amino)carbene Adducts of Antimony(III), Michael S. M. Philipp, Mirjam J. Krahfuss, Krzysztof Radacki, Udo Radius*, *European Journal of Inorganic Chemistry*, **2021**, *38*, 4007-4019, DOI:10.1002/ejic.202100632.

Detaillierte Darstellung der Anteile an der Veröffentlichung (in %)
Angabe Autoren/innen (ggf. Haupt- / Ko- / korrespondierende/r Autor/in) mit Vorname Nachname (Initialen)

Michael S. M. Philipp (MP), Mirjam J. Krahfuss (MK), Krzysztof Radacki (KR), Udo Radius (UR)

Autor	MP	MK	KR	UR	∑ in Prozent
Konzept	5%	0%	0%	5%	10%
Synthese	25%	0%	0%	0%	25%
Analytik	20%	5%	0%	0%	25%
Rechnungen	0%	0%	5%	2.5%	7.5%
Verfassen der Veröffentlichung	12.5%	0%	0%	5%	17.5%
Korrektur der Veröffentlichung	5%	0%	0%	5%	10%
Koordination der Veröffentlichung	0%	0%	0%	5%	5%
Summe	67.5%	5%	5%	22.5%	100%

Julius-Maximilians-
UNIVERSITÄT
WÜRZBURG

Fakultät für
CHEMIE UND
PHARMAZIE

Erklärung zur Autorenschaft

N-Heterocyclic Carbenes and Cyclic (Alkyl)(amino)carbenes as Ligands for p-Block Element Compounds, A Versatile Route To Cyclic (Alkyl)(Amino)Carbene-Stabilized Stibinidenes, Michael S. M. Philipp, Udo Radius*, *Zeitschrift für anorganische und allgemeine Chemie*, **2022**, e202200085, DOI: 10.1002/zaac.202200085.

Detaillierte Darstellung der Anteile an der Veröffentlichung (in %)
Angabe Autoren/innen (ggf. Haupt- / Ko- / korrespondierende/r Autor/in) mit Vorname Nachname (Initialen)

Michael S. M. Philipp (MP), Udo Radius (UR)

Autor	MP	UR	∑ in Prozent
Konzept	5%	5%	10%
Synthese	27.5%	0%	27.5%
Analytik	25%	0%	25%
Rechnungen	0%	5%	5%
Verfassen der Veröffentlichung	12.5%	5%	17.5%
Korrektur der Veröffentlichung	5%	5%	10%
Koordination der Veröffentlichung	0%	5%	5%
Summe	75%	25%	100%

13 Acknowledgement

Als Erstes ein riesiges Dankeschön an meinen Doktorvater **Prof. Dr. Udo Radius**. Vielen Dank Udo, dass ich erst meine Masterarbeit und nun auch noch meine Doktorarbeit bei dir in deinem durchweg tollen Arbeitskreis (Ich glaube auch die nächste Generation wird ganz dufte) machen durfte. Egal wann man Hilfe gebraucht hat, die Tür war buchstäblich offen, außer Todd war mal wieder in Plapperlaune. Du hast mir immer alle Freiheit bei der Bearbeitung meines Themas gelassen, was durch mich leider oft auch zu viel schwarzem Feststoff geführt hat. Zwei Jahre an vergeblicher Stibbinidensynthese brachten mir zwar vorerst nur viel Frust und einen Spitznamen ein, am Ende jedoch mündete die lange Versucherei umso mehr in Euphorie über die (natürlich gezielt) entdeckte neue Stibbiniden-Synthese-Route. Es war ein sehr emotionaler Moment für alle Anwesenden (Ich glaube ich habe beim Luis auch Tränen gesehen). Im Nachhinein war es ja eigentlich auch nur wie Brezeln backen! Wahrscheinlich werde ich sogar vermissen, dass jeden Moment noch eine Weihnachtskeksdose mit dubiosen Altlasten auftauchen könnte, oder dass jemand mit einem Kolben „Grignardüberaschung“ um die Ecke kommen könnte. Vielen Dank auf jeden Fall für all den Spaß, den ich in deiner Arbeitsgruppe (besonders auch in Hirschegg) und mit dem ganzen „Haus“ haben durfte.

Außerdem möchte ich der, für mich „alten Generation“ danken, angefangen bei **Rumpel**, der mich das erste Mal in den Arbeitskreis gebracht hat, sowie **Ulli**, **Heidi**, **Schnurres**, **Toni**, **Landmann**, **Maddi** und **Shorty**, die immer geholfen haben, wenn man Hilfe gebraucht hat. Danke auch, dass ich an den meisten coolen Promotionsfeiern dabei sein konnte.

Ein großes Danke auch an die „nicht ganz so alte Generation“. **Laura**, danke, dass du mich mittlerweile (sowie Katha und Miri auch) gut leiden kannst. Mit dir hatte man jedes Mal mega viel Spaß und deine immer gute Laune vermiss ich manchmal heute noch. Ich bin mir übrigens sicher, dass ich die sieben Krapfen geschafft hätte ;) Übrigens sorry nochmal, dass ich einfach eigenständig deine Line neu gefettet habe. Ich bin zu tiefst demütig. Dem blonden Engel **K. Untze** ein großes Danke für all die witzigen Anekdoten und schlauen Ratschläge. Ich bin vor allem sehr dankbar für meine noch intakten Hände … uff, das war knapp. **Katha** (und Felix), danke, dass ihr immer so lieb

und hilfsbereit zu einem wart, außer Katha wollte mich mal wieder auf die Schippe nehmen. Ich habe es einfach nie gerafft, was für einige Lacher sorgte. Danke auch **Miri** aka die Kristallkönigin für unsere gemeinsame Zeit bei den Röntgendiffraktometern und den daraus hervorgegangenen Premiumstrukturen, auch wenn es bei dir nie das Stibbiniden war. Du hast mal gemeint, dass Steffen und ich unser eigenes Generationsdingens aufgemacht hätten, also fahre ich mal mit der jungen Generation fort.

Steffen, danke, dass du so ein treuer und krass hilfsbereiter Kumpel bist. Danke für all die Hilfe und das Korrekturlesen. Wir haben ja nahezu zeitgleich im AKR angefangen und somit zahllose witzige und auch unerwartete Situationen zusammen mitgemacht. Von der Schlachtbank im alten Erdgeschoss, über das LAH-Debakel, das Destillationsmaleur, die Gasmaskenaktionen bis hin zu diversesten und unvorhersehbaren Situationen beim Zweimonats-Quench (Keksdose). Ich bin froh, dass wir das immer zusammen machen konnten. Danke auch für den sehr nicen Tauchurlaub zusammen mit Gregor und auch **Tobi**, den ich hier sehr gerne mit reinnehme, auch wenn er, laut eigener Aussage, nur zu 1/4 AKR-Mitglied ist. Vielen Dank Tobi, dass du seit dem ersten Semester so ein guter Freund bist. Ich werde mich immer sehr gerne an alle Ausflüge, Feiern und sonstige gemeinsame Gelegenheiten erinnern und hoffe, dass noch sau viele dazu kommen. Auf weitere Gin-Abende, Bouldersessions, Tauch-, Ski- und Wanderurlaube. Danke auch fürs Korrekturlesen, die gute Laune und den Beistand, wenn mal was nicht so gut gelaufen ist. Ich finds halt echt mittlerweile gar nicht mehr so schlimm, dass uns öfters Leute verwechseln :D Achtung fränkisches Lob: Könnt schlimmer sein! Zurück zum AKR. Danke **Luggi** (und auch Nicole) für die witzigen Abende an der Uni, im Park oder im Tscharlies. Besonders unterhaltsam wurde es, wenn eine Tischtennisplatte ins Spiel kam, ob in einem zwielichtigen Park oder in verschiedensten Kelleretablissements (haben wir viel zu selten gemacht). Ich vermisse auch jetzt schon die schier endlosen Heimwege über die Zeppelinstraße zusammen mit **Güü** und allen anderen, die auch dabei waren. Güü, du bist einfach ein ~~richtig feiner~~ äh, sau dufter Typ, muss ich echt sagen! Vielen Dank fürs Kristalle messen und für all die nicen Ratschläge aus der Welt der NMR-Losigkeit. Es hat mir auch immer Spaß gemacht zusammen mit dir den Lehrämtlern vor ihrem Examen noch die ein oder andere Weisheit mitzugeben. Ich hoffe auch, dass es noch weiterhin ein paar Loma, Bombe und Airport Abende hageln wird. Danke für all die

premiumhaften Main-Nachmittage und coolen Erlebnisse, ob zu Fuß auf den hohen Ifen mit Miri und dem König, oder mit dem Bike im Steinbachtal zusammen mit Dr. Rauch. Besonders unterhaltsam wars auch immer, wenn Alberto dabei war. In dem Zuge, danke auch an **Maaaaaaadiiiiiin** (ich kann hier leider kein Treppenhaus-Hallgeräusch simulieren … stells dir einfach vor) aka Alberto Luft aka Alberto Montenegro aka unzählige weitere Namen (Die kommen ja auch nicht von Nichts). Ohne dich wärs einfach viel viel viel langweiliger gewesen. Bleib einfach so ein fröhlicher Hirni, der du bis jetzt warst! Allerdings hoffe ich du verletzt dich nicht mehr so oft … achja und lass das mal mit den Plastiklaternen. Ich hoffe wir treffen uns immer wieder auf idiotische Ideen und Wetten. Ein fettes Danke an die Unzertrennlichen: **Luis** aka der gefeierte Fußgänger und **Gingi** ähhhhhöööhhhähhhhh Kimchi Kagawa. Es gibt auf dem Planeten einfach niemanden sonst, der so krass Pizza-Holo reinzimmern kann wie ihr beide. Danke auch für die nicen Geoguesser-Sessions, das Flaschenbolzen, die Sonnenuntergänge auf Dächern, die Main-Wiesen-Eskapaden und den Loma-Mittwoch. Steuert auch weiterhin mit so guter Laune durch die Gegend (und Tiefhöfe) und gebt manchmal dem alten Ehepaar **Melauni** und **Golk** was davon ab. Danke Melanie für die nicen Kuchen und für die witzigen Erlebnisse, ob auf Asphalt unter Sternen zusammen mit Steffen und Güü oder auf der Nature. Hoffe das machen wir mal wieder. Und denk an die Wette. Danke Golk für die witzigen Anekdoten, die krassen Bangertracks und die atemberaubenden Parkoursessions. Du bist bisher auf jeden Fall auch der unterhaltsamste DJ den wir hier oben bei Feiern hatten. To our part-time members **Jan** and **Lewis**, thanks a lot for the nice time and thanks Jan for all the shots. Vielen Dank auch meinem Praktikanten **Flo** (Ich glaube der Bericht kommt nicht mehr), und meinen mega coolen Laborantinnen **Franzi** und **Kirsten** sowie meinem swaggen Laboranten **Maggus**. Euch gebührt ein richtig fettes Danke, da ihrs ganz schön lange mit mir und meiner Chemie im Labor aushalten musstet. Ich hoffe, dass ich euch ein halbwegs passabler Lehrmeister und Laborbuddy war.

Ich möchte mich auch bei den anderen Arbeitskreisen bedanken, mit denen das Zusammenarbeiten und vor allem Feiern immer Spaß gemacht hat, insbesondere mit den Mitgliedern des AK Finze. Ein paar Ehemalige (und Flo ;)) aus dem Haus möchte ich dabei auch noch hervorheben: **Fabi Keppner** (Danke dass du mich in diese tolle WG gebracht hast!!!), **Flo Rauch**, **Felix**, **Anna Rempel**, **Jaqui** und **Anna Hanft** (Du

bist die beste Kommilitonin, die man sich ab dem ersten Semester hätte wünschen können). Vielen Dank, dass man mit euch so viel Spaß haben konnte.

Ein besonderer Dank gilt dem Team des Hauses, der NMR-Abteilung (**Rüdiger**, **Marie-Luise** und **Laura**) für die schier endlosen Messungen meiner Verbindungen und all die Geduld, **Alex** und **Tschisch** für Kristalldinge und Tschisch vor allem für das Retten der Daten!!!, **Christoph** für das versuchte Detektieren von Massesignalen, der CHNS-Abteilung (**Sabine** und **Liselotte**), den nicesten Hausdamen **Conny**, **Birgit** und **Gerti** (Danke, dass du zu uns immer so nett warst und danke für die Tasse auf meinem Schreibtisch!) den ebenso nicen Hausmeistern, **Alfred** und **Stefan Köper**, den Glasbläsern **Berti** und **Berni**, sowie **Manni**, **Herrn Obert** und dem Technischen Betrieb. Danke auch **Stephan Wagner** für die ganze Hilfe bei unseren Lehramtsseminaren.

Ich möchte mich auch bei meinem **Freundeskreis** und meinen **Mitbewohnern** bedanken. Ich liste jetzt aber mal lieber nicht alle Namen auf, sonst wird das mit dem Drucken so teuer. Der Dank kommt leider viel zu kurz, aber ich werde mich bei jedem von euch nochmal persönlich für all die schönen Stunden, den Zusammenhalt und die Unterstützung bedanken. Ohne so einen Freundeskreis würde das Leben keinen Spaß machen. Besonders möchte ich dabei auch nochmal dich **Finja** hervorheben. Du warst für mich die letzten zwei Jahre, aber vor allem in der finalen Phase sehr wichtig. Ich bin einfach sau froh, dass ich dich damals in die Wg geholt hab, mit dir wird’s einfach nie langweilig! Ich hoffe das wird auch noch sehr lange so bleiben.

Je mehr Leute ich hier gerade aufliste, desto mehr wird mir bewusst von wie vielen tollen Menschen das eigene Leben beeinflusst wird. Ganz großer Dank an alle!!!!!

Meine **Familie** hatte dabei den wahrscheinlich größten und besten Einfluss. Ihr seid einfach die Besten, die ich mir dafür wünschen könnte. Ihr habt mich immer unterstützt und mir das absolut bestmögliche Umfeld geboten. Ohne euch wäre ich nie so ein glücklicher und fröhlicher Mensch geworden. Ich hab euch einfach sau lieb!